2013

Evaluation of Gas-Assisted Gravity Drainage EOR Process Applicability in a Louisiana Oil Field through Experiments and Reservoir Simulation

Wagirin Ruiz Paidin
Louisiana State University and Agricultural and Mechanical College, ruizpaidin@yahoo.com

EVALUATION OF GAS-ASSISTED GRAVITY DRAINAGE EOR PROCESS APPLICABILITY IN A LOUISIANA OIL FIELD THROUGH EXPERIMENTS AND RESERVOIR SIMULATION

A Dissertation

Submitted to the Graduate Faculty of the
Louisiana State University and
Agricultural and Mechanical College
in partial fulfillment of the
Requirements for the degree of
Doctor of Philosophy

in

The Department of Petroleum Engineering

by
Wagirin Ruiz Paidin
B.S. in Mining, Anton De Kom Universiteit van Suriname, 2003
M.S. in Petroleum Engineering, Louisiana State University
and Agricultural & Mechanical College, 2006
May 2013

This work is dedicated to my mother and father: it all stems from the caring way that you have raised me and I shall remain forever grateful for all the opportunities that you have provided me with.

ACKNOWLEDGMENTS

This dissertation would not have been possible without the assistance of several individuals who, in one way or another, have contributed and extended their valuable guidance in the preparation and completion of this study. First and foremost, I am deeply grateful to my advisor, Dr. Dandina Rao, whose continued technical steering and mentorship have shaped me to become the research professional I am today.

Dr. Seung Kam, Dr. Stephen Sears and Dr. Christopher White who graciously agreed to be part of my examination committee and whose constructive criticism have only served to improve my research work. Dr. Kam-Biu Liu, the Dean's Representative, for his kind words after my final defense presentation.

The U.S. Department of Energy, Research Partnership to Secure Energy for America (RPSEA), Louisiana Board of Regents and ConocoPhillips for funding my various research interests, thereby providing not only the means, but also the validation of the work conducted.

The rest of the faculty members and staff of the Craft & Hawkins Department of Petroleum Engineering whose daily interactions have enriched my academic life and made it a joy to spend so much time on campus. A very special mention of Mr. Fenelon Nunes who has always been willing to provide technical guidance in and outside of the laboratory and whose tireless dedication to the department is very much appreciated.

Last, but not least, my family and friends for their tireless support and cajoling that have fueled me along this journey.

TABLE OF CONTENTS

LIST OF TABLES

LIST OF FIGURES

ABSTRACT

The Gas-Assisted Gravity Drainage (GAGD) process was developed as an alternative to conventional gas injection enhanced oil recovery (EOR) processes, which suffer from their inherent weakness of combating gravity segregation. The GAGD process, however, is aimed at taking advantage of this phenomenon and consists of using horizontal producers near the bottom of the payzone while injecting gas using vertical injection wells. It is hypothesized that the injected gas will rise to the top, thereby forming a gas cap while displacing reservoir brine/oil downward towards the producers. In this study, a single-well alternative to the multi-well GAGD process was investigated to determine the operating constraints that would result in maximum oil recovery, and the main areas of improvement/adaptation for implementation in the Buckhorn Field, an onshore Louisiana reservoir. In the newly proposed process, the gas injection and fluid production occur along the same wellbore; however, they would be located in different sections with the production completions in either a horizontal section of the well or in a lower-lying section of a vertical well.

The study was comprised of reservoir condition coreflooding experiments to elucidate the pertinent data to the field application of this single-well GAGD process. This data was then used in field-scale numerical simulations to optimize the proposed process with regards to maximum oil recovery by investigating various well locations/configurations, and production strategies. In order to frame the proposed processes' technical feasibility they were compared to other commonly implemented EOR processes, such as Continuous Gas Injection and Water-Alternating-Gas. Finally, an economic assessment of all of the investigated gas EOR processes was carried out to quantify the risk associated with their application. For this purpose, a cashflow

analysis was conducted using Excel after which Crystal Ball was utilized to generate the confidence intervals for selected economic performance indicators.

The numerical simulation study revealed that the multi-well GAGD process resulted in the highest oil recovery (50–58 %ROIP or 2.0–2.6 million STBO) while the economic study showed that all GAGD process variations would be profitable. However, the vertical single-well GAGD process ranked the highest based on the Internal Rate of Return and the Profitability Index.

1. INTRODUCTION

1.1 Problem Statement

The development of the GAGD process at LSU was initiated and led by Dr. D.N. Rao and currently, its development is in the final phase, namely a field implementation/test, in this case by an independent oil company in the Buckhorn field, an oilfield in North Louisiana. The design of the GAGD process was meant to overcome the shortcomings of traditionally implemented enhanced oil recovery (EOR) methods, such as the Constant Gas Injection (CGI) and Water Alternating Gas (WAG) processes. The GAGD process was developed as an alternative to these conventionally applied gas injection processes, which suffer from their inherent flaw of combating gravity segregation: the resulting under- and/or override of the injected water and/or gas, respectively, often results in disappointing field performances. The GAGD process, however, is aimed at taking advantage of the gravity segregation of the injected gas from the reservoir fluids and consists of placing horizontal producers near the bottom of the payzone while injecting gas using vertical injection wells. It is proposed that in the GAGD process the injected gas will rise to the top of the payzone, thus forming a gas cap while displacing reservoir brine and oil downward towards the producers. The gas cap will grow both in thickness as well as in lateral extent displacing fluids in an ever-increasing zone. Due to the gravity-stable injection of the gas and the location of the horizontal producers, it is hypothesized that the gas breakthrough of the injected gas can be delayed with proper selection of operational parameters.

In order to ensure that the application of the GAGD process in the Buckhorn field is successful, various measures need to be undertaken to maximize the GAGD oil recovery while minimizing the risk at the same time. As with any field application of a novel EOR process, one

needs to identify the main operative mechanisms of the first to guide the design of the field application. The effect of gas injection rate (capillary number), the type of gas injected, the pressure regime governing the gas injection, the wettability of the porous medium and the presence of fractures on the GAGD oil recovery were all determined through laboratory experiments. These experiments consisted of both visual model and coreflooding experiments. Rounding off the preparation of the field application is usually a field-scale numerical simulation of the novel EOR process to determine the operational parameters that would lead to the best options of implementing a field trial based on the maximum oil recovered. In these instances, numerical simulation is often used as a powerful tool to forecast what the ultimate recovery will be by determining what the resulting drainage patterns are based on the planned number of wells and their locations and trajectories, and operational details, such as the "ideal" gas injection and oil withdrawal rates, the maximum allowable gas-oil-ratio (GOR) and in conjunction with that, the targeted gas utilization factor (GUF). Other important parameters in the field application of a novel process are concerned with possible alternative configurations of the proposed method, not only to allow for increased flexibility of its application but also to improve the project's economic feasibility.

One such possible alternative is a single-well variety of the novel multi-well GAGD process. A viable alternative application configuration also increases a novel EOR method's appeal as it would mean that it would be potentially successful in reservoirs with, not only different, but also a wider range of characteristics. An example of potential environment that might be suitable for the implementation of the Single-Well GAGD process is an offshore reservoir due to the prohibitive cost of wells. One single offshore well can cost more than $200 Million making it difficult for even the major oil companies to afford the use of drilling patterns

of several wells that may be required to implement EOR processes offshore. Due to the rapid decrease of the reservoir pressure once production commences nearly two-thirds of the original oil in place is left behind as trapped oil. The combination of these factors makes offshore reservoirs a potential environment in which Single-Well GAGD could be successfully implemented.

1.2 Objectives

The objectives of this study are:

1. Conduct reservoir condition GAGD coreflooding experiments using reservoir cores and fluids, whenever possible, to derive the appropriate relative permeability curves from the experimental results for use in field-scale numerical simulation of the GAGD process in the Buckhorn field.
2. Perform a numerical simulation study in which the application of the GAGD process in the Buckhorn field is "optimized" by maximizing the ultimate recovery through the investigation of the effect of various operational parameters, such as the number of injection and production wells and their locations/trajectories, the gas injection and oil withdrawal rates, on the oil recovered.
3. Propose an alternative configuration of the GAGD process in which the injection as well as the production aspects occur in the same well, albeit using different well completions, and optimize the application of this alternative GAGD variation in the Buckhorn field using a similar methodology as described above.

4. Conduct a comparative economic analysis of the GAGD process and other selected EOR processes, in order to highlight the advantages of implementing the GAGD process in the Buckhorn field.

1.3 Methodology

In this study, coreflooding experiments were conducted to meet the objectives as outlined above. All coreflooding experiments were conducted at reservoir conditions of pressure (1500 psia) and temperature (238 °F), and whenever possible, actual reservoir cores and fluids, both oil and brine, were used. These precautions were taken in order to continue using as much relevant reservoir data in the subsequent field-scale simulation study. The relevant data in question were the water-oil and gas-liquid relative permeability curves that were generated from the pressure and production data collected during the coreflooding experiment using a coreflood simulator. The coreflood simulator in question calculates the required relative permeability curves by matching the experimental pressure and oil recovery data as closely as possible. Using relevant reservoir data in the simulation study as much as possible minimizes the risk that goes along with forecasting the performance of any field application of a novel EOR process. The simulation study was conducted using a commercial compositional simulator, CMG-GEM, as well as CMG's guided optimization package, CMOST. To perform the economic comparison of the various possible EOR processes in the Buckhorn field, a cashflow model was compiled in Excel after which Oracle's Crystal Ball add-in was used to perform a Monte Carlo-type simulation to generate a complete picture of their economic viability for this particular North Louisiana oilfield.

2. LITERATURE REVIEW

2.1 Literature Review on Current Status of the Gas-Assisted Gravity Drainage (GAGD) Process

2.1.1 Introduction

The development of the GAGD process at LSU resulted in a process patent and is now in the final phase, namely a field implementation, in this case by an independent oil company in the Buckhorn Field, an onshore north Louisiana oilfield. The design of the GAGD process was meant to overcome the shortcomings of the traditionally implemented Water Alternating Gas (WAG) process. In the WAG process a water slug is injected to improve the sweep efficiency of gas injection by using water to control the mobility of the displacement and to stabilize the front as stated by Christensen *et al.* (2001) and as is depicted in Figure 2.1.

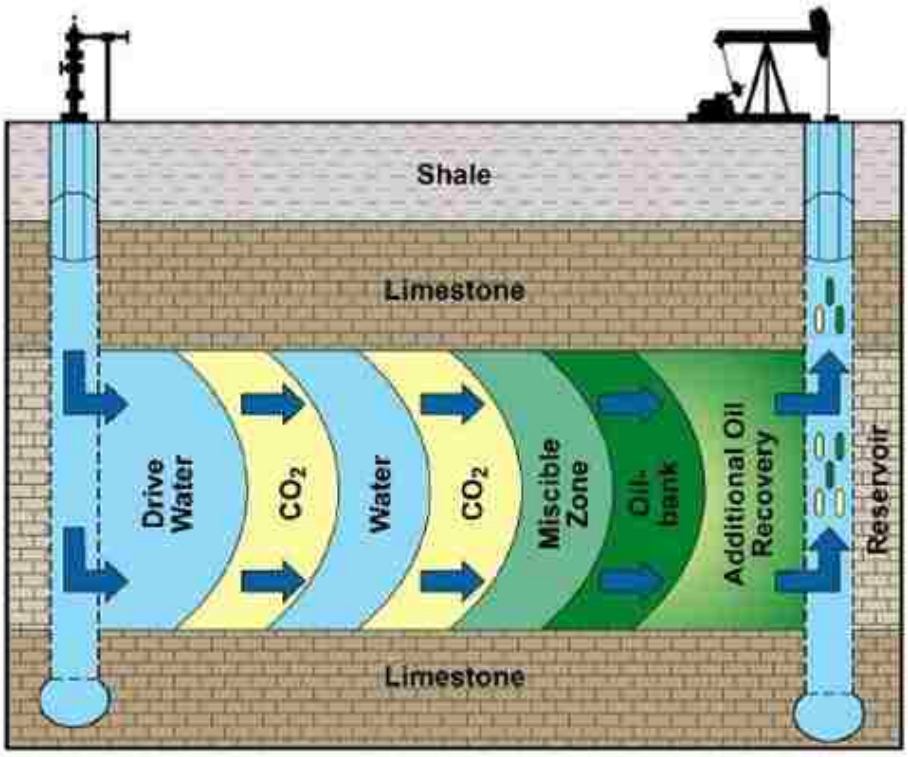

Figure 2.1: Idealized Schematic of the WAG Process (Adapted from US-DOE Website)

In their 2001 review of 59 field applications of the WAG process they have identified an average incremental increase of 5-10 percent with 14 of the fields reported to have problems with gravity overriding. This is caused by the difference in density between the injected fluids causing the gas to preferentially rise to the top and the water sinking towards the bottom of the payzone as is illustrated in Figure 2.2, instead of the initially envisioned stabilized piston-like displacement of Figure 2.1. Instead, the GAGD process uses the natural tendency of the gas to rise to the top and the descent of the injected water to the bottom by injecting gas into the reservoir using (existing) vertical wells and producing fluids from horizontal wells placed near the bottom of the payzone above the oil-water contact (Figure 2.3). As the gas rises it forms a gas cap at the top of the reservoir thus displacing and draining oil and water to the horizontal producers at the bottom. The use of horizontal producers increases the areal exposure to the reservoir thus leading to an increased well productivity.

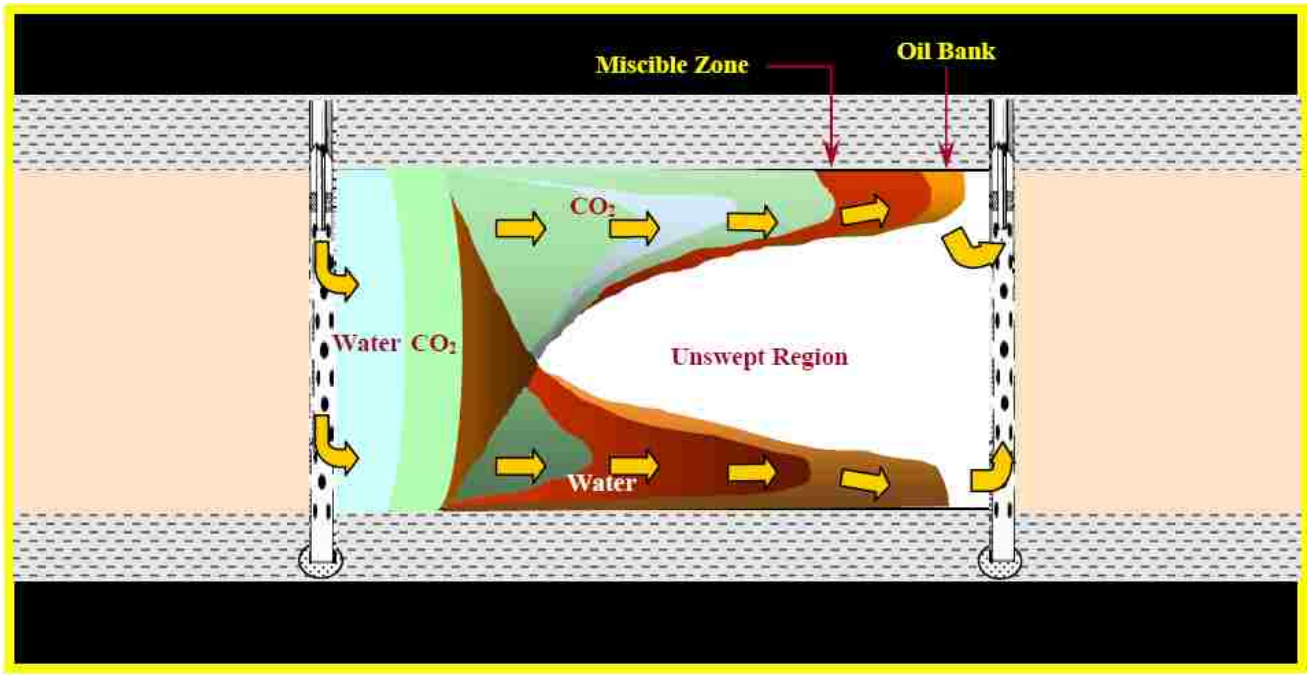

Figure 2.2: A More Realistic Schematic of the WAG Process (After Rao *et al.*, 2004)

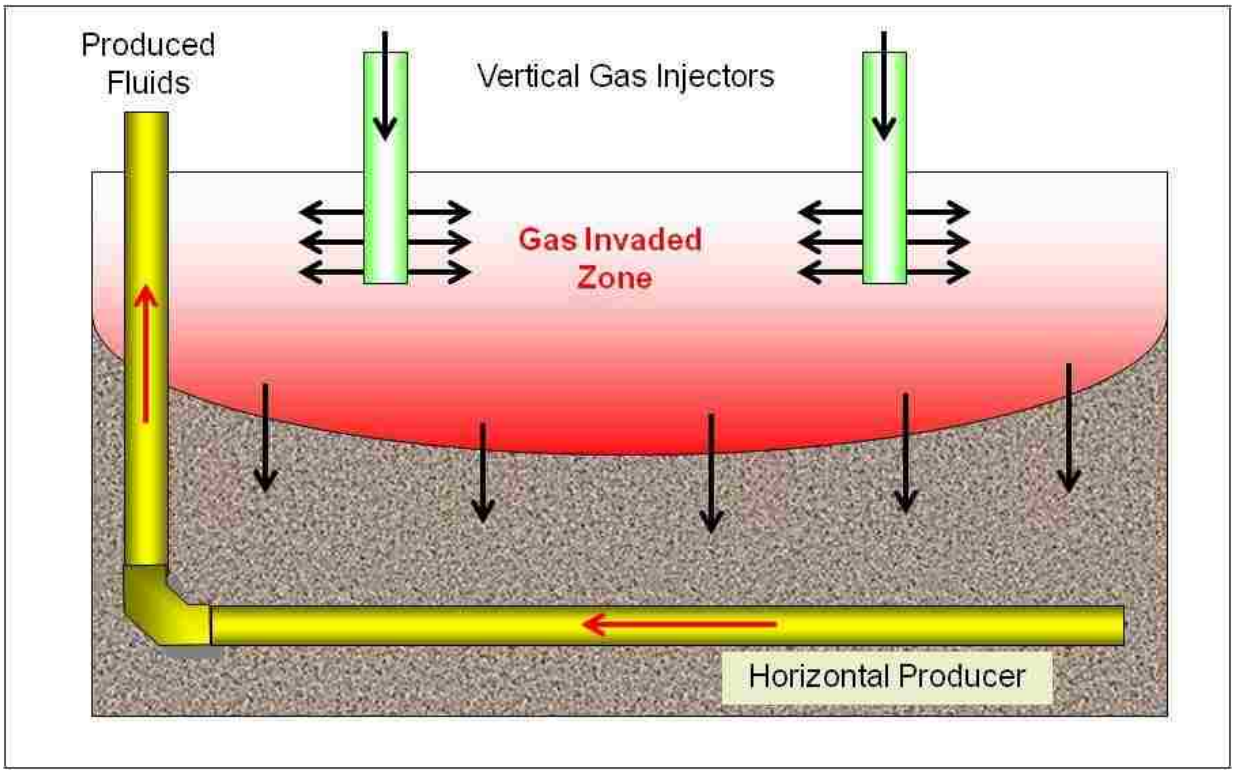

Figure 2.3: Schematic Representation of the GAGD Process

The GAGD process came to fruition with the financial assistance of the US Department of Energy and its development went through several stages:

1. Partially scaled physical/visual model experiments:

   These experiments were aimed at demonstrating the process and to identify suitable parameters by mimicking selected dimensionless numbers as observed in field projects. These dimensionless numbers were the capillary, Bond and gravity numbers. The visual experiments were also used to examine the effect of injectant miscibility, rock wettability and the presence of heterogeneities (fractures) on the GAGD recovery. Two types of models were used, a metal one that was based on a Hele-Shaw type model and a glass model, both of which contained silica sand/beads as the porous medium. Various gas/oil systems were used as proxies to the actual injectant/reservoir oil system, such as nitrogen or CO_2 as the injectant

and n-decane or soltrol as the oil phase. The conducted experiments revealed a log-linear relationship between the GAGD recovery and the three dimensionless numbers while in case of the gravity number this relationship persisted with the inclusion of field data as well as data from coreflooding experiments (Sharma, 2008). It was also shown that GAGD implementation under miscible conditions can lead to a near-perfect sweep of the model whereas the presence of fractures seems to enhance GAGD recovery as opposed to impede it due to the gravity-stable nature of the displacement: the fractures act as conduits for flow of the displaced reservoir fluids to the producer (Mahmoud, (2008); Paidin, (2007)). The wettability of the porous medium does seem to improve GAGD recovery slightly and this was accomplished by using glass beads that had been treated with organo-silanes thereby turning them oil-wet (Paidin, 2007).

2. Coreflooding experiments:

   The GAGD coreflooding experiments were conducted using both standardized as well as reservoir rock/fluid systems with cores of varying lengths and diameters. Initially, they were conducted with the objective of evaluating some of the same aforementioned parameters as well as mode of gas injection and core length effect. The results were as expected in that miscible floods performed better than those conducted under immiscible conditions while the long core experiments highlighted the effect of gravity segregation on the GAGD recovery (Rao, 2004). Reservoir conditions were also conducted with the specific goal of generating appropriate relative permeability curves for use in field-scale numerical simulation studies of the GAGD process using actual reservoir rocks and fluids.

2.1.2 The Field Application of GAGD

The process of implementing the GAGD process in the field was started in the second half of 2005 with a screening of two possible field options. Out of this screening, the Buckhorn field emerged as the most likely candidate for GAGD application. It is a previously waterflooded reservoir that had been shut in since 1972. The Buckhorn field is located in the Northeastern part of Louisiana and is a compartmentalized sandstone reservoir. It consists of four main units, or pods, of which one, the Buckhorn Dense Top, was selected for initial implementation of GAGD based on geological criteria. After the waterflooding had ended, it was estimated that the remaining reserves totaled about 4.7 million stocktank barrels. The wells in the Buckhorn Dense Top (from here on it will be referred to as the "Buckhorn Field") are said to be producing from the Buckhorn Sand (Oudumugsorn, 1971), the lowest (stratigraphically) producing zone in the Lower Tuscaloosa Formation. It has also been described as the most productive sand in the Buckhorn Field; the other producing sands being the S-2 Sand (also part of the Lower Tuscaloosa Formation) and the Washita-Fredericksburg Sand. The Buckhorn Sand was probably formed as a result of channel filling with the updip limit of the reservoir being formed by the pinchout of the sand against the edge of the channel. The porosity of the Buckhorn Sand ranges from 19.5 to 28.3 percent while the permeability ranges from 130.0 to 388.7 millidarcies. The original reservoir pressure was 4050 psia while the gravity of the oil in the Buckhorn Sand ranged from 39° to 42 °API.

The optimization process was designed as follows:

- Reservoir characterization – the reservoir characterization phase consisted of building a reservoir model based on the available geological data, such as well logs and reservoir maps. The appropriate fluid behavior model was also based on as much actual reservoir data as was

available at the time. This data consisted of actual reservoir fluids, oil and brine, and historical production data that was used to conduct the inversion process after which a forecast of the surface oil production rate was achieved using different CO_2 injection rates and well configurations.

- Optimization of production design – in the optimization stage of the production design various parameters were changed to assess their effect on the ultimate recovery. Among those parameters were the number of injector/producer well pairs, the location of the well pairs, the location of the horizontal producers above the oil-water contact, the CO_2 injection rates, the production rates and the lag time in between the start of injection and production.

As a result of the production design optimization it was decided that two injector/producer well pairs would be used in the selected locations as is illustrated in Figure 2.4. Both injection wells, G and G1 as denoted in Figure 2.4, had a total vertical depth of 8700 ft., while the horizontal wells' vertical section reached a depth of 8700 ft. The horizontal sections of the production wells, H and H1, each had a length of about 1200 ft.

In the field application of GAGD there are several possible sources for acquiring the required CO_2. One option is to source the CO_2 from Denbury Resources Inc. (DBI) by tying into the existing North-South running NEJD CO_2 pipeline originating at their CO_2 source field Jackson Dome, located near Jackson, Mississippi (see Figure 2.5). Yet another option would be to use tanker trucks to transport the daily required CO_2 volumes to the field location using already established roads. However, in this study only the pipeline construction alternative will be further investigated as it is considered a more permanent addition to the already expanding CO_2 pipeline network.

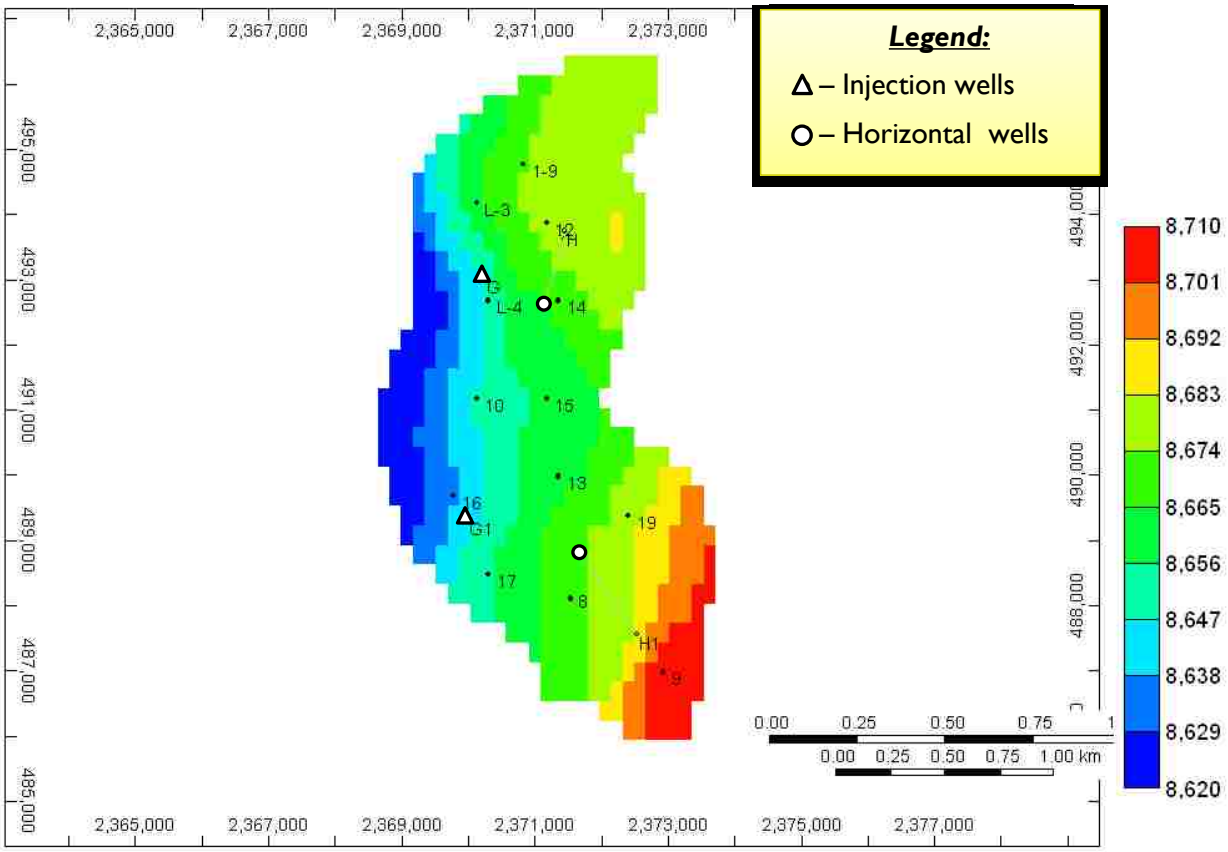

Figure 2.4: Planned GAGD Well Locations in the Buckhorn Field

2.2 Geological Description of the Buckhorn Field

A complete coring interval within the reservoir of the Buckhorn field has been interpreted by Omni Laboratories as sediments belonging to the Lower Tuscaloosa Formation. The lower Tuscaloosa sediments are part of the Tuscaloosa Group of east-central Louisiana and southwest Mississippi representing a complete depositional cycle (Spooner, 1964) and are of Upper Cretaceous age (Oudomugsorn, 1971). The transgressive, inundative, and regressive components within this depositional cycle are comprised of the lower, middle and upper units, respectively, of the Tuscaloosa Group. The area of interest as described in Spooner's article envelops the Buckhorn field and is highlighted in Figure 2.6. In general, the Lower Tuscaloosa unit is comprised of a sequence of beds that are in between the basal calcareous shales of the middle

Tuscaloosa and the sediments of Comanche age. It is typically composed of basal sand and conglomerate that is overlain by shale and lenticular sands. The principal historic geologic events during Tuscaloosa time that helped shape the area were the northern advance and the southern retreat of the Tuscaloosa sea which left a record in the geology column consisting of a northward thinning of the lower Tuscaloosa beds by onlap, a southward thickening of middle Tuscaloosa marine shale and a northward thickening of the upper Tuscaloosa regressive facies that eroded away part of the underlying middle Tuscaloosa unit.

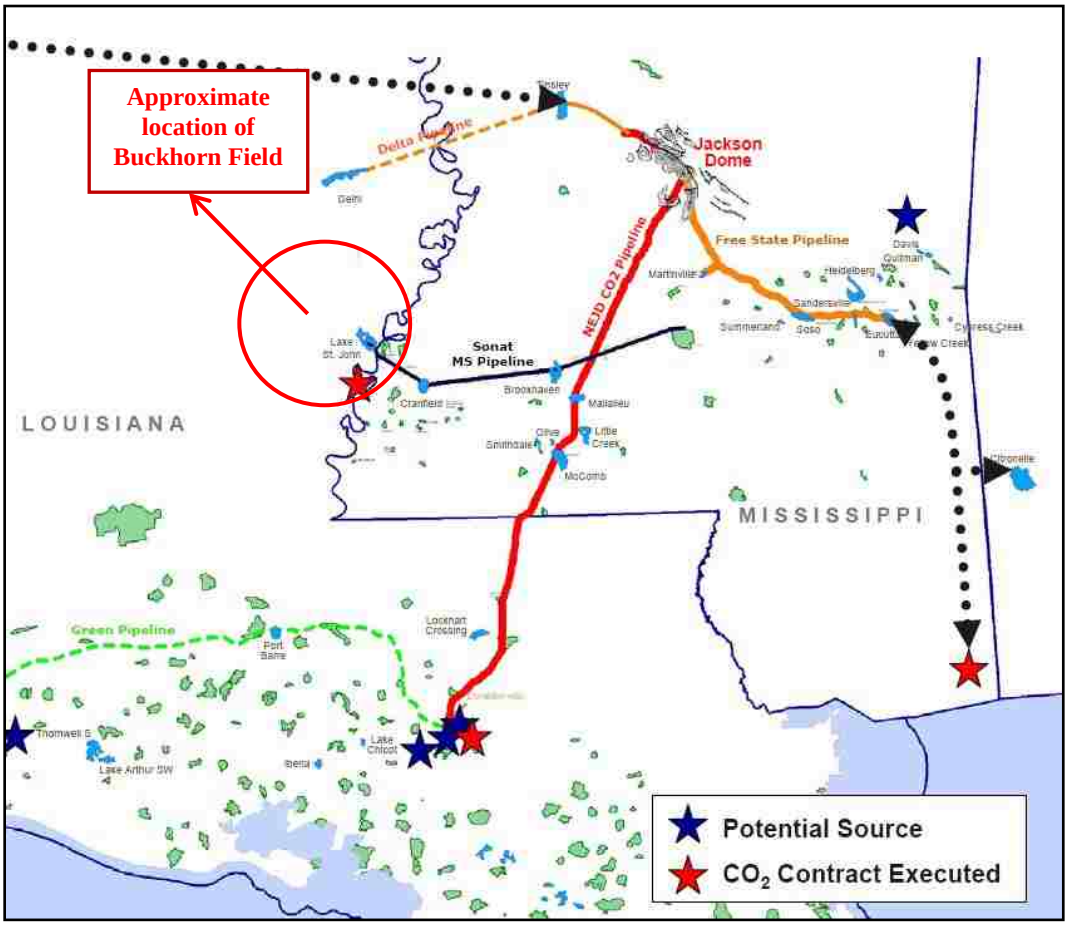

Figure 2.5: Location, Source and Origin of CO_2 to be used (Anonymous Online Presentation Downloaded on May 9, 2009 from: http://phx.corporate-ir.net/phoenix.zhtml?c=72374&p=irol-presentations)

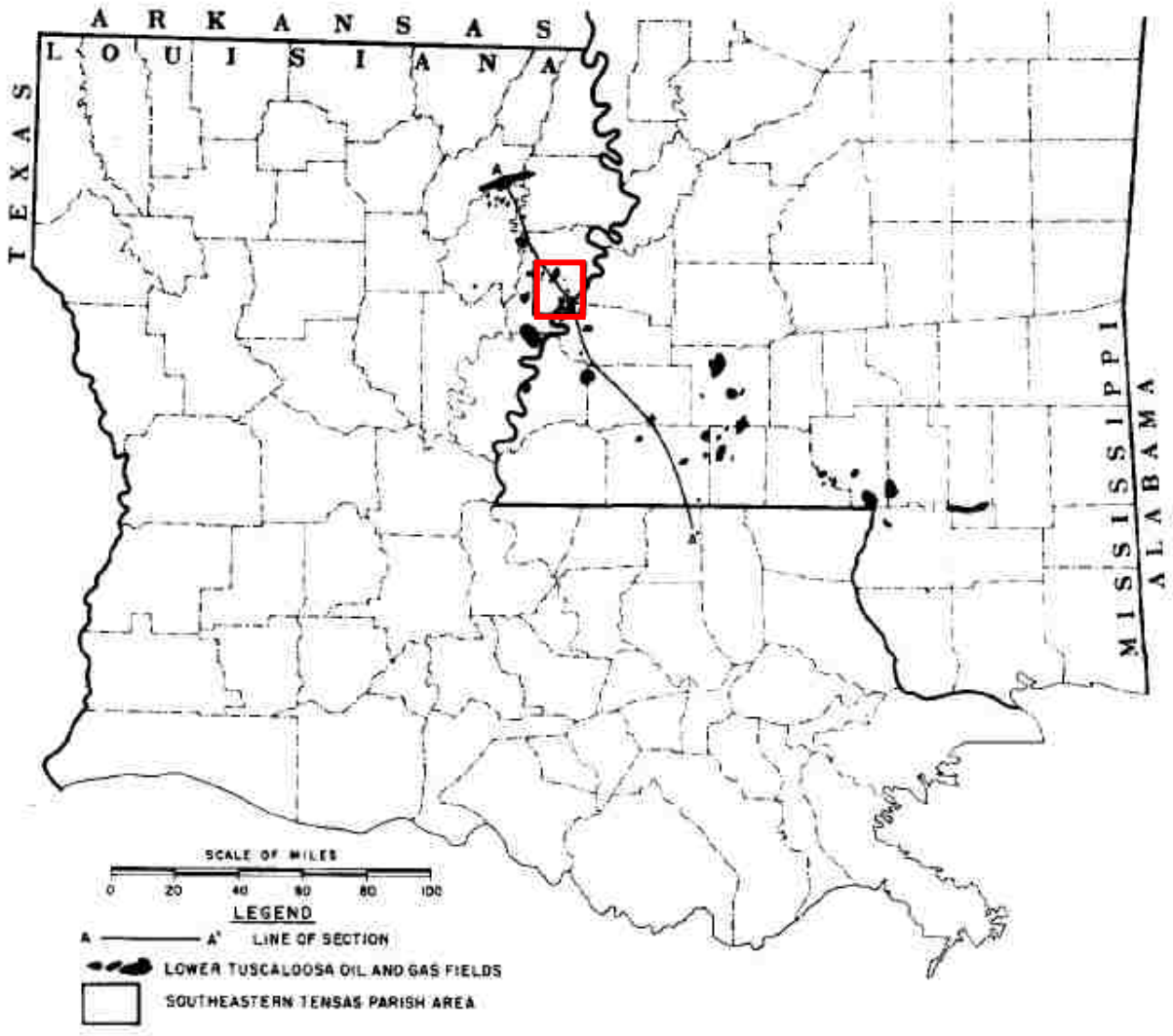

Figure 2.6: Index Map of Louisiana and Southern Mississippi Showing the Area of Interest (Tensas Parish) (After Spooner, 1964)

The stratigraphic column in the area of interest representing the Lower Tuscaloosa unit typically consists of 90 to 220 feet of shales (of varying color) and mudstones and fine-grained to conglomeritic, bentonitic sands. Of particular interest is that in those areas where the Lower Tuscaloosa exceeds 120 feet, a conglomeritic and usually porous and permeable sand occurs at the base and essentially forms a continuous reservoir. Most of the important fields in this area produce oil and gas from this sand and it is often termed Adams sand, Massive sand and

Buckhorn sand by various producers. Spooner (1964) defined the Buckhorn sand as the sand occurring below the upper 110 feet of the Lower Tuscaloosa and above the pre-Tuscaloosa unconformity. A typical sequence containing the Buckhorn sand is shown in Figure 2.7.

In his study, Spooner (1964) demonstrated that the Buckhorn sand is closely related to the pre-Tuscaloosa geomorphology, with sand deposition occurring mostly in the (stream) valleys that existed in the erosion surface of the pre-Tuscaloosa era. The thickness patterns visible in the buckhorn sand are indicative of the winding nature of the streams. Hydrocarbon traps are formed where the Buckhorn sand extends updip and is encased by the overlying Tuscaloosa shale. The Buckhorn field is an example of the salient or river bend type trap. This type of trap is usually formed by a broad river bend which changes directions sharply thereby forming upward projecting sand fingers with sand pinch out defining the trap on three sides (see Figure 2.8). Oudomugsorn (1971) supported this hypothesis by stating that from an investigation of the structural and isopach maps it could be deduced that the Buckhorn trap was formed as a result of a channel sand lying across a broad structural nose which has a very gentle slope towards the east/southeast of less than 120 feet per mile. The updip limit of the reservoir is where the sand pinches out against the edge of the channel while the eastern and southeastern boundaries are defined by either an oil-water contact or sand pinchout.

Finally, the latter author also posited that in all probability the hydrocarbons in the Buckhorn field were generated from source rocks that are part of the Washita-Fredericksburg and Tuscaloosa Groups, especially high organic content fine-grained sediments such as fossiliferous shales, mudstones, siltstones and limestone.

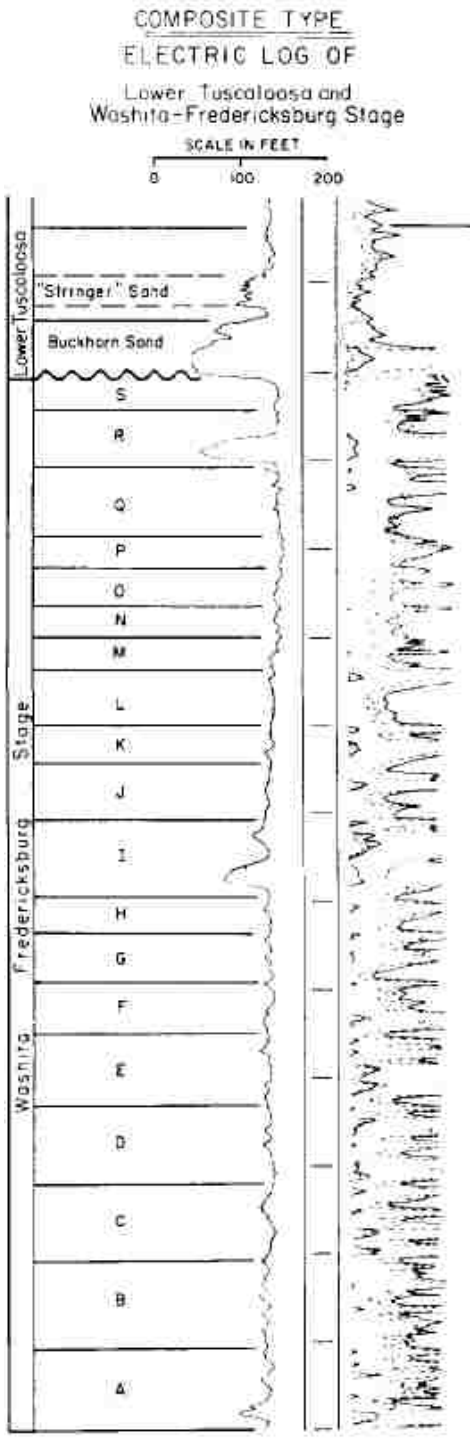

Figure 2.7: Composite Type Log of Lower Tuscaloosa Stage Depicting Buckhorn Sand Development (After Spooner, 1964)

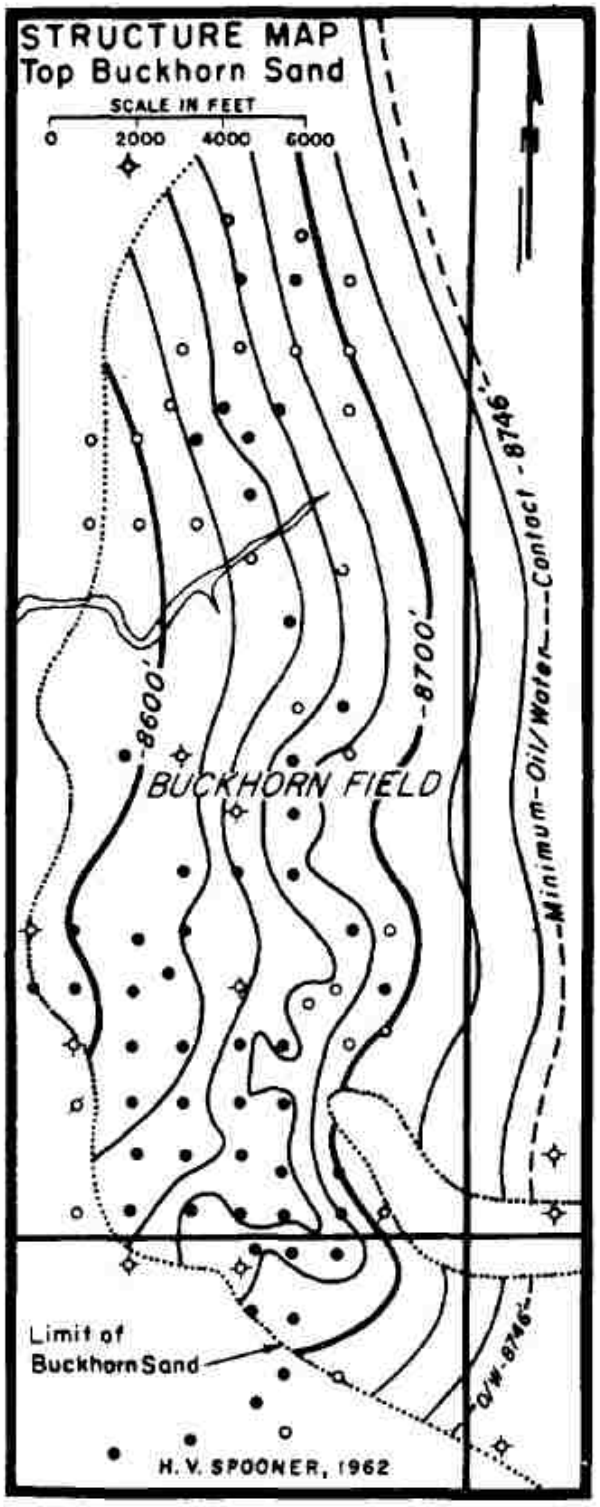

Figure 2.8: Buckhorn Sand Structure Map – Contours Indicate Depth in Feet below Sea-Level (After Spooner, 1964)

2.3 Literature Review on Current Status of Single-Well Gas EOR Processes for the Recovery of Light Oil

2.3.1 Introduction – Description of the Process

One of the many variations of gas injection as an enhanced oil recovery (EOR) process that has been applied in the field is the injection of gas continuously, a constant gas injection (CGI) flood, or in a cyclic manner, i.e. in a huff and puff mode. Either process has mostly been applied for the secondary and/or tertiary recovery in light oil reservoirs using the injection of CO_2, although the application in heavier oil reservoirs is not uncommon. The former is the most common way of conducting a gasflood while the huff 'n' puff process is a cyclic single well process that has been identified as the most likely applicable in reservoirs with limited areal extent or with a high degree of compartmentalization due to sealing faults. It has undergone a lot of research and most of what has resulted from said studies is applicable in general terms to continuous gas injection processes as well.

The huff 'n' puff process always consists of the following three stages (Miller and Hamilton-Smith, 1998):

1. The injection phase – gas (CO_2) is injected into the area near the wellbore.
2. The soak phase – the well is shut in for a pre-determined period of time to allow the injected gas to interact with the reservoir fluids (dissipation and/or dissolution) contained within the formation.
3. The production phase – the well is placed back on production.

In the soak phase the injected gas can possibly interact with the reservoir fluids as follows:

- It can act as a solvent thereby increasing the relative permeability to oil.

- It can imbibe into the rock matrix and release oil trapped due to capillary forces.
- It can reduce the relative permeability to water by acting as a blocking agent.
- It can add energy to the system to help drive fluids to the well.

In the case of the use of CO_2 as the injected gas some of the earliest proposed recovery mechanisms have been (Gondiken, 1987):

- Reduction of the oil viscosity due to the high solubility of CO_2 into oil, even at immiscible conditions.
- Swelling of the oil also caused by dissolution of CO_2 in it.
- The reduction of interfacial tension resulting in the enhanced ability of the oil to flow through the porous media that is the reservoir rock.
- The formation of carbonic acid when CO_2 reacts with hydrogen ions which in turn can react with the (carbonate) reservoir rock leading to a potential increase in reservoir permeability.

Subsequent history matches of field performance using numerical simulation have made it clear that the principal oil recovery mechanisms for the CO_2 huff 'n' puff process are oil swelling, oil viscosity reduction and gas relative permeability hysteresis (Denoyelle and Lemonnier, 1987). The gas relative permeability hysteresis (imbibition and drainage) results in gas and water blocking in the back production phase while the lower residual oil saturation to gas as compared to water results in an increase in oil recovery ($S_{org} < S_{orw}$).

The performance of a cyclic gas (CO_2) injection project is usually evaluated using the following parameters:

- Incremental oil recovery: the incremental oil recovery is usually calculated as the increment oil recovered over the baseline forecast production. The baseline production is often determined through regression analysis based on the production history prior to the huff 'n'

puff implementation. In case the forecast reached the economic limit a straight-line production profile was assumed with no further decline. The post-huff 'n' puff production is generally also fit using regression analysis.

- Gas utilization: it is defined as the volume of gas (CO_2) injected measured at standard conditions (unit: Mscf) divided by the estimated incremental oil (expressed per barrel incremental oil recovered). Another way of calculating the gas utilization factor is by relating the injected gas (CO_2) measured at reservoir conditions to a barrel of incremental oil recovered. The latter is referred to as the CO_2 reservoir utilization factor.
- Stimulation ratio: is defined as the average monthly oil production rate for the first month after the huff 'n' puff application divided by the average monthly production rate prior to the EOR process application.

2.3.2 Factors Affecting the Performance of Cyclic CO_2 Injection

Various researchers have investigated the important parameters affecting the performance of the huff 'n' puff process and in the process they have also come up with some notable production-response trends that are characteristic of this process.

Monger and Coma (1988) carried out a laboratory-scale evaluation of the CO_2 huff 'n' puff process for application in light oil reservoirs and identified the factors that affected the process performance in the laboratory. These results were then interrelated to field results to formulate a coherent, more complete, picture of which important factors affect a favorable field performance. The lab studies consisted of continuous and cyclic CO_2 coreflooding experiments using 32 °API stock-tank oil and watered-out Berea sandstone cores; a total of 32 experiments

were completed. The results from these experiments led to the identification and the assessment of the following performance affecting factors:

1. Mode of application: the experimental results using the watered-out Berea sandstone cores showed an average incremental oil recovery of 7 %ROIP over the waterflooding phase with an average total utilization factor of 5.81 Mscf/bbl. This indicated that the huff 'n' puff process was indeed effective at recovering residual oil after waterflooding. One of the parameters that were varied in the coreflooding experiments was the run pressure. The results suggested that conducting the process under immiscible conditions might be more favorable owing to the fact under those conditions a larger volume of CO_2 is injected. This results in oil production occurring earlier and more extensive (see Figure 2.9), and with an accompanied higher CO_2 retention.

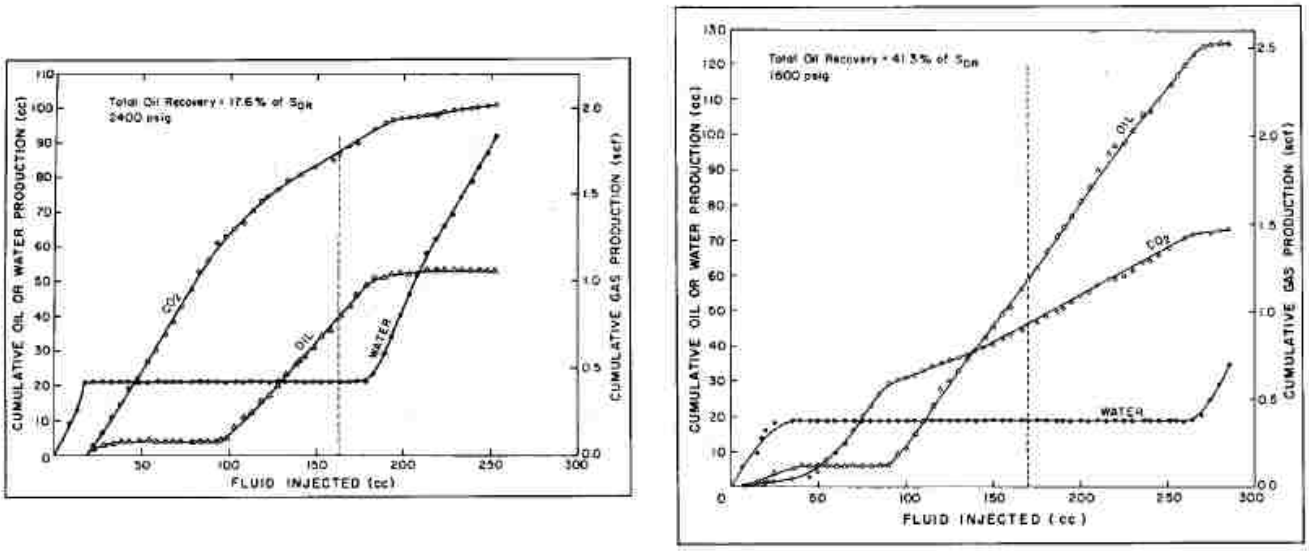

Figure 2.9: Production Profile of Cyclic CO_2 Flooding at 2400 psi (left) and 1600 psi (right) (After Monger and Coma, 1988)

2. Amount of CO_2 injected: another variable that was investigated was the CO_2 slug size and its effect on oil recovery. They found that there was a linear relationship between the amount of

CO_2 injected and the incremental oil recovery; both under immiscible as well as miscible conditions (see Figure 2.10). However, the total recovery efficiency was significantly less at miscible conditions (17.5 percent) as compared to that measured at immiscible conditions (41.3 percent) on both a slug-mass basis and a reservoir-slug volume basis. The implication of these results was that a disadvantage of the miscible application might be the accompanying reservoir contraction with pressure increase.

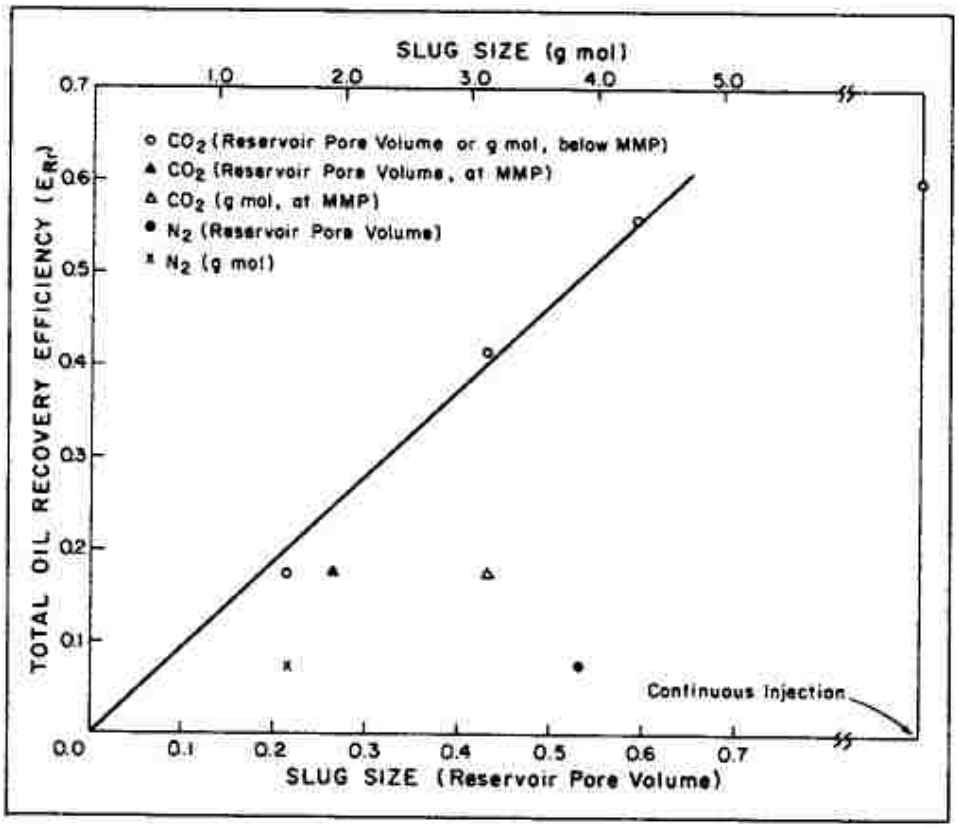

Figure 2.10: Relationship between Amount of CO_2 Injected and Total Recovery (Monger and Coma, 1988)

3. Soak period: the experimental results indicated that a soak period was necessary to obtain the maximum ultimate oil recovery.
4. Aquifer influx: the effect of aquifer influx was simulated through the introduction of additional water during the back production stage resulting in additional oil being recovered.

The most probable reason for this is the additional energy that an aquifer drive added to the oil production phase.

In the same study 14 field cases were also evaluated for the most pertinent factors affecting the huff 'n' puff field performance. In general, 6 to 16 MMscf of CO_2 was injected during the initial phase at a rate of several barrels per minute, followed by a shut-in period of 18 to 25 days after which the wells were placed on production. These field results are discussed in a dedicated paragraph to follow.

1. Pay zone thickness: in their evaluation of the field results a positive correlation was found between the stimulation ratio and the net pay or the perforation interval.
2. Reservoir oil viscosity: the stimulation ratio also improved slightly with a decrease in the reservoir oil viscosity making the case for the positive role played by viscous fingering of the injected gas in the huff 'n' puff process.
3. Reservoir pressure: a weak correlation was found that implied that as pressures neared the minimum miscibility pressure (MMP) this led to a slight impairment in both the utilization and stimulation factor. This phenomenon is supported by the occurrence that the displacement experiments performed at lower pressure performed better than those done at a higher run pressure. In a subsequent study Monger *et al.* (1991) conducted coreflooding experiments resulting in additional support for the hypothesis that a well-distributed initial gas saturation favorably affects huff 'n' puff performance. Figure 2.11 summarizes the aforementioned experiments in which a live oil composition was used with a bubblepoint pressure of 3300 psig. The results clearly indicate that the cyclic CO_2 recovery increased with decreasing run pressure.

Thomas *et al*. (1990) conducted laboratory and numerical experiments that indicated that the presence of a gas cap, gravity segregation and higher initial oil saturation favorably influenced the huff 'n' puff performance. Interestingly, their results highlighted the benefit of gravity override in the huff 'n' puff lab experiments: the lower density CO_2 migrated along the top of the core during the huff stage which resulted in the bypassing of oil with deeper penetration of the injected CO_2. The improved recovery was thought to be the result of a larger oil volume being contacted by the gas.

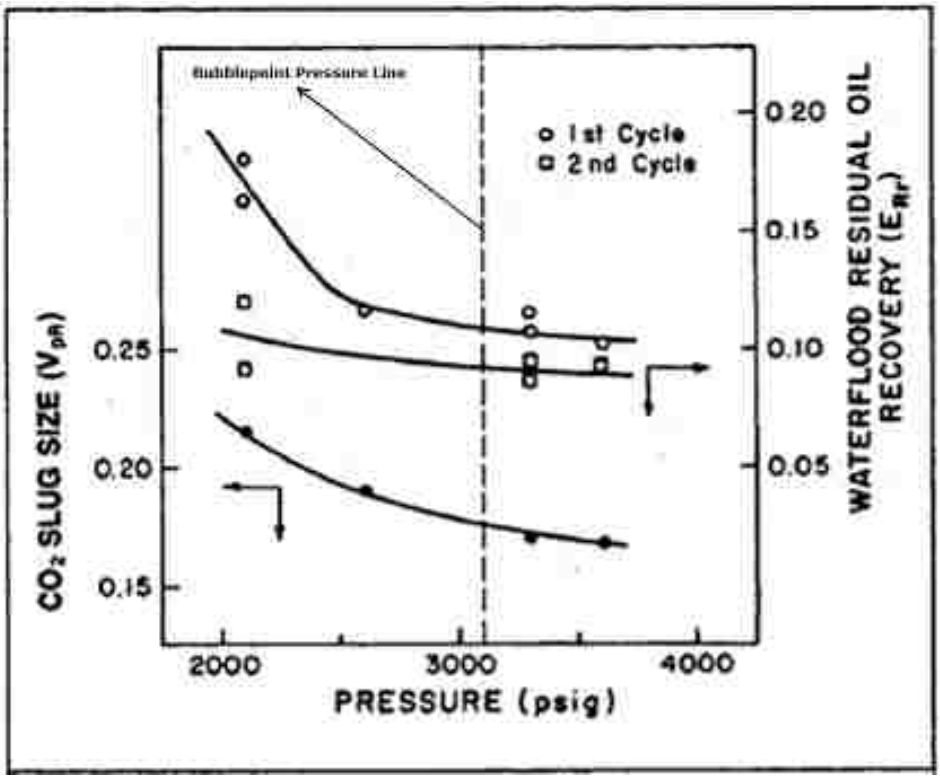

Figure 2.11: The Effect of Initial Gas Saturation on Huff 'n' Puff Performance (Monger *et al*., 1991)

The literature up to this point had been scarce as to instances of application of the huff 'n' process in low pressure or pressure-depleted reservoirs. This kind of application was highlighted by Monger *et al*. (1991) who combined laboratory coreflooding experiments with evaluations of

65 single-well field tests. In the experiments, watered-out cores were used at lower pressures to assess the immiscible recovery of light oil during the huff 'n' puff application. The results revealed that the application of huff 'n' puff at immiscible conditions was able to recover up to 18.0 percent of the waterflood residual oil with a utilization factor of 1.55 Mscf/bbl and a production profile that was very similar to those of experiments at higher pressures. According to their experiments, the lower-pressure results reveal two trends with pressure, namely that as pressure is lowered the retention of CO_2 increases and the gas utilization improves. The best first-cycle responses were adjusted for slug size and incorporated into Figure 2.12. It shows a smooth improvement in CO_2 utilization factor as the pressure was decreased and the process neared immiscible conditions, whereas the recovery efficiency improved as the process became more miscible.

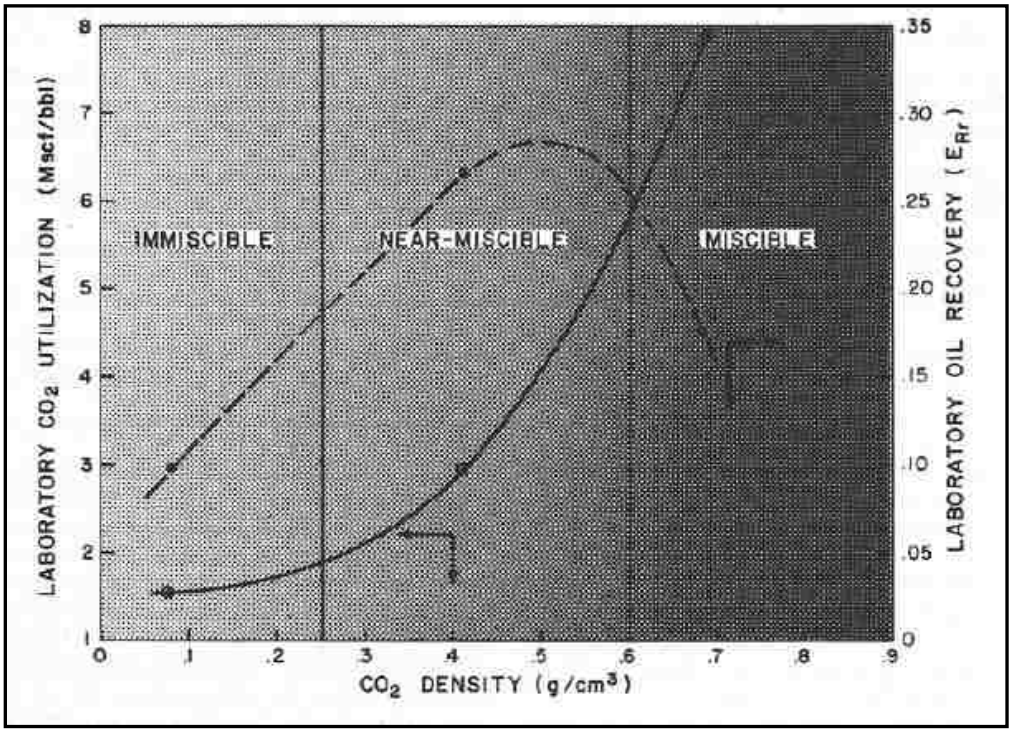

Figure 2.12: Correlation between CO_2 Utilization and Miscibility Inferred from Coreflooding Experiments (Monger *et al.*, 1991)

Based on 106 single-well CO_2 huff 'n' puff tests conducted in Louisiana and Kentucky in light oil (23 to 38°API) sandstone reservoirs of which 97 indicated incremental oil, Thomas & Monger-McClure (1991) presented field performance trends and developed correlations between huff 'n' puff performance and operational variables. Using the field response in terms of incremental oil, CO_2 utilization and stimulation ratio the following correlations were extracted:

1. Slug size: it was found that the mass of injected CO_2 was the best predictor of the stimulated oil production rate and the ultimate incremental recovery. They revealed a strong correlation between the mass of CO_2 injected and the production response as far as the incremental oil, and the observed post-injection rise in the production rate. It was concluded that the correlation could be used as a first-approximation predictive tool, assuming that the injected CO_2 contacts the oil within the targeted radius of treatment. A positive relationship between the stimulation ratio and the incremental oil produced was also revealed. These production response trends are depicted in Figures 2.13 to 2.15.
2. Target treatment radius: the evaluation of the field tests revealed that the field response did improve with the thickness of the payzone as more oil was contacted near the wellbore. This is also where the process efficacy is highest, although a project-wide positive relationship that was sufficiently strong could not be determined. Any inferences as far as target treatment radius were thus limited and the results suggested that it was dependent on reservoir conditions. A calculation assuming uniform displacement, a CO_2-saturation of 50 percent in the displacement zone and no mixing with the reservoir fluids in place resulted in an average estimated radius of CO_2 treatment of 73 ft applicable to the 30 successful field tests.

3. Soak period: based on their field test database, an optimal soak period of 1 month was suggested as soaks of this duration generated as much incremental oil per foot of exposed interval as projects with longer soak periods taking into account CO_2 losses during the soak.

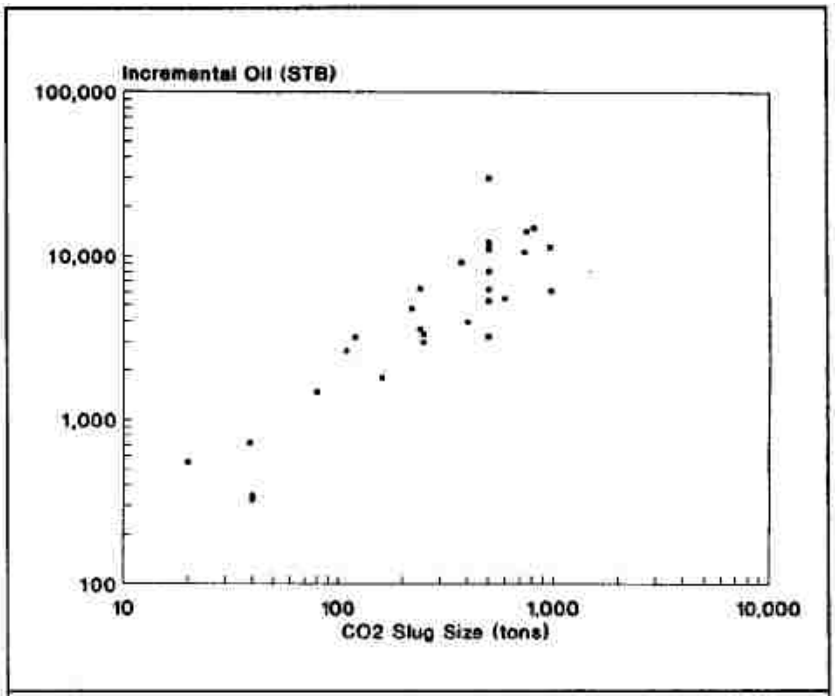

Figure 2.13: Correlation between Injected Mass of CO_2 and Incremental Oil (Thomas & McClure, 1991)

2.3.3 Operational Guidelines and Screening Criteria

Palmer *et al.* (1986) detailed the implementation of 11 CO_2 huff 'n' puff projects in 5 South Louisiana fields and came up with the following screening criteria based on these initial tests:

- High oil saturation near the wellbore.
- Reservoir pressure that was close to the minimum miscibility pressure.
- Thick payzone.
- Low reservoir permeability.

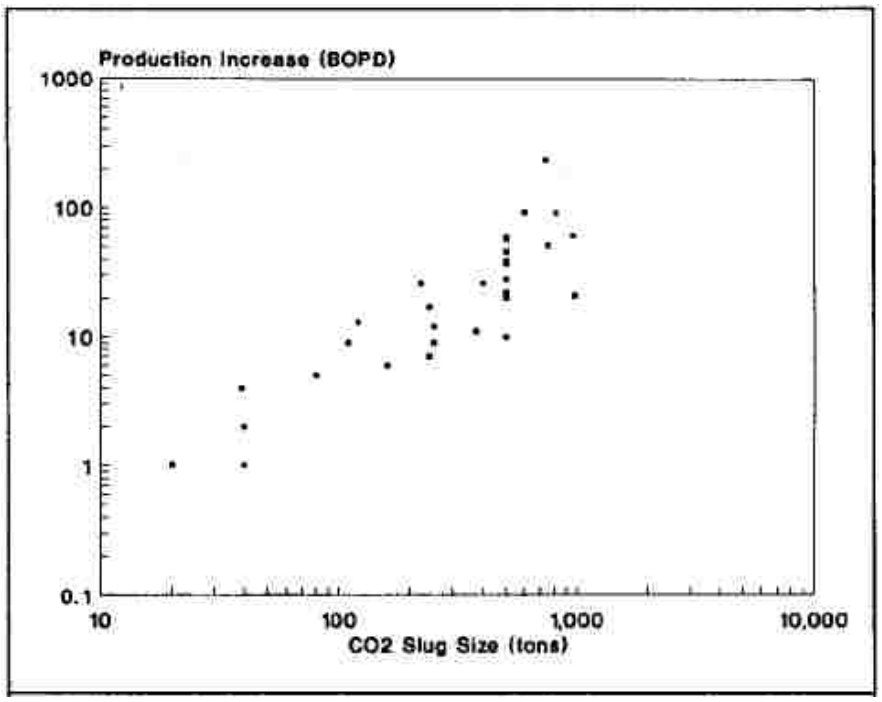

Figure 2.14: The Effect of Injected Mass of CO_2 on Stimulation Ratio (Thomas & McClure, 1991)

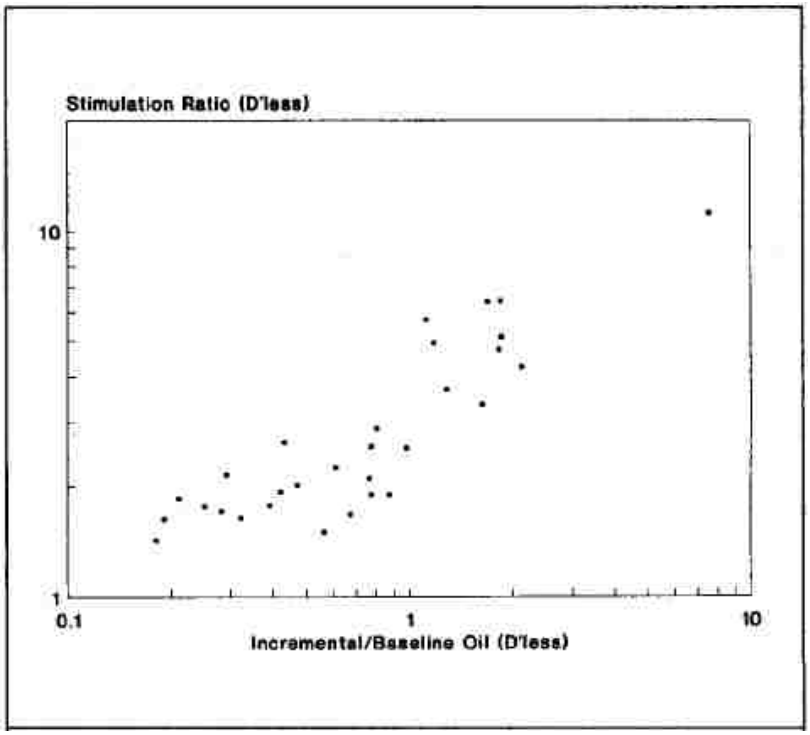

Figure 2.15: Relationship between Stimulation Ratio and Incremental Oil due to CO_2 Huff 'n' Puff (Thomas & McClure, 1991)

- Deep reservoirs.
- Reservoir temperature range: 185 to 240 °F.
- Oil viscosity range: 0.4 to 0.7 cp.
- Range of gas-oil ratios: 14 to 500 ft^3/bbl.

Most of the above screening criteria were supported by Thomas & Monger-McClure's (1991) evaluation of 106 CO_2 huff 'n' puff field tests in light oil reservoirs, but in contrast, they concluded that even though diverse types of reservoirs appear to be amenable to CO_2 huff 'n' puff, shallow reservoirs might be more likely to be economic, and that operating below the minimum miscibility pressure might be preferred.

Table 2.1: CO_2 Huff 'n' Puff Screening Criteria (Mohammed-Singh *et al.*, 2006)

Reservoir Parameter	Light Oil Reservoir	Medium Oil Reservoir	Heavy Oil Reservoir
Oil viscosity (cp)	0.4 – 8	32 – 46	415 – 3000
Oil gravity (°API)	23 – 38	17 – 23	11 – 14
Porosity (%)	13 – 32	25 – 32	12 – 32
Depth (ft)	1200 – 12870	2600 – 4200	1150 – 4125
Thickness (ft)	6 – 60	36 – 220	200
Permeability (mD)	10 – 3000	150 – 388	250 – 350

Mohammed-Singh *et al.* (2006) have formulated screening criteria for successful CO_2 huff 'n' puff operations based on design and production data from 16 huff 'n' puff projects implemented in the Forest Reserve oilfield, a medium heavy oil reservoir, over the past 20 years. Their screening criteria are tabulated in Table 2.1 and they have also proposed the following screening methodology:

1. Define project objectives.

2. Identify any site- or time-related advantages or disadvantages, such as favorably located gas sources or anticipated high capital investment, respectively, and near-well reservoir characteristics.
3. Develop a matrix of appropriate design and/or operating strategies for the specified objectives.
4. Optimize the objectives.
5. Explore feasible alternative improvements, such as the application of foam.
6. Develop project-specific screening criteria within the context above.

2.3.4 Worldwide Application of Huff 'n' Puff EOR

As mentioned before the huff 'n' puff process for the enhanced recovery of light oil has been applied in various reservoirs in various variations:

1. Classic CO_2 huff 'n' puff: Some reported examples on the application of the classic huff 'n' puff process have been:
    a. Monger & Coma (1988) evaluated 14 field tests in South Louisiana oil-bearing sands of which 9 were considered successful based on an average gas utilization factor of 1.54 Mscf/bbl and average reported incremental oil recovery of 8600 bbl. No operational issues were mentioned apart from "mechanical failures". 65 single-well cyclic CO_2 field tests were reported on by Monger *et al.* (1991) that were conducted in a pressure-depleted field in the Appalachian basin in eastern Kentucky (fractured dolomitic sandstone). On average, the field tests recovered 2300 bbl with an average utilization factor of 2.03 Mscf/bbl (based on the 12 most successful tests); again, no operational issues were reported on. All of the aforementioned field tests were

included in a later, more extensive, study by Thomas & Monger-McClure (1991) in which 106 single-well huff 'n' puff field tests were analyzed. The projects were implemented in 14 fields located in Louisiana and Kentucky and 97 of the tests showed incremental oil recovery. The tests were all performed in light oil-bearing (23 – 38 °API) sandstone formations (consolidated, unconsolidated and/or dolomitic. It was mentioned in their report that several operators improved oil production by opening wells on a small choke thereby increasing backpressure on the wells, while in one field project CO_2 breakthrough during the soak period was observed. It was speculated that it had traveled through fractures to the offset producer. Management of offset wells was therefore recommended whenever migration of the injected gas beyond the targeted treatment radius might be an issue in highly fractured reservoirs.

b. Twenty-eight huff 'n' puff projects in Texas were presented and discussed by Haskin & Alston (1989); the tests were performed in Gulf Coast Miocene reservoirs in east and south Texas that contained light oil (23 – 30 °API). The reported average incremental oil recovered was 1350 bbl with an average CO_2 utilization factor of 3.58 Mscf/bbl. No specific operational issues were reported.

c. Mohammed-Singh *et al.* (2006) summarized 20 years of design and performance data on sixteen CO_2 huff 'n' puff projects in the Forest Reserve field, Trinidad & Tobago. The oilfield in question contains multiple, stacked, complex deltaic sandstone reservoirs which are solution gas driven with some aquifer influx; the oil contained in these reservoirs was qualified as a medium oil (14 – 25 °API). The average recovery ranged from 1400 to 18000 bbl while the average CO_2 utilization was between 5 – 139 Mscf/bbl. It was reported that many wells that were gravel packed showed

increased sand production while the wells showing the best response to injection were in down-dip locations and may have benefited from aquifer influx and gravity drainage during the puff phase. “Mechanical difficulties” were experienced in 5 wells.

   d. The latter reference also contained an extensive overview of worldwide CO_2 huff ‘n’ puff field trials (see Table 2.2 on page 33).

2. Huff ‘n’ puff using a gas mixture: Miller & Hamilton-Smith (1998) summarized the successful application of cyclic gas recovery using a gas mixture (exhaust gas, i.e. N_2/CO_2 mixture) in the Big Sinking field of eastern Kentucky. The exhaust gas increased the production six times over the initial production rate with an average utilization factor calculated over 2 years of 0.85 Mscf/bbl. Within days of injection the gas had channeled to offset wells through a natural fracture trend requiring those wells to be shut in. The exhaust gas was generated using propane and at the time the cost per incremental barrel was calculated to be $2.35/bbl with an estimated investment payback period of 10 months.
3. Hydrocarbon gas huff ‘n’ puff:
   a. The previous reference also contained a summary on the use of rich gas (casing head gas) in the cyclic gas recovery of oil. The projected recovery was reported as 3.3 Mscf/bbl over a 3-year period. The casing head gas was gathered from other wells in the field in conjunction with a compressor driven an electric motor run with casing head gas. The calculated cost per incremental barrel was $1.65/bbl and an estimated payback period of 5 months.
   b. De Lino (1994) presented an extended evaluation of natural gas huff ‘n’ puff tests in the Miranga field, Bahia, Brazil. Three of the six wells involved displayed excellent

results with an average incremental oil recovery of 3000 barrels with a gas utilization factor of 0.5 – 4.6 MCF/bbl. No operational difficulties were reported, but local availability of natural gas and moderate to high injection pressures were proposed.

2.4. Literature Review on Current Status of Smart Well Technology

2.4.1 Introduction

Gao and Rajeswaran (2007) called smart well technology one of the most significant breakthroughs in production technology in recent times. Smart wells allow the operator to actively monitor, remotely choke or shut poorly performing selected zones thereby optimizing the oil production, without the need for physical intervention. Since the first application of smart well technology in August 1997 at Saga's Snorre Tension Leg Platform in the North Sea close to 600 smart wells had been drilled and/or completed by 2008 (MacPhail & Konopczynzki, 2008). The application of smart well technology has evolved over the years; not only has there been a significant increase in usage but the areas in which they have been used are also changing. Two important factors in these trends are the demonstrable and significant improvement in reliability of the smart well equipment, a result of reliability-driven engineering from the manufacturers' side, and the increase in the number of capabilities offered at an almost constant price level as a result of innovation by the well suppliers. During the first 7 years, the primary area of application was offshore (North Sea) with only 8 percent of the total number of smart wells being located on land. In the offshore environment, the significant additional investment needed for smart well technology application could more easily be justified against the already substantial cost of conventional offshore wells by emphasizing the benefits of avoiding costly interventions to modify the completion.

Table 2.2: Summary of Worldwide CO_2 Huff 'n' Puff Field Trials (Mohammed-Singh, 2006)

SPE paper	27677	15502	15502	15502	15502	15502	15502	15502	15502	15502	15502	15502
Field	Big Sink'g	Magnet	Picket Ridge	Field C	Field D	Withers N.	Field F	Thompson	Field I	Field J	Field K	W Col.
Basin	Appalachian	Withers									Manavel	
Province	Kentucky	Texas	Texas	Texas	Texas	Texas	Texas	Texas	Texas	Texas	Texas	Texas
Country	USA	USA	USA	USA	USA	USA	USA	USA	USA	USA	USA	USA
Formation		Magnet W	Picket Ridge					Frio			Olig	S Andres
Depth (ft)	1300	5500	4570	4900	4650	5250	5250	5200	7796	4100	5000	2600
Thickness (ft)	60	21	7	12	9	8	8	25	15	15	?	?
Porosity (%)	13	23	30	31.8	31	25	25	27	?	30	30	30
Permeability (mD)	19	1700	1200	534	350	450	400	500	15	500	1000	560
Sw Current (%)	50											
Pressure initial (psi)	400											
BHP (psi) current	150	1310	930	1430	1350	860	1030	1540	1200	750	900	500
Temperature (°F)	68	154	138	155	150	150	150	153	175	149	149	116
Oil gravity (° API)	36	26	25	24.4	23	25.7	25.7	25.2	37	25	26	30
Oil viscosity (cp)		2.3	2.5	4.6	3.2	2.5	2.9	2.7	1.6	4.4	4.2	8
Transmissibility(mDft/cp)		15522	3360	1393	984	1440	1103	4630	141	1705		
Produced WOR	90%	9-24	12-16	24-106	72	12-100	6.1	1.75	0.3	0	15-99	45536
Pre-CO_2 oil rate (bbl/d)		16-86	23-27	3-41	12	12-60	54	12	21	56	9-85	12-30
% Primary Recovery												
So (start of cyclic CO2)		73	80	68	69	80	75	73	?	85	?	?
Type of reservoir	WD											
# of wells / # treatment	240/290											
CO2 Util'n (Mcf/bbl)	1.1	1.1	8.2			2.8	10.2				2.4	10.2
Project Success	Success											
Incremental oil (STB)	180000	3697	122	0	0	1766	490	3	0	0	1656	391
CO^2 injected (MMSCF)	210	4	1	8	5	5	5	4	4	4	4	4
Days of soak	10	12	7	25	20	17	17	36	23	23	21	13
Note: WF = water flood, DD= depletion drive, swd= strong water drive, wwd= weak water drive; LA & KY = Louisiana and Kentucky												

SPE paper	18977	20208	20208	20208	20208	20208	20208	20208	20208	20208	20208	16720
Field	Paradis	West Cote	b	c	d	e	f	g	h	I	k	Timbalier
Basin		Blanche Bay		Lake Barre					Bayou Sale	Lafitte		
Province	Louisiana	Louisiana	LA & Ky	Louisiana	LA & Ky	LA & Ky	LA & Ky	LA & Ky	Louisiana	Louisiana	LA & Ky	Louisiana
Country	USA	USA	USA	USA	USA	USA	USA	USA	USA	USA	USA	USA
Formation	Main py	Minnelusa	Sand	Up M	Sand	Sand	Sand	Sand	St. Marry	Sand	Sand	
Depth (ft)	10200	8140	10330	12870	4909	1200-3000	6248	1300	10060	8900	9837	4878
Thickness (ft)		21	48	20-50	12-17	6-24	7-35	34-58	30	na	15-34	
Porosity (%)	26	29	26	25	32	32	32	13-16	31	27	24	32
Permeability (mD)	1033	322	1033	139	2500	3000	300-500	10	500	250	252	500-2500
Sw Current (%)												25
Pressure initial (psi)												2390
BHP (psi) current		3847	2406	2500	2235	560-1400	2900	100	1795	3947	5100	2235
Temperature (°F)		165	212	240	138	80-100	166	68	206	185	192	138
Oil gravity (° API)	36	23-38	23-38	33	23-38	23-38	23-38	23-38	23-38	34	23-38	26
Oil viscosity (cp)	0.5	1.3		0.4						0.7		
Transmissibility(mDft/cp)		5202										
Produced WOR		9	15.6	1	71	8.3		5:5	0.37	0.43		99%
Pre-CO_2 oil rate (bbl/d)	23	19	25-31	47	13-18	9-53		1-70	54	72		15
% Primary Recovery												18
So (start of cyclic CO2)												34-60
Type of reservoir	tertiary	WF	WF	DD	SWD	SWD	SWD	DD	WWD	SWD	DD	b/water
# of wells / # treatment	11	1	2	3	4	9	2	66	1	1	3	2
CO2 Util'n (Mcf/bbl)	1.9	2.7	1.5-2.7	0.3	0.9-1.9	0.72-2.68		0.6-2.1	0.7	0.71		1.1-3.2
Project Success	Success											Success
Incremental oil (STB)	27000	3233	6148-11410	29830	5516-14863	2612-11051		321-6326	12115	9118		14000
CO^2 injected (MMSCF)	16											23
Days of soak	21	31	19-21	25-33	26-161	28-63	20-23	Jul-36	47	17	16-54	4-7 weeks
Note: WF = water flood, DD= depletion drive, swd= strong water drive, wwd= weak water drive; LA & KY = Louisiana and Kentucky												

The number of land-based smart wells has increased in recent years to 52 percent of the total number of smart wells in use primarily due to the large-scale adoption of intelligent well technology by Saudi Aramco for their Maximum Reservoir Contact (MRC) wells (Abdulaziz *et al.*, 2008). Figure 2.17 depicts the evolving trends as far as location and application area for smart wells over the period 1997 to 2008.

Apart from the previously mentioned capabilities of a smart well system it is also capable of collecting, transmitting and analyzing completion, production and reservoir data. In order to do this it requires such common elements as flow control devices, feed-through isolation packers, control, communication and power cables, down-hole sensors, and surface data acquisition and control. Even though hydraulic motive power systems are dominant, a variety of electric and hybrid electro completions have also been implemented.

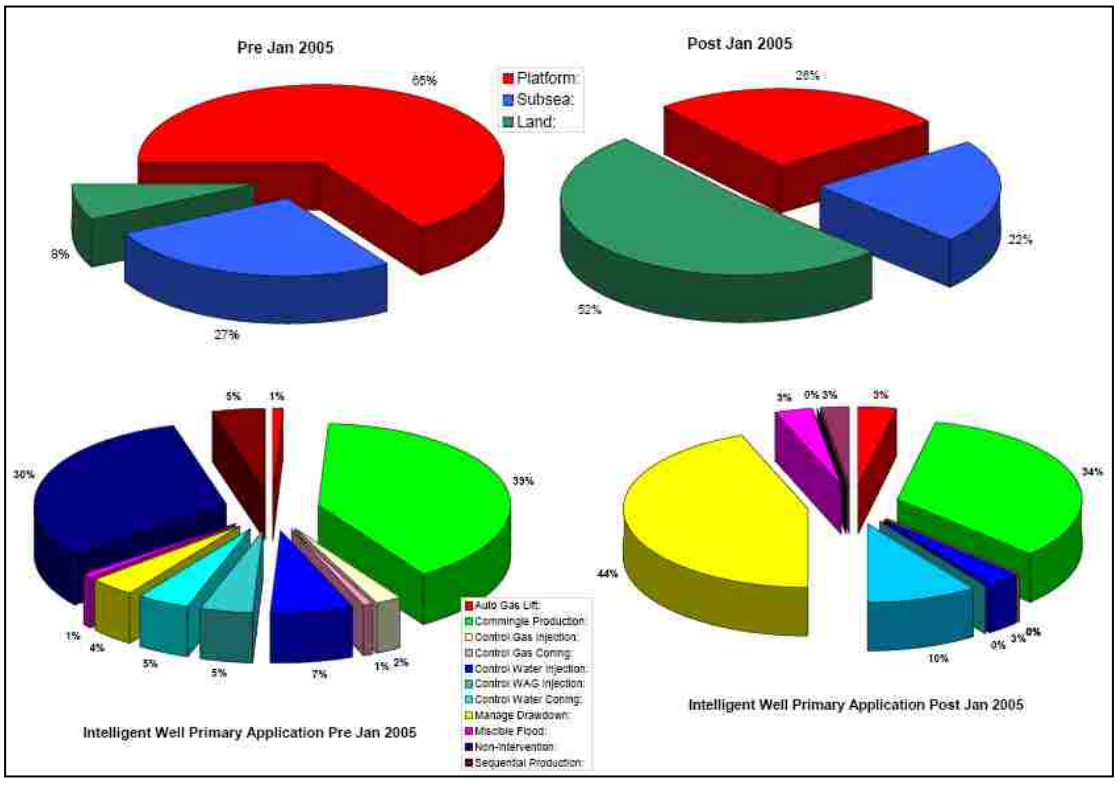

Figure 2.16: Location and Application Distribution of Smart Wells over the Years (MacPhail & Konopczynzki, 2008)

2.4.2 Reservoir Management Opportunities using Smart Well Technology

Part and parcel of stimulating the uptake of any new technology by the oil industry is convincing parties involved of the added benefit or value of said technology. In the case of smart well technology, the value added can include the following (Glandt, 2005):

1. Quantifiable value:
    a. Reduction in number of wells needed to drain a reservoir.
    b. Reduction in well intervention costs.
    c. Flexibility in well operation, i.e. the ability to respond almost immediately to changes, both expected as well as unexpected, in the production/injection performance.
    d. Increased ultimate recovery due to improved well management.
2. Qualitative value:
    a. Data acquisition in the early phases of production enhances the probability of success of subsequent infill wells.
    b. Identification of the important key parameters for optimization of reservoir management decisions.
    c. Provide the means to mitigate any unexpected downside from new developments.
    d. Health, safety and environmental advantages due to unmanned operations.
    e. Smaller environmental footprint as a result of the decrease in the number of wells needed.
    f. Being able to use abandoned wells to acquire relevant data.

Some of the many opportunities for smart well technology enhanced reservoir management were listed by Glandt (2005) as:

1. Optimal sequential production: in an intelligent well that intercepts multiple oil zones a remotely operated valve would be able to open perforations to the most productive zone at any time to access otherwise deferred oil without sacrificing reserves. This is compared to the typical bottoms-up sequence of production in which only one zone is produced at a time followed by plugging it up when the economic limit is reached after which the next zone up is perforated.
2. Commingled production from a stacked reservoir: in the case when the installed tubing does not pose any inflow restrictions controlled smart commingling provides an intervention-less means of optimizing the net oil at surface by controlling the inflow from the various zones based on the range of rates and water cuts.
3. Fluid transfer between formations for sweep/pressurization: smart completions have a definite place in dumpflooding operations in which fluid from an over- or underlying interval is transferred to the productive interval in a controlled manner to maintain pressure or serve as a driving agent (Figure 2.18).
4. Production from oil rims: if a horizontal is completed in an oil rim it would be very sensitive to early water/gas breakthrough whereas with smart completions any breakthrough at one location along the wellbore can be shut in and the offtake moved to another location thereby giving the coned water/gas the opportunity to recede back. When draining across multiple compartments the zonal control becomes even more valuable with increasing heterogeneous character across compartments.
5. Drive recovery processes: subsea wells in drive processes are very suitable for remote flow control at injection and/or production wells when optimizing sweep efficiency because of the high intervention costs.

6. Flow profiling: in- and outflow information along wells is important to the ensuing stimulation and also plays an important role in understanding unswept or undrained oil. Nowadays, Distributed Temperature Sensing (DTS) is a fiber-optic based technology that can provide a temperature profile along the well that can be translated into a flow profile.

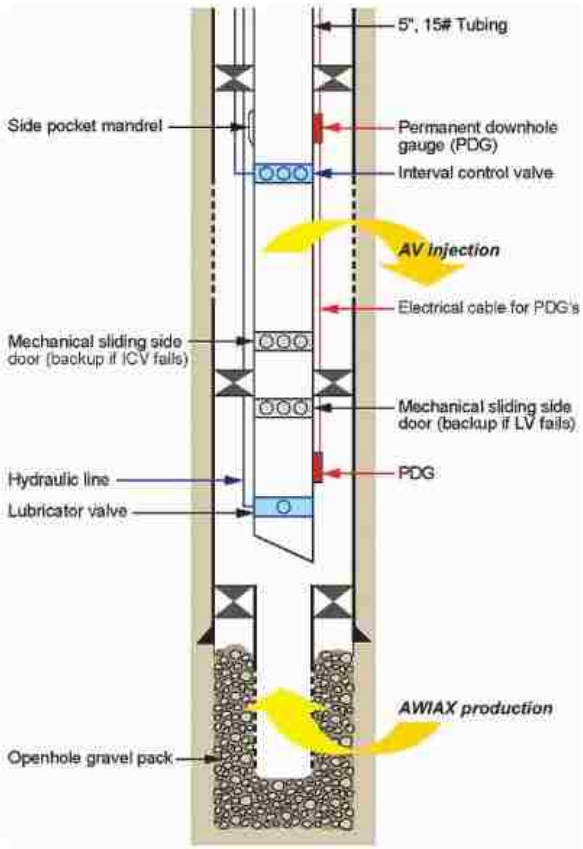

Figure 2.17: Well Schematic of Internal Gas Injection well (after Lau *et al.*, 2001)

7. Intelligent multilaterals: the use of inflow control to optimize production becomes even more compelling in multilaterals that are very effective in reducing the well costs (cost per unit length of contacted rock) and using the available platform space optimally. The ability to control the inflow from each leg solves the problems that can result from unexpected production behavior in any of the legs that may compromise the total production.

8. Waterflooding: flow control along horizontal wells and the ability to modify injection and production profiles in order to affect the sweep efficiency is currently still very new.
9. Swing gas producers: used in the North Sea to meet a heightened gas demand in colder seasons.
10. Connector wells: smart wells can play an important role in addition of reserves through downhole linkage oil accumulations that are inaccessible from current platforms to another one that is, thus preventing the need for expensive additional tiebacks.
11. Downhole production testing: long-term production testing of a reservoir can be done with downhole flow meters and pressure sensors using a depleted reservoir as a sink.
12. Smart abandonment: by equipping abandoned wells with sensors allows reservoir monitoring without disturbing production or adding extra complexity to the producing wells.
13. In-situ gas lift: smart oil wells that intercept gas zones could use wireline-operated gas lift mandrels or surface-controlled electric valves to provide controlled access to the gas for lifting purposes.
14. Downhole reservoir imaging.

2.4.3 Comparison of Smart Wells to Conventional Wells

Even though it may be evident that the application of smart well technology might be quite beneficial, it still remains necessary to be able to quantify the expected gain (in terms of the effect on the net present value, NPV, of the project) as a function of parameters such as operational controls, geologic uncertainties and economic parameters. Schiozer & Silva (2009) came up with a methodology to do just that; in order to compare the performance of conventional

and smart wells, they devised a methodology of production strategy optimization while considering the availability of various production capacities among other variables.

The methodology consisted of two parts, the first of which was focused on production strategy optimization, while the second part dealt with geological and economic uncertainties. The main steps of the methodology were:

a) Definition of the basic economic model;
b) Selection of production capacities;
c) Development of an optimization methodology for production strategy;
d) Optimization of available strategies using the following steps:
    - Choose an initial platform capacity;
    - Define an initial strategy to be optimized;
    - Test with a schedule for the wells' perforations;
    - Optimize the maximum water cut;
    - Optimize the number and location of wells;
    - Reschedule the wells' perforations if needed;
    - Re-optimize the water cut;
    - Return to the first step and restart the optimization process with another available platform until all platform options have been optimized.
e) Combination of the strategies including cross-validation;
f) Comparison of the optimized strategies and selection of the best alternative for each well/platform capacity;
g) Comparison of the optimized strategies but now with inclusion of geological or economic uncertainties.

Some of the important premises in their study were:

- Fixed parameters are time interval between valve opening, maximum producer flow, and minimum bottom-hole pressure (BHP) of the injectors.
- The main objective function is the NPV.
- The optimization is based on reactive control of the valves as opposed to pro-active.
- No possibility of valve failure.

Their study revealed that the same number and location of wells were obtained for all platform capacities with the smart wells showing slightly superior performance. With increasing platform capacity, the increase in oil production when using smart wells becomes less pronounced because as the liquid flow rate limitation increases the penalty of producing water decreases, i.e. the conventional wells produce more oil because they are allowed to produce more water. However, the water production in all cases is lower when smart wells are deployed. They concluded that the influence of the platform capacity (or production restrictions) on the production is larger than the type of well used.

When they included geological uncertainty in their comparison, it was found that as water production increased as a result of higher reservoir heterogeneity the efficiency of smart wells increased/became more effective. Again, the water production was much lower when smart wells were used compared to conventional wells. Incorporation of economic uncertainty into the models did not reveal any clear case for the use of smart wells but did highlight the need for a detailed economic evaluation on a case by case basis. An NPV risk curve (graph of frequency versus NPV) did, however, reveal that the highest benefits of implementing smart well technology were observed for those cases with higher heterogeneities, high uncertainty, optimistic economic outlook models and lower production capacities.

3. EXPERIMENTAL APPARATUS AND PROCEDURES

3.1 Framing of the Laboratory GAGD Experiments

The development of the GAGD process at LSU was funded by the US Department of Energy and consisted of several, at times, concurrent stages:

1. Partially scaled physical/visual model experiments:

   These visual experiments were aimed at demonstrating the potential merits of the GAGD process and to identify suitable operational parameters for further investigation by matching the range of selected dimensionless numbers as those that were observed to be important in similar gas flooding field projects, namely the capillary, Bond and gravity number. To this end, partially-scaled physical models were used that enabled the recording of the frontal advancement of the injected fluid throughout the porous medium. This was accomplished by incorporating translucent panels into at least two sides of the physical model to allow an unobstructed view of the GAGD displacement process. The visual model experiments were also used to examine the effect of injected fluid miscibility, wettability of the porous medium and the presence of heterogeneities (fractures) on the GAGD recovery. Various gas/oil systems were used as proxies to any actual injectant/reservoir oil systems, such as nitrogen/CO_2 as the injectant and n-decane/soltrol as the reservoir oil phase, while glass beads and/or silica sand were used as the porous medium in these experiments. The visual model experimental results revealed a log-linear relationship between the GAGD recovery and all three dimensionless numbers which, in the case of the gravity number, persisted even with inclusion of actual field data in the visual model experimental data (Sharma & Rao, 2008). It was also shown that miscible GAGD implementation could lead to a near-perfect sweep of the model whereas the presence of fractures seemed to enhance, rather than impede,

GAGD recovery: the fractures actually served as flow conduits to the producer (Paidin & Rao, 2007; Mahmoud & Rao, 2008). Also, the application of the GAGD process in an oil-wet porous medium led to slightly better recovery results compared to its application in a similar, albeit water-wet porous medium. An oil-wet porous medium was produced by chemically altering the initial water-wet state of borosilicate glass beads by treating them with organo-silanes (Paidin & Rao, 2007).

2. Coreflooding experiments:

   The initial coreflooding experiments were conducted using standard as well as reservoir rock/fluid systems with outcrop and reservoir cores of varying lengths and diameters. The objective of these high pressure and temperature coreflooding experiments was to evaluate effect of the mode of gas injection and core length on GAGD oil recovery. The results were as expected in that miscible floods performed better than immiscible ones, while the long core experiments highlighted the effect of gravity segregation on the GAGD recovery.

The process of implementing the GAGD process in the field began in the second half of 2005 with a pre-screening of two possible field options. Out of this screening, the Buckhorn Field emerged as the most likely candidate for GAGD application at the time. It is a previously waterflooded reservoir that had been shut in since 1972. It is located in the Northeastern part of Louisiana (Tensas parish) and is a compartmentalized sandstone reservoir. It consists of four main units, or pods, of which one was selected for the initial implementation of the GAGD process based on certain favorable geological criteria, such as relative thickness, homogeneity of the sand and potential target reserves. After the waterflooding had ended it was estimated that the remaining reserves totaled about 4.7 million stocktank barrels. An important part of the optimization of the GAGD application in this field is the use of numerical simulation to forecast

the potential maximum ultimate recovery when the process is applied under ideal operational conditions. To this end, actual field data needs to be incorporated in the characterization of the reservoir simulation model as much as possible including the pertinent relative permeability curves. At this point it can be stated that the reservoir condition corefloods conducted during this study were specifically aimed at generating appropriate relative permeability curves for use in field-scale numerical simulation studies in support of the design of the GAGD process application in the Buckhorn field.

3.2 Materials

3.2.1 Fluids

In order to maintain a high level of relevance to the Buckhorn field, actual reservoir fluids were used as much as possible when conducting the reservoir condition experiments. In those instances when the use of actual reservoir fluids was not possible, care was taken to synthesize the requisite fluids according to the compositional analyses of the respective fluids, be it reservoir brine or live oil. At various stages of the experimental work, samples of both reservoir brine as well as stock tank oil were provided by the small independent oil company that had undertaken the challenge of implementing the GAGD process in the Buckhorn field.

The provided reservoir brine was analyzed by a commercial laboratory that provided the compositional analysis of the Buckhorn reservoir brine as summarized in Table 3.1, while Table 3.2 shows an overview of the type and amount of salts that went into preparing the synthetic reservoir brine when needed. For the preparation of synthetic reservoir brine, the various salts were added to deionized water in the correct amounts followed by thorough stirring and evacuation of any dissolved gas with a vacuum pump. All salts were purchased from Fisher

Scientific and, thus, were all of lab grade purity, i.e. 99.9 percent. When there was an opportunity to use actual reservoir brine, it was always filtered using Whatman No. 5 filter paper under vacuum conditions. This step was taken as a precaution to prevent any undue plugging of the porous medium from occurring during the coreflooding experiments. The provided reservoir brine almost always was a semi-clouded solution with visibly suspended particles which, if not removed prior to the coreflooding experiment, would certainly lead to plugging of the core sample and, thus, impede the flow-through experiment.

Table 3.1: Brine Composition Analysis Results for the Buckhorn Brine from a Commercial Laboratory

Test	Method	Parameter	Concentration	Units
pH	150.1	pH	5.61	pH Units
Calcium, Total	200.7	Calcium	11000	mg/L
Magnesium, Total	200.7	Magnesium	620	mg/L
Potassium, Total	200.7	Potassium	430	mg/L
Sodium, Total	200.7	Sodium	67000	mg/L
Alkalinity as $CaCO_3$	2320B	Alkalinity	21.3	mg/L
Hardness as $CaCO_3$	2340C	Hardness as $CaCO_3$	24000	mg/L
Hardness as Carbonate	2340C	Hardness as Carbonate	21.3	mg/L

In the coreflooding experiments, actual reservoir oil was always used as the oleic phase, either as live or stocktank oil. The composition of the provided stocktank oil was analyzed by a commercial laboratory and their analysis was corroborated through gas chromatography within our research group; a Varian CP 3800 Gas Chromatograph was used for that purpose. The composition of the provided stock tank oil is shown in Table 3.3.

The live or recombined oil composition was also determined by the same commercial laboratory and the analysis results are shown in Table 3.4.

Table 3.2: Amount of Salts Required (in Grams per Liter) to be Dissolved in Distilled and Deaerated Water to Prepare Synthetic Buckhorn Brine in the Laboratory

Salt Name	Formula	gm/liter
Sodium Chloride	NaCl	133.26
Potassium Chloride	KCl	0.82
Calcium Chloride (Hydrate)	$CaCl_2.2H_2O$	40.35
Magnesium Chloride (Hydrate)	$MgCl_2.6H_2O$	5.19
Sodium Sulfate (Hydrate)	$Na_2SO_4.10H_2O$	0.54
Sodium Bicarbonate	$NaHCO_3$	0.03
Total Dissolved Solids: 170000 mg/liter		

Table 3.3: Composition of Buckhorn Stocktank Oil

Components	Carbon No.	Mole %	Components	Carbon No.	Mole %
Methane	C1	0.002	Hexadecanes	C16	3.266
Ethane	C2	0.042	Heptadecanes	C17	2.950
Propane	C3	0.566	Octadecanes	C18	2.865
i-Butane	iC4	0.440	Nonadecanes	C19	2.467
n-Butane	nC4	1.160	Eicosanes	C20	2.012
i-Pentane	iC5	1.502	Heneicosanes	C21	1.751
n-Pentane	nC5	1.447	Docosanes	C22	1.520
Hexanes	C6	3.830	Tricosanes	C23	1.416
Benzene	C6	0.000	Tetracosanes	C24	1.282
Heptanes	C7	8.677	Pentacosanes	C25	1.168
Toluene	C7	0.095	Hexacosanes	C26	0.990
Octanes	C8	12.067	Heptacosanes	C27	0.864
M/P-Xylene	C8	1.066	Octacosanes	C28	0.823
O-Xylene	C8	0.936	Nonacosanes	C29	0.738
Nonanes	C9	5.785	Triacontanes	C30	0.667
Decanes	C10	7.567	Hentriacontanes	C31	0.610
Undecanes	C11	5.765	Dotriacontanes	C32	0.522
Dodecanes	C12	4.659	Tritriacontanes	C33	0.463
Tridecanes	C13	4.938	Tetratriacontanes	C34	0.394
Tetradecanes	C14	4.309	Pentatriacontanes	C35	0.378
Pentadecanes	C15	3.918	Hexatriacontanes	C36+	4.083

Notes:
(1) Corrected Properties of Liquid @ 60 / 60 ^oF
Specific Gravity = 0.8854
Molecular Weight = 249.66
(2) Corrected Properties of C_{50+} @ 60 / 60 ^oF
Specific Gravity = 1.2298
Molecular Weight = 1161.27

Table 3.4: Composition of Buckhorn Live Oil

Components	Carbon No.	Mole %	Components	Carbon No.	Mole %
Methane	C1	25.464	Hexadecanes	C16	2.688
Ethane	C2	0.000	Heptadecanes	C17	2.353
Propane	C3	0.044	Octadecanes	C18	2.322
i-Butane	iC4	0.089	Nonadecanes	C19	2.266
n-Butane	nC4	0.300	Eicosanes	C20	1.678
i-Pentane	iC5	0.752	Heneicosanes	C21	1.336
n-Pentane	nC5	0.757	Docosanes	C22	1.153
Hexanes	C6	2.556	Tricosanes	C23	1.155
Benzene	C6	0.000	Tetracosanes	C24	1.045
Heptanes	C7	5.667	Pentacosanes	C25	0.933
Toluene	C7	0.831	Hexacosanes	C26	0.813
Octanes	C8	7.820	Heptacosanes	C27	0.737
M/P-Xylene	C8	1.246	Octacosanes	C28	0.650
O-Xylene	C8	0.394	Nonacosanes	C29	0.592
Nonanes	C9	4.369	Triacontanes	C30	0.540
Decanes	C10	5.136	Hentriacontanes	C31	0.475
Undecanes	C11	4.335	Dotriacontanes	C32	0.408
Dodecanes	C12	3.860	Tritriacontanes	C33	0.366
Tridecanes	C13	3.854	Tetratriacontanes	C34	0.312
Tetradecanes	C14	3.638	Pentatriacontanes	C35	0.294
Pentadecanes	C15	2.897	Hexatriacontanes	C36+	3.865
Properties of C_{6+} Reservoir Fluid @ 60 / 60 ^{o}F:					
Mole percentage = 72.584					
Specific Gravity = 0.8329 (38.4 °API)					
Molecular Weight = 207.2					
GOR = 166.9 scf/bbl					

For the initial phase of the GAGD coreflooding experiments live oil was prepared by combining Buckhorn stocktank oil and pure methane gas in a floating piston transfer vessel to create a representative live fluid sample. Instead of adding a bevy of gaseous components, the decision was made to lump them all into the methane component of the live oil composition to simplify the mixing procedure. It was determined that this simplified method of live oil preparation would not affect the GAGD coreflooding oil recovery results disadvantageously due to the relatively small amounts of the gaseous components in the live oil composition compared

to methane (please refer to Table 3.4). After the addition of the methane to the stocktank oil, the mixture was pressurized to slightly above the initial reservoir pressure and was allowed to equilibrate for 24 hours during which the transfer vessel was inverted several times to allow the mixture to properly achieve equilibrium.

The reservoir crude oil was also filtered through Whitman No. 5 filter paper prior to being utilized in any of the coreflooding experiments, however, the reservoir stocktank oil was not de-aerated. The SARA analysis results are tabulated below (Table 3.5). It was performed by Pencor, a division of Core Laboratories LP, on two stocktank samples.

Table 3.5: Topped SARA Analysis Conducted on Buckhorn Stocktank Oil

Topped:	50.8	weight %
Remaining:	49.2	weight %
Saturates:	70.69	weight %
Aromatics:	25.26	weight %
Resins:	3.71	weight %
Asphaltenes:	0.34	weight %
Notes: Topping performed at 60 °C under nitrogen stream for 42 hours. Asphaltenes: heptane insoluble, methylene chloride soluble fraction. Oil: Heptane soluble fraction. Residual*: Heptane and methylene chloride insoluble fraction (*includes weight loss during processing and/or sediment).		

The Buckhorn live oil was further characterized by determining its bubble point pressure and measuring its viscosity as a function of pressure at a temperature that is representative of the reservoir, namely 238 °F. The bubble point pressure was measured using the Constant Composition Expansion (CCE) method wherein a sample of the live Buckhorn oil is housed in a floating piston transfer vessel which allows the expansion of the sample's volume by draining water that is housed on the opposite side of the piston. The live oil sample was initially pressurized to 4000 psi with water at ambient temperature, thereby ensuring that the fluid is in

single phase. During each step a small amount of water was drained thereby allowing the live oil to expand and depressurize in a very controlled manner. Afterwards the transfer vessel was agitated several times until the pressure stabilized. These steps were repeated until the live oil sample had gone well into its two-phase region. The bubble point pressure was then determined from a plot of the stabilized pressure versus the cumulative water drained as is shown in Figure 3.1.

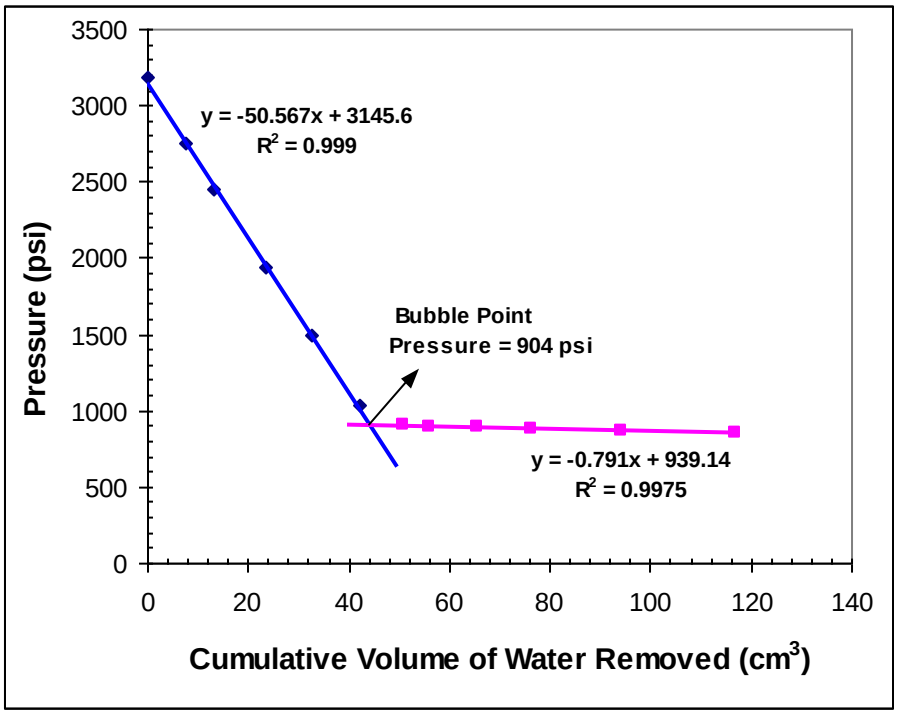

Figure 3.1: Bubble Point Pressure of Buckhorn Live Crude Oil at 75°F

The bubble point pressure of the Buckhorn live oil is indicated on the graph as the intersection of the two distinct linear sections of the curve, each representing the two- (pink line) and single-phase (blue line) region, respectively. A linear function was fit through the data of each region using simple linear regression resulting in the linear functions as noted in the graph.

Solving for the intersection of the two linear functions provided an exact value of the bubble point pressure, i.e. 904 psi.

The viscosity of the Buckhorn live crude oil was measured using an electro-magnetic viscometer at a reservoir temperature 238°F by a commercial laboratory. This viscometer contains a stainless steel piston, which is magnetically driven back and forth inside a measurement chamber and the travel time recorded to determine viscosity of the sample. Viscosity measurements were carried out over a wide range of pressures at pressures from much above the reservoir pressure to atmospheric pressure and the results were summarized in Figure 3.2.

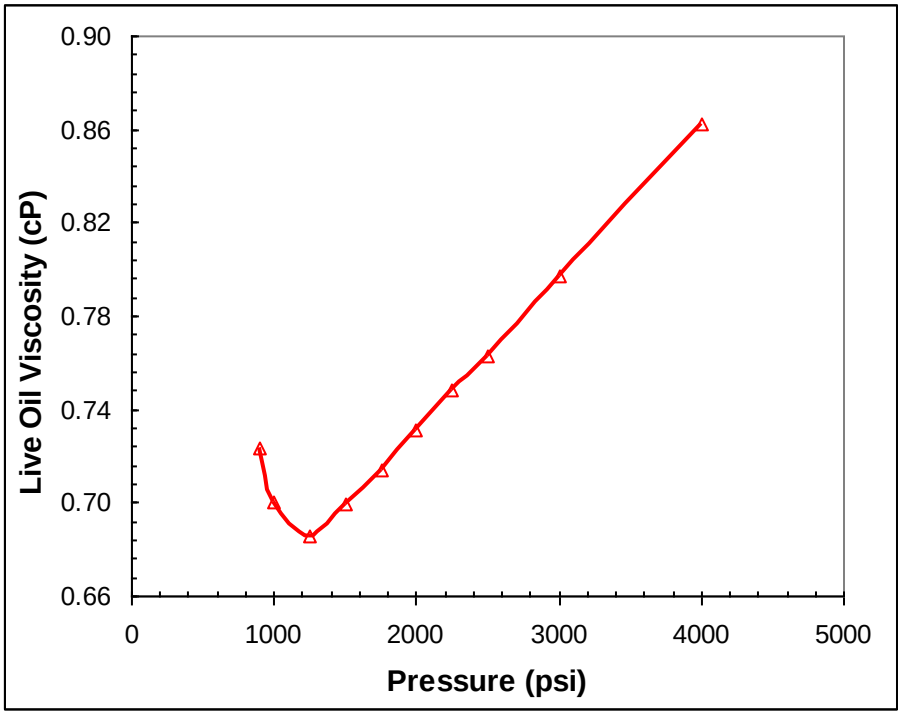

Figure 3.2: Viscosity Determination of Buckhorn Live Crude Oil at 238^{o}F

The last fluid used in the GAGD coreflooding experiments is CO_2 which was purchased from AirGas and was provided in pressurized cylinders (size 200) containing a syphon tube

(diptube). This enabled the extraction of the gas in a liquid phase which allowed for the appropriate pressurization (through compression) to the required injection pressure without the disadvantage of not having enough injected gas volume. The gas had a purity of 99.99 percent according to the vendor's specifications.

3.2.2 Rocks

The provided reservoir core samples were taken from the "Anderson 23 No. 1 well" and were analyzed by Omni Laboratories, Houston, Texas. The provided core material covered a cored depth interval extending from 8694.00 ft. to 8714.80 ft. (continuous core). In summary, the description of the rock samples ranges from micaceous/very fine- to fine-grained sandstone to medium-grained sandstone and subsequently possesses a wide grain size range of 0.03 mm to 0.28 mm (determined from thin section analysis). The porosity also reflects this wide range in grain size and is reported to be in the range of 13.9 to 23.9 percent. A more detailed description is provided in Table 3.6, however, the listed sample depths are not representative of the true depth as those were changed internally to match cores with logs.

The depositional environment was interpreted by the commercial laboratory based on a detailed sedimentological examination of approximately 21 feet of slabbed conventional core material. The cored interval contains sediments from the Lower Tuscaloosa Formation indicative of a fluvial-deltaic environment. The sediments in the core represent sediments from various facies, such as distributary channel, distributary mouth and prodelta facies (Omni Laboratories, 2011). They summarized the various depositional facies as follows:

- Distributary channel:

Core depth of 8694.0 to 8699.0 ft.: this facies consists of very fine- to coarse -grained sandstones and as such, these sediments have good reservoir quality with a core plug porosity of 16.1-23.9 percent and Klinkenberg permeability values ranging from 856-1630mD. This unit lacks pervasive fractures.

Table 3.6: Overview of Anderson 23 No. 1 Sample Properties

Sample Depth (ft)	Rock Name	Average Grain size (mm)	C.A. Porosity in % (NCS)	C.A. Permeability in mD (Klink.)	Reservoir Quality
8694.50	Very fine- to coarse-grained sandstone	0.06-0.60	23.9	1530	Good
8695.50	Fine- to medium-grained sandstone	0.27	19.8	1110	Good
8696.50	Very fine- to coarse-grained sandstone	0.05-0.60	22.4	1630	Good
8697.45	Very fine- to coarse-grained sandstone	0.05-0.70	17.5	1200	Good
8698.50	Very fine- to coarse-grained sandstone	0.05-0.58	16.1	856	Good
8699.50	Micaceous, very fine- to fine-grained sandstone	0.06	13.9	0.025	Poor
8700.50	Micaceous, very fine- to fine-grained sandstone	0.06	17.7	0.115	Poor

- Distributary mouth bar:

  Core depth from 8699.0 to 8706.15 ft.: this interval displays the characteristic coarsening upward sequence of a distributary mouth bar lithofacies and consists of very fine- to fine-grained micaceous sandstones interbedded with dark gray to black shale layers. The reservoir quality is poor with core plug porosity values from 13.9-17.7 percent and permeabilities in the range of 0.025-0.115 mD. The lateral extent of the interbedded shale layers is not known.

- Prodelta:

  Core depth from 8706.15 to 8714.8 ft.: it consists of dark gray to black shales interbedded with siltstones and very fine-grained sandstones. No porosity or permeability measurements

or petrographic analyses were conducted in this interval, but it is expected that the permeability is very low (this unit would serve as a flow barrier).

The provided samples were large-diameter cores that were split along their axis and as such were not readily usable for the coreflooding experiments. The first step in core preparation was the extraction of several 1.5 inch-diameter core plugs with the use of bench drill press and a suitable diamond coring bit (a 2 percent NaCl solution was used as coolant and to provide lubrication during the coring process). The ends of the extracted plugs were then cut with a diamond rock saw and carefully polished to achieve parallel and smooth surfaces: the resulting core plugs were all about 2 inches in length. Before proceeding, the core plugs were thoroughly cleaned of any in-situ fluid content by using the standard Soxhlet extraction method (please refer to §3.3.4.1). In order to minimize the effect of the dead volume on the coreflooding results and to improve the diameter-to-length ratio, three core plugs were assembled into one composite core that was then used in all of the experiments. Tissue paper was placed in between the core plugs to provide hydraulic connectivity and good capillary contact, after which the composite core was wrapped in Teflon tape. The practice of using tissue paper as the bridging material in between core plugs that make up a composite core had been successfully utilized by several other researchers (Hinkley and Davis, 1986; Nadeson, et al., 2001; Zekri and Almehaideb, 2002). Hinkley and Davis (1986) conducted steady-state fractional flow experiments using composite cores in which the saturation profile along the length of the core was monitored using a microwave saturation scanner. Their scanning results revealed that the most effective bridging material for water-wet Berea core plugs were thin sheets of paper sheets. Figure 3.3 shows the experimental saturation profile of a Berea composite core during a steady-state fractional flow experiment using two different flow rates. The composite core was composed of four one foot-

long segments. In the figure the joints are denoted by dotted lines and in this particular experiment the first joint was bridged with a layer of diatomaceous earth, the middle joint was left empty while the last one was bridged with layers of thin paper sheets. The depicted saturation profile clearly shows a distinct saturation discontinuity where the joint was left empty with the thin paper sheets being the most effective at providing good capillary contact, i.e. resulting in a smooth saturation profile.

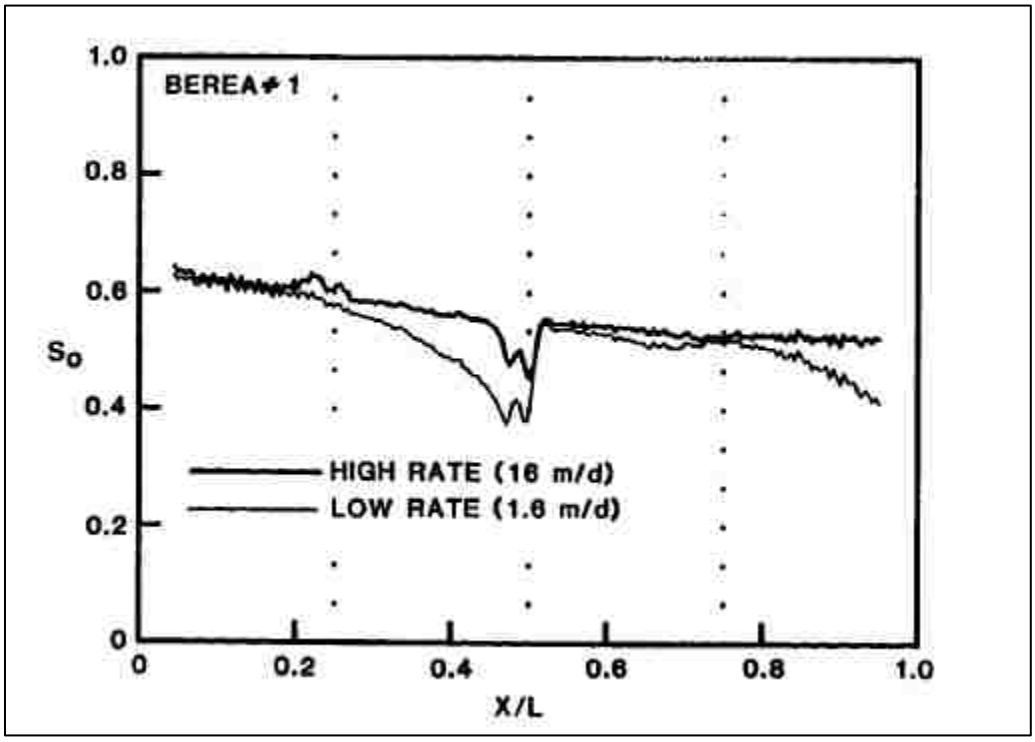

Figure 3.3: Scanned Saturation Profile – Effect of Bridging Material (Hinkley and Davis, 1986)

In this study, Kimwipe tissue paper was used as bridging material while the joints in between the core plugs were additionally covered with glass fiber tape that was soaked with epoxy resin to provide a sturdier seal. After curing of the epoxy resin, the composite core was inserted in a Viton rubber core sleeve and contained in a Hassler-type coreholder. Figure 3.4

depicts the aforementioned process of assembling the three reservoir core plugs into one composite core.

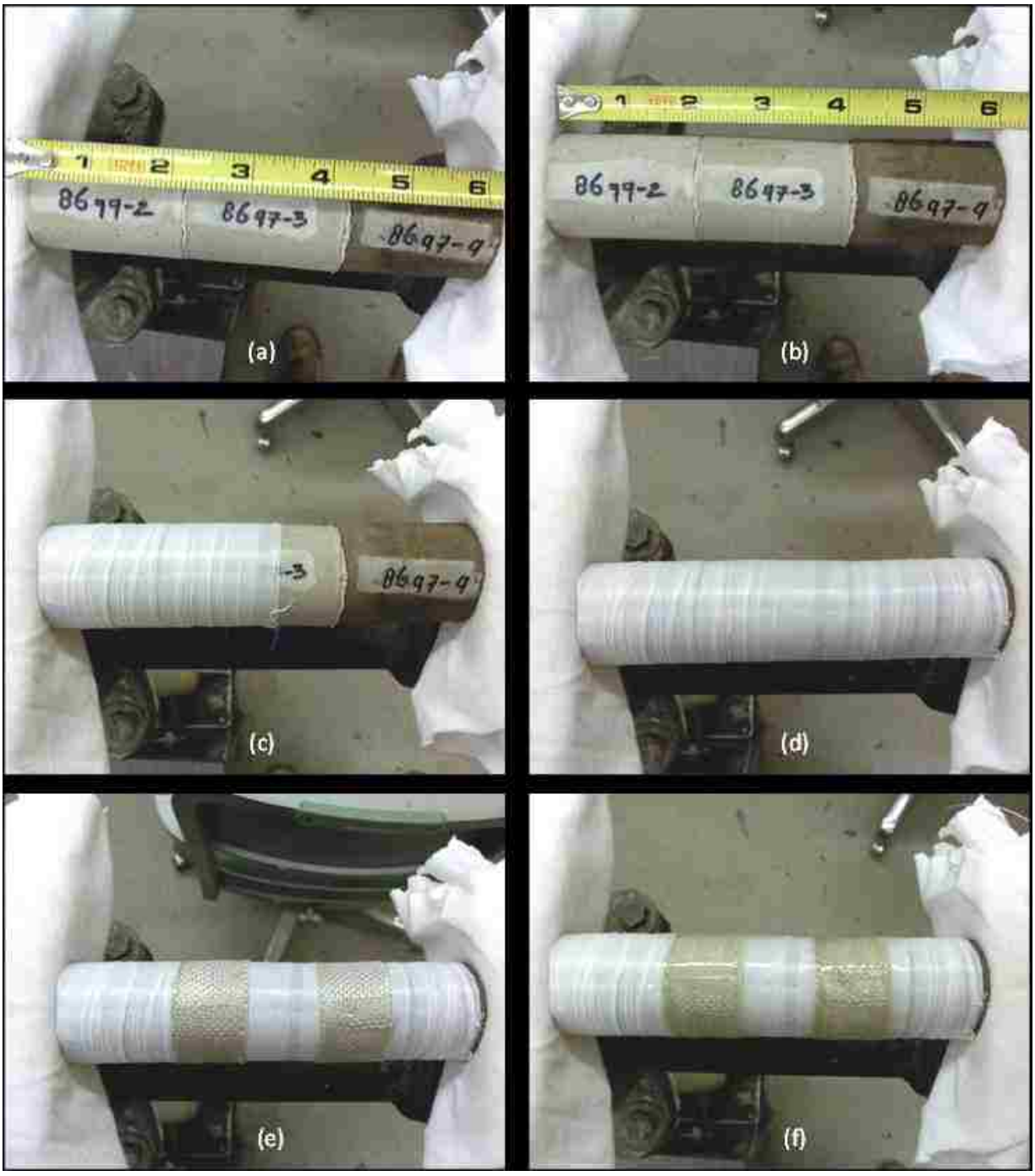

Figure 3.4: Preparation of Composite Core for Coreflooding Use – (a & b) Placement of Core Plugs in Sequence with Tissue Paper in Between; (c & d) Wrapping of Composite Core with Teflon Tape; (e) Seams Covered with Glass Tape and Epoxy Resin (d)

3.3 Experimental Apparatus

Since an important aspect to the coreflooding experiments was that they were to be representative of the field conditions, care was taken to perform them under reservoir pressure and temperature conditions as much as possible. A back pressure regulator was used to ensure that a minimum pressure of 1500 psi was maintained throughout the experiments whereas a heating tape and glass wool were used to heat and insulate the coreholder, respectively, thereby maintaining a constant temperature of 238 °F throughout. The same heating/insulation measures were also applied to the floating piston transfer vessels that contained the fluids used.

The experimental setup used in this round of experiments was adapted from the previously used design with some minor modifications. The complete experimental setup is depicted in the diagram in Figure 3.5 (on page 57), and consists of the following:

1. The coreholder assembly – the main component was a Hassler-type coreholder with a maximum pressure rating of 5000 psi. It was manufactured by Phoenix Company and was designed to hold a 1.5 inch diameter core with a length of up to 12 inches. As mentioned before, a heating tape manufactured by Omegalux as well as glass wool insulation material was used as part of the coreholder assembly to maintain a constant working temperature of 238 °F.
2. Constant rate pump – a positive displacement pump was used in the coreflooding experiments in conjunction with the floating piston transfer vessels. The pump used was a compact Series 1500 Lab Alliance pump with dual heads, a controllable set rate of up to 12 cc/min and a maximum working pressure of 5000 psi.
3. Floating piston transfer vessels – two types of floating piston transfer vessels were used in the coreflooding experiments. To house the reservoir brine, a transfer vessel made of

Hastelloy was used while a stainless steel one was used to house the reservoir oil as well as the injectant. The Hastelloy transfer vessel was manufactured by CoreLab and has a pressure rating of 5000 psi as well. The internal volume is 2000 cc and the floating piston is made of Teflon. The stainless steel transfer vessel has a similar internal volume but is made completely of stainless steel. It was manufactured by TEMCO, Inc.

4. Wet test meter – to measure the gas production a wet test meter was utilized. Manufacturer: GCA Precision Scientific.
5. Back pressure regulator – this piece of equipment was used to maintain a constant outlet pressure of 1500 psi during the coreflooding experiments. The back pressure regulator used was of the diaphragm-type and had a maximum working pressure of 4500 psi. It was also manufactured by TEMCO, Inc.
6. Hand pump – a hand pump was used to apply the overburden pressure through the use of hydraulic oil as the pressured medium. Manufacturer: Enerpac.
7. Pressure gauges – a combination of digital and dial pressure gauges were used. The digital pressure gauges (P_1 and P_2 in Figure 3.5) were employed when high accuracy readings were required such as the inlet and outlet pressure readings, while the dial gauges (P_3 and P_4 in Figure 3.5) were used as pressure monitoring devices. All pressure gauges were manufactured by Ashcroft, but the digital pressure gauges had a maximum pressure rating of 5000 psi with 0.25 percent (of full scale) accuracy.

In addition, a graduated cylinder was used to collect the liquid effluents while any produced gas was vented to the outside. In Figure 3.5 the red lines indicate possible sources of dead volume that were minimized by flowing through the bypass flow line prior to the start of any experiment or subsequent experimental phase. This reduced the dead volume to only the

flow lines on either side of the coreholder which were kept as short as possible for this very reason. On average, the dead volume was minimized to 2.1 cc using the depicted experimental setup.

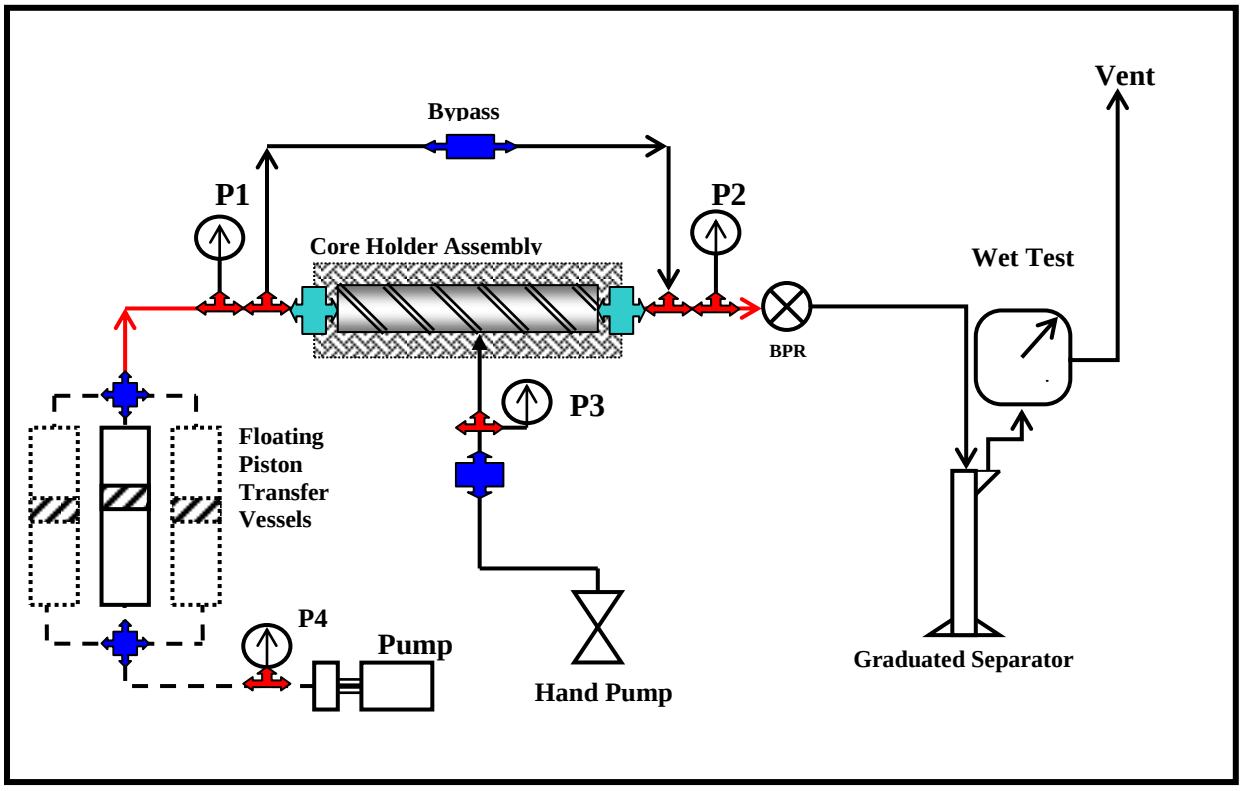

Figure 3.5: Schematic Drawing of the Experimental Coreflooding Setup

3.4 Experimental Procedure

This study consisted of two sets of coreflooding experiments with the same goal, namely to further assess the effectiveness of applying GAGD in the Buckhorn field. It was the intent to perform a sequence of experiments aimed at mimicking the field condition-application of GAGD as closely as possible with the following experiments: a horizontal waterflood followed by a vertical gas flood.

This was partially achieved in the first set of experiments, but in the second set of experiments it was decided that only a vertical gas flood was to be performed as most of the

reservoir had not been waterflooded yet. Each set of experiments also included a thorough cleaning of the composite core prior to the start of the sequence, saturation of the core with brine followed with saturation with stock tank oil thereby driving down the brine saturation to connate conditions. At this point, the composite core was ready to be used in the sequence of experiments. The following is a more detailed explanation of the experimental protocol that was followed.

3.4.1 Core Cleaning

The core cleaning phase is intended to thoroughly clean the cores of all fluids prior to the start of the experiments. The aim of this is to prepare the core for re-establishment of a native wetting state. This entails saturating the cleaned core samples with reservoir fluids, thereby attaining representative initial fluid saturations as best as possible and exposing the previously cleaned rock pore surfaces to the reservoir fluids at reservoir conditions in order to get back the native wetting state. Therefore, the composite core was thoroughly cleaned using a Soxhlet-type extractor with a solution of 50 percent toluene and 50 percent methylchloride. The composite core was cleaned according to the apparatus directions for at least 4 hours and up to 8 hours if the core was especially oil-saturated. The boiling rate of the toluene/methylchloride cleaning solution was set at such a level to allow for one complete re-circulation of the fluid in about 15 to 20 minutes. After completion of the extraction process, the core was placed in a 160 °F oven to dry overnight in order to make sure that the cleaning solution had completely evaporated out of the core.

3.4.2 Horizontal Waterflood

The GAGD coreflooding experiments were conducted in two main steps: first, a horizontal waterflood was conducted and then, a (GAGD) gasflood was performed. The waterflood consisted of the following sequential steps:

1. Load the cleaned and dried core in the coreholder assembly. Maintain an overburden pressure that is 500 psi greater than the core pressure at all times during the experiments.
2. Remove all of the air from the core by pulling vacuum on it using a vacuum pump. This minimizes the possibility of air entrapment.
3. Determine the pore volume of the core by injecting brine into the core using a very low constant injection rate while keeping the core confined and measuring the injected volume. The brine injection needs to be stopped when the core pressure sharply increases signaling that the core is completely saturated with brine.
4. Pressurize the core by flowing brine through the core and using a back-pressure regulator set at the reservoir pressure of 1500 psi at the outlet end. This pressure was maintained throughout the following procedure.
5. Determine the absolute permeability by injecting brine into and flowing through the core at four different flow rates to (up to 10 pore volumes). By measuring the stabilized flowing pressure and knowing the (constant) injection rate the absolute permeability can be calculated using the Darcy equation for linear liquid flow:

$$k = \frac{Q*\mu*L}{A*\Delta P} \quad \text{.....} \quad (3.1)$$

, with all of the variables in consistent units.

6. Flood the core with stock tank oil until the connate brine saturation is reached. Connate brine saturation is attained when no more brine is being produced. Monitor the oil and water production, the pressure drop, and measure the end-point (effective) permeability (3-4 pore volumes) using the same equation above.
7. Wrap the coreholder with a heating tape set at 238 °F and allow the core to age for up to a week to attain a representative native wetting state.

All of the aforementioned steps were performed at the reservoir temperature of 238 °F while the injected fluids were also brought to the same temperature before being injected into the already heated core. In order to ensure that the displacement during the brine flood would be stabilized, i.e. that any rate and/or length effects on the recovery are diminished, the brine was injected such that Leas & Rapoport's (1953) scaling coefficient was greater than 1.0. At values of greater than 1.0 it had been established that the flooding behavior becomes independent of rate and length. The scaling coefficient was defined as: $Lv\mu_w$ $[\frac{cm^2 * cp}{min}]$……..……(3.2)

3.4.3 CO_2 Injection

After conclusion of the waterflood, a CO_2 injection needs to be performed which would be a representation of the GAGD-type gas displacement that would occur in the Buckhorn field. The tertiary CO_2 injection was done in one of two ways: horizontal or gravity-stable, i.e. with the core's long axis oriented vertically:

1. In case of a gravity-stable CO_2 injection, place the core vertically and wait for 24 hours to allow the fluids to re-distribute themselves in the core while performing the following step in the meantime. If a tertiary gas injection is to be conducted, proceed to the next step.

2. Load CO_2 into one side of a floating piston transfer vessel and pressurize the gas to the required pressure of 1500 psi by injecting water on the other side of the piston, thereby compressing the gas.
3. Wrap the transfer vessel with a heating tape set at the reservoir temperature of 238 °F and allow the gas to attain equilibrium over several hours. Drain water as required to maintain the CO_2 pressure at 1500 psi.
4. Perform a tertiary gravity-stable CO_2 flood until no more oil is produced while monitoring the oil, water and gas production, the pressure drop, and measure the end-point (effective) permeability (3-4 pore volumes).

3.5 Reservoir Simulation Study

The simulation study was conducted using various CMG (Computer Modelling Group) tool packages, namely:

- WinProp:

  This simulation package was used to generate an appropriate fluid model of Buckhorn's reservoir fluid system to be used in the field-scale simulation of the GAGD process. The aim of generating a representative fluid model is to capture the full range of PVT behavior that is expected during the GAGD field application as completely as possible, which entails capturing the interaction of the injected CO_2 with the reservoir oil, including swelling and/or viscosity reduction of the oil due to dissolution of the CO_2, miscibility attainment of the injected gas with the oil, and any preferential extraction of oil components. In order to meet this objective as much actual laboratory measured fluid data was used in the fluid model, including but not limited to, the composition of the reservoir live oil (using a C_{6+}-lumped

component to represent any heavier components), viscosity measurements, and the lab-determined bubble point pressure. Using actual lab data for calibration of the resulting fluid model again tries to minimize any inherent risk as much as possible within the constraints.

- GEM:

  CMG-GEM is a commercial equation-of-state compositional simulation package "which can simulate all the important mechanisms of a miscible gas injection process, i.e. vaporization and swelling of oil, condensation of gas, viscosity and interfacial tension reduction, and the formation of a miscible solvent bank through multiple contacts" (GEM Manual, 2011). It was used because it was expected that the GAGD process efficiency would be highly dependent on the interaction between the injected gas and the oil's various components. GEM was used in conjunction with Builder, which as the name implies was used to build the base reservoir model. In Builder, a 3-D model of the Buckhorn reservoir was compiled by combining isopach maps and structure maps of the top of the main sand structure. The location and the orientation of the injector and production wells were also defined in Builder, as well as pertinent relative permeability curves that were generated from the reservoir condition coreflooding experiments.

  Apart from the Buckhorn reservoir model, a simple block-shaped synthetic model was also compiled to investigate the effect of the gas injection rate, the oil withdrawal rate and the presence of flow barriers on the GAGD performance one at a time. Even though this block model had a very simple shape it did resemble the full-scale field model in the sense that it shared some the same reservoir qualities. By keeping the reservoir geometry simple and by only using the minimum number of wells it was intended to isolate the effect of each parameter investigated on the GAGD oil recovery.

- CMOST:

  CMOST is a relatively new addition to the suite of simulation packages that CMG offers and is typically used to conduct a guided or automated sensitivity analysis, to optimize (maximize or minimize) an objective function of interest, e.g. the cumulative oil produced or the producing water-oil-ratio (WOR), or to perform a history match. In this study, it was used to determine the optimum operating conditions for two variations of the proposed alternative of the GAGD process, namely a single-well version of GAGD, SW-GAGD. One variation consisted of using a single vertical well that had completions in two separate zones with the top-most completions being used as injection ports while the lower-most completions served as the production end. The other alternative is using a single well that has an offset (horizontal) leg at the bottom of a vertical section. Again, the top-most completions (in the vertical well section) were to be used as injection ports while the horizontal leg has the production completions.

3.6 Economic Study

3.6.1 Putting Together the Appropriate Cost Model

For this study, a GAGD cost model was constructed that was as detailed and current as possible. To this end, various professionals in the field of petroleum field development were consulted to gather the most applicable cost elements to be included in the cost model. The cost model was part of the overall cash flow analysis that was implemented in order to evaluate the economic performance of the field implementation of not only the conventional GAGD process, but also of the other EOR methods of interest including the proposed single-well GAGD configurations.

The resulting cash flow analysis is a reflection of the petroleum fiscal regime or system (PFS) that applies to Northern Louisiana. In essence it is a concessionary fiscal system, otherwise known as a royalty/tax system, a reference to the two most obvious elements of the PFS. Under this PFS, private ownership of the resources is allowed through the transfer of rights to the contractor (the contractor bears all the risks and most of the rewards) and the payment of bonuses, royalties and taxes to the state and/or federal government. The most important payment-related components in a royalty/tax system are:

1. Royalty – usually a percentage of the gross revenue.
2. Additional deductions – these are taken out of the net revenue after royalty and are comprised of the operating costs (OPEX) and the capital expenditures (CAPEX), including depreciation, depletion and amortization allowances and tangible and intangible drilling costs.
3. Taxation – deducted from the net revenue after royalty and fiscal deductions, encompassing state and/or local taxes and federal income tax.

The various components are illustrated in the flow chart depicting the PFS in Northern Louisiana (Figure 3.6). A cash flow analysis involves the calculation of the net cash flow, i.e. "the summation of all revenues, expenses, taxes and investments on a year-by-year basis" (Iledare, 2001) according to the following formula:

$$NCF_t = GR_t - ROY_t - CAPEX_t - OPEX_t - BONUS_t - TAX_t - OTHER_t \quad (3.3)$$

, where:

- NCF_t = After-tax net cash flow in year t,
- GR_t = Gross revenues in year t,
- ROY_t = Total royalties paid in year t,

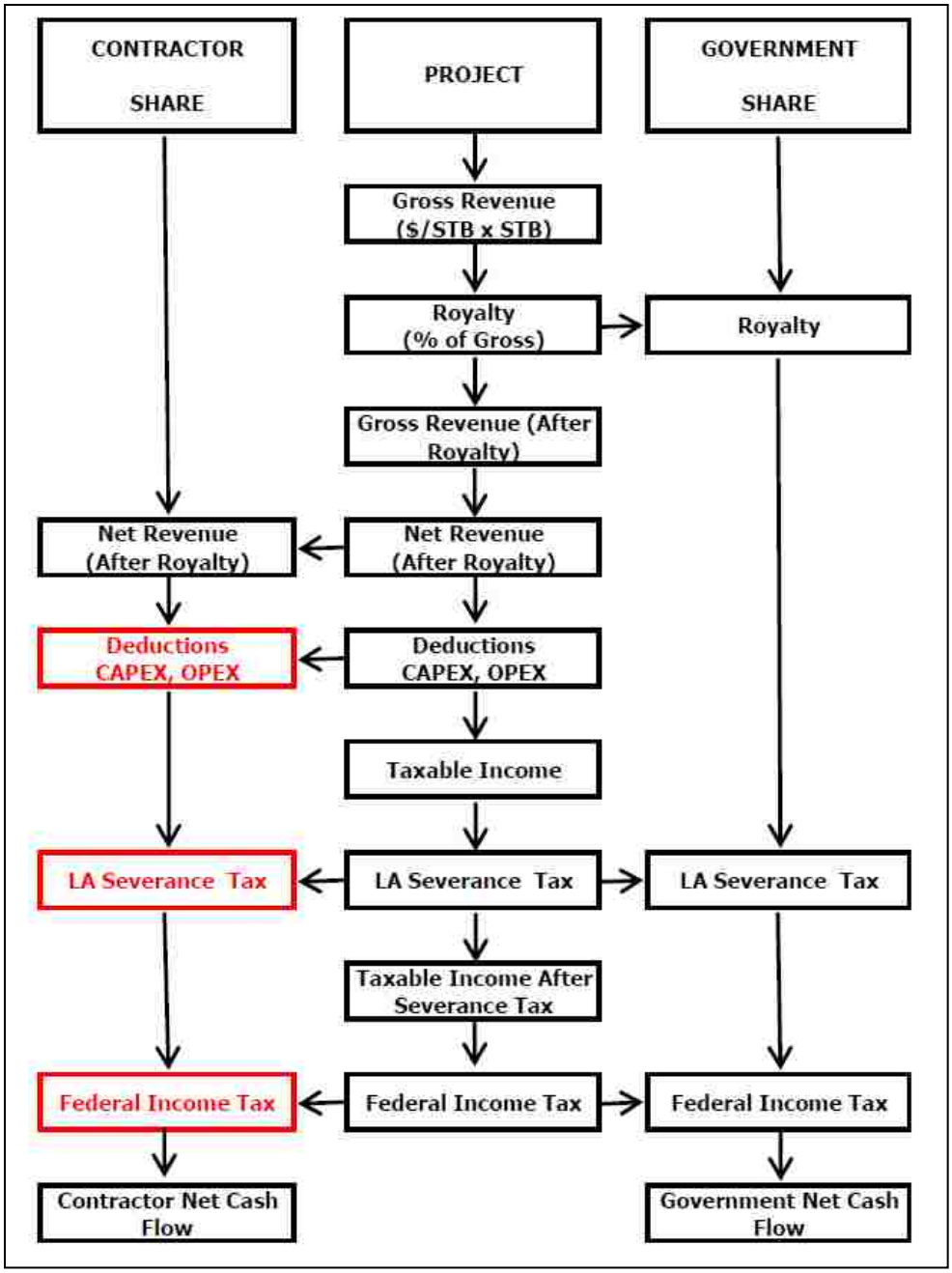

Figure 3.6: Flow Chart of Northern Louisiana PFS Components

- $OPEX_t$ = Total operating expenditures in year t,
- $BONUS_t$ = Bonus paid in year t,
- $CAPEX_t$ = Total capital expenditures in year t,

- TAX_t = Total taxes paid in year t,
- $OTHER_t$ = Other costs paid in year t.

In order to account for the time value of money the calculated cash flows were discounted using the appropriate discount factor that is reflective of the corporate cost of capital. The summation of the net cash flow is referred to as the net present value and for a specific field, F, and given the specific fiscal regime, f, can be calculated as:

$$PV(F,f) = \sum_{t=1}^{k} \frac{NCF_t}{(1+D)^{t-1}} \quad (3.4)$$

, where:

- D = Discount factor.

3.6.2 Cost Model

This section outlines how the capital and operating expenditures were determined and applied to the cost model.

1. Capital Expenditure (CAPEX):

Capital Expenditure, CAPEX, is a one-off cost usually incurred at the beginning of a project (also referred to as a front-end cost prior to production). During implementation of the GAGD process, CAPEX would primarily be generated from the drilling of two vertical and two horizontal wells as well as the installation of the facilities required to manage the process. The cost of drilling and completing the wells are based on a study of Louisiana Wellbore Completions Schematics and Formation Tops by Dr. Don Goddard (Goddard, 2006). Using the chart of average drilling cost per foot in Figure 3.7 the cost of drilling a vertical well can be inferred. In addition, the Authorization for Expenditure (AFE) costs table of a 5000' (Figure 3.8) and a 10000' well contained in the report (Goddard, 2006), were used to interpolate the tangible

and intangible cost of drilling and completing the required number of wells. The total AFE costs were determined to be $1.1 million and $5 million, respectively. Therefore, a 8700' vertical injection well should cost about $5 million, allowing for some inflation. It is often assumed that the cost of a horizontal well is roughly twice as much as that of an equivalent vertical well which means that one 9500' horizontal producing well should cost about $10 million including completions.

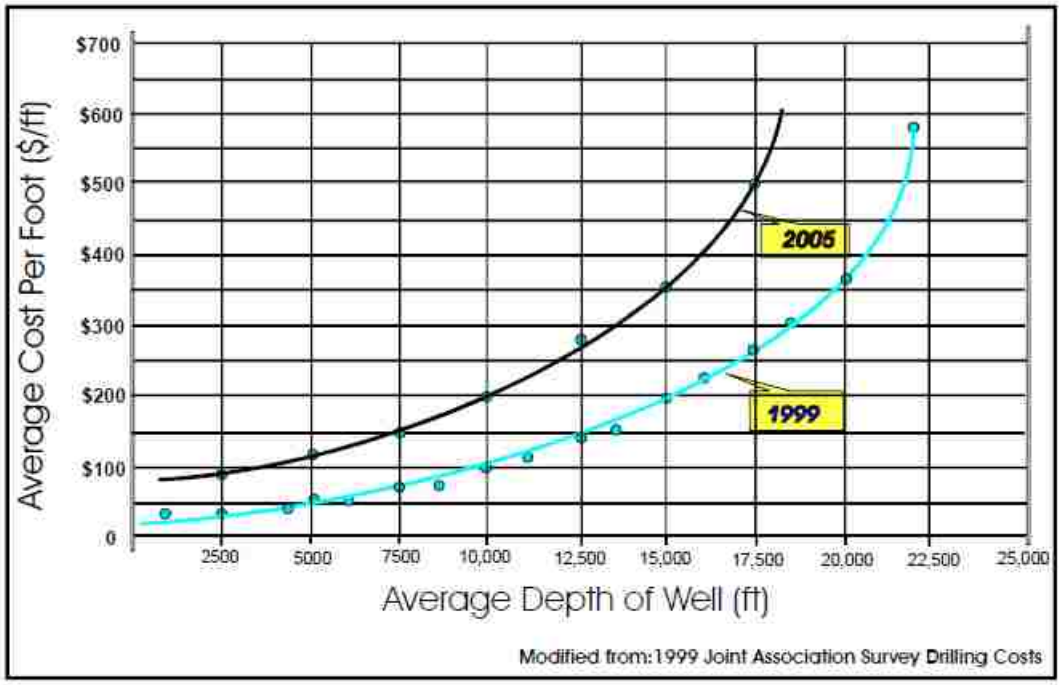

Figure 3.7: Graph of Average North Louisiana Drilling Cost per Foot (After Goddard, 2006)

After the wells are drilled and completed, the facilities needed to carry out the process must be installed or built. This operation would be considered small compared to the large 10- to 30-well gas flooding operations, therefore the facilities costs would be far less than that of a large-sized operation. The equipment needed would include: two compressors, a driving engine, various heat exchangers, separator, pulsation dampeners, and a concrete housing structure. To determine these total costs Dresser-Rand Inc. in Baton Rouge, LA, was contacted and one of

their salesmen, Mr. Fisher, provided a quote of $1.5 million for the compression equipment. Mr. Dan Nelson of Compressor System Inc. provided a cost estimate of $5 million to build a facility housing all of the equipment above. Therefore, the total facilities would add another $5 million to the aggregate CAPEX cost.

Estimate for a 5000' Straight Hole w/1000HP Rig (Precompletion Estimate Included)

ESTIMATED INTANGIBLE COSTS

	Day Rate	Days	Precompl.	DRILLING COST	PRECOMPL. COST	TOTAL AFE
Surveys and Permits/Environmental				$10,000	$2,500	$12,500
Rig Move (Mob. & Demob.)	$5,000	4		$20,000	$0	$20,000
Drilling Per Day	$5,000	5	3	$25,000	$15,000	$40,000
Fuel, Lubes and Water	$1,000	5	3	$5,000	$3,000	$8,000
Rental Equipment	$1,000	5	3	$5,000	$3,000	$8,000
Drill Bits				$20,000	$2,000	$22,000
Drilling Mud & Chemicals		5	3	$75,000	$0	$75,000
Mud Logging	$800	2		$1,600	$0	$1,600
Cement & Squeeze Services				$50,000	$15,000	$65,000
Casing Crews & Tools				$15,000	$10,000	$25,000
Open Hole Logging+MWD/LWD				$100,000	$0	$100,000
Sidewall Cores & Analysis				$5,000	$0	$5,000
Transportation	$5,000	5	3	$25,000	$15,000	$40,000
Labor	$2,000	5	3	$10,000	$6,000	$16,000
Supervision	$850	5	3	$4,250	$2,550	$6,800
P&A Costs	$25,000	3	0	$75,000	$0	$75,000
Pipe Inspection				$10,000	$5,000	$15,000
Overhead	$500	5	3	$2,500	$1,500	$4,000
Insurance	$400	5	3	$2,000	$1,200	$3,200
Communications	$250	5	3	$1,250	$750	$2,000
				$461,600	**$82,500**	**$544,100**

TANGIBLE COSTS

	Depth (Ft)	Diameter	$/Ft			
Drive Pipe		30"	220 (not needed)	$0	$0	$0
Conductor		20"	60 (not needed)	$0	$0	$0
Surface Casing		16"	16 (not needed)	$0	$0	$0
Intermediate Casing	400	8-5/8"	25	$10,000	$0	$10,000
Production Liner	5,000	5 1/2 "	12	$0	$60,000	$60,000
Wellhead Equipment				$50,000	$10,000	$60,000
TOTAL TANGIBLES				**$60,000**	**$70,000**	**$130,000**
TOTAL AFE COSTS				**$521,600**	**$152,500**	**$674,100**

Figure 3.8: Example AFE for a 5000' Well (After Goddard, 2006)

Lastly, to estimate the cost of constructing a pipeline from the CO_2-source to the Buckhorn field the chart in Figure 3.9 was consulted which is taken from a natural gas transmission pipeline cost analysis study (Parker, 2004).

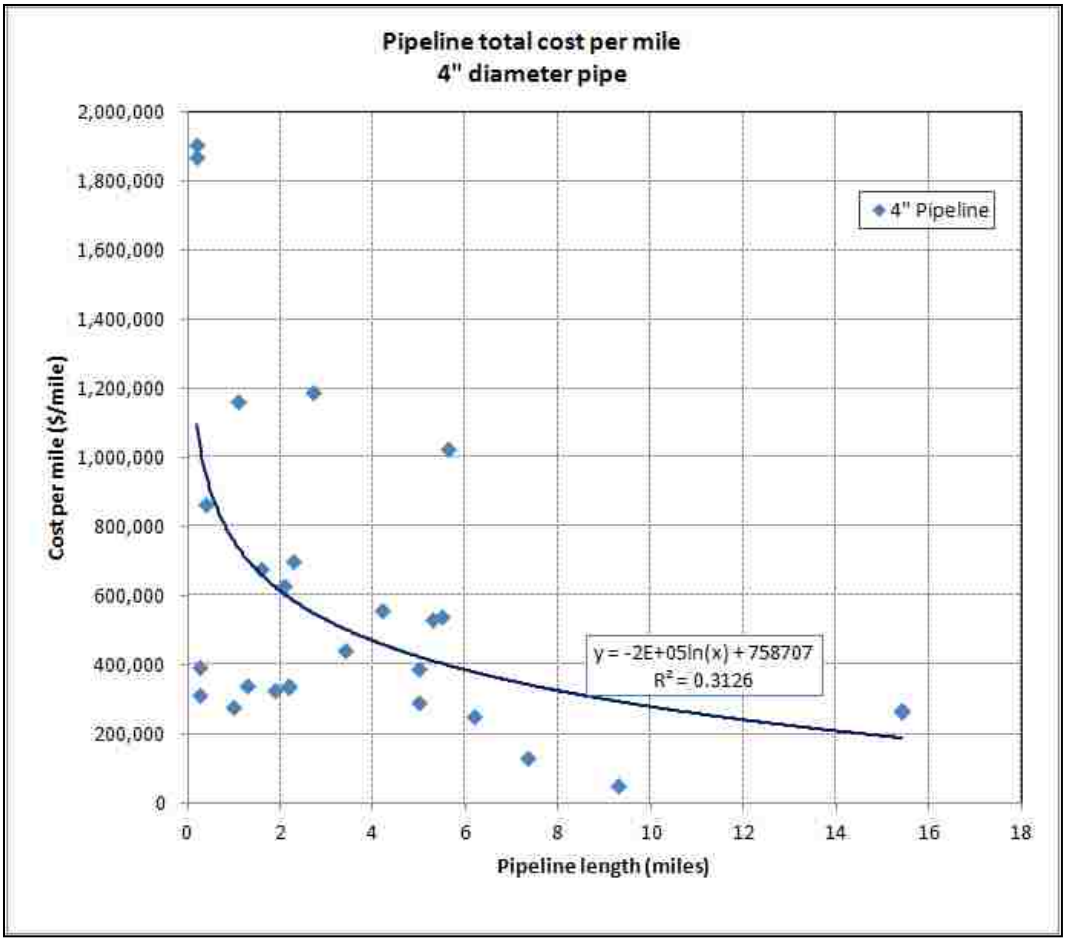

Figure 3.9: Plot of the Total Cost of Pipeline Construction per Mile – 4" Diameter (After Parker, 2004)

The distance from the delivery point of CO_2 is 10 miles plus a safety factor of two to account for the meandering involved in constructing the pipeline (e.g. avoiding large structures or sensitive areas), hence the envisioned designed requirement of 20 miles of pipeline. Using these natural gas transmission pipeline costs (Parker, 2000) an estimated cost of laying a 4 inch diameter, 20 mile pipeline can be estimated to be about $4.1million. The aggregate CAPEX cost used in the cost model is ultimately estimated to be $21.2 million when 2 vertical and 2 horizontal wells are employed. The aforementioned costs can be adjusted based on the number and type of wells used in any given EOR application, e.g. for the conventional GAGD application:

$$\begin{aligned}\boldsymbol{CAPEX} = \; & \boldsymbol{Drilling\ cost}\ (2\ horizontal + 2\ vertical\ wells) \\ & + \boldsymbol{Facilities}\ (Compressor + Diesel\ Engine + Concrete\ floor\ structure \\ & + Heat\ exchangers + Seperators + Pulsation\ Dampener) \\ & + \boldsymbol{20\ miles\ of\ pipeline} \ldots\ldots\ldots\ldots\ldots\ldots\ldots\ldots\ldots\ldots\ldots\ldots\ldots\ldots\ldots\ldots\ldots\ldots\ldots\ldots\ldots . (3.5)\end{aligned}$$

$$\begin{aligned}\boldsymbol{CAPEX} & = (2 * \$10\ million * 2 * \$5\ million) + \$5\ million + (20\ miles * \ \$159{,}566/mile) \\ & = \$38.2\ million\end{aligned}$$

The total investments are then incorporated into the cashflow analysis by dividing them into two parts, the investments that are expended at the start of the project and those that will be depreciated over a certain period once the project has officially started, usually taken as five years. The bulk investments in the first year and the depreciation amounts thereafter are determined in the cashflow by means of the independent variable $CAPEX_{expensed}$ (expressed as a percentage).

2. Operating Expenditure (OPEX):

OPEX was garnered from the CO_2 cost, and the overhead and maintenance costs. The closest CO_2 source to the BH site is the Jackson Dome in Mississippi owned and operated by Denbury Resources Inc. According to DBI's investor's report, their current price of CO_2 is $\$0.15/Mcf\ to\ \$0.30/Mcf$, and since the daily injection volume varies from 0.5 MMscf to 2 MMscf, the daily CO_2 cost ranges from \$150/day to \$1200/day.

The annual OPEX was determined from U.S. Energy Information Administration's report on oil and gas lease equipment and operating costs (1994 through 2009) (EIA, 2010). It listed the lease equipment and well costs for an 8000' well as \$23.7 million for a 10 well- lease, and the direct annual operating costs for an 8000' well as \$1.1 million, also based on a 10 well-lease.

Both cost estimates were for secondary recovery operations and can be adjusted to the number of wells operative in the lease at present.

3. Royalty and Taxes:

According to Veazey & Associates, a local reservoir engineering consulting firm, landowner royalty rates vary and are negotiable. Royalties can range from one-eighth (12.5 percent) to one-third (33.3 percent), but usually are one-fifth (20 percent). Louisiana Taxes are generally classified into Severance Taxes and Ad Valorum Taxes. For oil, the severance taxes are fixed at 12.5 percent of the gross value (after royalty and fiscal deductions). Lastly, in our analysis we applied a federal income tax of 20 to 40 percent on the taxable income.

Based on the following well-count applicable for each of EOR processes evaluated, some of the aforementioned CAPEX and OPEX cost components were scaled accordingly:

- Multi-well ("conventional") GAGD: four;
- Horizontal and vertical single-well GAGD: two;
- CGI: four;
- WAG: four.

To assess the feasibility of the proposed GAGD field application, specific economic performance indicators were calculated and used to evaluate this project. These were the Net Present Value (NPV), Internal Rate of Return (IRR), Performance Index (PI) and Growth Rate of Return (GRR). These economic performance indicators were calculated using the following formulas:

- $NPV = \sum_{t=0}^{8} \frac{NCF_t}{(1+r)^t}$ ..... (3.4)
- $PI = \frac{NPV}{Total\ Investment}$ ..... (3.6)

- $GRR = \left[PI^{1/t} * (1 + Discount\ Rate)\right] - 1$ ..... (3.7)
- IRR – is the value of the discount rate given the specific field, F, and the reigning fiscal regime, F, at which the NPV equals zero:

  $IRR\ (f, \mathrm{F}) = \{D \mid PV\ (f, \mathrm{F}) = 0\}$ ..... (3.8)

The aforementioned equations were coded in an Excel spreadsheet that was used in conjunction with Crystal Ball software to evaluate this project and perform a thorough sensitivity analysis on the effect of selected input variables on the previously mentioned economic performance indicators. The selected independent variables and their assumed probability distributions are:

1. $CAPEX_{expensed}$:

   Triangular distribution – Minimum = 20%, likeliest = 30% & maximum = 40%.

2. CO_2 Price:

   Uniform distribution – Minimum = \$0.15/Mcf & maximum = \$0.30/Mcf.

3. Discount Rate:

   Triangular distribution – Minimum = 5%, likeliest = 10%, & maximum = 20%.

4. Production Scheme:

   Discrete Uniform distribution – Possible values: 1 to 12. In the design optimization stage the application of the various EOR processes in the Buckhorn Field was simulated using CMG's compositional simulator GEM to predict the production profiles as a function of the operational constraints. A total of 12 different production schemes were thus generated for each EOR process. In the cashflow analysis each scheme was then assigned a number from 1 to 12 and coded in such a way that Crystal Ball could access each production profile by sampling from the assigned probability distribution.

5. Royalty rate:

   Triangular distribution – Minimum = 12.5%, likeliest = 20% & maximum = 33.3%.

6. Federal Income Tax (FIT):

   Triangular distribution – Minimum = 20%, likeliest = 30% & maximum = 40%.

7. Oil Price:

   The assignment of an appropriate probability distribution to the oil price variable was not as straight-forward as was the case for the aforementioned independent variables. To that end, the historical oil prices for the period of January 1986 till present were used as a starting point (EIA website). This oil price data has been plotted in Figure 3.10.

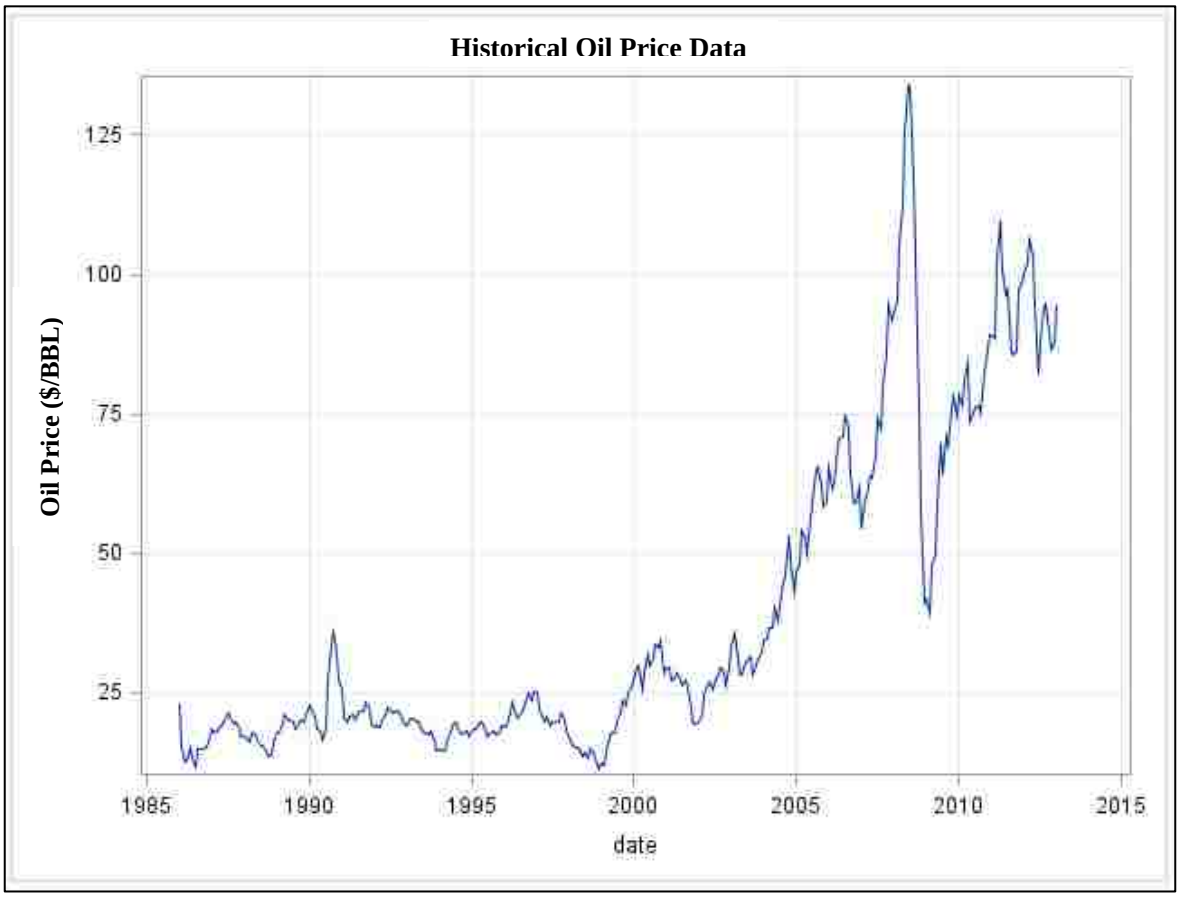

Figure 3.10: Historical Oil Price Data – 1986 to 2013 (EIA Website)

The figure above reveals the volatile nature of the historical oil price which adds a certain degree of complexity/uncertainty in any forecast of future oil prices. In order to provide reasonable forecast range for the oil price, this historical data was treated as a time series, in which the value of the dependent variable, in this case the oil price, is not merely a function of the independent variable, time, but also of the value of the dependent variable at previous time steps. The oil price data was analyzed using the time series analysis procedures available when using SAS software, more specifically using the ARIMA procedure. According to the SAS documentation available online the ARIMA procedure is described as (http://support.sas.com/documentation/cdl/en/etsug/60372/HTML/default/viewer.htm#etsug_arima_sect001.htm):

> The ARIMA procedure analyzes and forecasts equally spaced univariate time series data, transfer function data, and intervention data by using the autoregressive integrated moving-average (ARIMA) or autoregressive moving-average (ARMA) model. An ARIMA model predicts a value in a response time series as a linear combination of its own past values, past errors (also called shocks or innovations), and current and past values of other time series.

Using this procedure, a 95-percent confidence interval was constructed for the entire forecast result range which enabled the calculation of the three oil price values used in the cashflow analysis, the so-called low, mean and high oil price. The oil price forecast results generated in this manner are tabulated in Table 3.7 and have also been graphed in Figure 3.11. The figure not only shows the actual oil price data for the past ten years (denoted by round markers), but also includes shaded bands on either side of the fitted model results (solid line) indicating the 95-percent confidence interval. Averages were calculated of the predicted oil price as well as the limiting values of the 95-percent confidence interval to generate the values required as input in the cashflow analysis.

Table 3.7: SAS Forecast of Future Oil Prices

Date	Oil Price ($/BBL)	Std. Error ($/BBL)	95% Confidence Limits ($/BBL)	
May-2013	100.34	9.88	80.98	119.71
Jun-2013	100.66	11.18	78.76	122.57
Jul-2013	101.61	12.34	77.43	125.79
Aug-2013	101.56	13.40	75.30	127.82
Sep-2013	100.95	14.38	72.77	129.13
Oct-2013	100.15	15.30	70.16	130.14
Nov-2013	99.66	16.17	67.97	131.34
Dec-2013	98.60	16.99	65.30	131.89
Jan-2014	99.92	17.77	65.08	134.76
Feb-2014	99.95	18.60	63.49	136.40
Mar-2014	102.95	19.42	64.89	141.01
Apr-2014	104.32	20.20	64.72	143.91
May-2014	104.02	20.95	62.95	145.08
Jun-2014	104.34	21.68	61.84	146.83
Jul-2014	105.28	22.39	61.41	149.16
Aug-2014	105.23	23.07	60.02	150.44
Sep-2014	104.62	23.73	58.11	151.13
Oct-2014	103.82	24.38	56.05	151.60
Nov-2014	103.33	25.00	54.33	152.34
Dec-2014	102.27	25.62	52.06	152.47
Jan-2015	103.59	26.21	52.22	154.97

Following this methodology, a triangular distribution was assigned to the oil price variable in the Crystal Ball cashflow analysis that was defined according to: Minimum = $68.28/BBL, likeliest = $101.32/BBL & maximum = $134.37/BBL. The assignment of a triangular distribution is meant to function as a proxy for the often implemented practice of defining a low, medium and high value to a given portfolio element in order to assess the risk that is associated with the implementation of the project.

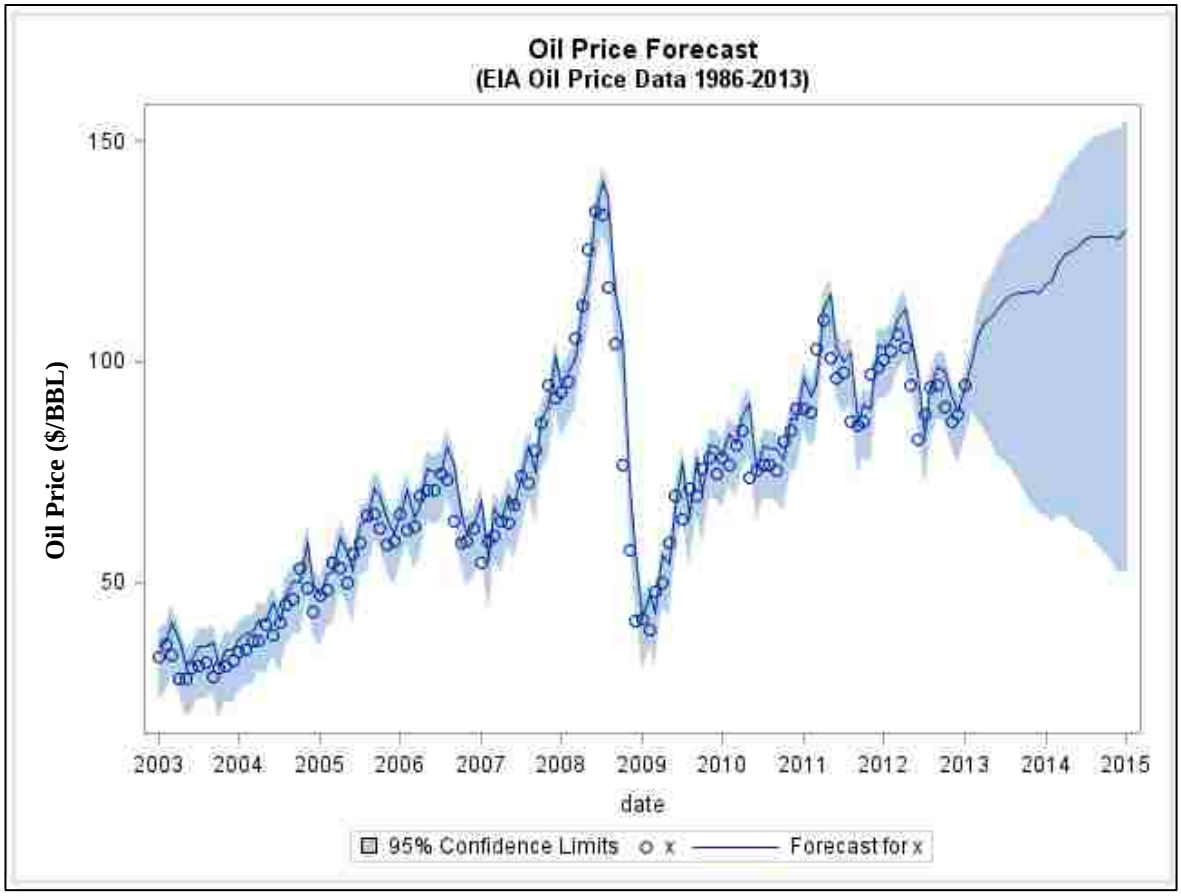

Figure 3.11: Predicted Oil Prices Showing 95-Percent Confidence Interval

4. RESULTS AND DISCUSSION

4.1 GAGD Coreflooding Results

The coreflooding experiments were initiated early on in the technical feasibility study of the GAGD field trial in the Buckhorn field. During this first phase of coreflooding experiments not all of the required elements were available, in the sense that only reservoir stocktank oil was at hand to conduct the displacement experiments with. In order to facilitate progress, it was decided to use a synthesized reservoir brine as well as Berea sandstone core material as a stand-in for the actual reservoir rock.

After the start of the field trial, core samples were retrieved during the drilling process as well as current reservoir brine and stocktank oil which were made available to conduct more representative GAGD coreflooding experiments. As opposed to the coreflooding experiments conducted with the Berea sandstone core, all of the CO_2 injection was conducted in a gravity-stable manner.

The results of each phase of the coreflooding experiments will be discussed separately in the subsequent paragraphs, starting with the Berea GAGD coreflooding results after which the Buckhorn GAGD coreflooding results will be presented.

4.1.1 Berea GAGD Coreflooding Results

The core flood experiments were conducted in three steps. The preliminary oil flood was used to measure the connate water saturation of the core. After restoring the initial reservoir conditions, brine was injected into the core to determine the secondary recovery. Tertiary gas injection followed the secondary flood to evaluate the efficiency of CO_2 injection. For tertiary gas injection two separate procedures were used after waterflooding: one was a non-gravity

stable (horizontal) gas injection followed by GAGD, and the other one was GAGD injection immediately after waterflooding.

4.1.1.1 First Berea Sequence: Restoration (Oilflood) – Waterflood – Traditional (Non-Gravity Stable) CO_2-Injection – GAGD

- Oil-flood (drainage): This cycle constitutes the process of injection of stocktank oil and live oil into the core initially saturated with brine to calculate the connate water saturation, the original oil in place (OOIP) and the relative permeability of oil. The stocktank oil was injected first to replace the water, so less live oil is needed. The use of the stocktank oil was also more helpful to restore the original wettability state in a shorter amount of time. The results for this first sequence are summarized in Table 4.1.
- Brine flood (imbibition): This cycle constitutes the process of brine injection into the core, which was at connate water saturation, to get the waterflood residual oil saturation in the core. Brine was injected at stable flow rates into the core. The results of this step can be an indicator of the extent of feasible secondary oil recovery. The end point permeability of the rock to brine at the end of this cycle can also be used to infer wettability. The high waterflood oil recoveries, low end point water permeabilities and a sharp breakthrough with negligible oil production thereafter indicate a typical water-wet case (Figures 4.1 and 4.2).
- Tertiary gas injection flood (non-gravity stable): The CO_2 is miscible with oil under the pressure and temperature conditions used. CO_2 was injected into the horizontal core at low flowrate. The water was produced with very little oil at first. No more water was produced after 0.9 pore volume injection. The oil was recovered continuously with very low rate until 2 pore volume injection.

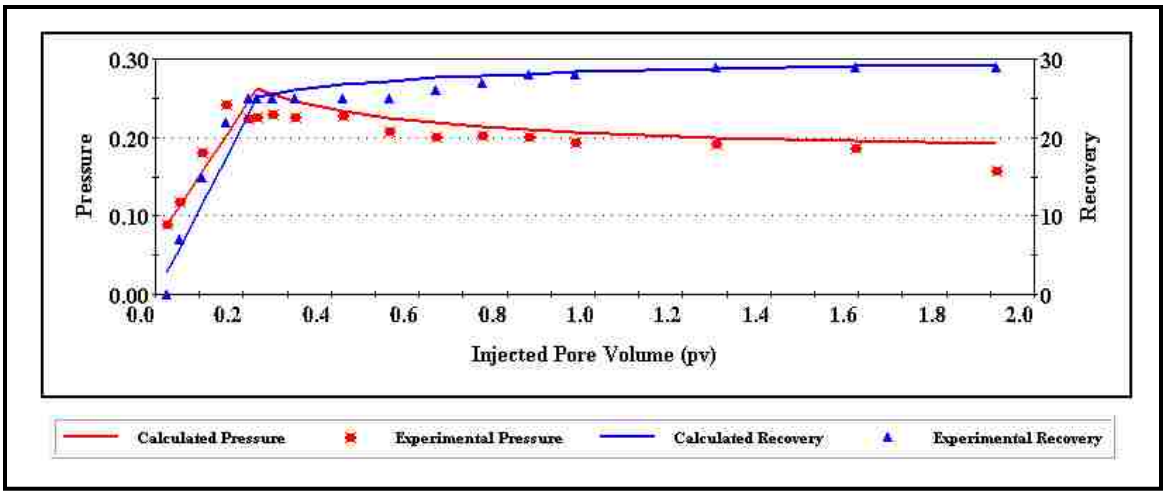

Figure 4.1: Recovery and Pressure Drop during Waterflooding (First Sequence)

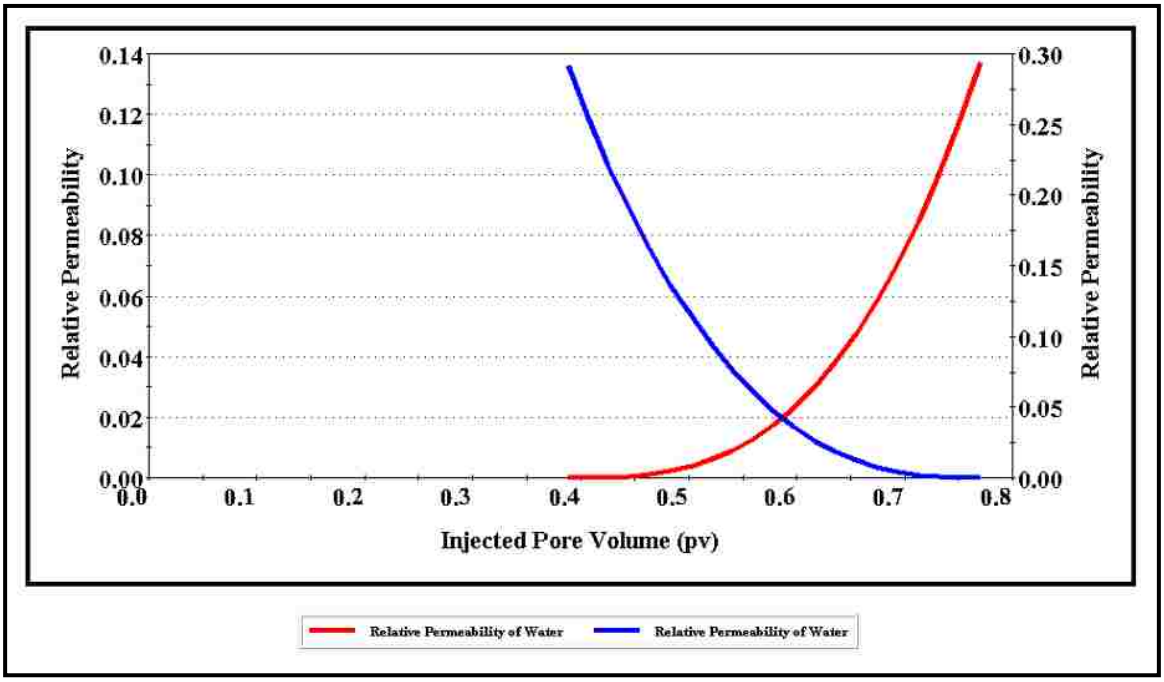

Figure 4.2: Relative Permeability Curves of Water and Oil during Waterflooding (First Sequence)

- Gas-assisted gravity drainage (GAGD): In order to check the benefit of the GAGD technique compared to the traditional gas injection, the coreholder was placed vertically after the first stage of tertiary gas injection. After waiting overnight, CO_2 was injected from the top of the

core to check if there was going to be any incremental recovery. During the first 40 minutes no liquid was produced (about 0.4 pore volume injection). After that, the oil was produced continuously at a very low rate, until 1.5 pore volume injection. From Table 4.1 it can be seen that nearly 20 percent more oil was recovered. On core scale, the gravity effect is much less pronounced than is expected on oilfield scale. Hence, we can expect more benefit when implementing the GAGD process in the field. The experimental results indicate that the GAGD process is more effective than traditional tertiary gas injection.

Table 4.1: Experimental Results of the First Sequence

Steps	Sw (%)	So (%)	Kro	Krw	Incremental Oil Recovery (%)	Total Oil Recovery (%)
Oil-flood	47.65	52.35	0.4			
Waterflood	77.06	22.94		0.141	56.17	56.17
CO_2-injection (Non-gravity stable)	59.19	15.14			13.96	70.13
CO_2-injection (GAGD)	59.19	5.2			19.94	90.0

4.1.1.2 Second Berea Sequence: Restoration (Oilflood) – Waterflood – GAGD

This sequence is similar to the previous one except that a GAGD injection was started directly after waterflooding. The oilflood and waterflood procedures were the same as in the first sequence. The test results are shown in Table 4.2.

Table 4.2: Experimental Results of the Second Sequence

Steps	Sw (%)	So (%)	Kro	Krw	Incremental Oil Recovery (%)	Total Oil Recovery (%)
Oilflood	59.19	40.81	0.49			
Waterflood	86.5	13.5		0.187	66.93	66.93
GAGD CO_2-injection	57.46	3.06			25.58	92.5

The second sequence had a higher original water saturation, hence, the relative permeabilities were a little bit higher than in the previous sequence (Figure 4.3 and 4.4). The tertiary recovery by the GAGD process was higher than the recovery by the traditional non-gravity stable gas injection, but it was less than the total tertiary recovery in the first sequence. However, considering that the residual oil saturation was lower in this sequence (only 3 percent) the GAGD injection process performed very well as a tertiary recovery technique.

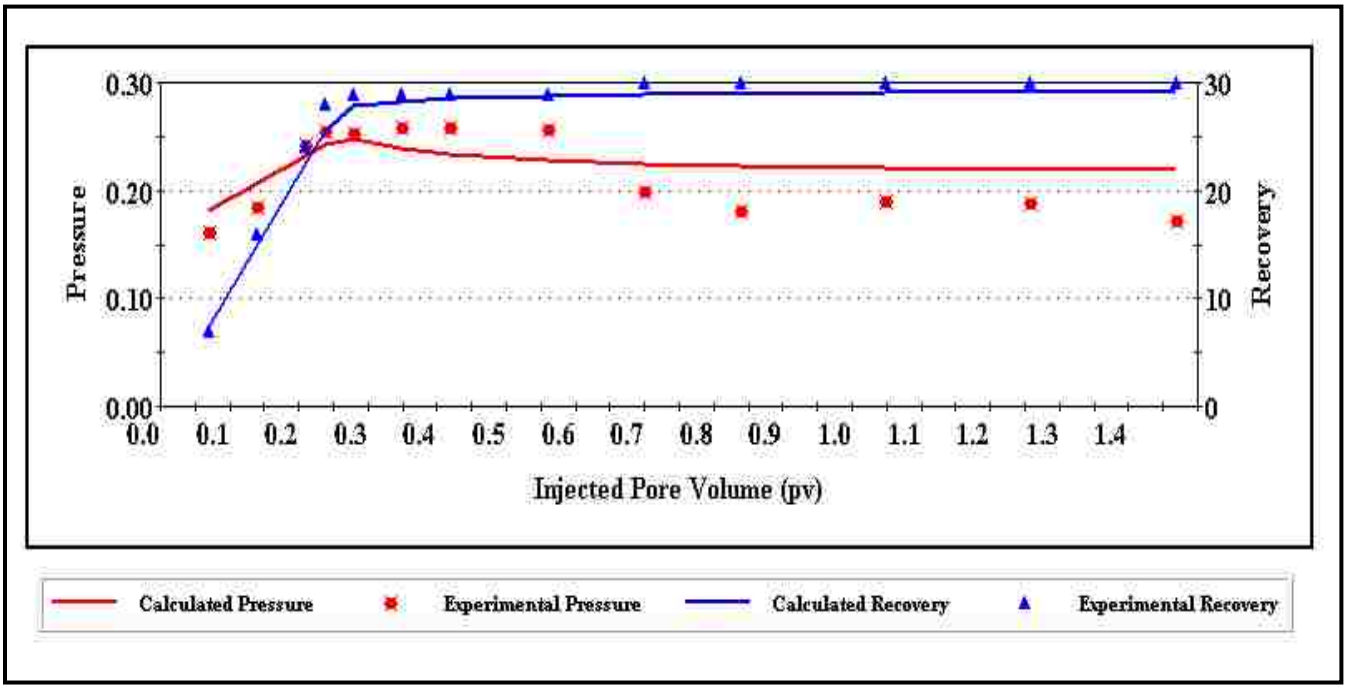

Figure 4.3: Recovery and Pressure Drop during Waterflooding (Second Sequence)

From Figure 4.5 it can be seen that the GAGD process is more economical than the non-gravity drainage: in the GAGD process most of the oil had been recovered after injection of less than 0.3 pore volume. However, in the non-gravity stable process, the oil was recovered continuously at a very low rate until more than 4 pore volumes of CO_2 had been injected.

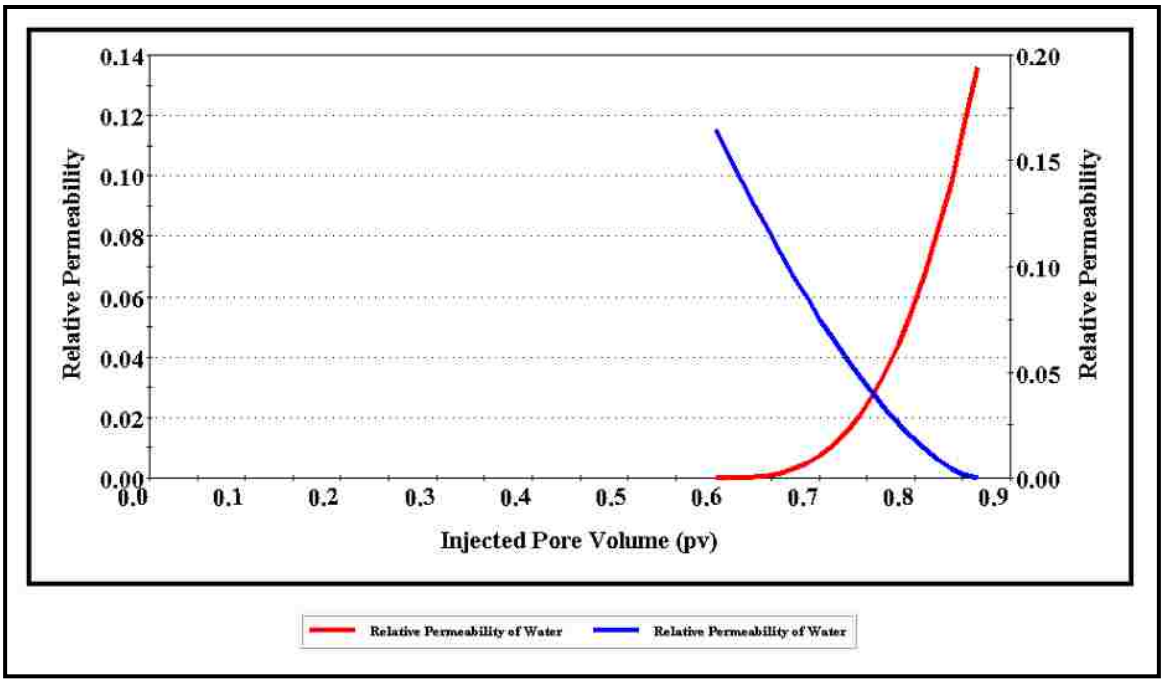

Figure 4.4: Relative Permeability Curves of Water and Oil during Waterflooding (Second Sequence)

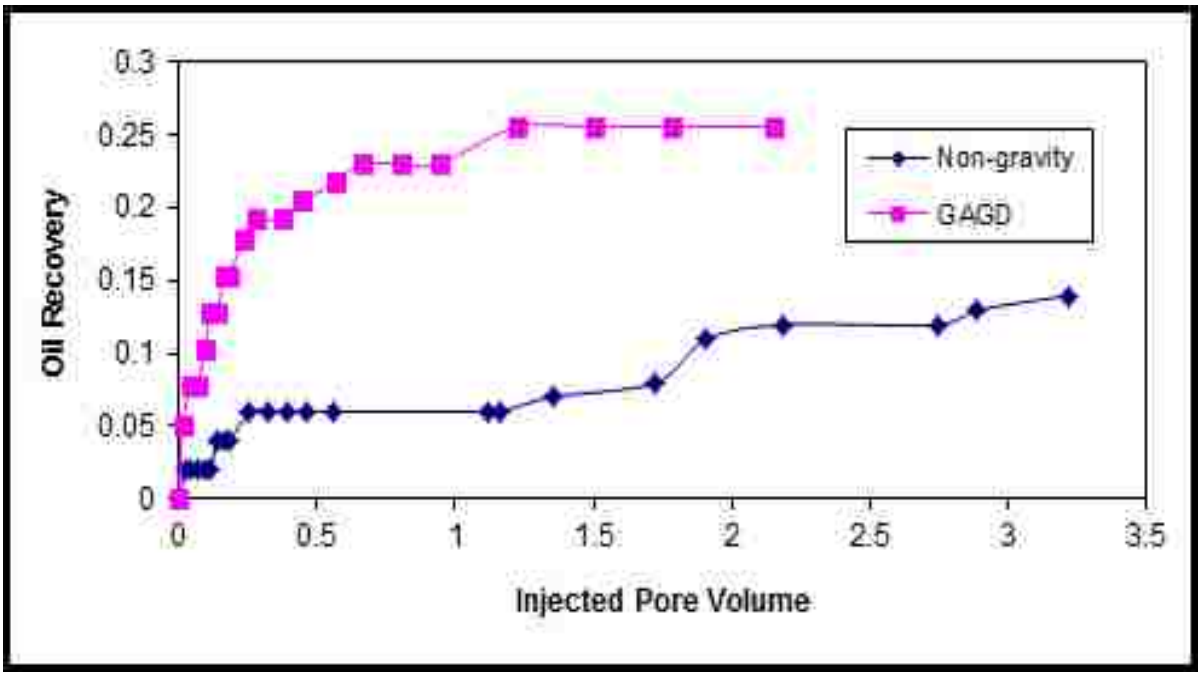

Figure 4.5: Comparison of the Tertiary Recovery between GAGD and Traditional Non-Gravity Stable Gas Injection

4.1.2 Buckhorn GAGD Coreflooding Results

4.1.2.1 First Buckhorn Sequence: Restoration (Oilflood) – Waterflood – GAGD CO_2-Injection

- Oilflood: This first step is very important in restoring the composite core to its native wetting state and consists of injecting stock tank oil into the core initially saturated with brine. The production data from this cycle was also used to calculate the connate water saturation, the original oil in place (OOIP) and the relative permeability of oil to brine. The results for this first sequence are summarized in Table 4.3. After reaching connate brine saturation the core was left to age at reservoir temperature for up to a week before continuing with the next step.
- Brine flood: Reservoir brine was injected into the core, which was at connate water saturation, until the waterflood residual oil saturation in the core was attained. The brine flood results can be an indicator of the extent of feasible secondary oil recovery through the implementation of a waterflood. The end point permeability of the rock to brine at the end of this cycle can also be used to infer wettability. The experimental data was used to generate the oil/water relative permeability curves to be eventually used in field-scale reservoir simulation. An in-house coreflood simulator was used for this purpose (Figures 4.6 to 4.8). Ultimately, the brine flood resulted in a recovery factor of 58.4 %OOIP.

Table 4.3: Experimental Results of the First Experimental Sequence

Steps	Water Saturation (%)	Oil Saturation (%)	Oil Relative Permeability	Water Relative Permeability	Incremental Oil Recovery (%)	Total Oil Recovery (%)
Oilflood	32.4	67.6	0.056			
Waterflood	71.2	28.1		0.58		58.4
GAGD CO_2 - injection	71.2	28.1			N/A	N/A

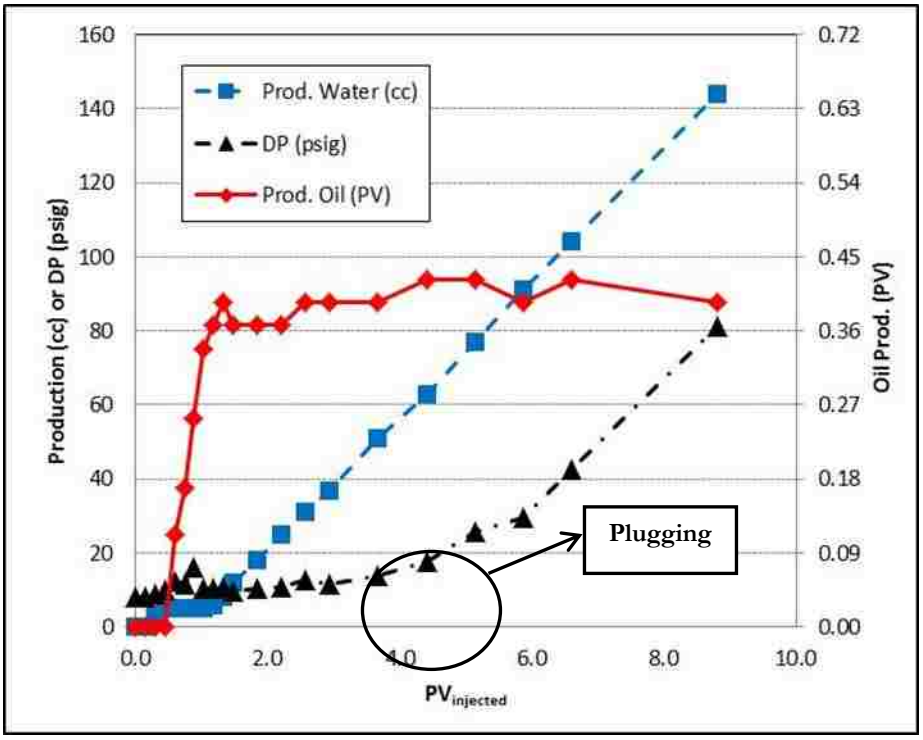

Figure 4.6: Experimental Recovery and Pressure Drop Profile during Waterflooding (First Sequence)

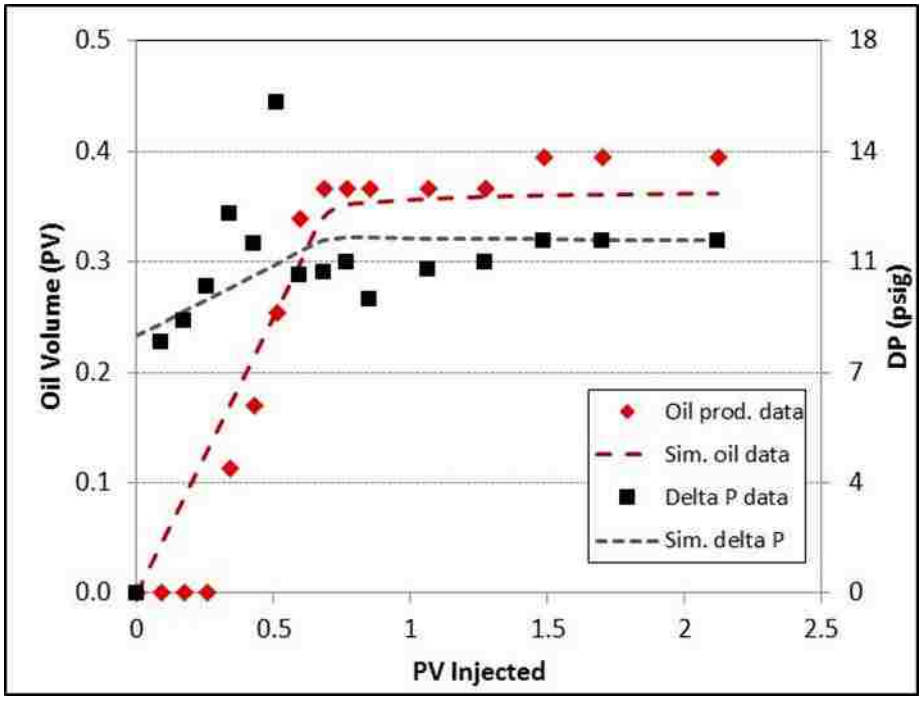

Figure 4.7: History-Matched Recovery and Pressure Drop Profile during Waterflooding (First Sequence)

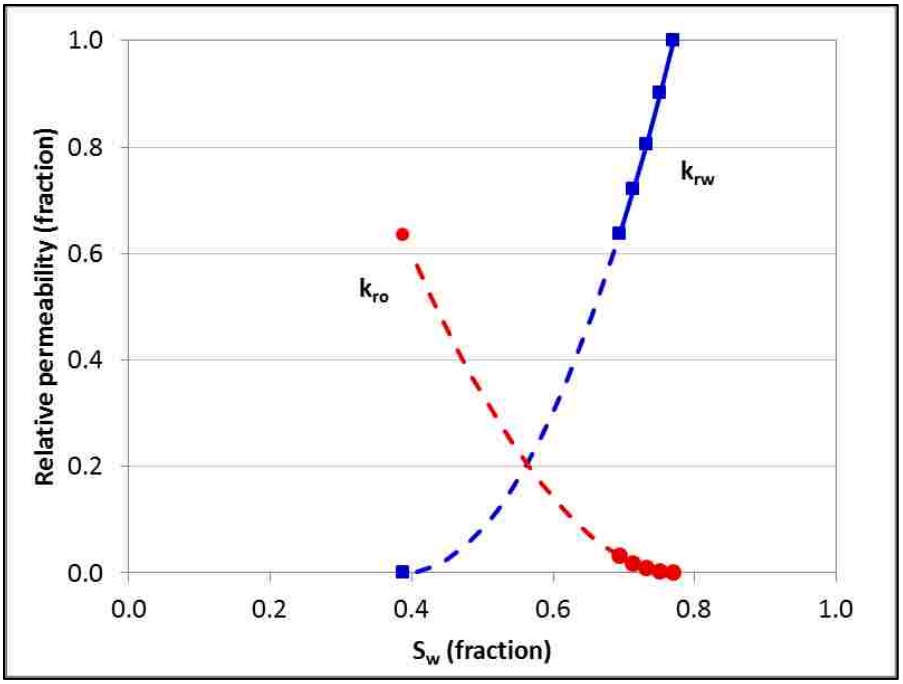

Figure 4.8: History-Matched Relative Permeability Curves of Water and Oil during Waterflooding (First Sequence)

During the brine injection the transfer vessel containing the brine was heated to 238 °F with a heating tape part of which was also wrapped around the injection line as best as possible. However, the injection line was not insulated with glass wool at this time which resulted in the brine cooling off sufficiently before entering the core to cause the core fluids to cool off appreciably over time. It is suspected that as a result the heavier ends in the oil dropped out of solution as the core cooled off. This led to an increased plugging of the core as is evidenced by the continually-increasing pressure drop during the latter part of the brine injection.

- GAGD: In order to assess the applicability of the GAGD technique in a tertiary mode, the coreholder was placed vertically after the brine flood. After waiting overnight, CO_2 was injected from the top of the core to displace any remaining oil in a gravity-stable manner. However, due to the plugging that occurred in the previous stage no additional oil was

recovered at the experimental conditions of pressure and temperature. In order to avoid this from happening, it was decided that only a secondary-mode gravity-stable gas flood was to be performed during the next sequence of experiments. This was deemed appropriate as much of the reservoir had not been waterflooded yet.

4.1.2.2 Second Buckhorn Sequence: Restoration (Oilflood) – GAGD CO_2-Injection

After the first sequence of experiments it was necessary to clean the composite core using the process described earlier. After thoroughly cleaning and cooling the core plugs they were again assembled into one composite core and mounted in the coreholder. It went through the same first two steps similar to the first experimental sequence until the core was at connate brine saturation. Table 4.4 summarizes the results of the second sequence of experiments and as can be seen, the initial brine saturation was slightly higher than the first round. This can possibly be attributed to the cleaning process which has been found to sometimes change the wettability towards more water-wet conditions.

Table 4.4: Experimental Results of the Second Experimental Sequence

Steps	Water Saturation (%)	Oil Saturation (%)	Oil Relative Permeability	Water Relative Permeability	Incremental Oil Recovery (%)	Total Oil Recovery (%)
Oilflood	50.4	49.6	0.012			
GAGD CO_2 - injection	33.9	9.6				80.7

The GAGD flood was conducted after a two-day equilibration period following the oilflood to allow the fluids to redistribute in the core. Figure 4.9 shows the oil and water production profiles during the CO_2-flood which continued until no more liquid was produced. The gas was injected at an average injection rate of 1 cc/min and an outlet pressure was

maintained at 1500 psi. From the production profile it can be seen that liquid production occurred almost instantaneously with the start of gas injection: the brine production leveled off at 20 minutes into the flood while the oil production continued at a very low rate until at 22 cc of oil was produced at 240 minutes. This accounted for a recovery factor of 80.7 %OOIP. The slight "jump" in the oil production profile reflects the overnight wait after the first day of gas injection. This resting period allowed for the remaining fluids to redistribute due to gravity drainage as well as for the injected gas to attain equilibrium with the residual oil saturation remaining after the first injection period. This additional recovery is indicative of the inherent efficiency of conducting a gravity-stable gas injection.

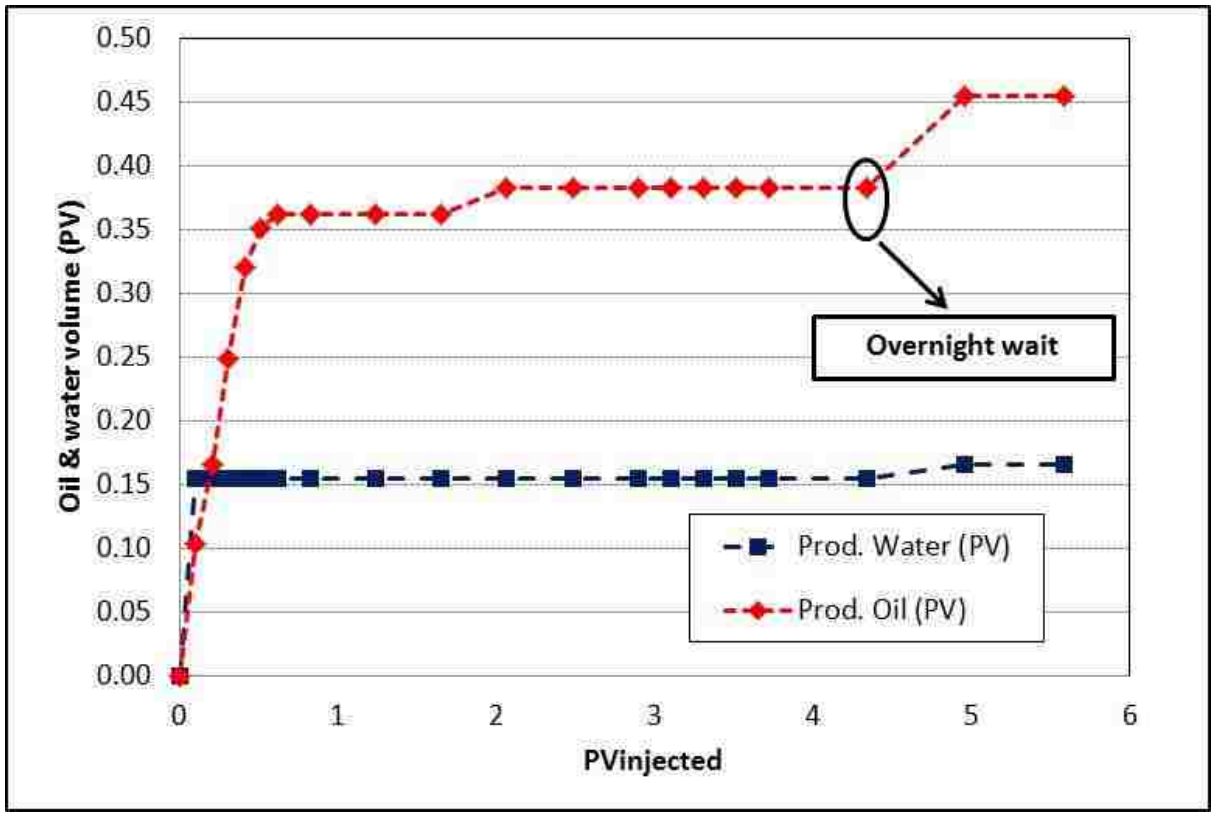

Figure 4.9: Experimental Recovery Profile during Gravity-Stable (GAGD) CO_2 Injection (Second Sequence)

4.2 Reservoir Simulation Study

4.2.1 Experimental Relative Permeability Curves

The coreflood experiments conducted with reservoir cores and fluids at representative reservoir conditions resulted in the brine-oil relative permeability curves as depicted in Figure 4.8. The endpoint permeability to CO_2 at residual fluid saturation was measured at the end of experimental sequence # 2 and was used to calculate the CO_2-liquid relative permeability curves using the available Corey-type correlations in the numerical simulator that was used in this simulation study (the compositional simulator CMG-GEM). The required three-phase relative permeability data was then calculated using the aforementioned two-phase relative permeability curves and Stone's (II) Model. The coreflooding experiments using Berea cores in the previous stage of GAGD development resulted in relative permeability data that were significantly different from the relative permeability data resulting from reservoir core experiments: Figures 4.10 and 4.12 show the relative permeability curves from both experimental stages side by side to accentuate these differences. A closer look at the brine-oil relative permeability curves in particular show the significant differences between the Berea-derived and the reservoir core-derived data. The relative permeability curves resulting from the Berea coreflooding experiments clearly indicate a water-wet wetting state if the Craig's rules-of-thumb are employed (Craig, 1993) (see Table 4.5), while on the other hand the implied wetting state of the reservoir core is not as straight-forward. Even though all of the criteria for a water-wet porous medium are met the relative magnitude of the brine and oil end-point permeabilities is significantly different compared to the Berea sandstone curves. It can also be observed that the end-point permeabilities when using the reservoir core show a completely opposite picture than was observed in the Berea sandstone core system.

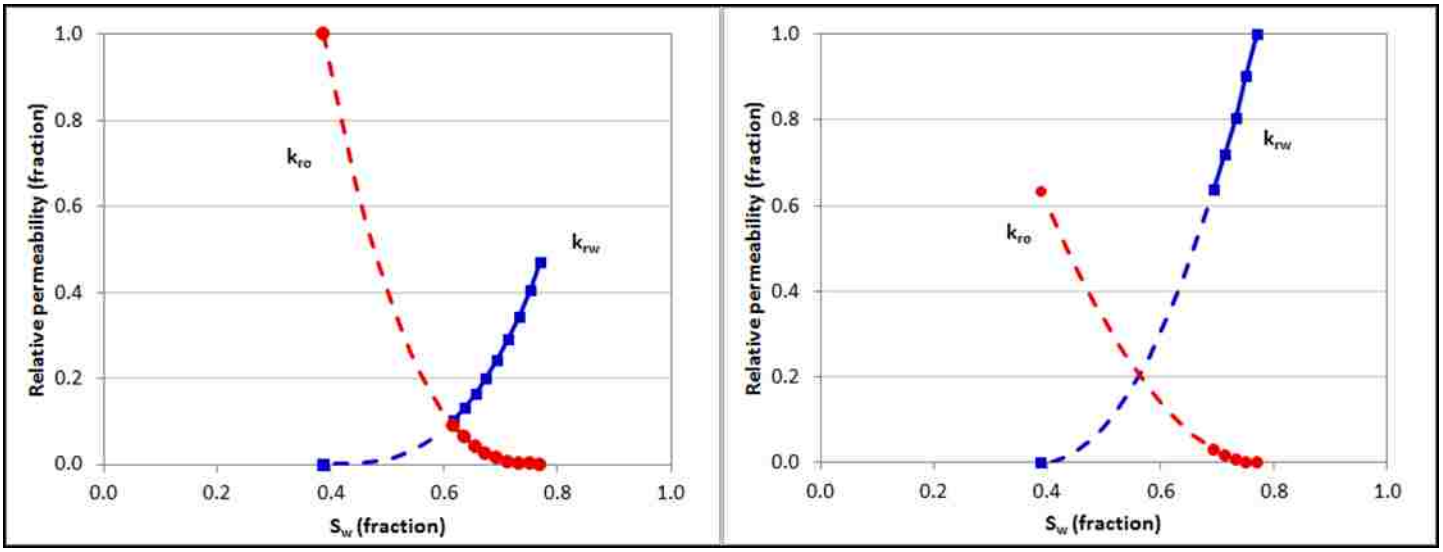

Figure 4.10: Experimentally Determined Brine-Oil Relative Permeability Curves: Berea (Left) and Reservoir Core (Right)

The Berea sandstone and the reservoir core relative permeability data were used in a simulation study in which the GAGD performance in the Buckhorn field is assessed using the same reservoir model and numerical simulator that was used in the previous development stage.

Table 4.5: Rules of Thumb for Inferring Wettability from Relative Permeability Curves (Craig, 1993)

	Water-Wet	**Oil-Wet**
Connate water saturation	Usually greater than 20 to 25 percent	Generally less than 15 percent, frequently less than 10 percent
Saturation at which oil and water relative permeabilities are equal	Greater than 50 percent water saturation	Less than 50 percent water saturation
Relative permeability to water at maximum water saturation; i.e. at floodout	Generally less than 30 percent	Greater than 50 percent and approaching 100 percent.
Relative magnitude of oil and water relative permeability at S_w = 50%	Oil relative permeability > water relative permeability.	Oil relative permeability < water relative permeability

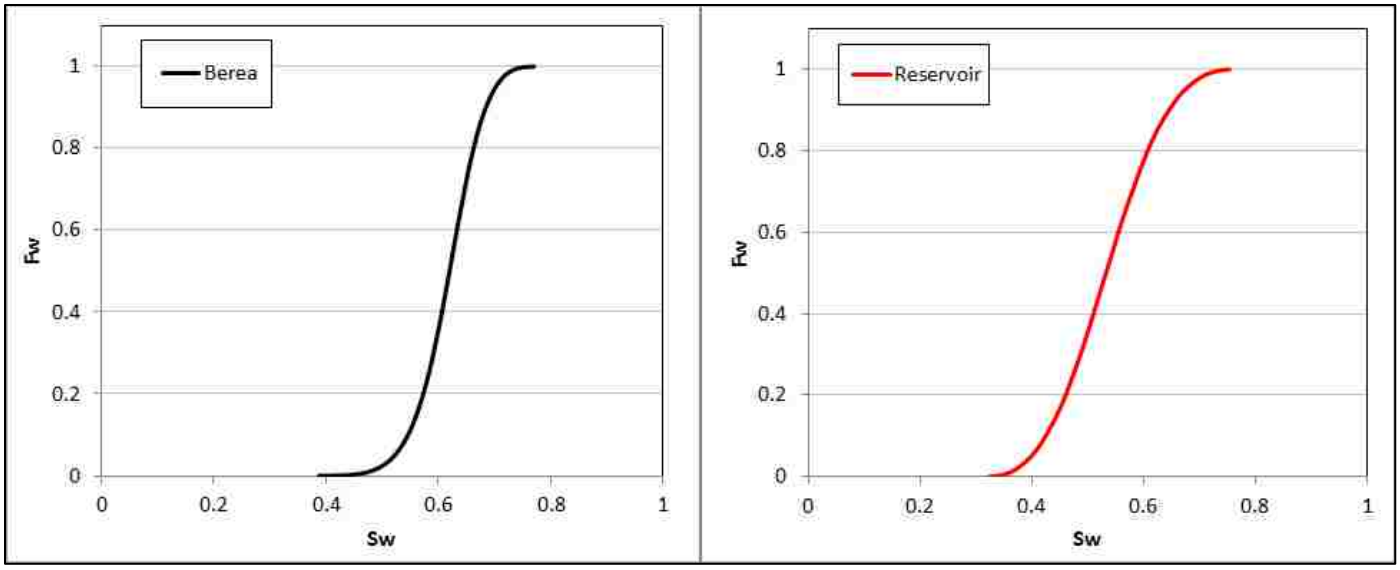

Figure 4.11: Experimentally Determined Fractional Flow Curves: Berea (Left) and Reservoir Core (Right)

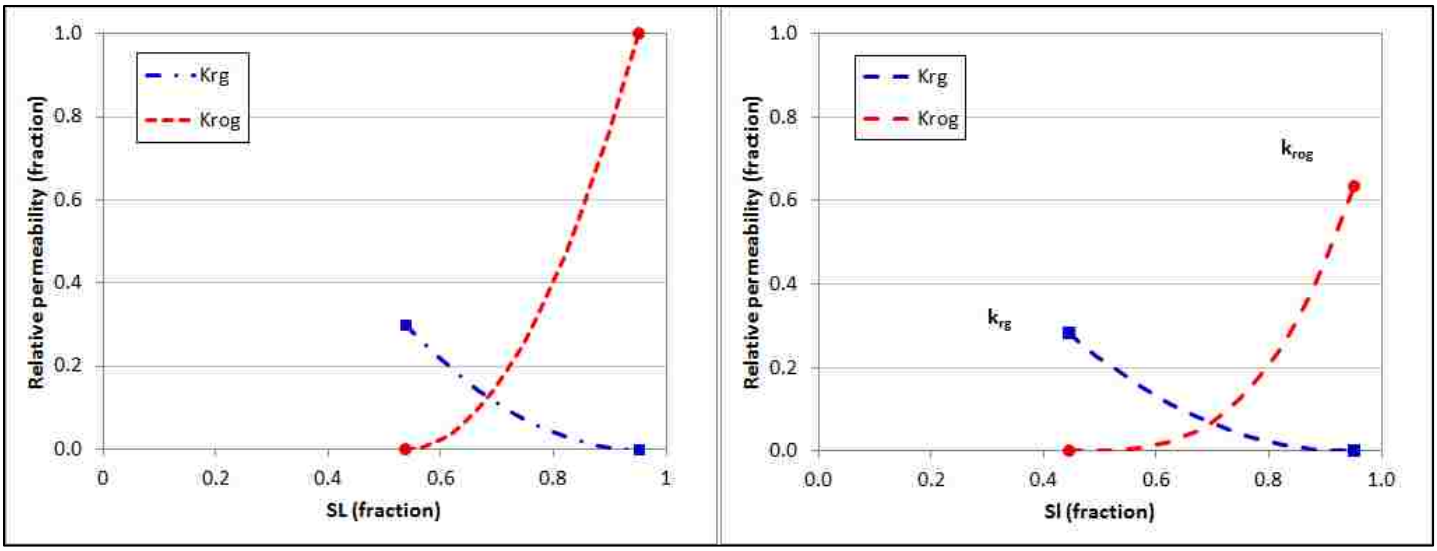

Figure 4.12: Experimentally Determined CO_2-Liquid Relative Permeability Curves: Berea Core (Left) and Reservoir Core (Right)

4.2.1.1 Reservoir Model Description

The reservoir model is a 3D model that was compiled using digitized isopach (thickness) and structure maps (top of the formation) of the Buckhorn field and consists of 12000 grid blocks. The GAGD field application was designed to be conducted using two well pairs, each

consisting of 1 vertical injector and 1 horizontal producer (shown in Figure 4.13A and B). For details on the reservoir characterization as well as the precise GAGD well locations and trajectories please refer to Technical Progress Report No. 19499R04 (Rao D. N., 2006).

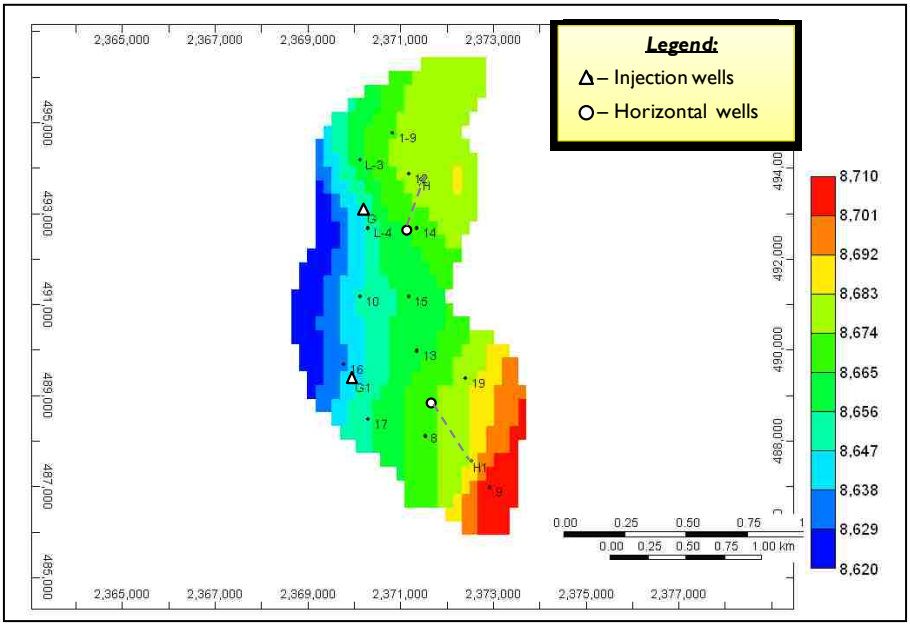

Figure 4.13A: Areal View of Buckhorn Reservoir Model with GAGD Wells

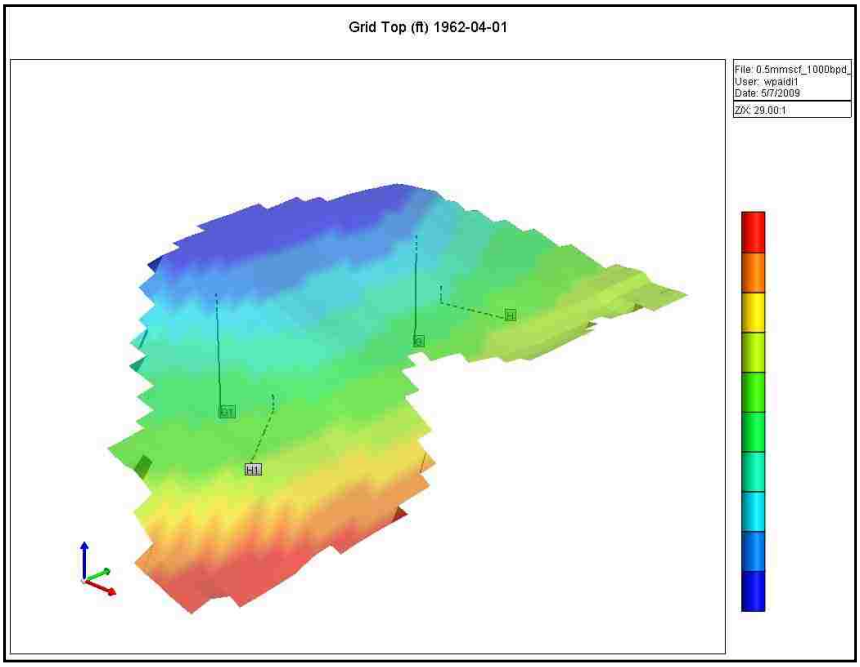

Figure 4.13B: Areal (Top) and Three-Dimensional (Bottom) View of the Selected Buckhorn Dense Pod (From confidential internal report)

4.3 GAGD Performance – Full-Scale Simulation Results

The study of the dependence of the multi-well GAGD oil recovery on various operational constraints and reservoir parameters obstruction was conducted with CMG's CMOST which is described as their "history matching, optimization, sensitivity analysis, and uncertainty assessment tool" (CMG CMOST Manual, 2011). In this study, it was also used as an optimization tool to, in effect, maximize the GAGD oil recovery by varying specific selected variables over a wide range of values. According to the CMG CMOST manual:

> An optimization task is used to identify optimal field development plan and operating conditions that will produce either a maximum or minimum value for objective functions the user specifies. These objective functions may be physical quantities, such as cumulative oil produced, recovery factor, and cumulative steam oil ratio. (Page 12)

The objective function in this part of the study was the recover factor, RF, either calculated as the oil produced divided by the original oil in place, units: %OOIP, or as the produced oil divided by the residual oil in place, units: %ROIP. The default optimization method is referred to as the CMG Designed Exploration and Controlled Evolution (DECE) Optimizer which is a proprietary optimization method that mimics the way reservoir engineers commonly go about solving history matching and/or optimization problems. Unique to this optimizer is the ability to incorporate a user's engineering judgment and understanding of the reservoir by allowing them to control which parameters actually influence the outcome through the use of an influence matrix.

CMG CMOST was used to investigate the effect of the following operational constraints and/or reservoir parameters on the multi-well GAGD oil recovery in three separate simulation studies:

1. The maximum CO_2 injection rate and oil production rate:

The general dependence of the multi-well GAGD performance on the operational constraint was studied by allowing either to vary within the following defined ranges: gas rate – 0.5 to 5 MMSCF/D (6 equal intervals); and oil rate: 500 to 3500 STBO/D (6 equal intervals). In all of the simulations, the Buckhorn Field was produced for 8 years. The CMOST results have been summarized in Figures 4.14 to 4.16. Figure 4.14 depicts the effect of the gas injection rate on the GAGD RF (in %ROIP).

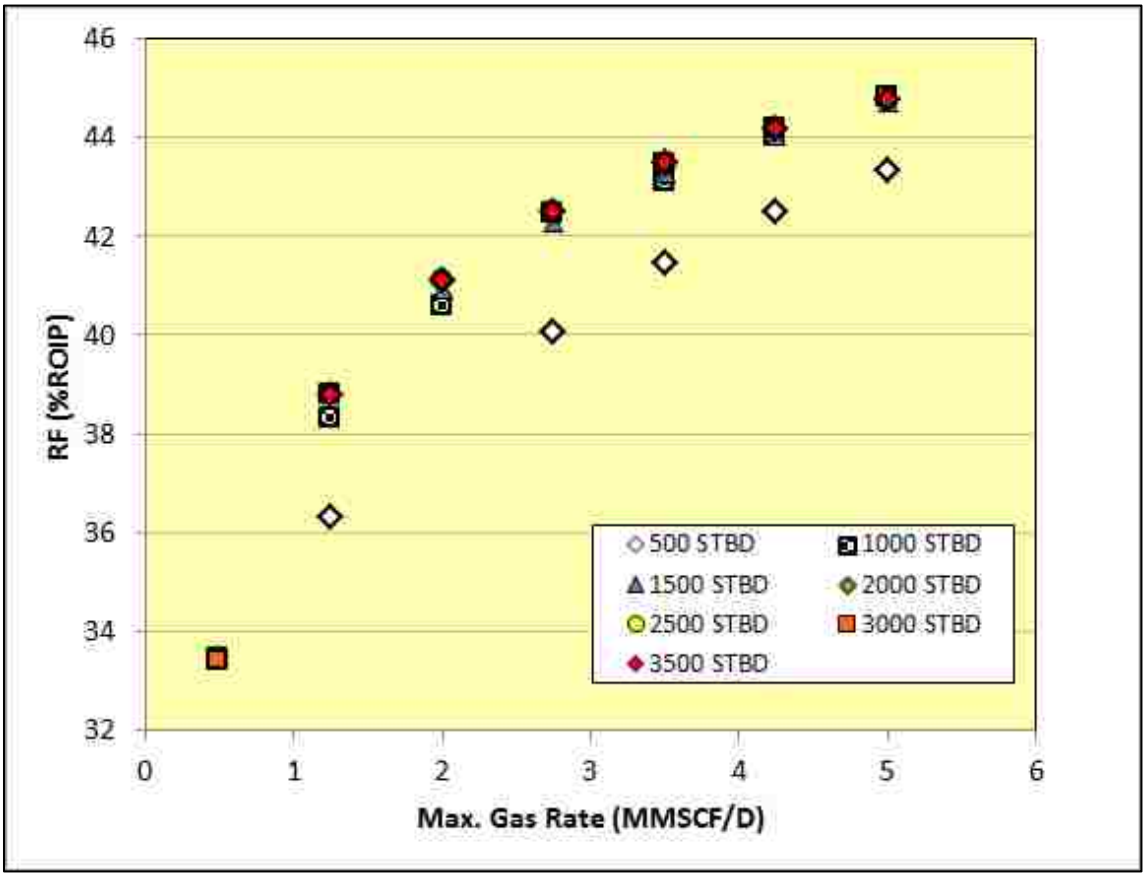

Figure 4.14: Multi-Well GAGD Recovery Factor vs. Gas Injection Rate – Reservoir Model

The figure shows that there seems to be a strong dependency of the RF on the gas injection rate: as more CO_2 is injected, more oil is ultimately recovered. The experimental results have also been grouped by the oil production rate and it is quite evident from the relative lack of

scatter in the data points that the oil production rate does not affect the RF strongly at all. This is substantiated by Figure 4.15 which shows the effect of the oil production rate on the multi-well GAGD RF (also in %ROIP).

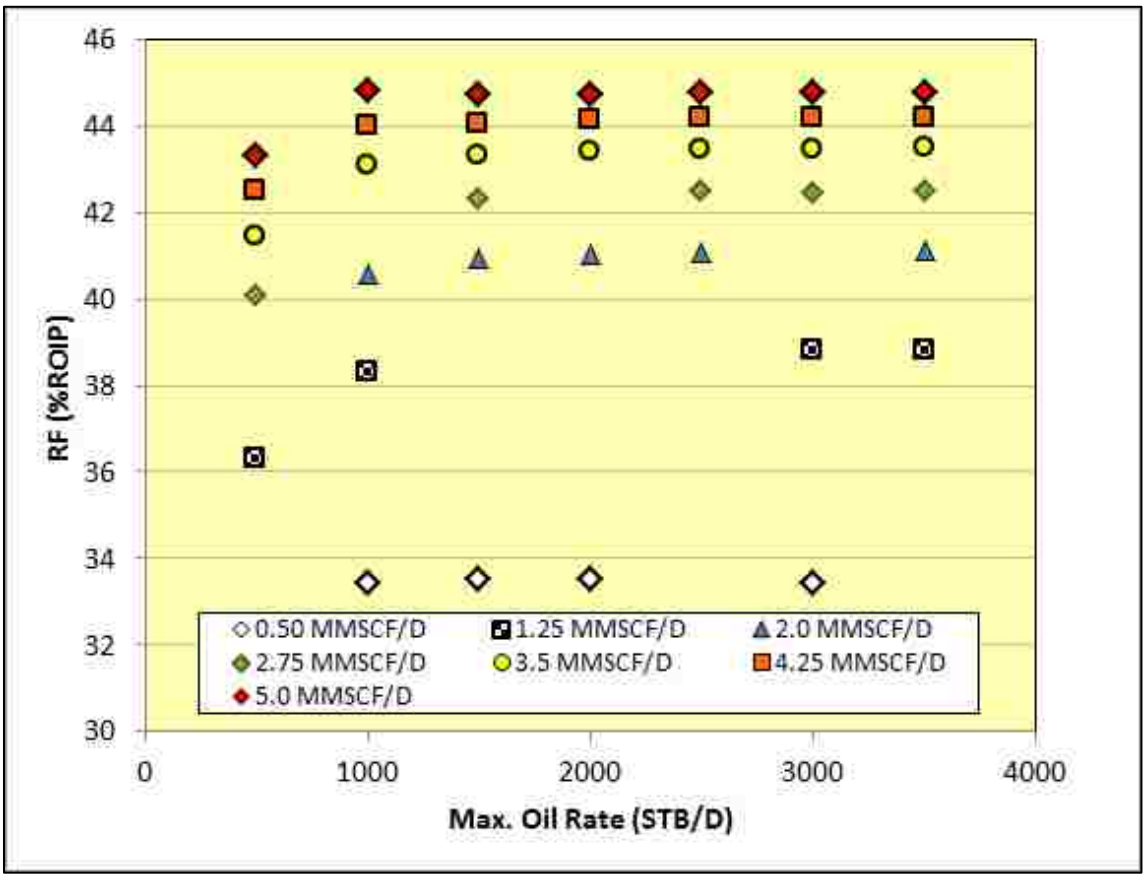

Figure 4.15: Multi-Well GAGD Recovery Factor vs. Oil Production Rate – Reservoir Model

The results have again been grouped, but this time by the gas injection rate. The figure clearly shows that the RF is influenced mostly by the gas injection rate rather than by the oil production rate. As the gas rate is increased, the RF results move up higher and higher, whereas there is no trend visible with relation to the oil production rate. The RF-values were also plotted as a function of both operational constraints as can be seen in the contour plot of Figure 4.16.

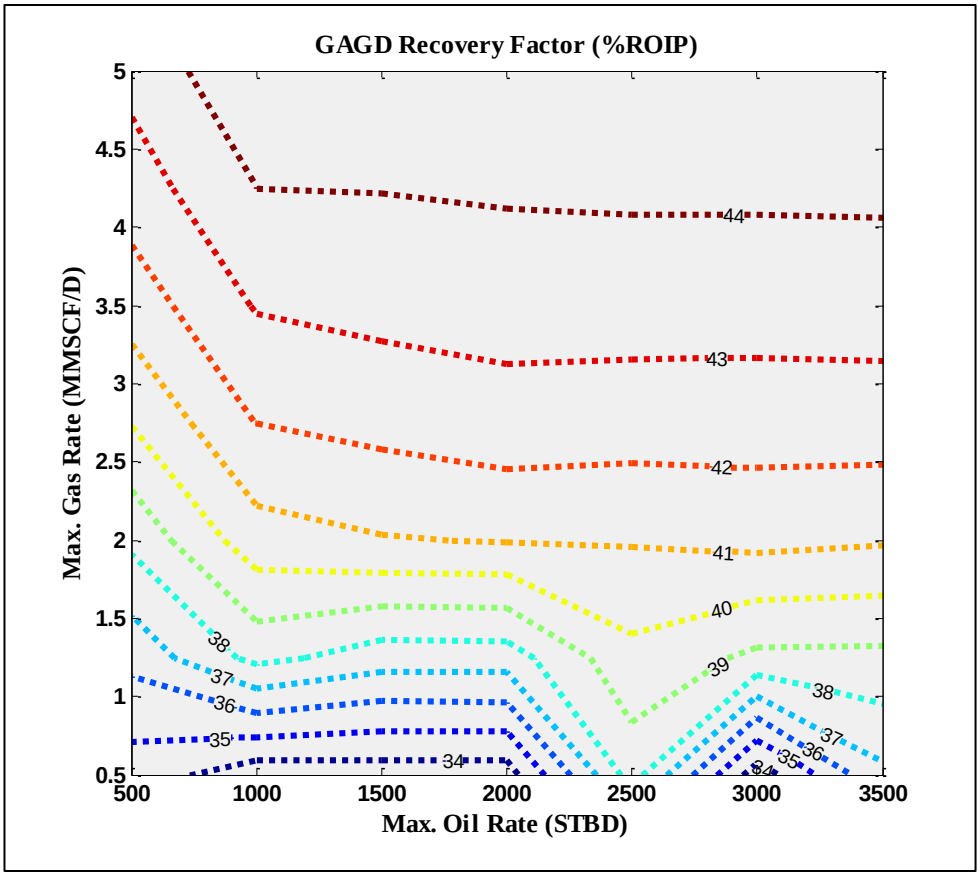

Figure 4.16: Contour Plot of Multi-Well GAGD Recovery Factor – Reservoir Model

The contour plot shows a broad overview of how the RF changes as different values of the operational constraints are chosen during the optimization study. It is very useful in showing that at some point there comes a point of diminishing returns which in turn is very helpful in choosing the final operational constraints to be used to generate the oil production history needed for the economic analysis.

2. The grid block size:

   In order to confirm the absence of the effect of numerical dispersion and/or a capillary transition zone on the oil recovery, a refined full-scale reservoir model was composed with grid refinement in the Z-direction, i.e. instead of using four grid blocks in the vertical

direction the refined reservoir model utilized 12 grid blocks in said direction. This effectively reduced the grid block thickness from 8.8 feet to 2.9 feet in the thickest part of the reservoir model. For the most part, the same operational constraint ranges were used with this refined reservoir model in the CMOST exploration study. The CMOST RF results (in %ROIP) are displayed in Figure 4.17.

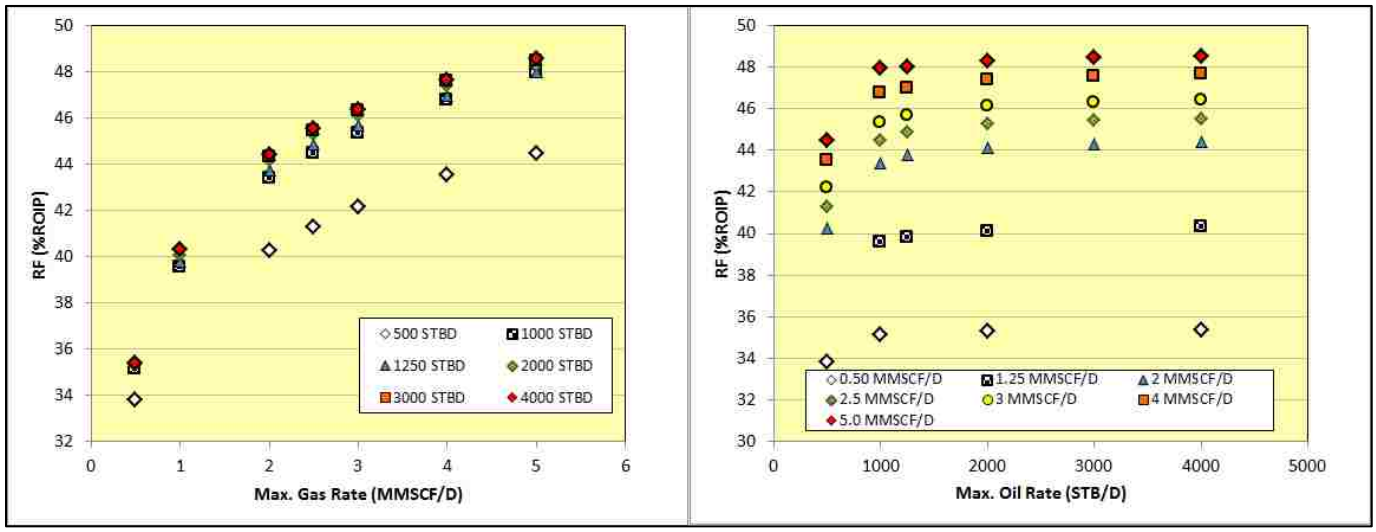

Figure 4.17: Multi-Well GAGD Recovery Factor vs. Gas (Left) and Oil (Right) Rate – Refined Reservoir Model

The RF-values resulting from using the refined reservoir model are very similar to the previously shown results using the four-layered model: there is a strong positive correlation with the gas injection rate while the oil production rate does not seem to influence the ultimate recovery as much. In order to compare the simulated RF results as a function of the number of layers they have been plotted in a column chart that includes error bars based on the standard deviation of each sample population (please refer to Figure 4.18). The column chart below shows that when the error bars are taken into account, there seems to be no significant difference between the RF-results of the four-layered and the refined reservoir model simulations.

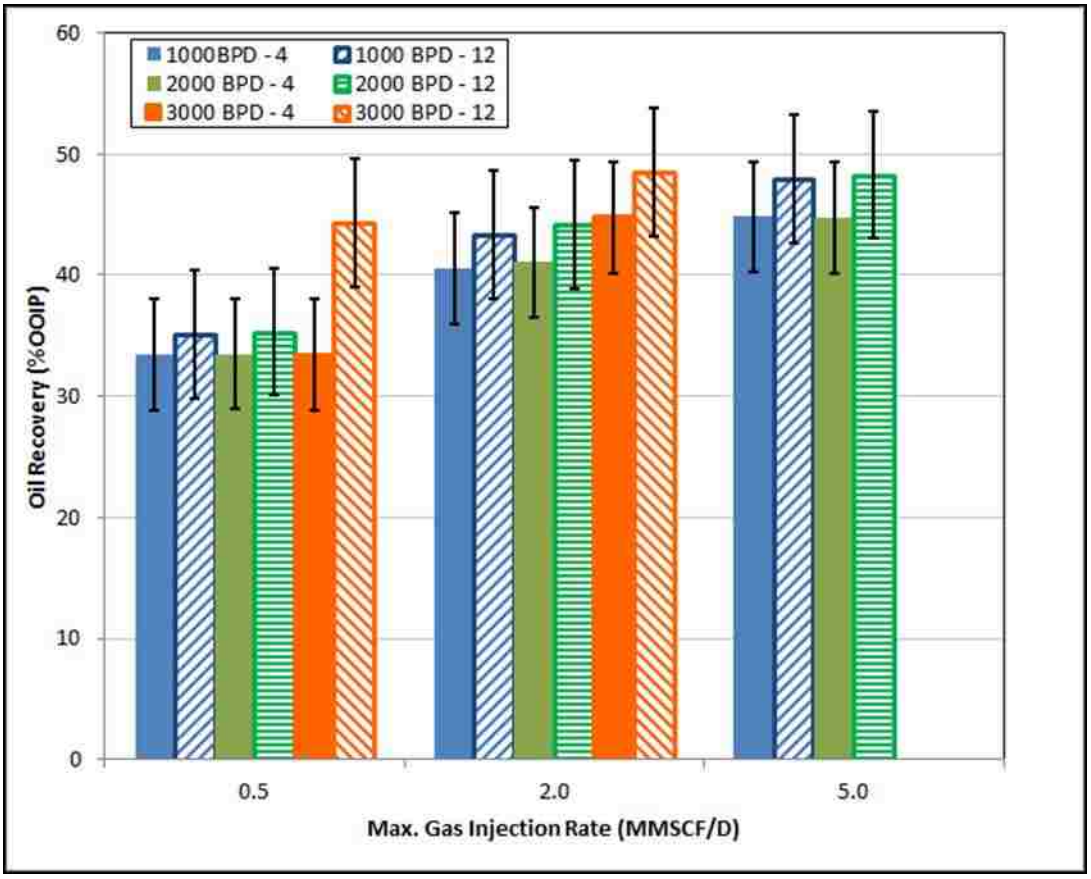

Figure 4.18: Comparison of the Effect of Grid Refinement on Multi-Well GAGD Recovery

3. The presence of a flow barrier:

   Even though no well logs were available that confirmed the presence of field-wide shale layers that would impede fluid flow, the effect of its occurrence was investigated using the refined reservoir model. Shale layers usually have a very low permeability and as such, a flow barrier was defined in the reservoir model to mimic the effect a field-wide shale layer would have on the ultimate oil recovery. A horizontal permeability reduction factor of 1 percent was utilized to define the flow barrier while its location was chosen in the CMOST study as layer 3, 6 or 9, i.e. the refined (12-layered) reservoir model was used at this point. In

the whole of the simulation study, the vertical permeability was defined by using a scaling factor, also known as the k_v/k_h-ratio, equal to 0.10. The CMOST simulation results have been summarized using similar charts as before. Figure 4.19 shows a side-by-side depiction of the simulated RF (in %ROIP) as a function of the operational constraints.

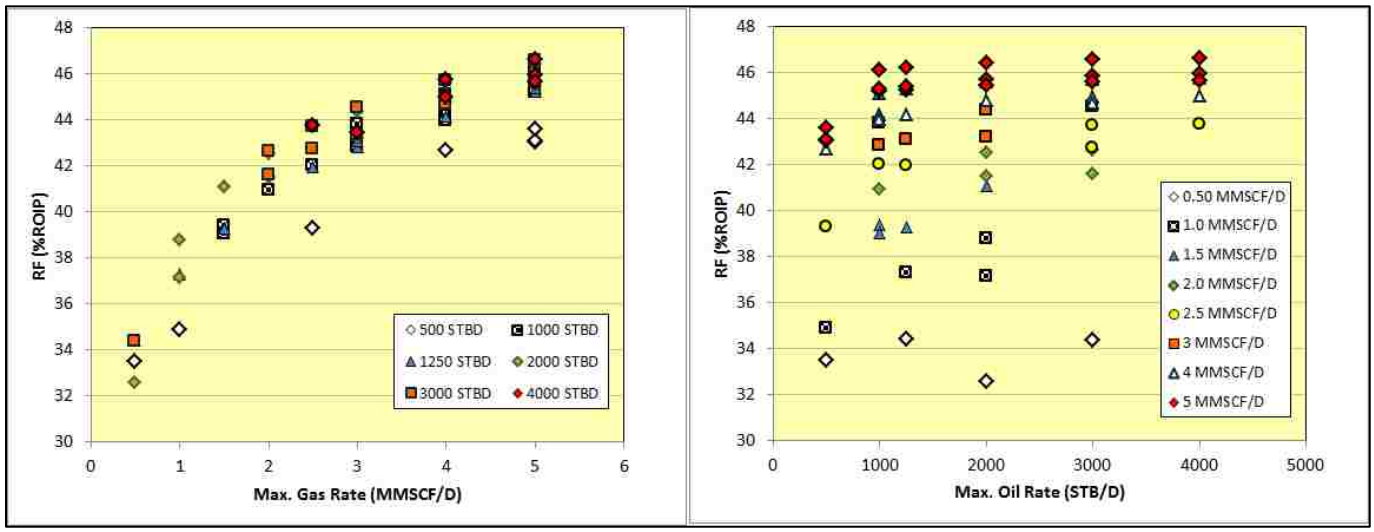

Figure 4.19: Multi-Well GAGD Recovery Factor vs. Gas (Left) and Oil (Right) Rate – Reservoir Model With Flow Barrier

Again, the overall results are very similar to what was previously revealed although the scatter in the RF-results as a function of the gas rate seems to be slightly greater indicative of the effect of the presence of the flow barrier. The presence of the flow barrier is also evident in the graph depicting the results as a function of the oil rate where a despite the significant scatter a slight linear trend is visible when viewing the grouped results. This means that there seems to be a dependency on both the gas injection (mainly) as well as the oil production rate (slightly). The main dependence on the gas injection rate is further supported if the results are plotted as a function of the relative position of the flow barrier, but grouped by the gas injection rate (Figure 4.20).

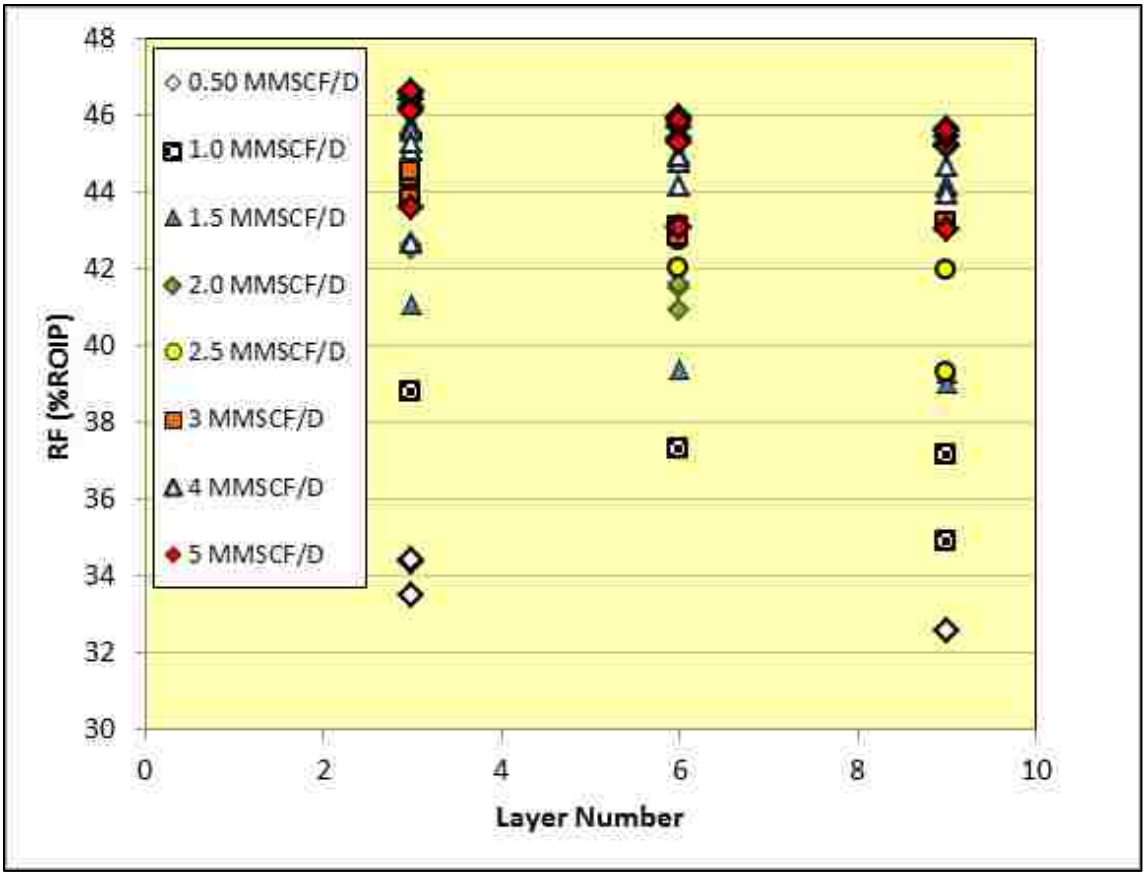

Figure 4.20: Multi-Well GAGD Recovery Factor vs. Flow barrier Position – Reservoir Model

The figure above shows that regardless of the position of the flow barrier, the RF increases as the gas injection rate is increased. The question, however, still remains whether the presence of a field-wide shale layer would have a negative impact on the ultimate recovery. This can be answered when the RF-results are compared to the barrier-free CMOST results (please refer to Figure 4.21). The column chart provides an easy means of assessing the effect of a field-wide flow barrier on the ultimate oil recovery and the incorporated error bars (again, one standard deviation) reveal that there seems to be no significant effect due to the presence of a shale layer in the Buckhorn Field.

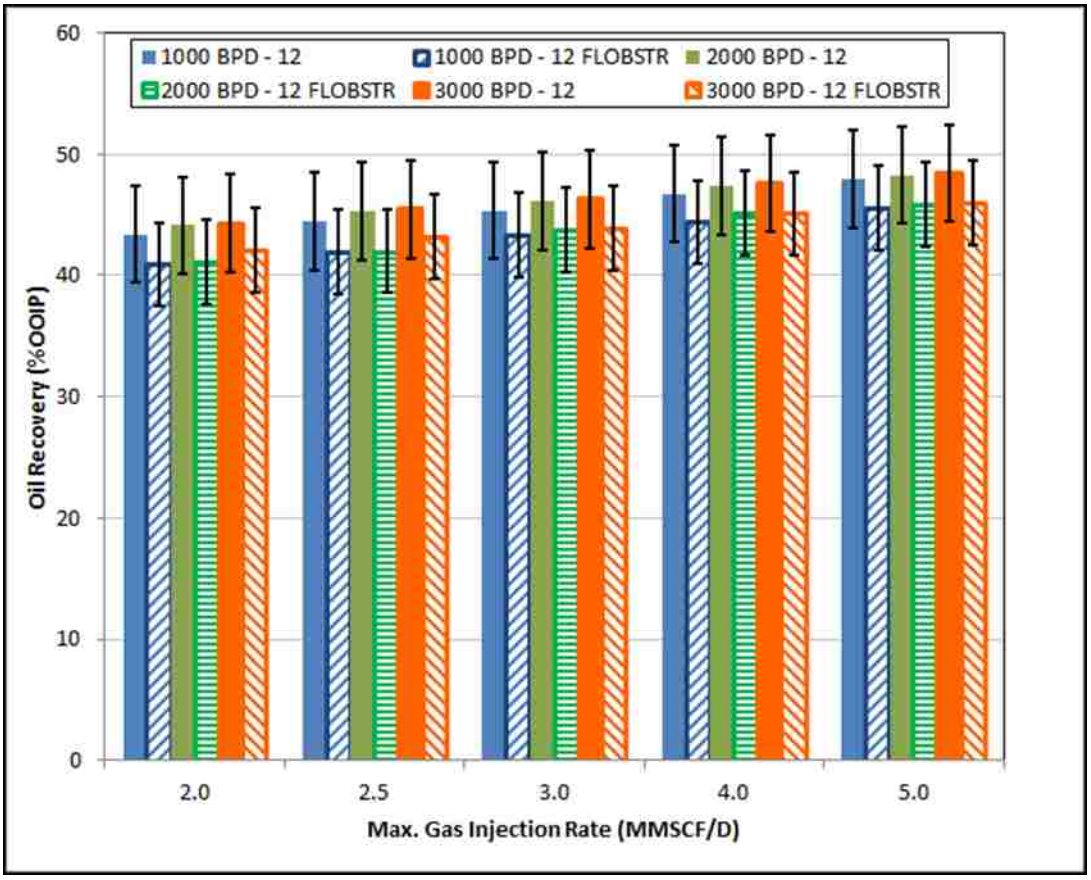

Figure 4.21: Comparison of the Effect of Flow Barrier on Multi-Well GAGD Recovery

Even though the ultimate recovery is not negatively affected by the presence of a shale layer in the field, it does have an effect on the overall fluid drainage pattern. This is evident when the gas saturation over time is tracked in the Buckhorn Field. The gas saturation evolution (maximum gas injection rate: 1MMscf/day; maximum oil production rate: 1000 STB/day) is depicted in Figures 4.22A and 4.22B showing a cross-sectional view through the reservoir. In the graph one of the vertical injection wells, G1, is visible. In this scenario, the gas is injected across the whole length of the wellbore and the flow barrier occurs in layer 6. As can be seen from the figure, the flow barrier (shale layer) affects the manner in which the gas zone grows laterally. Figure 4.22A shows the gas saturation profile two years after the start of the gas injection and the

shale layer clearly hampers the gas that is injected beneath the flow barrier from contributing to the growing gas zone above it. Instead it grows laterally beneath the flow barrier itself pushing itself further downdip than would have occurred without it.

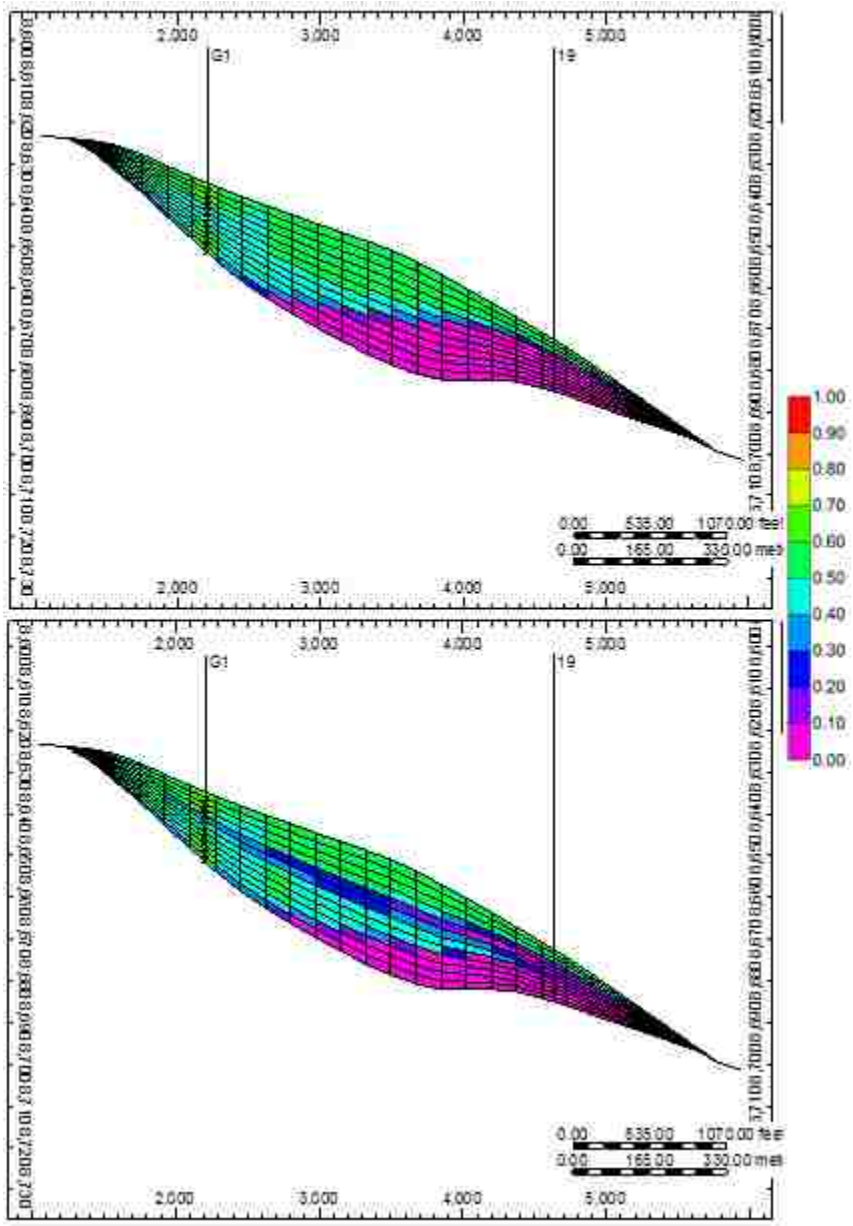

Figure 4.22A: Gas Saturation Profile in the Presence of Flow Barrier – 2 Years after Start of Multi-Well GAGD

The presence of the shale layer is felt throughout as is depicted in Figure 4.22B showing the gas saturation four years after the start of the project: the injected gas is never fully able to enter the shale layer itself and thus, cannot displace all of the oil contained within it. This indicates that any reduction in the ultimate recovery is possibly due to oil being trapped in the shale layer.

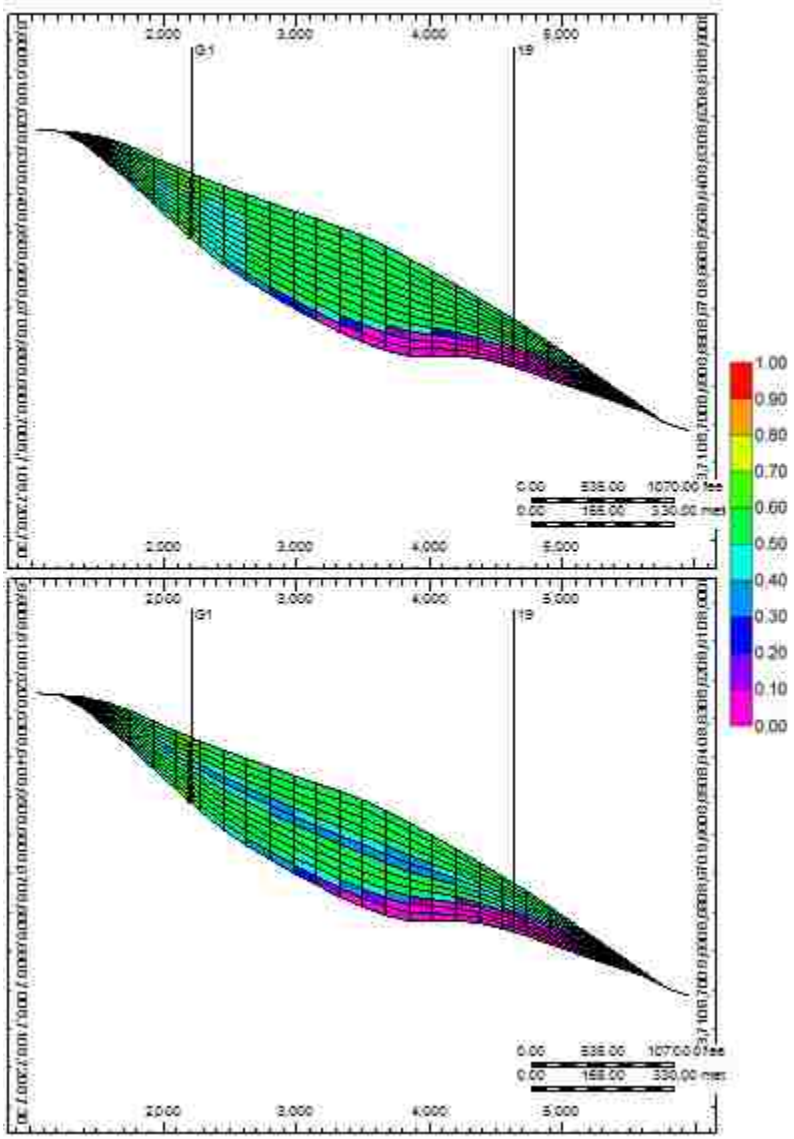

Figure 4.22B: Gas Saturation Profile in the Presence of Flow Barrier – 4 Years after Start of Multi-Well GAGD

All of the CMOST exploratory results were taken into consideration to determine the appropriate values of the operational constraints to investigate the GAGD performance in the Buckhorn Field. Ultimately, the values of the operational constraints that were used in this field-scale numerical simulation study of the GAGD development using both Berea and reservoir core permeability data were:

- Three levels for the CO_2 injection rate – 1, 2 and 3 MMscf/day/well. These rates were set maximum allowable rates, i.e. the rate was constricted to not exceed these values.
- Four levels for the oil withdrawal rate (500, 1250, 3000 and 5000 BPD/well). Again, the production rates were defined as maximum allowable fluid rates.
- A maximum injection pressure 4500 psi.
- A minimum wellbore pressure in the producers of 500 psi.
- All simulations ran approximately 8 years from 2006 to 2014.

Using the values as outlined above, oil production profiles were generated that were then used as input in the economic assessment of the multi-well GAGD process in the Buckhorn Field. The subsequent simulation studies of any other EOR process as described in the sections to follow had the same objective.

In order to highlight the effect of utilizing the relative permeability data derived from coreflooding experiments using Berea sandstone versus reservoir core material in the simulation study, the simulation results for total GAGD recovery (in %ROIP) for both have been summarized in Tables 4.6A and 4.6B and Figure 4.23A and B. The simulation results indicate that as the injection rate is increased it leads to an increase in the GAGD recovery. These trends are more clearly visible in the three-dimensional column chart of Figure 4.23B. It depicts the

effect of the CO_2 injection rate and the oil withdrawal rate on the GAGD recovery simulation results when using the reservoir core data. It can be clearly seen that an increase in the GAGD recovery is attained when both the gas injection as well as the oil production rate are increased for both cases (when either Berea or reservoir core data was used). Closer examination of the column chart in Figure 4.22A shows that the dependency of the recovery factor on the gas injection rate is stronger when the reservoir rock data is used as opposed to the Berea data where an increase in the gas injection rate only marginally improves the oil recovery.

The differences in relative permeability curves between the corefloods using reservoir cores versus Berea cores do not appear to result in oil recovery numbers that show a diverging or conflicting picture, but rather, the beneficial trend of higher recoveries with increasing oil withdrawal rates highlights the gravity-stable displacement occurring during application of the GAGD process.

Table 4.6A: GAGD Performance Simulation Results – Berea Sandstone

Gas injection rate (MMSCFD/well)	**1**	**2**	**3**
Max. Oil Prod. Rate (BPD/well)	**Incremental Recovery (%ROIP)**	**Incremental Recovery (%ROIP)**	**Incremental Recovery (%ROIP)**
500	54.6	57.8	59.3
1250	54.0	56.0	57.1
3000	53.4	55.0	55.8
5000	53.1	54.6	55.5

Table 4.6B: GAGD Performance Simulation Results – Reservoir Rock

Gas injection rate (MMSCFD/well)	**1**	**2**	**3**
Max. Oil Production Rate (BPD/well)	**Incremental Recovery (%ROIP)**	**Incremental Recovery (%ROIP)**	**Incremental Recovery (%ROIP)**
500	47.7	51.7	54.6
1250	50.3	55.0	57.4
3000	50.6	55.4	57.7
5000	50.6	55.4	57.8

For any gas injection process it is important to maximize the incremental oil recovery per unit of injected gas volume, a parameter also referred to as the gas utilization factor (GUF), often in units of MSCF/STB. For the conventionally used gas injection EOR processes, such as the continuous gas injection or Water-Alternating-Gas process, this gas utilization factor typically falls within the range of 6-12 MSCF/STB (Brock and Bryan, 1989; Kulkarni and Rao, 2004) depending on whether the gas injection process is applied under miscible conditions or not. Implementing a gas injection EOR process under miscible conditions often leads to a more efficient use of the injected gas for oil recovery purposes, thus, ultimately resulting in lower GUF-values. The simulation results from our study have shown the GUF to be possibly quite lower indicating the improved efficiency of the GAGD process when applied in the Buckhorn Field. The gas utilization factors for both stages of the simulation study are summarized in Table 4.7 and clearly indicate a higher efficiency of the GAGD process when compared to the previously mentioned conventional gas injection EOR processes.

Table 4.7: Gas Utilization Factor of GAGD Application in Buckhorn Field

	Berea	Buckhorn	Berea	Buckhorn	Berea	Buckhorn
Gas Injection Rate (MMSCFD/well)	**1**		**2**		**3**	
Production Rate (BPD/well)	**Gas Utilization Factor (Mscf/STB)**		**Gas Utilization Factor (Mscf/STB)**		**Gas Utilization Factor (Mscf/STB)**	
500	2.0	2.5	3.2	4.7	3.7	6.7
1250	1.4	2.5	2.7	4.7	3.7	6.7
3000	1.4	2.5	2.8	4.7	3.9	6.7
5000	1.4	2.5	2.8	4.7	4.0	6.7

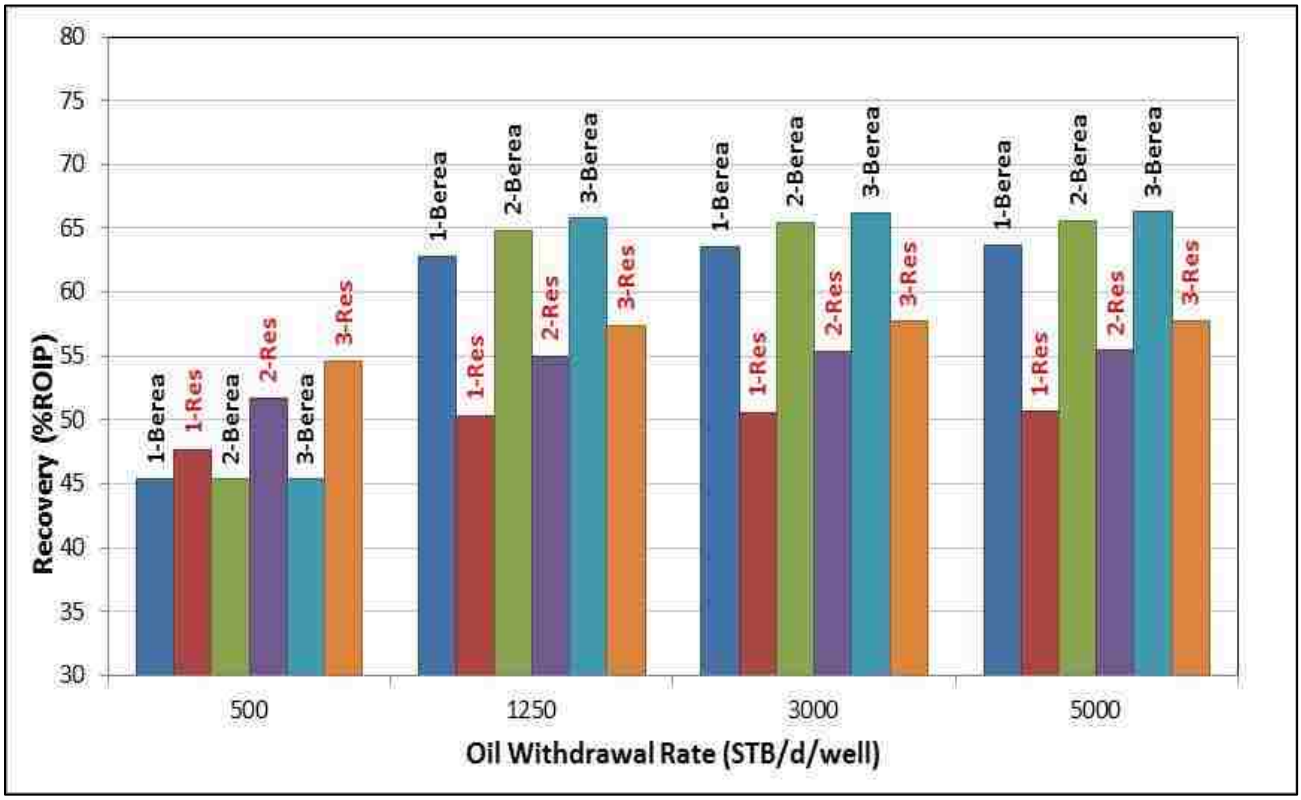

Figure 4.23A: Comparison of GAGD Recovery as Function of Gas Injection and Oil Production Rate – Berea (Black); Reservoir Core (Red)

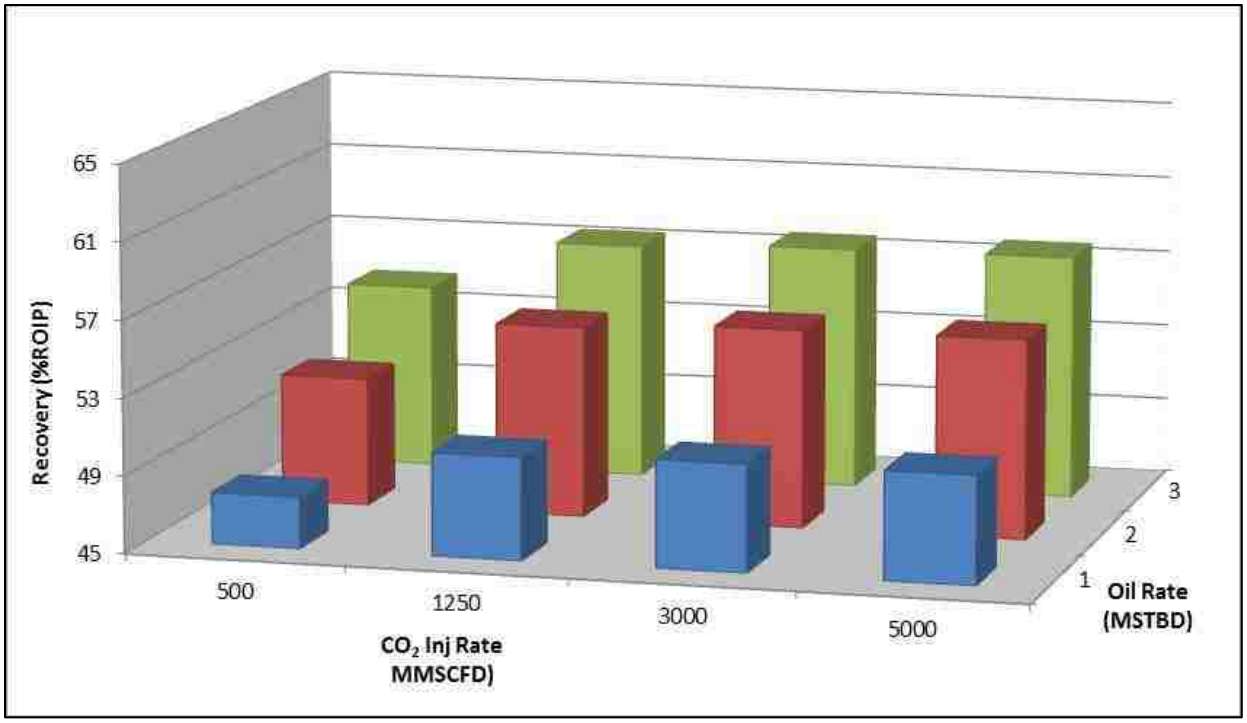

Figure 4.23B: Graph of the Effect of Varying Gas Injection and Surface Oil Rate on Incremental Recovery in Buckhorn Reservoir Rock-Fluid System

4.4 Single-Well GAGD Application in the Buckhorn Field

4.4.1 Introduction

One of the possible alternative ways of applying the GAGD process in the field is the so-called single-well application (SW-GAGD) in which a vertical well (either existing or newly drilled) is completed in such a way that the uppermost perforations are used to inject the displacing gas while the lower perforations are used to produce the reservoir fluids. This is a departure from the conventional GAGD process application in which multiple well pairs are used to drain a reservoir. Each well pair consists of a vertical gas injector and a horizontal producer which ideally has its horizontal leg as close as possible to the bottom of the payzone and/or the oil-water contact. In the proposed alternate configuration multi-completion single wells will be used to produce as much oil from the Buckhorn field through the injection of CO_2 in the upper

perforations and producing reservoir fluids from the lower completions. A diagram of the single-well GAGD process is depicted in Figure 4.24 (adapted from a drawing by Saikia (2012)).

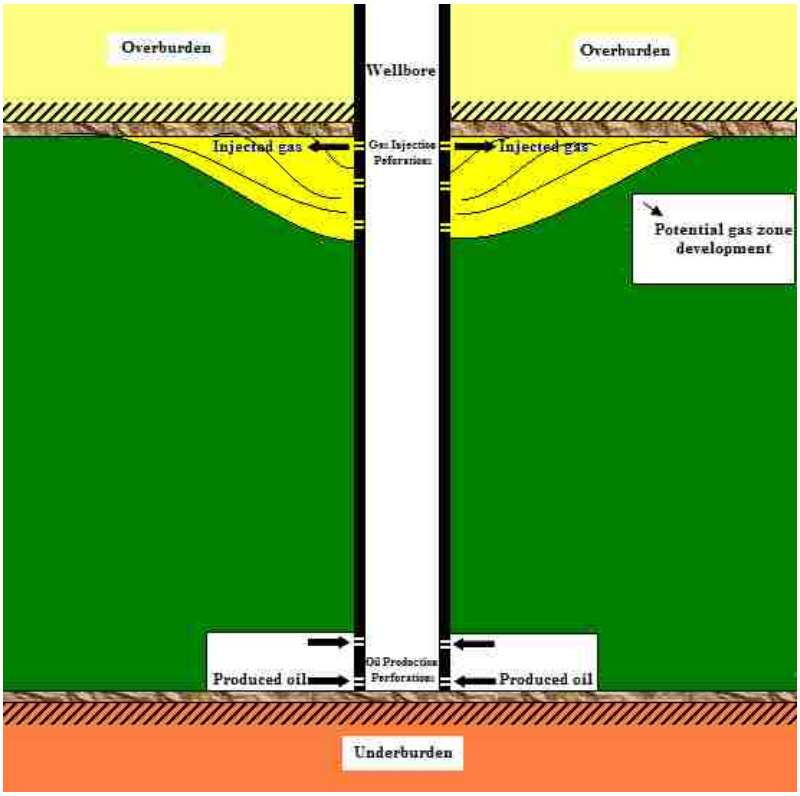

Figure 4.24: Schematic Drawing of the Vertical Single-Well GAGD Process (Saikia, 2012)

4.4.2 Objective

The objective of this phase of the simulation study is to investigate the potential oil recovery in the Buckhorn field when the GAGD process is applied using single wells with multiple completions. To this end, field-scale numerical simulations were conducted using CMG's GEM, a compositional simulator. The GAGD oil recovery as referred to in this study is taken as the incremental recovery over the initial oil recovery during the primary depletion and waterflooding stage of the field development and as such, is always expressed in terms of percentage of the residual oil in place, %ROIP.

4.4.3 Numerical Study of the SWGAGD Process

4.4.3.1 Block SWGAGD Model – Description

As a starting point of the current simulation study the previously compiled reservoir and PVT model were used, as well as the most recent relative permeability curves derived from coreflooding experiments using reservoir core samples. However, they were applied not in the full-scale field model, but rather, in a much simpler block-shaped reservoir model to investigate the importance of the gas injection and oil production rate, the presence and severity of flow barriers, and the configuration of the SWGAGD well on the ultimate oil recovery. The dependence of the SWGAGD oil recovery on the gas and oil rate was investigated over a wide range of values, as was the location and magnitude of the flow restriction (mimicking a field-wide shale layer).

In order to be able to isolate the effect of the aforementioned parameters on the SWGAGD recovery, it was decided to compile a very simple synthetic, block-shaped reservoir model that was very homogeneous, but at the same time it incorporated some of the same model parameters as the full-field numerical model. Some of the shared parameters were: the reservoir fluid model, the liquid-liquid and gas-liquid relative permeability curves and a representative value for both the porosity and the horizontal permeability, namely 23.5 percent and 200 mD, respectively. The block reservoir model had an area of 50 acres and a thickness of 25 feet with a total number of gridblocks of 6250. All simulations conducted with the synthetic block models spanned 10 years. Figure 4.25 shows a side (cross-sectional) view of the synthetic block model with the vertical SWGAGD well visible in the center of the model. The vertical SWGAGD has its production completions in layers 8 to 9 while gas is injected in layers 1 and 2.

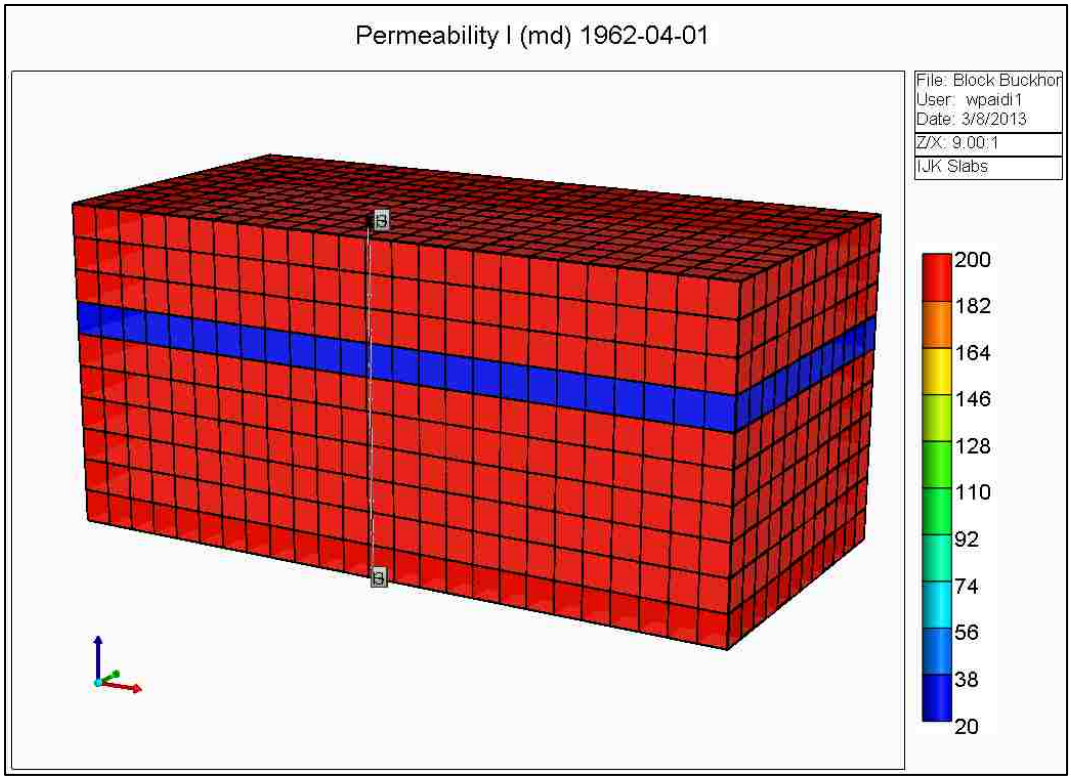

Figure 4.25: Cross Sectional View through SWGAGD Block Model

Apart from the vertical trajectory of the SWGAGD well as depicted above, another variation of the SWGAGD process investigated was one in which the production occurred from the horizontal section of the well as is depicted in the schematic drawing in Figure 4.26. The choice for placing the production completions in an offset (horizontal) section of the SWGAGD well was made to possibly improve the drainage patterns due to the increased well exposure of a horizontal well. The decrease in the well drawdown by using this configuration might also lead to higher SWGAGD recoveries, and perhaps improved gas efficiency. A block synthetic model of this alternate configuration was also composed in a similar manner as before and is shown in Figure 4.27A and B. In this configuration all of the production completions are along the horizontal section of the well which is fully contained in layer 9.

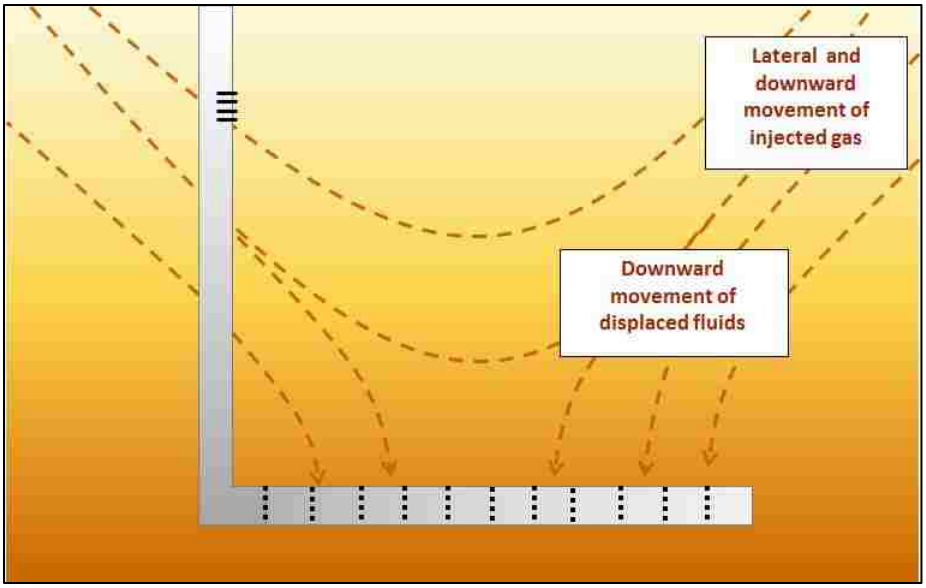

Figure 4.26: Schematic Drawing of the Horizontal Single-Well GAGD Process

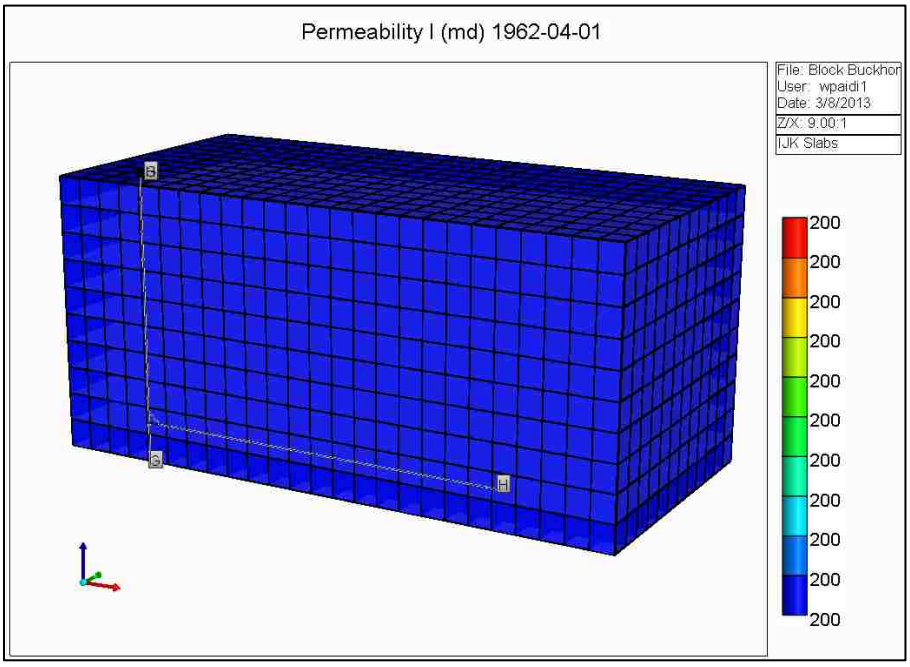

Figure 4.27A: Cross Sectional View through SWGAGD Block Model – Horizontal Variation

The aforementioned synthetic block reservoir models were used to explore and optimize both variations of the single-well GAGD process as was previously done with the multi-well GAGD process.

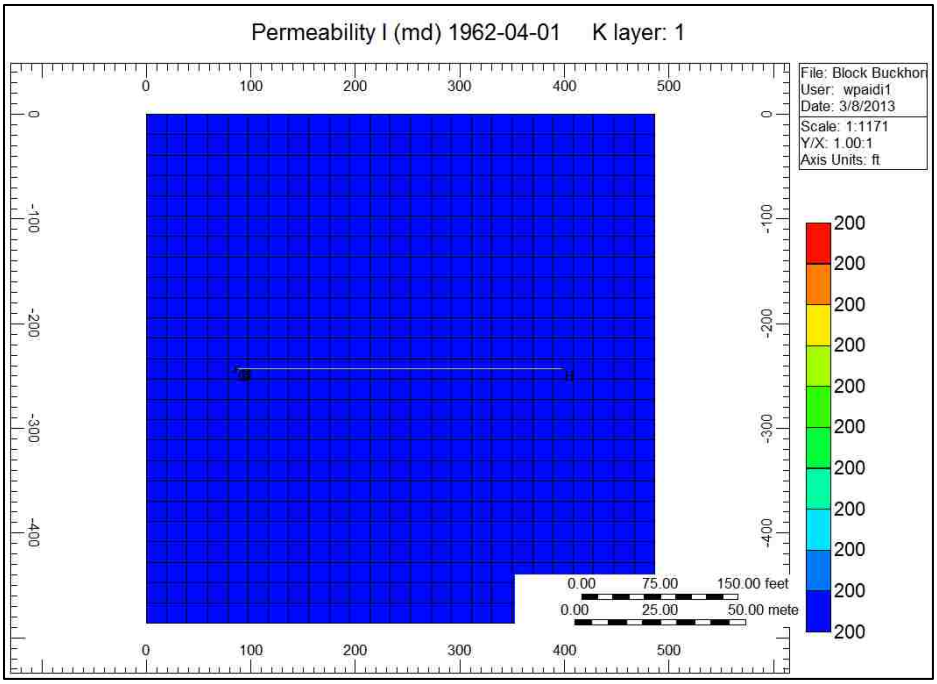

Figure 4.27B: Areal View SWGAGD Block Model – Horizontal Variation

In both variations of the SWGAGD process (vertical versus horizontal well) the same range of values was used in the optimization study as follows:

- CO_2 injection rate:

  The gas injection rate was defined within the range of 0.5 to 2MMSCF/day for a total of 10 possible values that are equally spaced.

- Oil production rate:

  The oil rate was varied from 100 to 3000 BPD divided over 10 equal intervals.

- Depth of the flow obstruction:

  In this case, a flow obstruction was again defined as a layer with a permeability that was 10 percent of the original horizontal permeability value. The position of the layer was varied within the 10 possible layers but restricted to layers 4 to 8. This means that neither the injection nor the production completions were ever in the layer that was defined as the flow

barrier. The logic behind this choice is that in most cases completions are not performed in a shale layer or other tight/impermeable layer, which the flow obstruction is a proxy for. Figure 4.25 shows the depth of the flow barrier as layer 4 (Z-direction increases downwards).

4.4.3.2 Block SWGAGD Model – Results

The results of the optimization of the vertical SWGAGD process using the synthetic block model are summarized in Figures 4.28-30. The recovery factor is plotted on the Y-axis against the optimization variables in each of the subsequent figures. Each recovery value is the combined effect of varying three optimization results and as such the interpretation of the depicted results may not necessarily be straight-forward. To aid in the interpretation of the CMOST results the various data points have been grouped by either the gas injection or the oil production rate.

Despite the combined effect of three different variables on the SWGAGD recovery factor, there is a very clear, not necessarily linear, trend visible when the recovery factor is plotted against the gas injection rate: an increase in the gas injection rate results in an increase in the SWGAGD oil recovery regardless of the value of the oil production rate or the depth of the flow barrier (Figure 4.28). The lack of significant scatter in the data indicates that the recovery factor is very dependent on the choice of the gas injection rate (as was expected). When looking at the graph of the plotted recovery factor against the oil production rate (Figure 4.29) it is clear that there is quite a bit of scatter in the data, as well as a lack of any discernible trend in the recovery factor with regards to the oil rate.

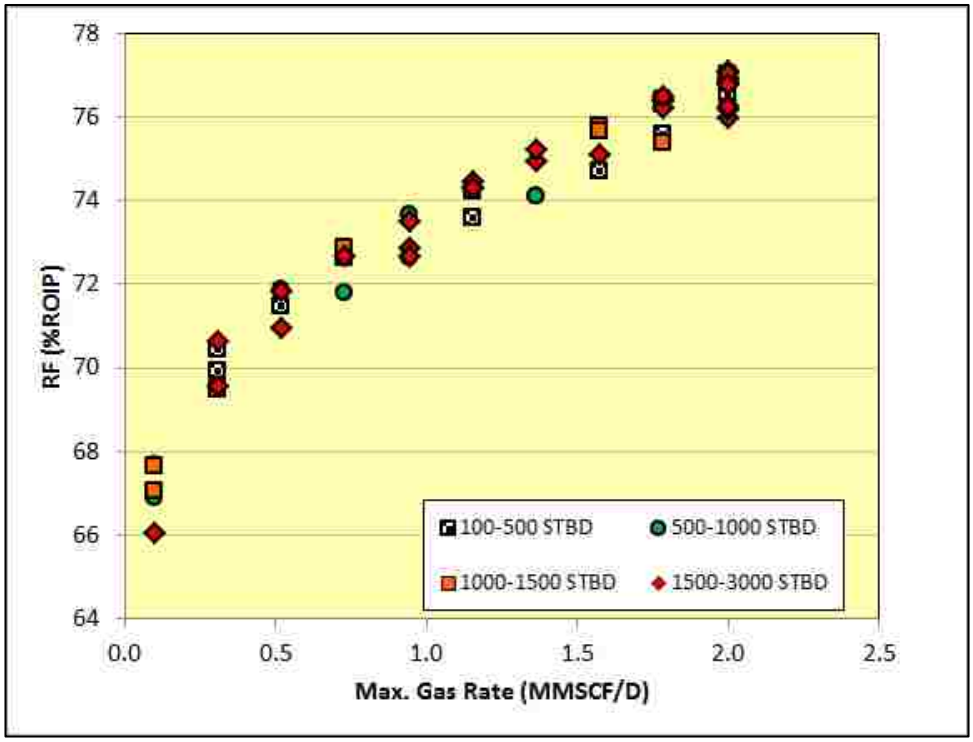

Figure 4.28: Vertical SWGAGD Recovery Factor vs. Gas Injection Rate – Block Model

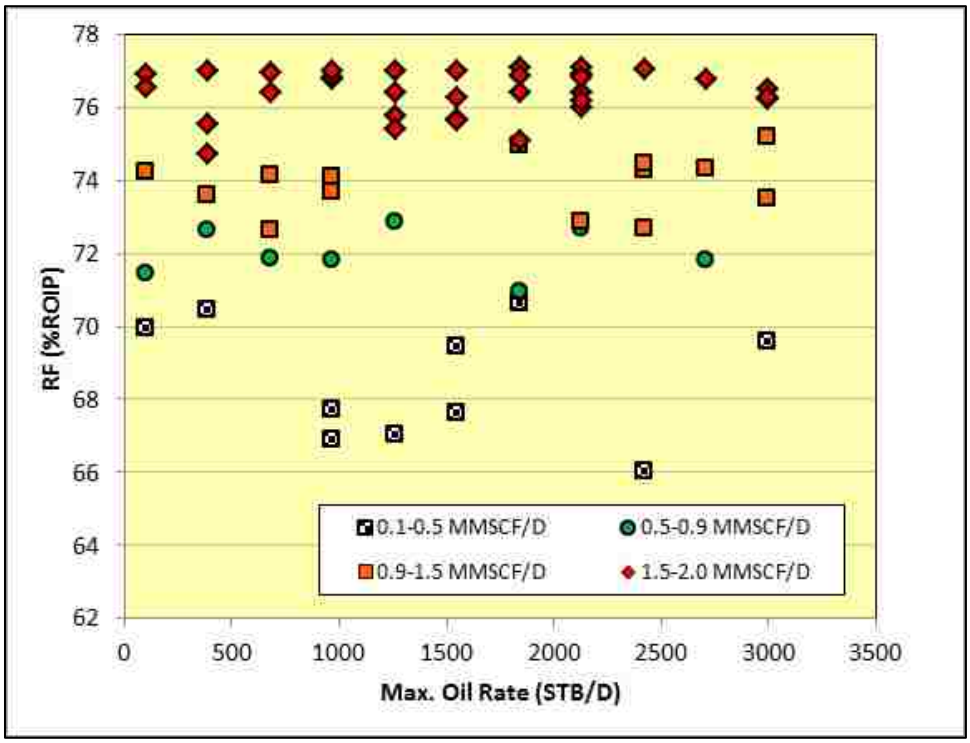

Figure 4.29: Vertical SWGAGD Recovery Factor vs. Oil Withdrawal Rate – Block Model

However, because of the grouping of the data based on the gas injection rate a correlation does appear. Upon a closer examination of the graphed results it is evident that as the gas rate is increased this resulted in an increase of the RF leaving only the effect of the depth of the flow barrier to be assessed.

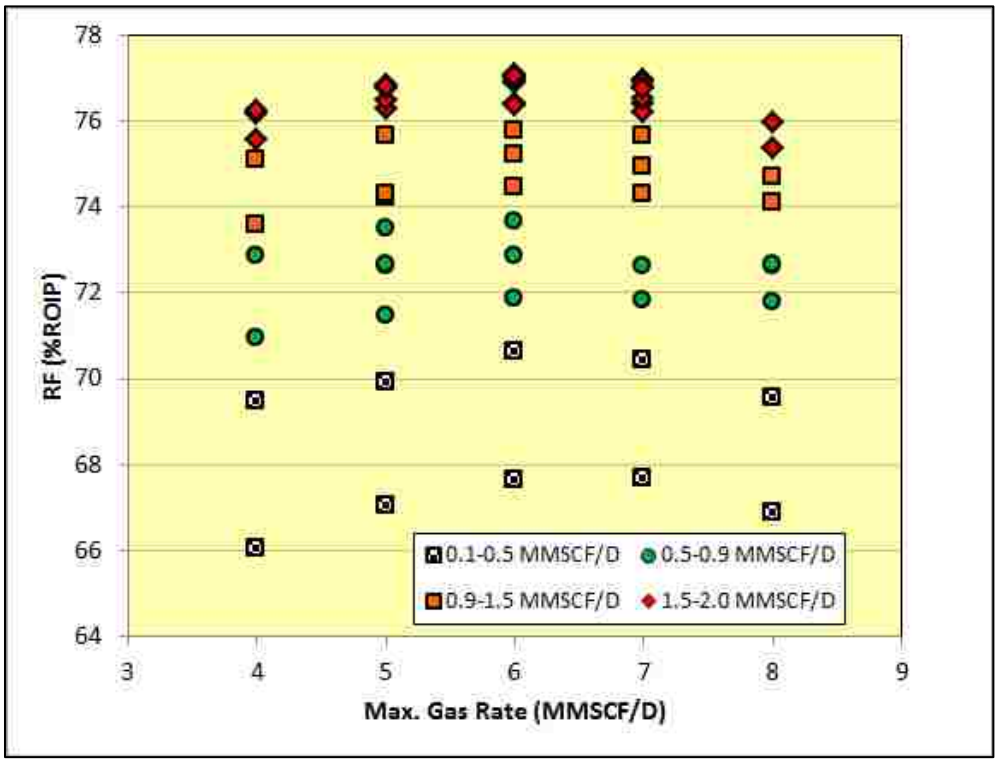

Figure 4.30: Vertical SWGAGD Recovery Factor vs. Depth of Flow Barrier – Block Model

A similar picture emerges when the recovery factor is plotted against the depth of the flow barrier (with a horizontal permeability of 10 percent of the rest of the reservoir) as there is again a lot of variability in the optimization results (Figure 4.30 above). However, there does seem to be a slight maximum visible when looking at the location of the optimum cases for the flow barrier being located in layer 6 (which is exactly in the middle of the synthetic block model). When the flow barrier occurs right in the middle of the reservoir it apparently seems to have a stabilizing effect on the displacement in the vertical SWGAGD configuration. Key to the

graph is that the presence of a flow barrier does not impede the SWGAGD recovery regardless of its relative location. A strong correlation with the gas injection rate is again very clear from this graph.

The same trends as described above for the SWGAGD optimization study using the vertical well configuration were also seen in the optimization study of the horizontal SWGAGD variation. Figures 4.31 to 4.33 show the recovery factor as a function of the gas injection and oil production rate, and the depth of the flow obstruction layer.

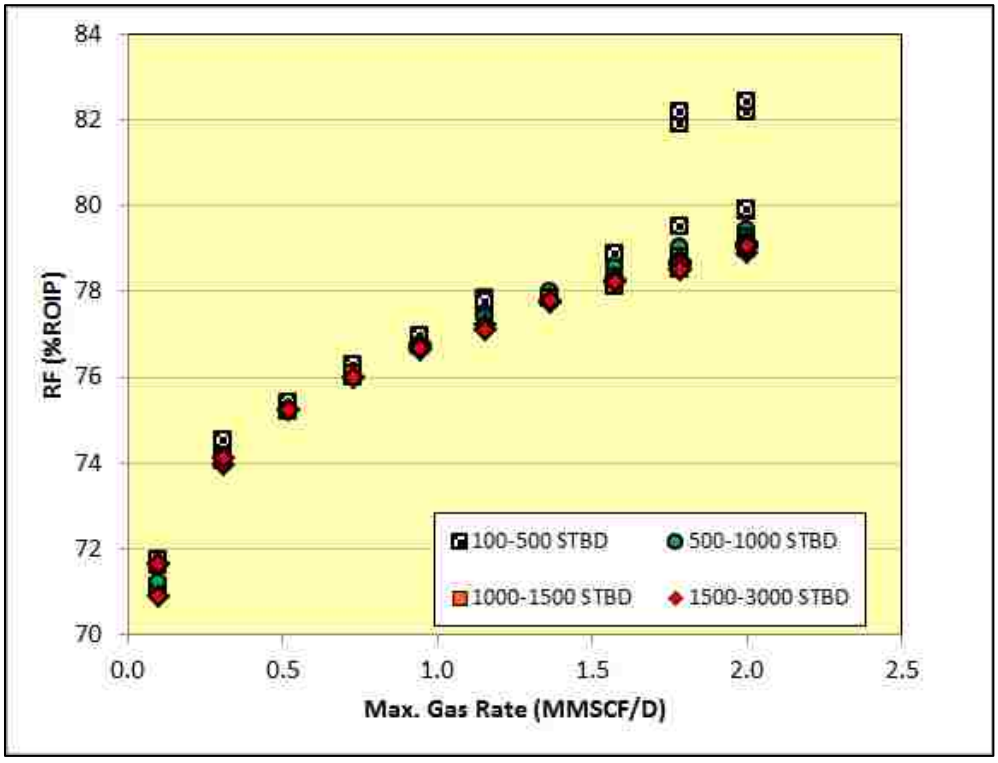

Figure 4.31: Horizontal SWGAGD Recovery Factor vs. Gas Injection Rate – Block Model

Apart from the fact that a strong positive relationship is revealed between the SWGAGD recovery factor and the gas injection rate (Figure 4.31), it is also worth noting that the oil recovery values are higher when compared to the vertical SWGAGD results. This indicates that using one horizontal well for both injection and production purposes does indeed lead to better

oil recovery results as was hypothesized before. Some of the highest RF-values were attained with the lower oil production rates in combination with the highest gas injection rates.

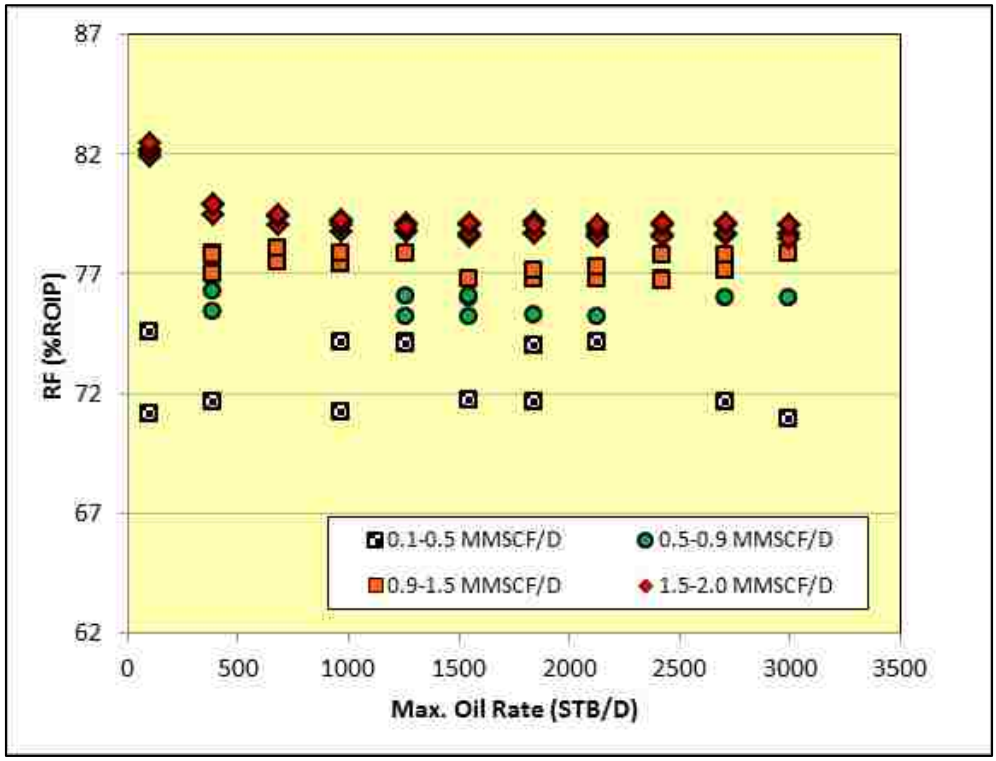

Figure 4.32: Horizontal SWGAGD Recovery Factor vs. Oil Withdrawal Rate – Block Model

The optimization of the horizontal SWGAGD process using the synthetic block model again showed that the oil recovery has very little dependency on either the oil rate (Figure 4.32) or the depth of the flow barrier (Figure 4.33), implying that when the SWGAGD process efficiency is to be simulated using the full-scale field model it will be the gas injection rate that shall prove to be the dominant factor influencing the ultimate oil recovery. As for the gas efficiency comparison between the two variations of the SWGAGD process it can be seen from Figure 4.34 that even though using a horizontal well does indeed result in better oil recovery numbers it does come at the cost of utilizing the injected gas less efficiently. This is indicated by the higher producing gas-oil-ratios of the horizontal SWGAGD process as compared to that of

the vertical configuration. This is possibly offset by the higher attained RF-values for the horizontal SWGAGD process as is evident from the RF-contour plots for both variations of the SWGAGD process in Figure 4.35.

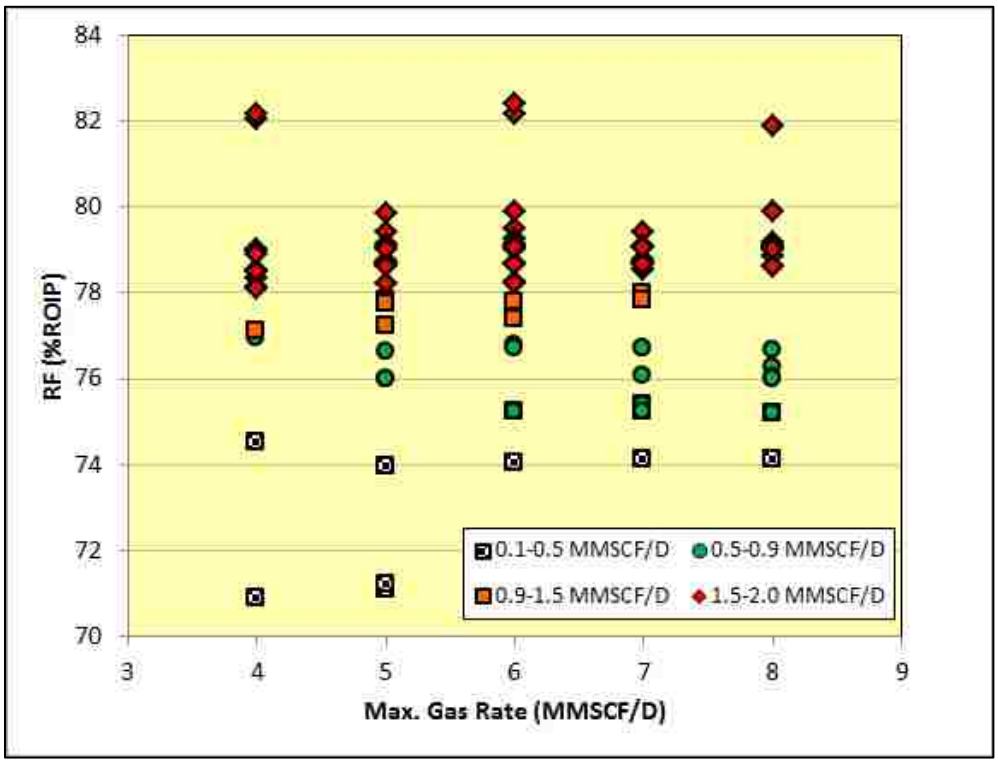

Figure 4.33: Horizontal SWGAGD Recovery Factor vs. Depth of Flow Barrier – Block Model

4.4.4 Field-Scale Simulations of the SWGAGD Process

The optimization study as described above was extended to the full-scale reservoir model to investigate whether the same trends as were seen with the synthetic block model would translate to the reservoir model. In order to accomplish this task, the contour plots of the block model RF as a function of gas injection and oil rate were assessed to choose appropriate values. As a result, the gas injection rate was chosen from within the range of 0.25 to 3 MMSCF/day while the oil production rate ranged from 500 to 3000 BPD.

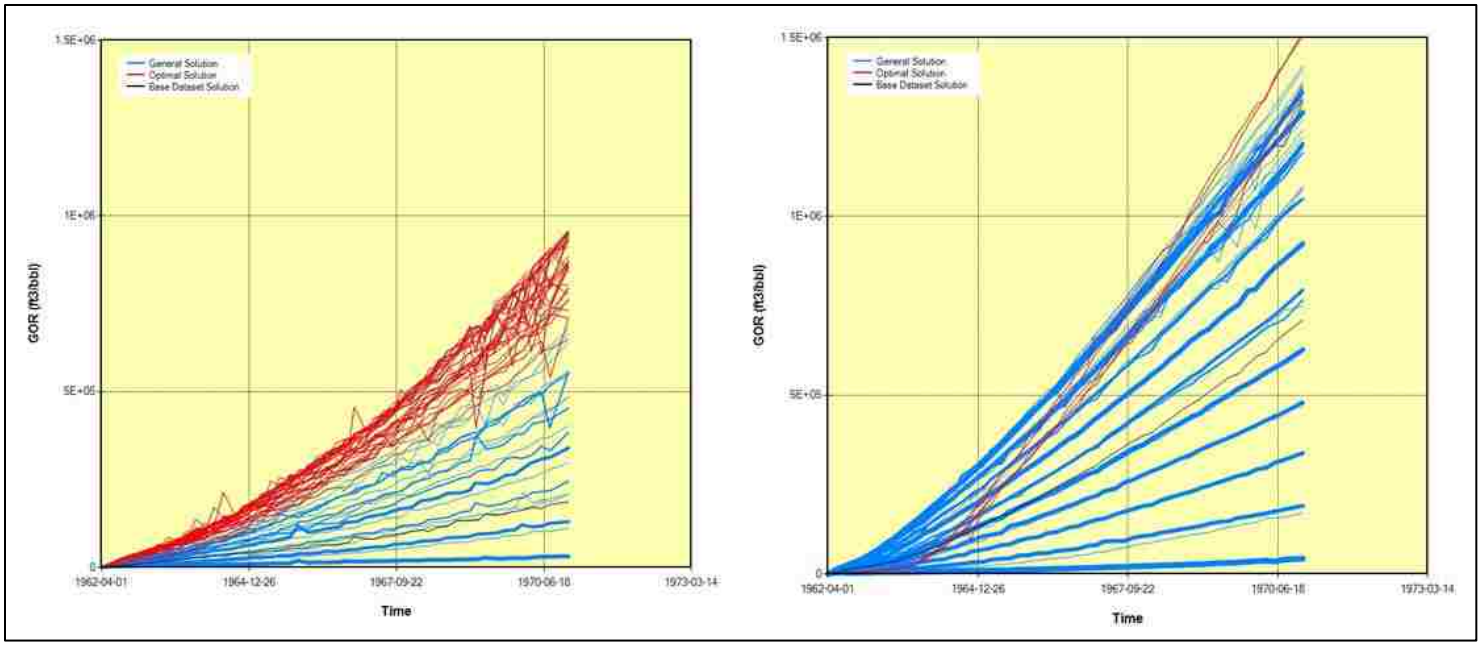

Figure 4.34: Gas Efficiency of Vertical (Left) and Horizontal (Right) SWGAGD – Block Model

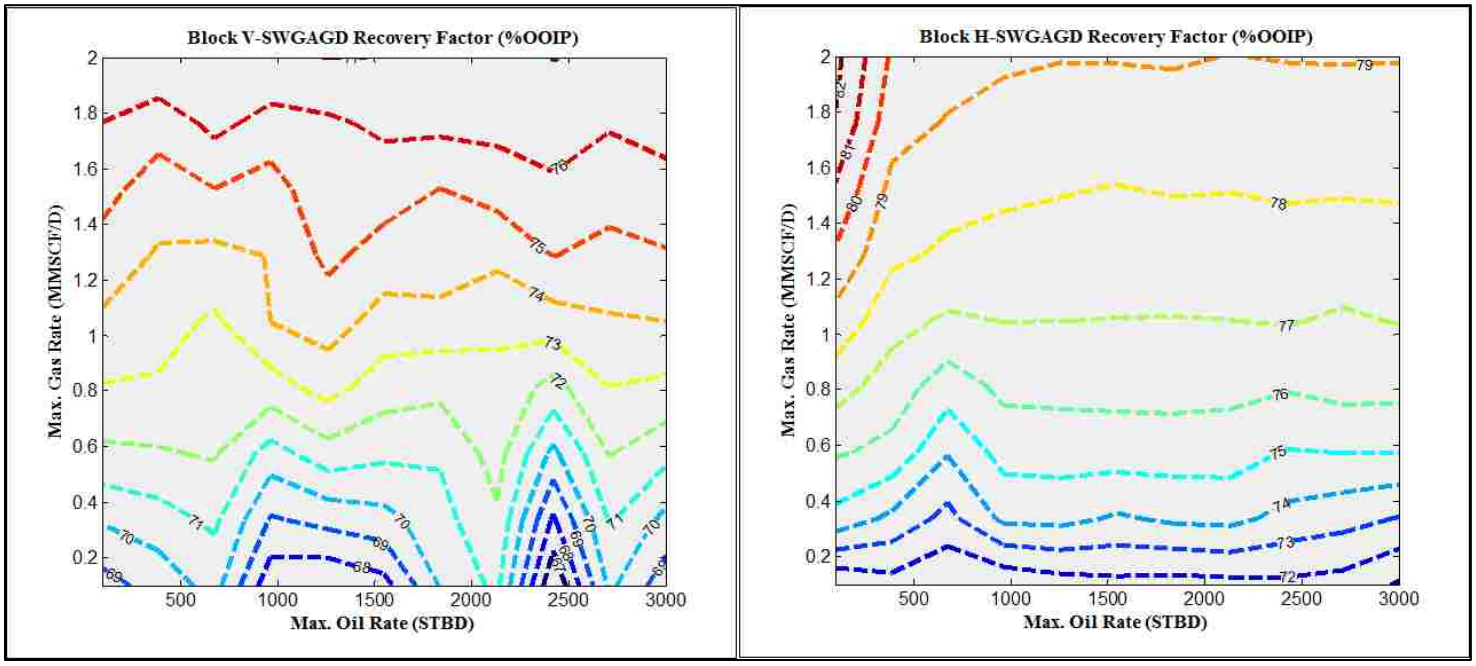

Figure 4.35: Contour Plots of Vertical (Left) and Horizontal (Right) SWGAGD Recovery – Block Model

4.4.4.1 Location of the GAGD Wells

It is expected that the final location of the GAGD dual-completion wells will an important aspect of the field application of SWGAGD. One of the ways of determining the future location of these wells is to place them such that they will be most effective in draining the remaining oil in place after the primary production and waterflooding stage. Maps of oil saturation could be helpful in finding the optimum well location but unfortunately at the end of the first production stage the oil saturation distribution map of the Buckhorn field did not prove to be helpful as can be seen in Figure 4.36. The areas of high oil saturation are too large to facilitate the decision where to place the GAGD wells. Another option would be to examine maps of so-called productive capacity which in this context was taken as the product of the oil saturation, the pay thickness, the effective porosity and the reservoir permeability. Figure 4.37 indicates that there are two defined areas with the highest production capacity potential that could be suitable for GAGD well placement. This option is depicted in Figure 4.38. The GAGD wells are indicated in the figure by red dots. The simulations were set up in a very similar manner to the previously discussed conventional GAGD runs in that there was a 6-month stagger between the well located in the Northern part of the field compared to the one in the Southern part of the Buckhorn field

4.4.4.2 Field-Scale Simulation Results – Vertical SWGAGD

The optimization study as described above was extended to the full-scale reservoir model to investigate whether the same trends as were seen with the synthetic block model would translate to the reservoir model. In order to accomplish this task, the gas injection rate was

chosen from within the range of 0.25 – 3 MMSCF/day while the oil production rate ranged from 500 to 3000 BPD.

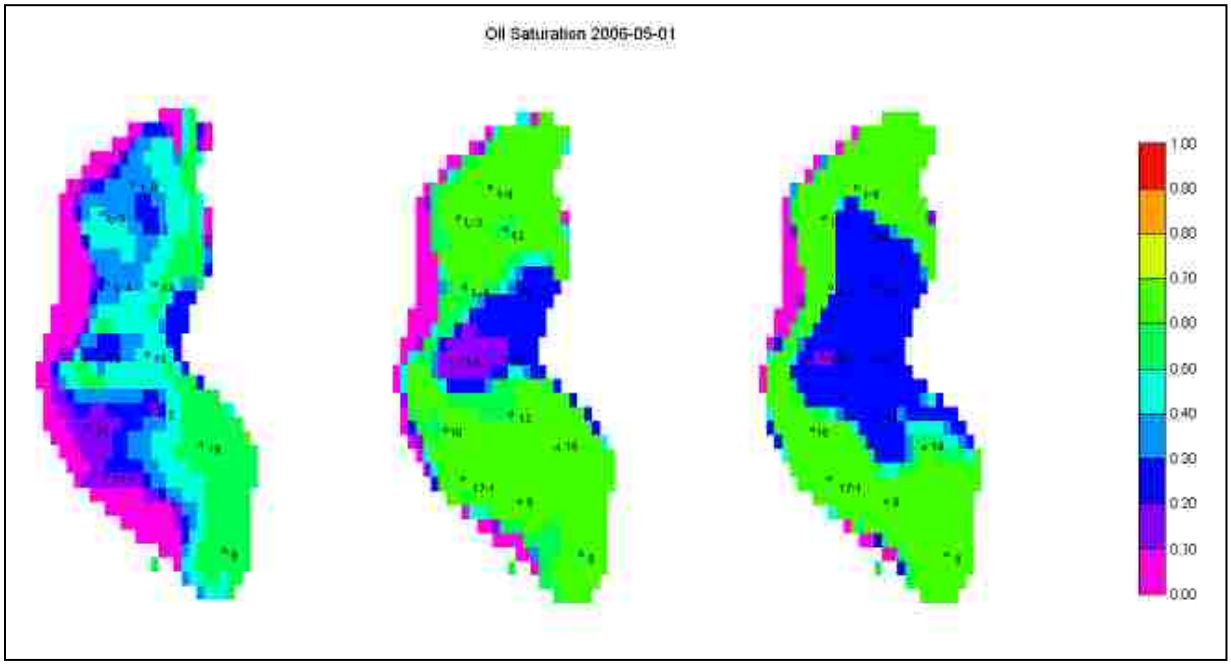

Figure 4.36: Oil Saturation Maps Prior to the Start of SW-GAGD – From Left to Right: Layer 1, 2 & 3

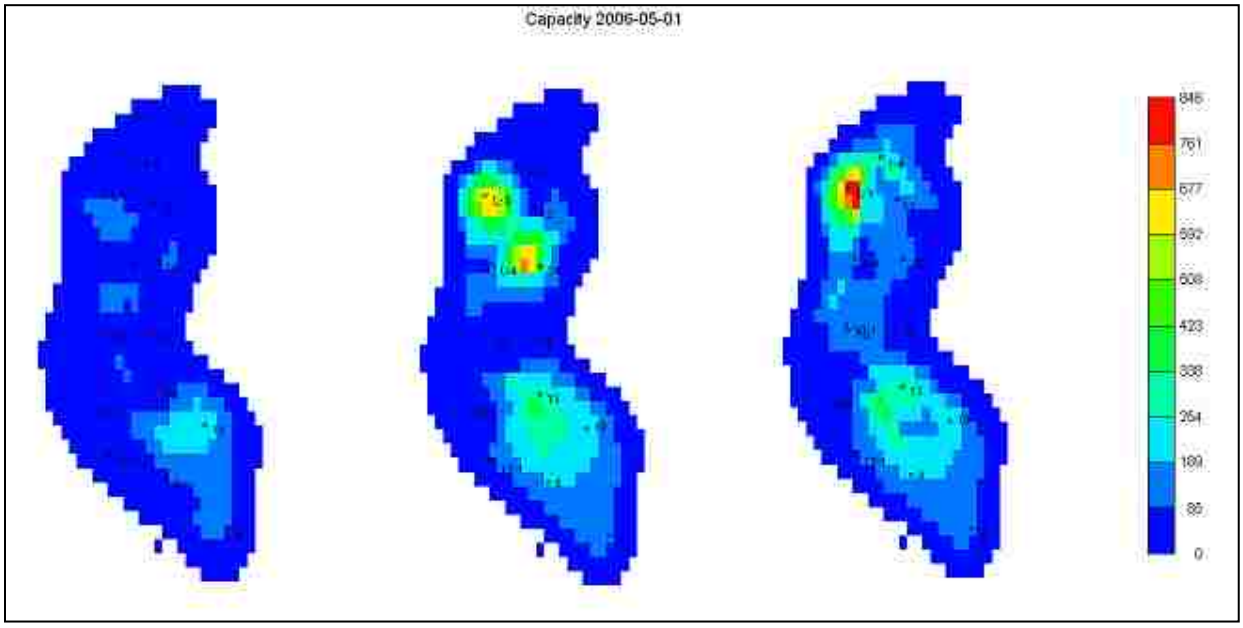

Figure 4.37: Production Capacity Maps Prior to the Start of SWGAGD – From Left to Right: Layer 1, 2 & 3

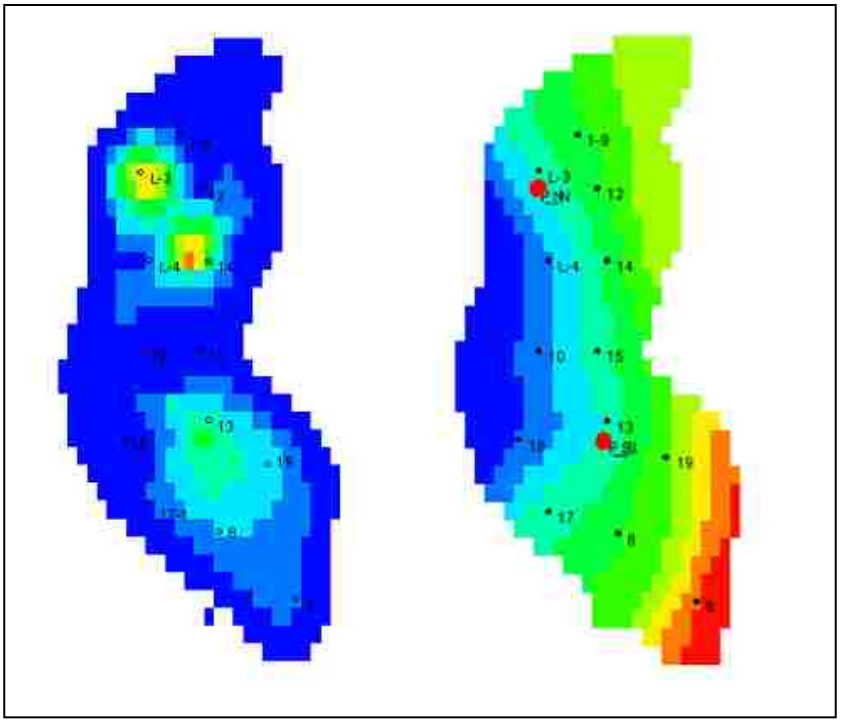

Figure 4.38: Location of SWGAGD Well Coinciding with Maximum Production Capacity (Red)

The results from the optimization study were very surprising, in that it they revealed a very different picture from what had been observed with the synthetic block model. In this case, the reservoir optimization of the vertical SWGAGD process showed that there was not as clear a trend in the recovery data when plotted in terms of the gas injection rate (Figure 4.39). This was compounded by the presence of quite a bit of scatter as well. However, the data does show that with increasing gas injection rate the recovery factor does seem to decrease in general. This is probably the result of early breakthrough occurring resulting in a displacement that is suboptimal. In order to make sense of the plotted results, the data was grouped as a function of the oil production rate and it can be seen that the lower oil production rates resulted in the highest RF-values. Furthermore, there is a very clear negative correlation visible, i.e. increasing the oil production rate results in a decrease of the ultimate oil recovery. This phenomenon was further substantiated by Figure 4.40.

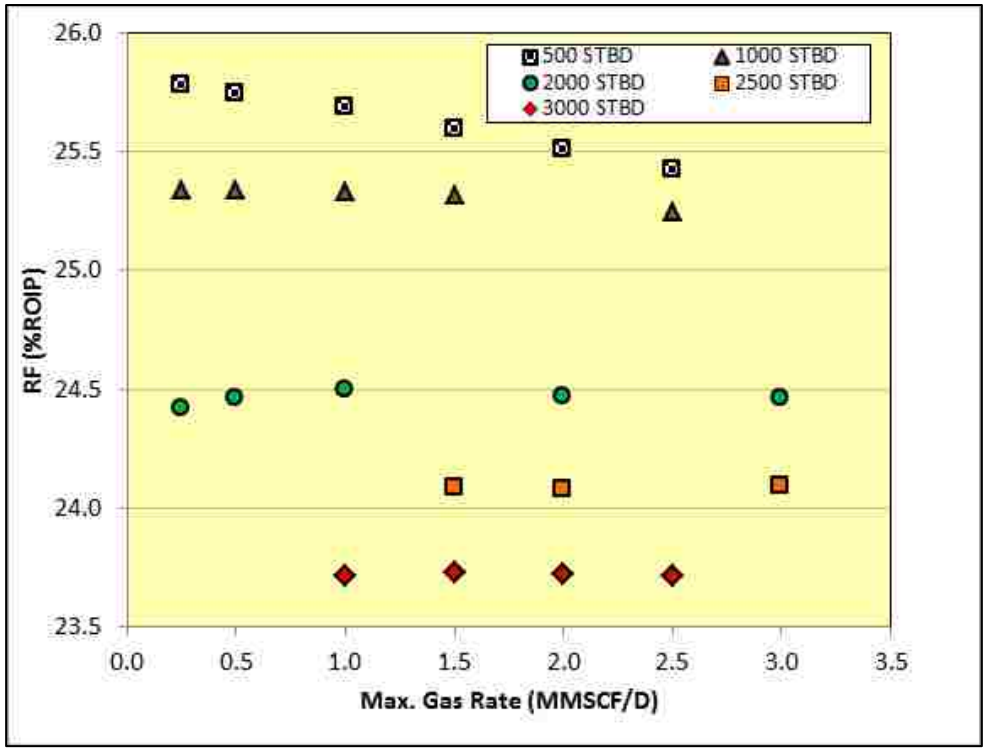

Figure 4.39: Vertical SWGAGD Recovery Factor vs. Gas Injection Rate – Field Model

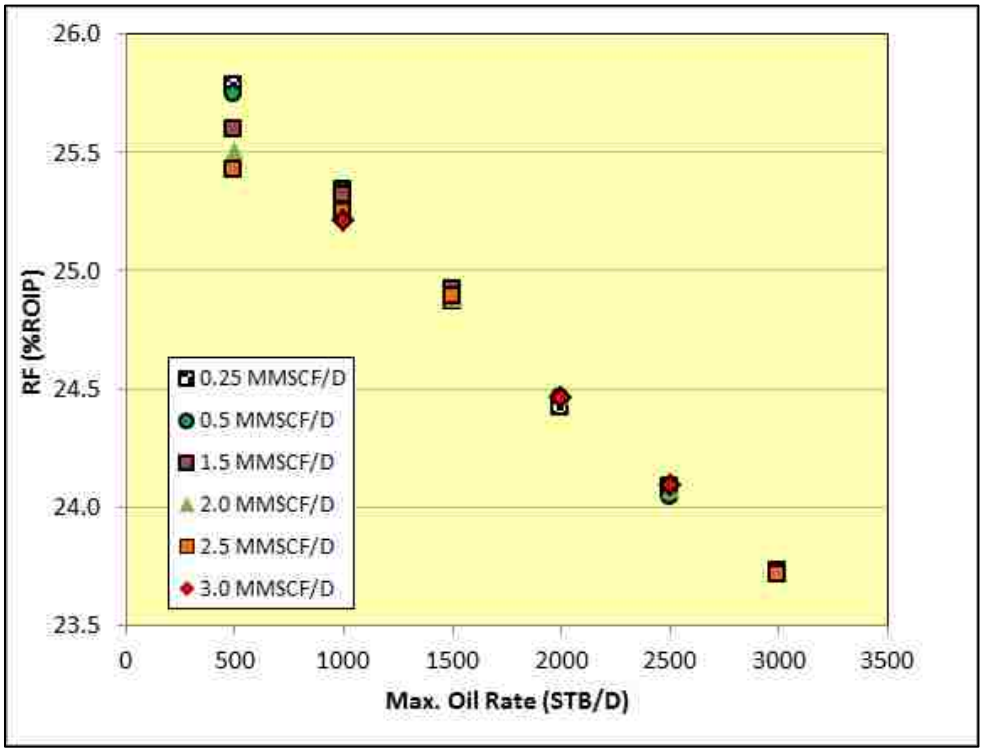

Figure 4.40: Vertical SWGAGD Recovery Factor vs. Oil Rate – Field Model

As opposed to the synthetic model results, the vertical SWGAGD recovery data in terms of the oil production rate did show a very clear linear relationship, but this time around a decreasing trend rather than an increasing trend (see Figure 4.40 on the previous page). The lack of scatter in the simulation data points indicates that the recovery factor is very responsive to changes in the maximum allowed oil rate. There seems to exist a delicate balance between the reservoir voidance due to the oil withdrawal rate and the void replacement due to the injected gas that needs to be appropriately chosen in order for the displacement to result in a maximum oil recovery.

In order to facilitate the choice for the optimum combination of gas injection and oil withdrawal rates for the field-scale simulation of the vertical SWGAGD process, the gas utilization factor (GUF) optimization results were plotted against the gas injection and oil rate in a contour plot (see Figure 4.41). A cut-off value of 8MCF/STB was used for the GUF which meant that injecting gas at a lower value than 3MMSCF/D could still result in an optimum case with regards to the oil recover factor. The following values were chosen for the CO_2 injection and oil production rate:

- Gas injection rate: 0.25, 1 and 2 MMSCF/D;
- Maximum oil withdrawal rate: 500, 1000, 15000 and 2000 STB/D.

A maximum injection pressure of 4500 psi and a minimum bottom-hole pressure of 500 psi were also used for the injection and production wells, respectively. The simulation results of the vertical SWGAGD application in the Buckhorn Field are summarized in Table 4.8 and are also depicted in Figure 4.42. The latter figure also shows the average GUF as a function of the gas injection rate.

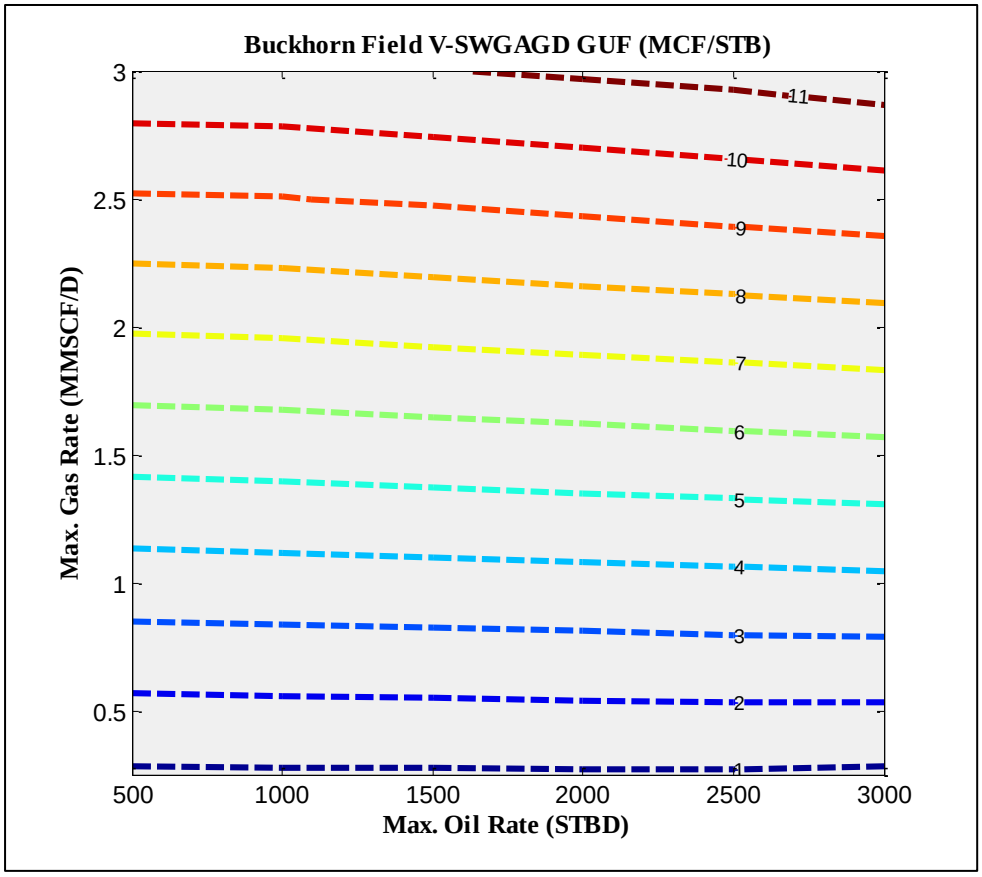

Figure 4.41: Vertical SWGAGD GUF vs. Gas and Oil Rate – Field Model

Table 4.8: Summary of Vertical SWGAGD Oil Recovery Simulation Results

Gas Injection Rate (MMSCFD/well)	0.25	1	2
Max. Oil Production Rate (BPD/well)	**Incremental Recovery (%ROIP)**	**Incremental Recovery (%ROIP)**	**Incremental Recovery (%ROIP)**
500	34.8	34.6	34.4
1000	34.2	34.2	34.1
1500	33.5	33.6	33.6
2000	32.9	33.0	33.0

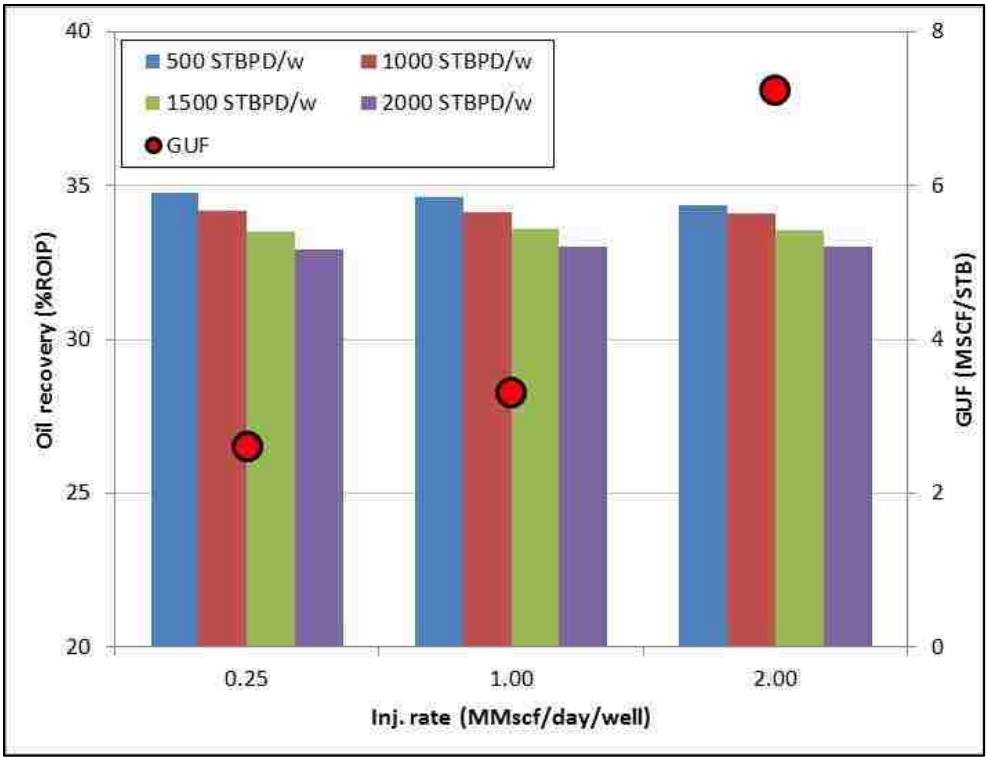

Figure 4.42: Column Chart of Vertical SWGAGD RF and GUF – Field Model

4.4.4.3 Field-Scale Simulation Results – Horizontal SWGAGD

In order to choose the best combination of values for the gas injection and the oil production rate for use in the simulation of the horizontal SWGAGD process, it was also optimized using CMOST in an exploratory way as was done for the vertical configuration. The same types of figures were also used to aid in the choice. As was done before, the data points were grouped by either the gas injection or the oil production rate to facilitate an easier interpretation of the simulation results. Interestingly, when examining the various graphs of the recovery factor as a function of the gas injection (Figure 4.43) and the oil rate (Figure 4.44) a picture emerges that is the opposite as was seen in the optimization of the vertical SWGAGD field-scale application, but very similar to the optimization of the same process using the synthetic block model. A strongly positive relationship is seen between the recovery factor and the gas injection rate while Figure

4.44 seems to indicate that the performance of the horizontal SWGAGD process seems to be insensitive to the oil production rate. It is also clear that the resulting ultimate recovery is quite a bit higher than was seen for the vertical SWGAGD process.

A contour plot of the GUF (Figure 4.45) was again used as a guide for choosing the simulation parameter values for the vertical SWGAGD process; the following ranges were chosen:

- Gas injection rate: 1, 2 and 3 MMSCF/D;
- Maximum oil withdrawal rate: 500, 1000, 1500 and 2000 STB/D.

Again, a maximum injection pressure of 4500 psi and a minimum bottom-hole pressure of 500 psi were also used for the injection and production wells, respectively. The run time for each of the simulations was set to be 8 years. The oil recovery results are tabulated in Table 4.9 and shown in Figure 4.46.

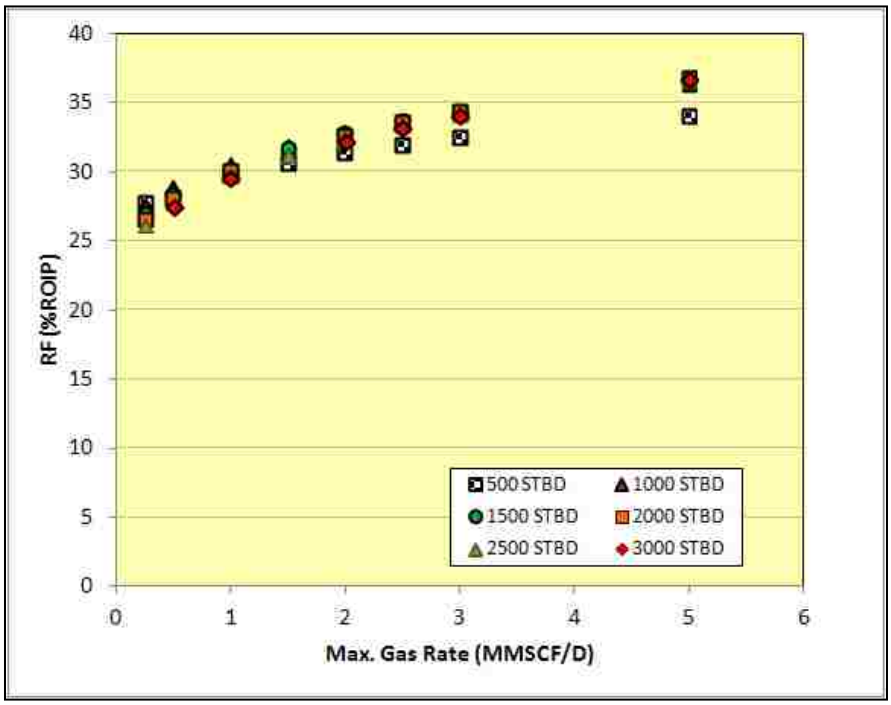

Figure 4.43: Horizontal SWGAGD Recovery Factor vs. Gas Injection Rate – Field Model

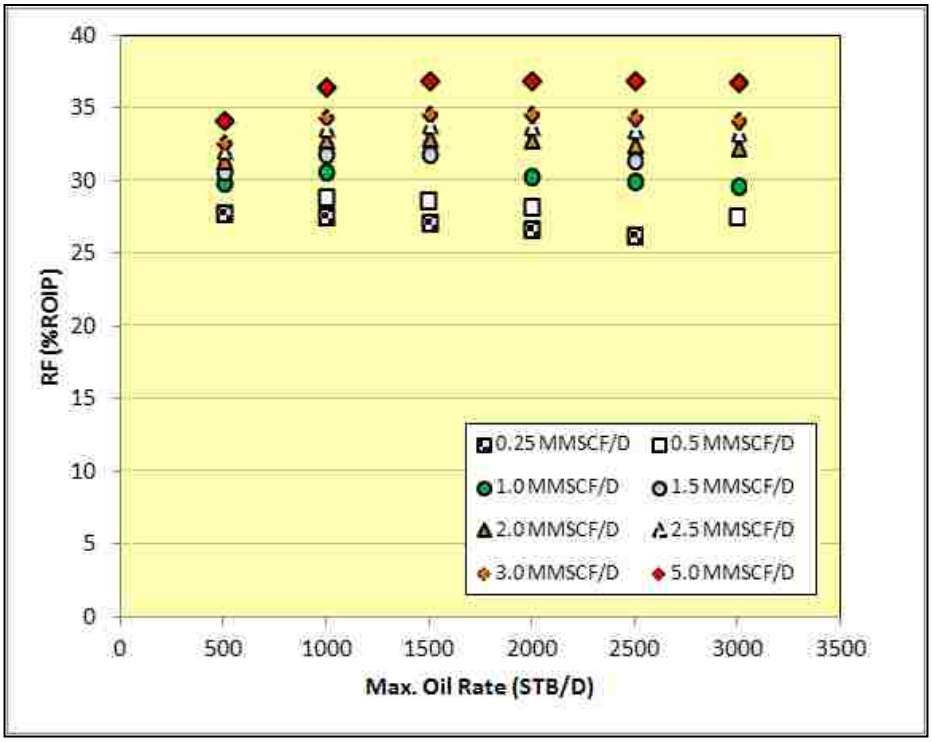

Figure 4.44: Horizontal SWGAGD Recovery Factor vs. Oil Rate – Field Model

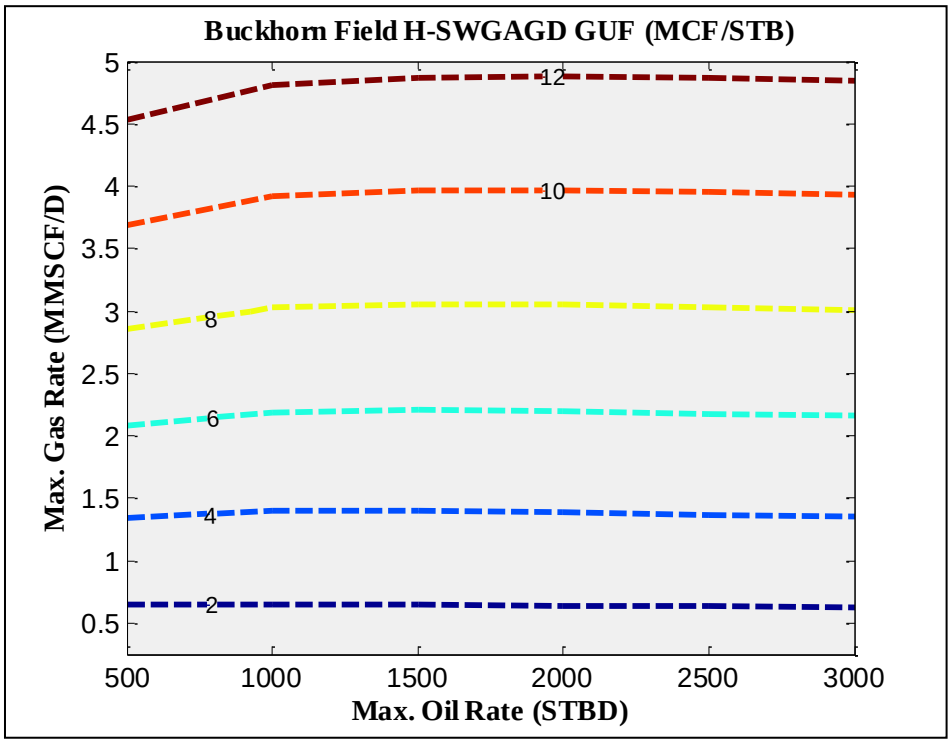

Figure 4.45: Horizontal SWGAGD GUF vs. Gas and Oil Rate – Field Model

Table 4.9: Summary of Horizontal SWGAGD Oil Recovery Simulation Results

Gas Injection Rate (MMSCFD/well)	1	2	3
Max. Oil Production Rate (BPD/well)	**Incremental Recovery (%ROIP)**	**Incremental Recovery (%ROIP)**	**Incremental Recovery (%ROIP)**
500	40.1	42.3	43.8
1000	41.2	44.2	46.2
1500	41.0	44.4	46.6
2000	40.7	44.1	46.5

The results do indicate that the oil recovery results are significantly higher than when the vertical SWGAGD configuration was assessed by about 8.5%ROIP on average. However, as was expected from the exploratory optimization phase, the injected gas is not as efficiently used at times as is indicated by the higher GUF values (Table 4.10) at similar levels of gas injection and oil production rate. In the case of using a horizontal well section for production purposes it not only positively affect oil production by increasing the drainage area and exposure, but it also provides more pathways for the injected gas to be produced along with any reservoir oil/water. This was previously indicated by the comparison of the cumulative GOR-values for both single-well GAGD configurations.

Table 4.10: Gas Utilization Factor of Horizontal SWGAGD Application in Buckhorn Field

	Vertical	**Horizontal**	**Vertical**	**Horizontal**
Gas Injection Rate (MMSCFD/well)	**1**		**2**	
Max. Oil Prod. Rate (BPD/well)	**Gas Utilization Factor (Mscf/STB)**		**Gas Utilization Factor (Mscf/STB)**	
500	3.5	3.0	3.3	5.8
1000	2.3	3.0	3.3	5.5
1500	2.3	3.0	3.3	5.5
2000	2.3	3.0	3.3	5.5

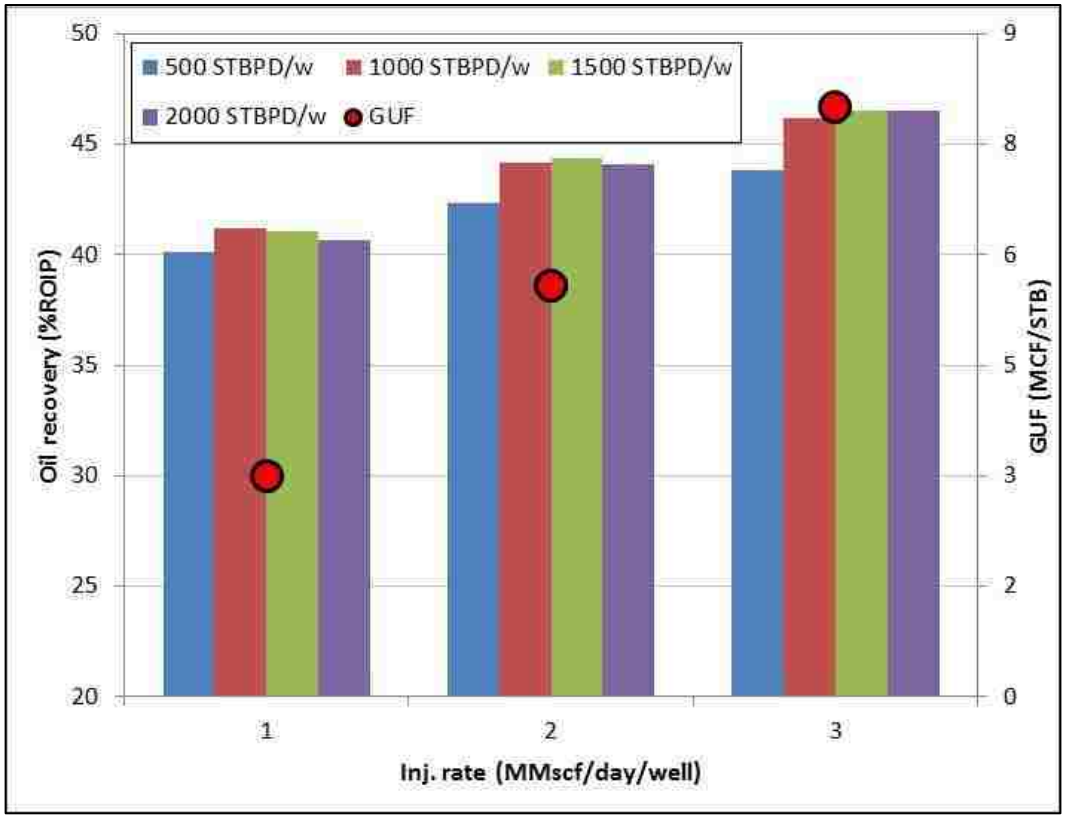

Figure 4.46: Column Chart of Horizontal SWGAGD RF and GUF – Field Model

4.5 The Application of Alternative Processes in the Buckhorn Field

The Buckhorn Field is relatively homogeneous with no prevalent faults or field-wide shale layers that might acts as flow barriers. It had undergone waterflooding after the primary depletion leaving behind a sizable target for EOR. As such, it had been identified as a good candidate for the first field trial of the GAGD process. In this study, a new configuration of the conventional GAGD process was proposed, namely a single-well variation that used the same well to contain both the injection as well as the production completions. The latter may possible be along the offset part of a horizontal well. In order to complete the technological feasibility study of this new process, two other conventionally applied EOR processes were also assessed through field-scale numerical simulation.

These alternative EOR processes were continuous gas injection (CGI) and the water-alternating-gas (WAG) process.

4.5.1 Numerical Study of a CGI Application in the Buckhorn Field

Just as before, the simulation of the CGI process in the Buckhorn Field was preceded by an exploratory optimization study to investigate the dependence of the CGI ultimate recovery on various parameters, such as the gas injection arte and the oil production rate. In this version of the CGI application in the Buckhorn field two well pairs will also be used to facilitate an easier comparison to the other EOR methods that were already studied. Figure 4.47 shows the location of the two vertical injection wells and the two vertical production wells in the field.

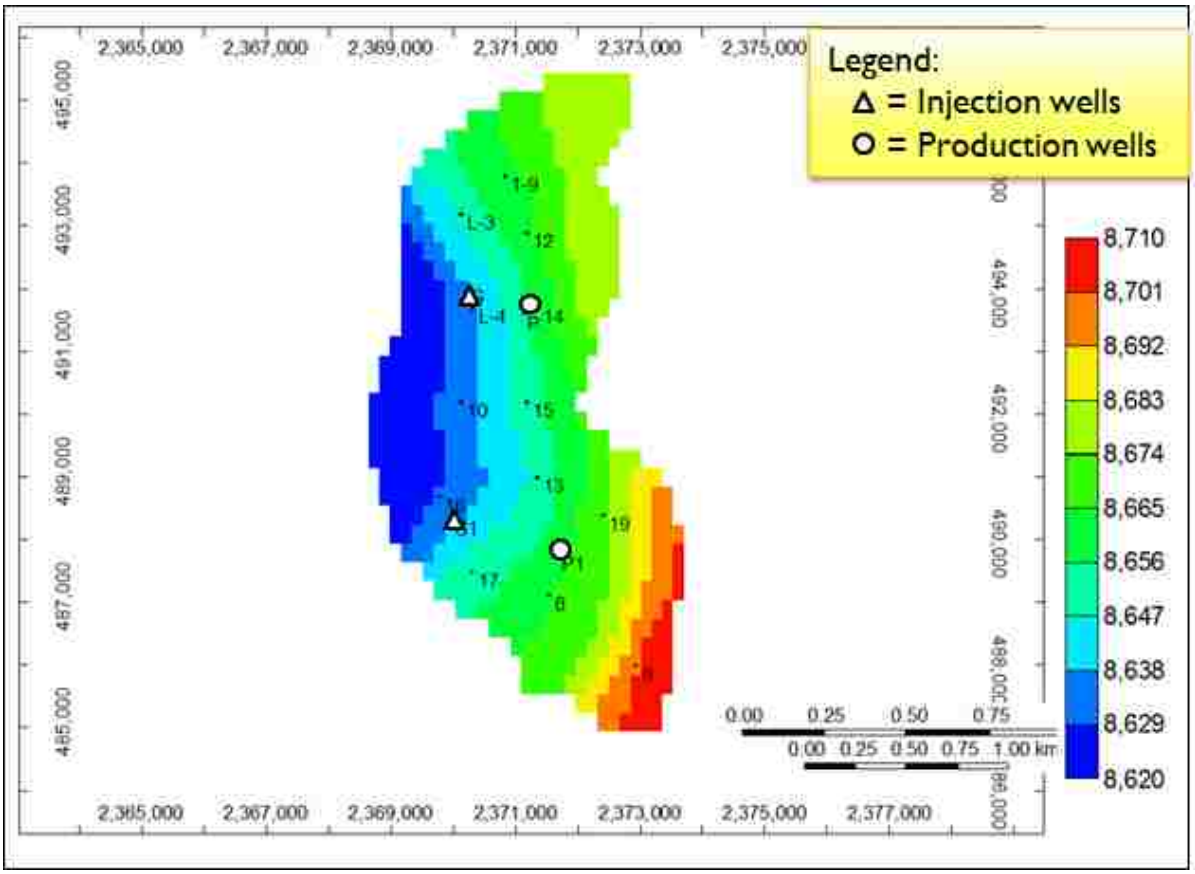

Figure 4.47: Proposed Location of Wells in Buckhorn Field – CGI

Not surprisingly, the exploratory optimization of the CGI process revealed that there is a strong possibility for the existence of a linear relationship between the oil recovery and the gas injection rate (depicted in Figure 4.48). In this CMOST study the gas injection rate was allowed to vary between 0.5 to 3 MMSCF/D while the oil production rate varied from 500 to 2000 STBD. And again, there seems to be no relationship between the CGI recovery factor and the oil rate. The grouping of the data by the gas injection rate clearly reveals that the CGI oil recovery is highly dependent on the gas injection rate value. The range of the gas injection rate was chosen with the help of Figures 4.49 and 4.50 in which the RF- and GUF-values, respectively, were plotted as contour plots as a function of the gas injection and oil production rate. These graphs clearly show that as long as the gas injection rate is chosen to be less than 3 MMSCF/day the GUF-value will be no higher than about 7 MCF/STB.

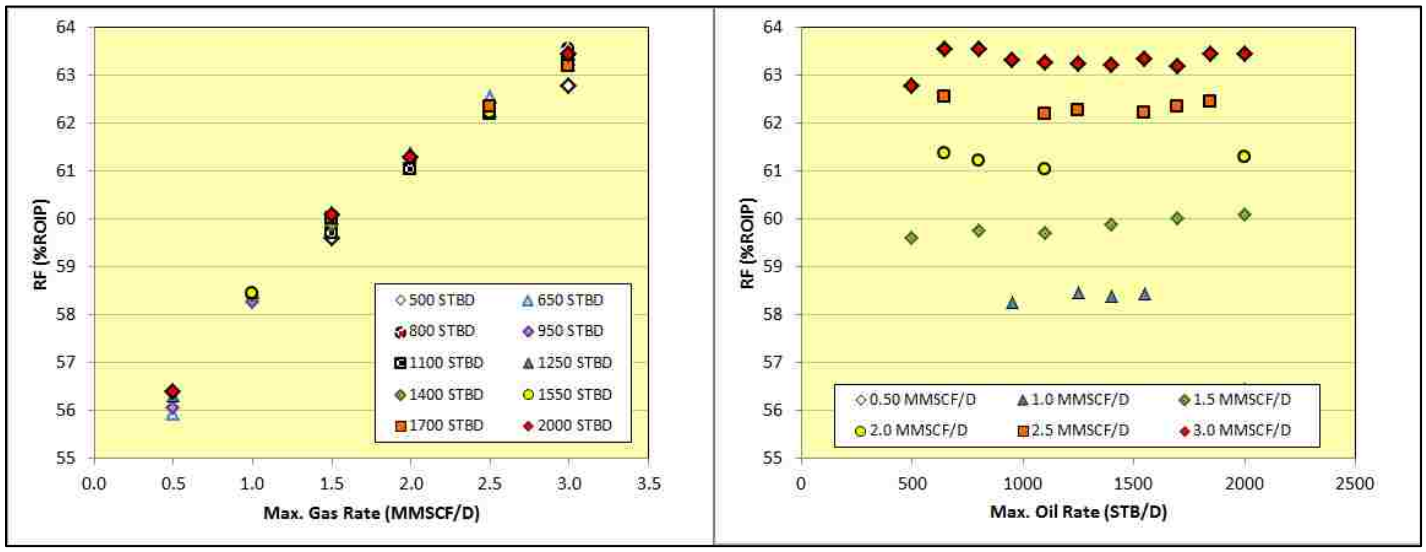

Figure 4.48: Dependence of CGI Recovery on Gas (Left) and Oil (Right) Rate – Field Model

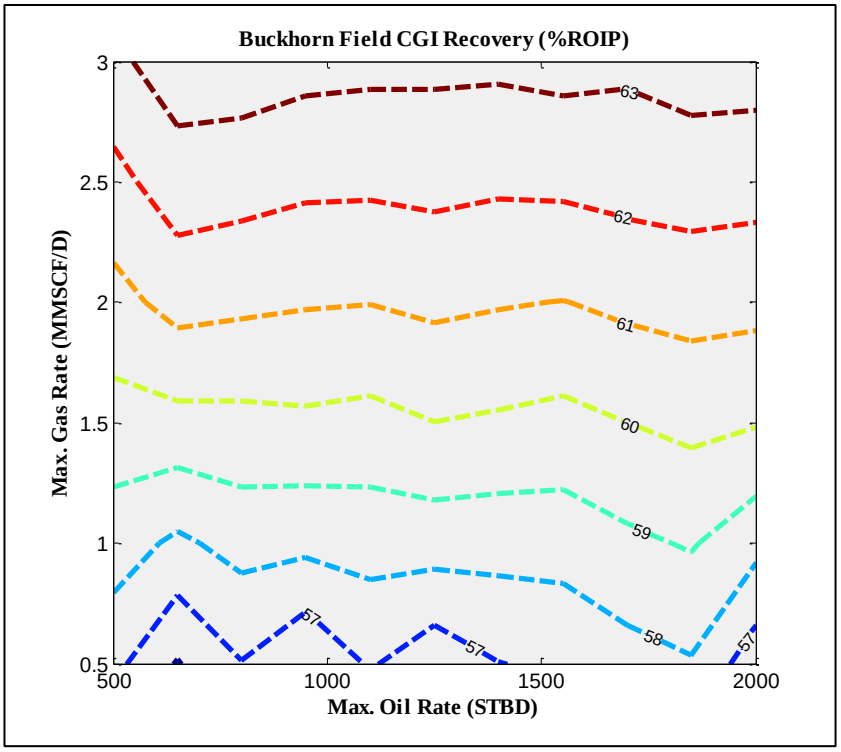

Figure 4.49: CGI Buckhorn Field Recovery Contour Plot

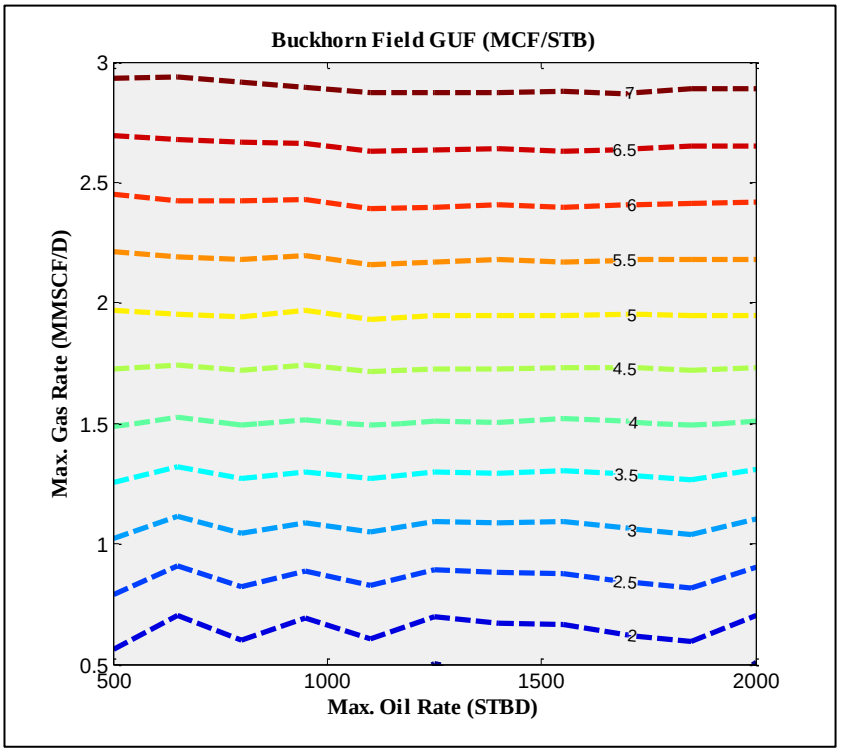

Figure 4.50: CGI Buckhorn Field GUF Contour Plot

Based on the preceding the following values were chosen for use in this phase of the simulation study:

- Gas injection rate: 1, 2 and 3 MMSCF/D;
- Maximum oil withdrawal rate: 500, 1250, 3000 and 5000 STB/D.

All of the other constraints were kept consistent with the previous simulations, i.e. a minimum bottomhole pressure of 500 psi was maintained for the production wells while the gas was injected at a pressure no higher than 4500 psi. The simulation results reveal a similar picture to what was observed with the field-scale application of the GAGD process in that there is an increase in the CGI recovery as the gas injection rate is increased; please refer to Table 4.11 and Figure 4.51.

The tabulated oil recovery results definitely show the lack of a correlation between the ultimate recovery and the oil rate. It is also worth noting that further increasing the gas injection rate would indeed lead to an increase in the oil recovery, however, the GUF value would become prohibitive with regards to the gained incremental recovery.

4.5.2 Numerical Study of a WAG Application in the Buckhorn Field

As was mentioned in the literature review, the development of the WAG process came about as a means of controlling and improving the vertical sweep efficiency by countering the potential sinking of the injected water to the bottom of the payzone with the injection of a lighter (gas) phase. However, due to thickness of oil reservoirs in general this inevitably still results in a potential bypassing of part of the reservoir by the injected fluid phases.

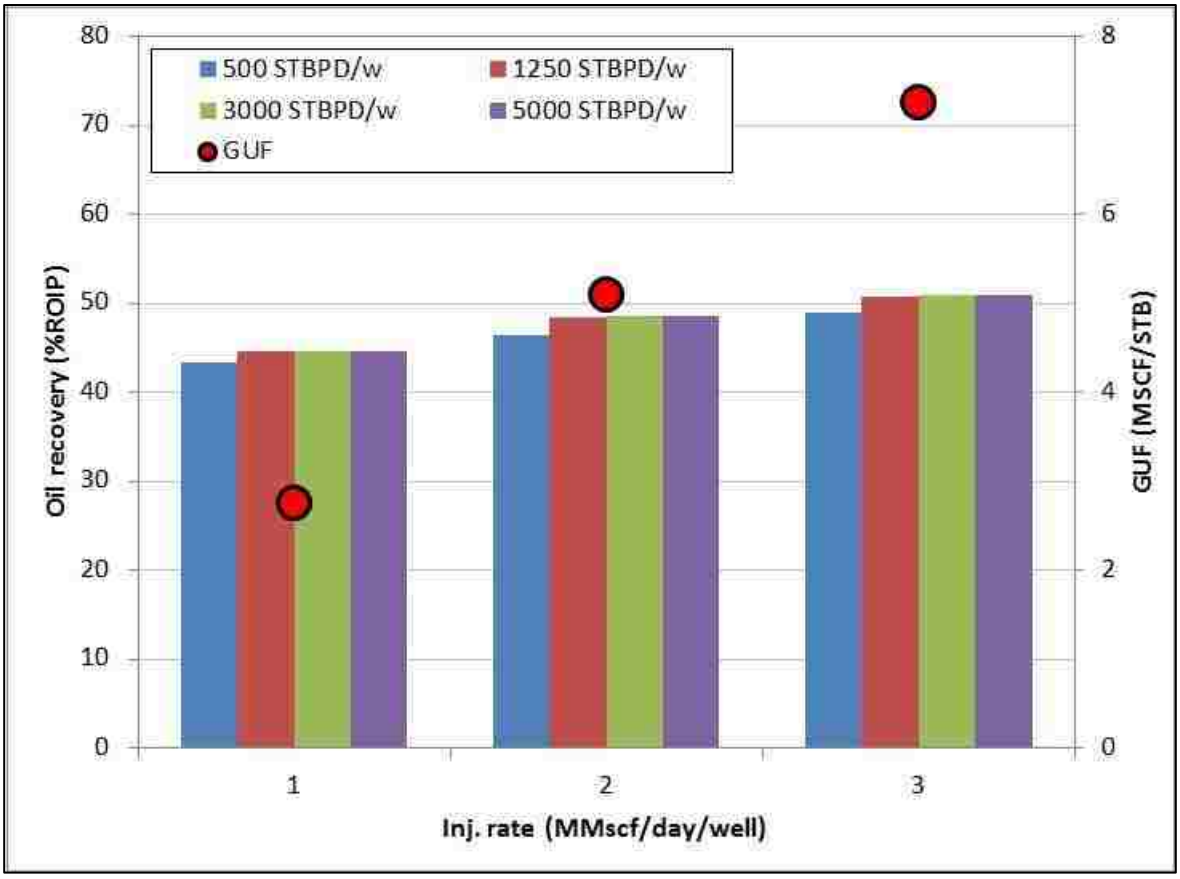

Figure 4.51: Column Chart of CGI Oil Recovery and GUF Values

Table 4.11: Summary of CGI Oil Recovery Simulation Results

Gas Injection Rate (MMSCFD/well)	1	2	3
Max. Oil Production Rate (BPD/well)	**Incremental Recovery (%ROIP)**	**Incremental Recovery (%ROIP)**	**Incremental Recovery (%ROIP)**
500	43.3	46.5	49.0
1250	44.7	48.4	50.7
3000	44.6	48.5	50.9
5000	44.6	48.5	51.0

The numerical simulation of the WAG process in the Buckhorn Field proceeded in a very similar manner to the previously studied EOR processes. The same well locations were used for

the injection and the production wells (all vertical wells) as in the CGI process as well as the same number of wells. The injection cycles were of equal duration and the simulation time was equally divided to span 2 cycles each of water and CO_2 injection. No attempt was made to optimize the duration and number of cycles and no inclusion of hysteresis in the liquid-liquid relative permeability curves was introduced.

The exploratory optimization study of the WAG process in the Buckhorn Field also followed suit with the exception that the oil rate was excluded as a dependent variable as the previous optimization/simulation study phases had revealed the lack of dependence between the oil recovery and the oil rate time and again. Instead, the gas and water injection rate were chosen as the independent variables to be optimized. The range of the gas injection rate was defined to be between 1 and 3 MMSCF/D while the water injection rate varied between 5000 and 20000 STBWPD. As was stated earlier, the duration (and subsequently, the number) of injection cycles was not part of this study. The plot of the WAG recovery versus the gas injection rate (left-hand side of Figure 4.52) again shows a strong positive relationship to the gas injection rate, however, significantly more scatter is visible in the data. It is evident from the grouping of data points by water injection rate, that the latter does affect the ultimate WAG RF in the Buckhorn Field. On the other hand, the graph of the WAG recovery data as a function of the water injection rate (right-hand side of Figure 4.52) has quite a lot more scatter than is visible in the previously mentioned plot. However, due to the fact that it represents a means of voidance replacement rather than just void creation (i.e. the oil production rate) there is a slight decreasing trend visible in the scattered data points. It seems that as the water injection rate is increased past a certain value there is no increase in the recovery attained, however, as the gas injection rate is increased, the WAG RF is improved.

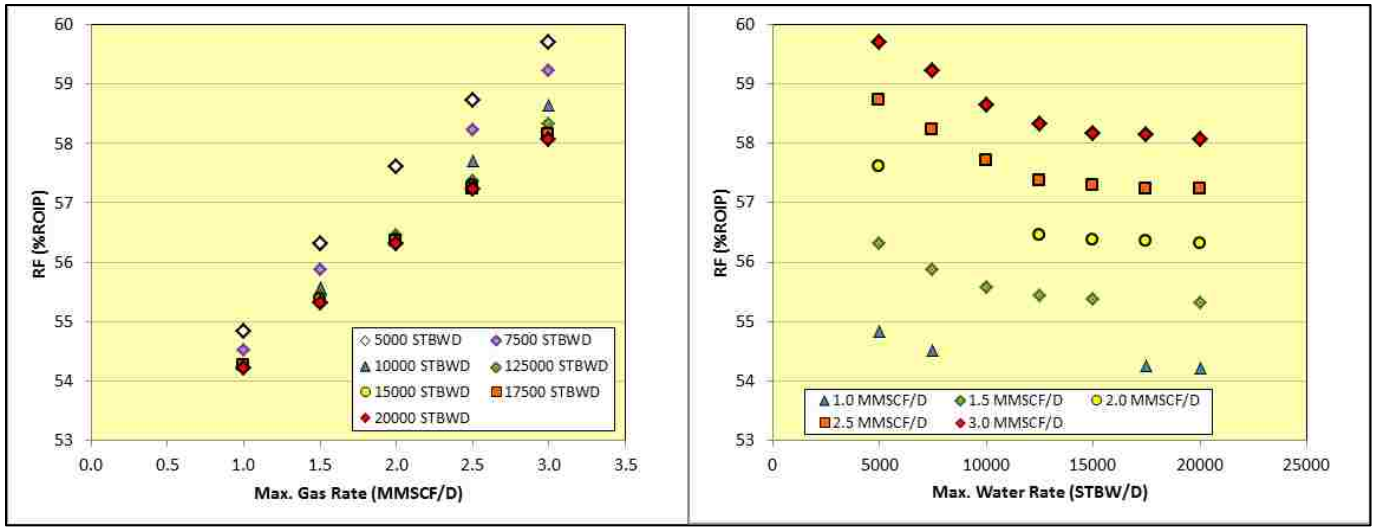

Figure 4.52: Dependence of the WAG Recovery on Gas (Left) and Water (Right) Injection Rate

To facilitate the choice of the optimum values for the operational constraints various contour plots were constructed. Figure 4.53 shows the one depicting the WAG RF as a function of the gas and water injection rate.

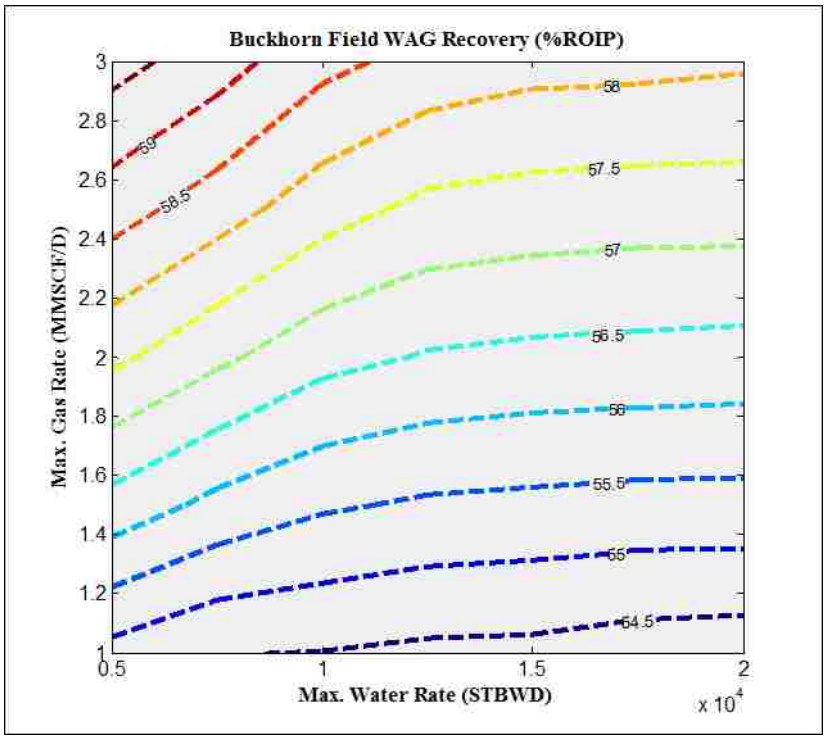

Figure 4.53: WAG Buckhorn Field Recovery Contour Plot

The aforementioned trends in the ultimate oil recovery are also evident from this contour plot: an increase in the gas rate results in an increase of the RF and while this is also true for the water rate, there is definitely a point of diminishing returns visible. The efficiency of the WAG application in the Buckhorn Field is summarized in Figure 4.54 depicting the water and gas utilization factor contours.

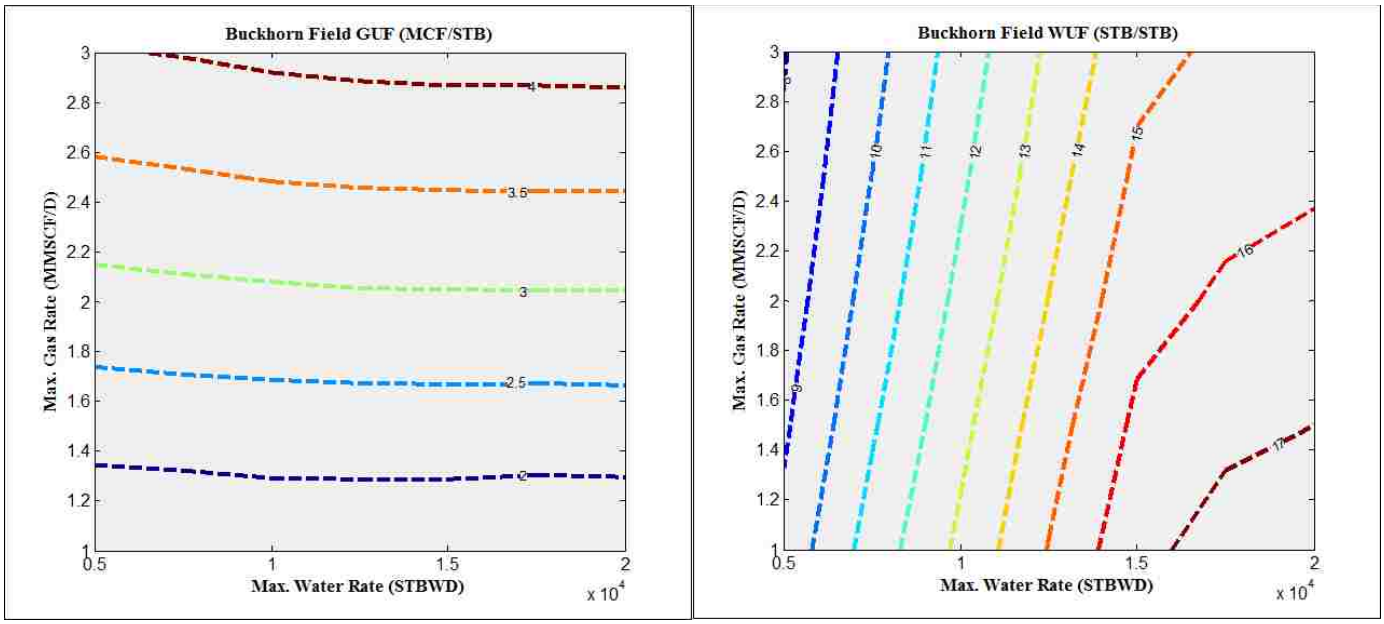

Figure 4.54: WAG Buckhorn Field Gas and Water Efficiency Contour Plot

Taking the previous observations into consideration the WAG process was simulated using the following values for the dependent variable:

- CO_2 injection rate: 1, 2, 3 and 5 MMSCF/D;
- Water injection rate: 5000, 10000 and 15000 STBWD;
- Cycle ratio and tally: 1-to-1 and 4;
- Maximum oil production rate: 1250 STB/D.

The simulation results of the WAG application in the Buckhorn Field are summarized in Table 4.12 in terms of the gas and water injection rates and are depicted in Figures 4.55 and 4.56.

Table 4.12: Summary of WAG Oil Recovery Simulation Results

Gas Injection Rate (MMSCFD/well)	1	2	3
Water Injection Rate (BPD/well)	**Incremental Recovery (%ROIP)**	**Incremental Recovery (%ROIP)**	**Incremental Recovery (%ROIP)**
500	43.3	46.5	49.0
1250	44.7	48.4	50.7
3000	44.6	48.5	50.9
5000	44.6	48.5	51.0

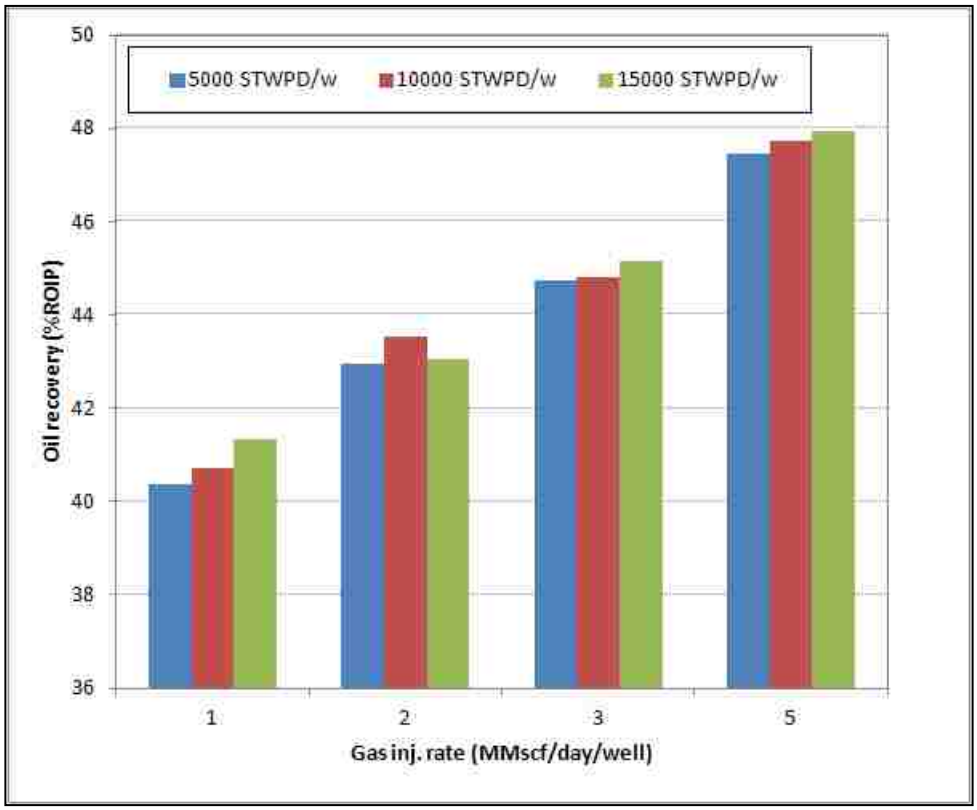

Figure 4.55: Column Chart of WAG Recovery Factors vs. Gas Injection Rate

There is a need to plot the WAG recovery results in terms of both the gas and water injection rate as the optimization had revealed that either one of them seemed to have an influence on the ultimate oil recovery.

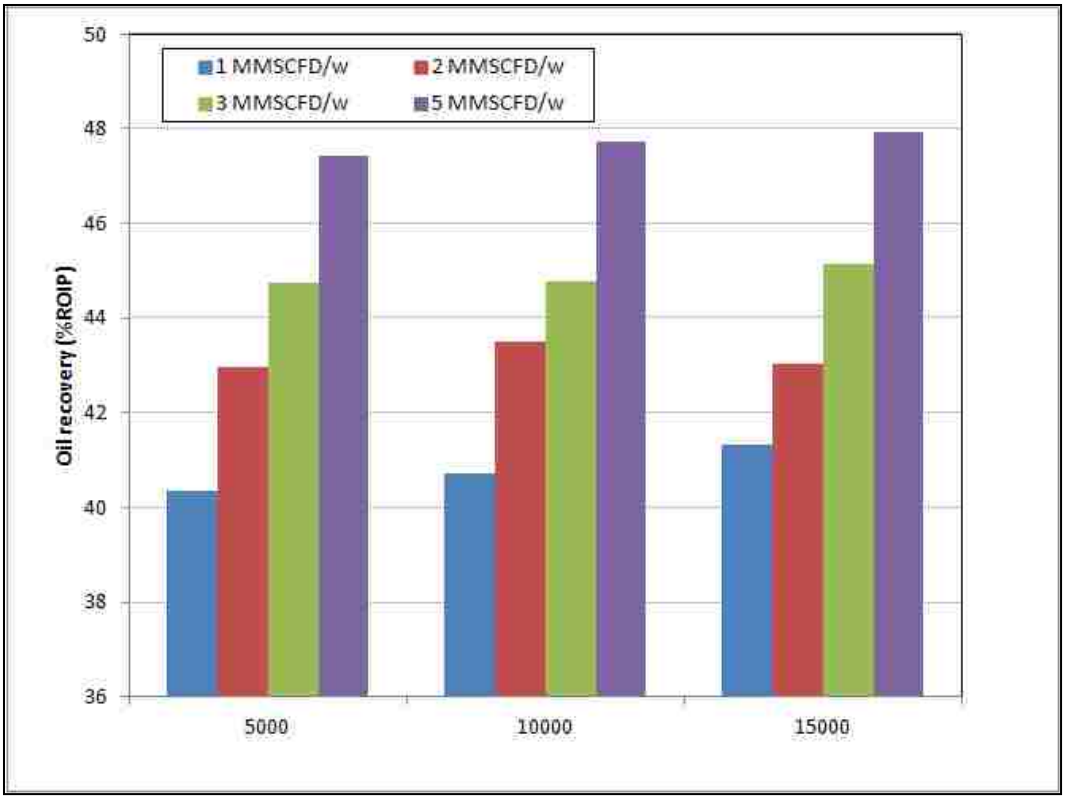

Figure 4.56: Column Chart of WAG Recovery Factors Water Injection Rate

The results as shown in Figure 4.55 clearly show that by increasing the gas injection rate more oil is recovered, however, when the WAG recovery results are plotted as a function of the water injection rate (Figure 4.56) it is clear its influence on the oil recovery is even more pronounced when compared to the effect of the water injection rate.

4.6 Economic Assessment of Various Gas Injection EOR Processes for the Buckhorn Field through Reservoir Simulation

The simulation results of the various EOR processes were used as input for the economic analysis that formed the basis for the comparison being made in this section. One method is by using the least and most favorable values for each of the input variables as described in section 3.6.2. In this manner, the range of the selected economic performance indicators can be attained. However, these numbers only show the two extreme possibilities of the economic performance

of the projects. Using statistical modeling software, such as Crystal Ball, affords the possibility of conducting a Monte Carlo simulation in which each of the input variables is assigned a probability distribution that is randomly sampled at which instant the sampled values are used to calculate the performance indicators of that individual trial. This process is repeated for n = 1000 times to generate a population of trials. This population is then used to calculate a probability distribution for each of the economic indicators themselves, thereby allowing incorporation of parameter uncertainty in the evaluation of the project. Selected important statistical parameters of the various probability distributions that were generated for each of the economic performance indicators are summarized in the following tables (Table 4.13 to 4.17) for each of the EOR processes in question.

Table 4.13: Probability Distribution Description of Economic Performance Indicators – Multi-Well GAGD

Statistics	NPV ($)	PI	GRR	IRR
Mean	37,168,771	5.0	32.4%	203%
Median	38,046,045	4.9	32.7%	179%
Standard	15,071,791	1.8	6.2%	132%
Variance	2.27E+14	3.1	0.4%	175%
Skewness	0.0850	0.2676	-0.28	0.59
Kurtosis	2.91	2.87	3.07	2.59
Coeff. of	0.41	0.3519	0.1904	0.65
Minimum	-1,552,081	0.9	10.5%	12%
Maximum	92,174,898	10.6	49.5%	666%
Range Width	93,726,979	9.8	39.1%	653%
Mean Std. Error	476,612	0.1	0.2%	4%

The mean NPV-values of the investigated EOR applications for the Buckhorn Field indicate that all of the development plans would generate a profit at the current assumed economic parameters. This is more readily evident in Figure 4.57 which shows a comparison of the NPV performances for all the different CO_2 EOR methods.

It should be pointed out that the Excel cashflow analysis was set up in such a way as to stop when the calculated net value stream for any given year after the start of the project became negative, i.e. the total costs were greater than the generated income after tax for that particular year. By setting up the spreadsheet calculations in this manner it was not necessary to adjust the production profiles as a function of a particular cut-off value for any of the usual production metrics, such as: the oil production rate, the producing gas-oil-ratio, etc.

Table 4.14: Probability Distribution Description of Economic Performance Indicators – CGI

Statistics	NPV ($)	PI	GRR	IRR
Mean	28,684,709	4.5	31.0%	160%
Median	28,616,027	4.4	31.2%	161%
Standard Deviation	11,141,042	1.5	5.7%	82%
Variance	1.24E+14	2.3	0.00	0.67
Skewness	0.2094	0.5392	-0.12	0.31
Kurtosis	2.89	3.45	2.8534	2.53
Coeff. of Variability	0.39	0.3386	0.18	0.5103
Minimum	65,999	1.0	14.1%	19%
Maximum	64,991,811	11.3	46.7%	440%
Range Width	64,925,812	10.3	32.6%	421%
Mean Std. Error	352,311	0.0	0.18%	2.58%

Table 4.15: Probability Distribution Description of Economic Performance Indicators – WAG

Statistics	NPV ($)	PI	GRR	IRR
Mean	29,901,737	4.6	31.7%	145%
Median	29,053,707	4.4	31.9%	143%
Standard Deviation	9,455,483	1.3	4.7%	36%
Variance	8.94E+13	1.6	0.2%	13%
Skewness	0.3951	0.5854	-0.01	0.23
Kurtosis	3.01	3.18	2.85	2.83
Coeff. of Variability	0.32	0.2792	0.1473	0.25
Minimum	8,230,750	1.8	16.8%	49%
Maximum	63,716,121	9.2	46.4%	264%
Range Width	55,485,372	7.4	29.6%	215%
Mean Std. Error	299,009	0.0	0.1%	1%

Table 4.16: Probability Distribution Description of Economic Performance Indicators – Vertical Single-Well GAGD

Statistics	NPV ($)	PI	GRR	IRR
Mean	34,751,210	7.5	38.9%	240%
Median	34,599,931	7.4	39.2%	243%
Standard Deviation	9,508,088	2.0	4.9%	99%
Variance	9.04E+13	4.1	0.2%	99%
Skewness	0.1402	0.4271	-0.09	0.20
Kurtosis	2.91	3.31	2.83	2.35
Coeff. of Variability	0.27	0.2690	0.1253	0.41
Minimum	10,385,154	2.6	24.8%	56%
Maximum	69,697,947	15.6	52.6%	520%
Range Width	59,312,793	13.0	27.7%	464%
Mean Std. Error	300,672	0.1	0.2%	3%

Table 4.17: Probability Distribution Description of Economic Performance Indicators – Horizontal Single-Well GAGD

Statistics	NPV ($)	PI	GRR	IRR
Mean	35,744,531	5.3	33.9%	168%
Median	35,314,655	5.2	34.0%	167%
Standard Deviation	11,273,835	1.6	4.9%	72%
Variance	1.27E+14	2.4	0.2%	51%
Skewness	0.3106	0.5036	-0.06	0.21
Kurtosis	3.14	3.08	2.95	2.25
Coeff. of Variability	0.32	0.2932	0.1461	0.43
Minimum	5,893,513	1.6	16.6%	33%
Maximum	77,884,412	11.3	48.7%	367%
Range Width	71,990,898	9.7	32.1%	334%
Mean Std. Error	356,510	0.0	0.2%	2%

Based on the data in the summary table for the multi-well GAGD process, the mean IRR is very favorable and is quite a lot higher than the traditionally accepted corporate discount rate of 10 percent. Compared to the other three parameters for the same EOR process, the GRR has the least variability as reflected by its coefficient of variability. The same is true for the variability of the GRR of the other EOR processes.

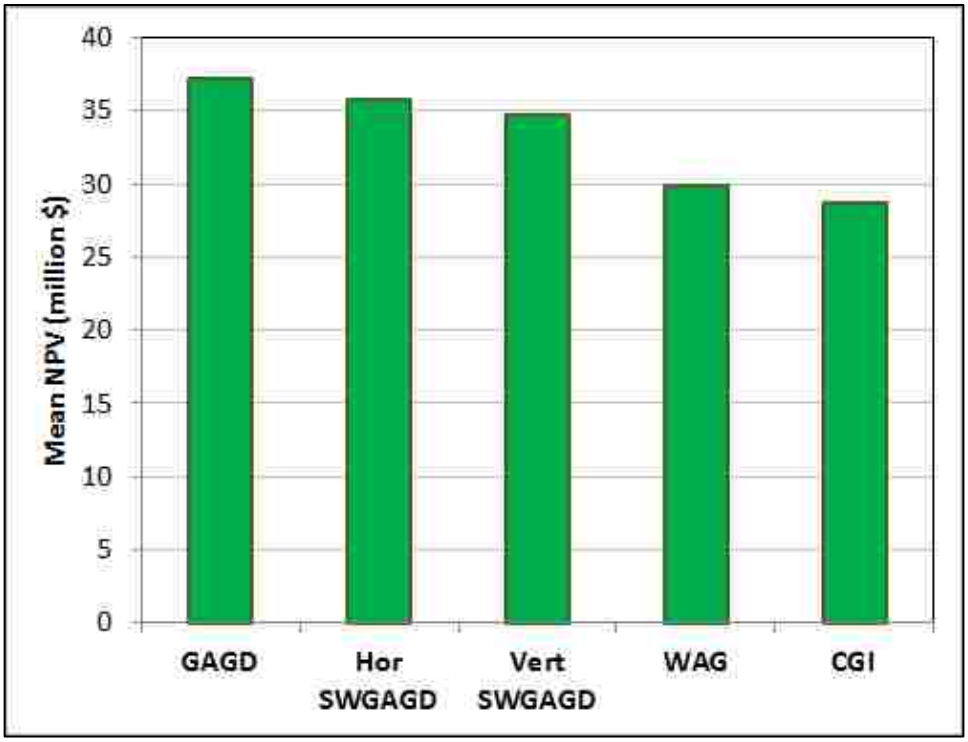

Figure 4.57: Comparison and Ranking of Mean NPV Performance of the Various CO_2 EOR Options for the Buckhorn Field

A thorough sensitivity analysis of the economic performance indicators was also performed using Crystal Ball for each of the studied EOR processes. The results were graphed in tornado charts showing the relative sensitive of the economic performance indicator in question as a function of the independent variables. Figure 4.58 shows an overview of the sensitivity analysis performed of the multi-well GAGD process and it is clear that the oil price contributes the most to the variability in the results for most of the economic performance indicators. Furthermore, the NPV is also sensitive to the following dependent variables (in descending order of influence): the production scheme (i.e. the operational parameters), the royalty rate, the discount rate, the federal income tax and the $CAPEX_{expensed}$.

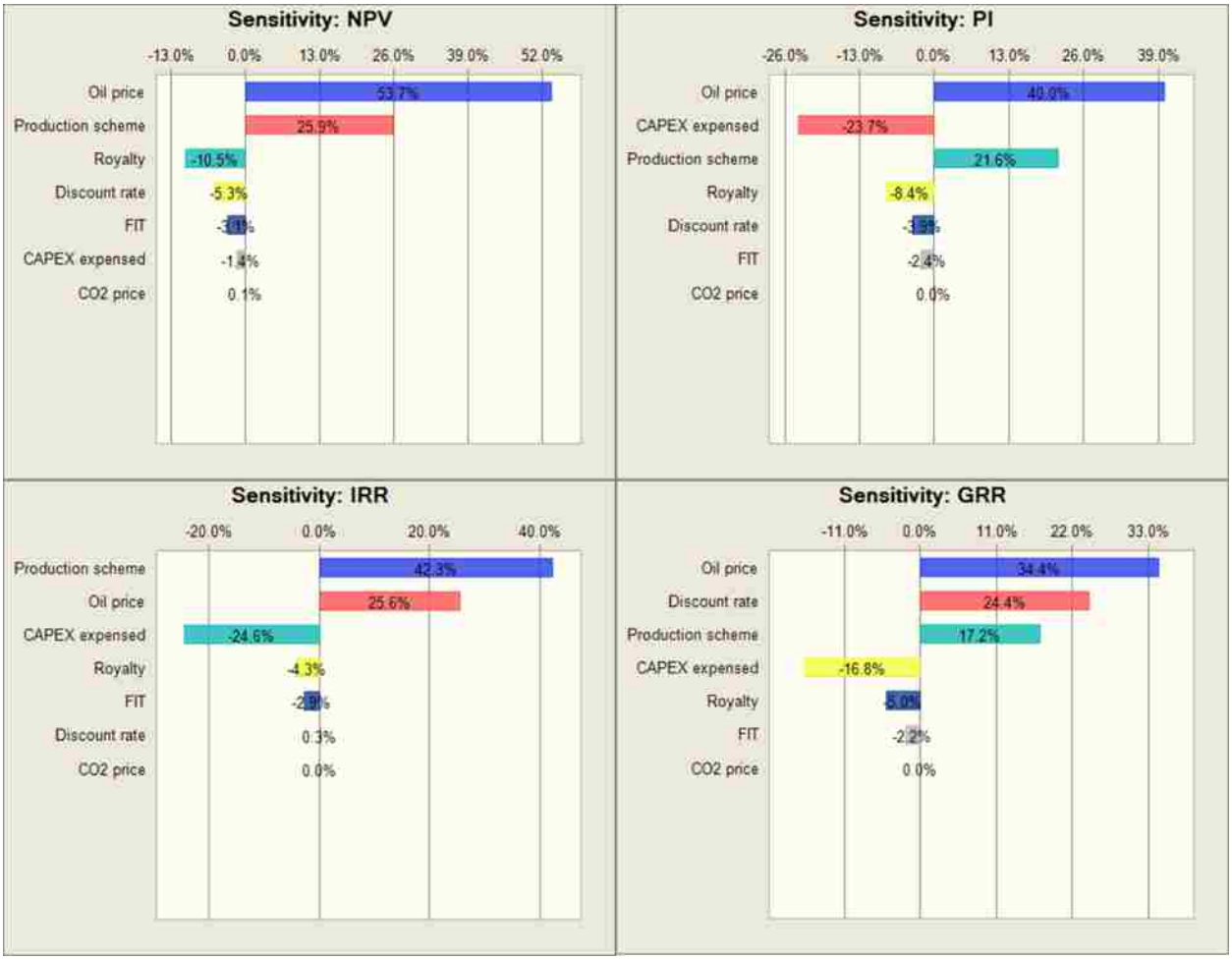

Figure 4.58: Sensitivity Charts of the Economic Performance Indicators – Multi-Well GAGD

The sensitivity analysis results of the NPV for the other EOR processes are depicted side-by-side in Figures 4.59 and 4.60. The tornado graphs show that for all of the investigated EOR processes the NPV seems to be most sensitive to the oil price by a factor of on average 5 compared to the next most influential independent variable. It is clear that these graphs display quite a bit of difference in not only which of the dependent variables has the most influence on the NPV in the various development plans, but also the magnitude of said influence.

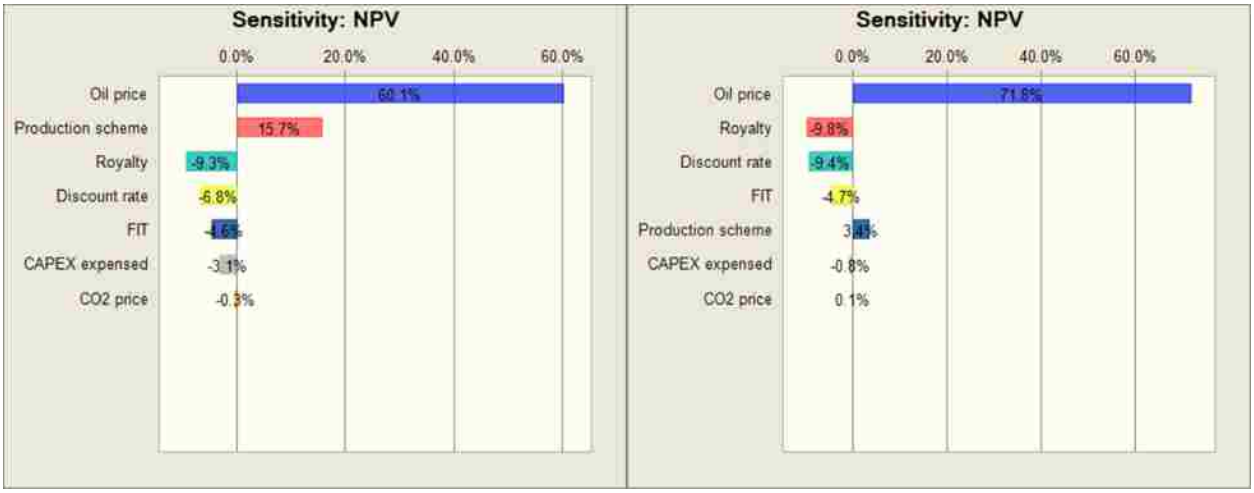

Figure 4.59: Sensitivity Charts of the NPV – CGI (Left) and WAG (Right)

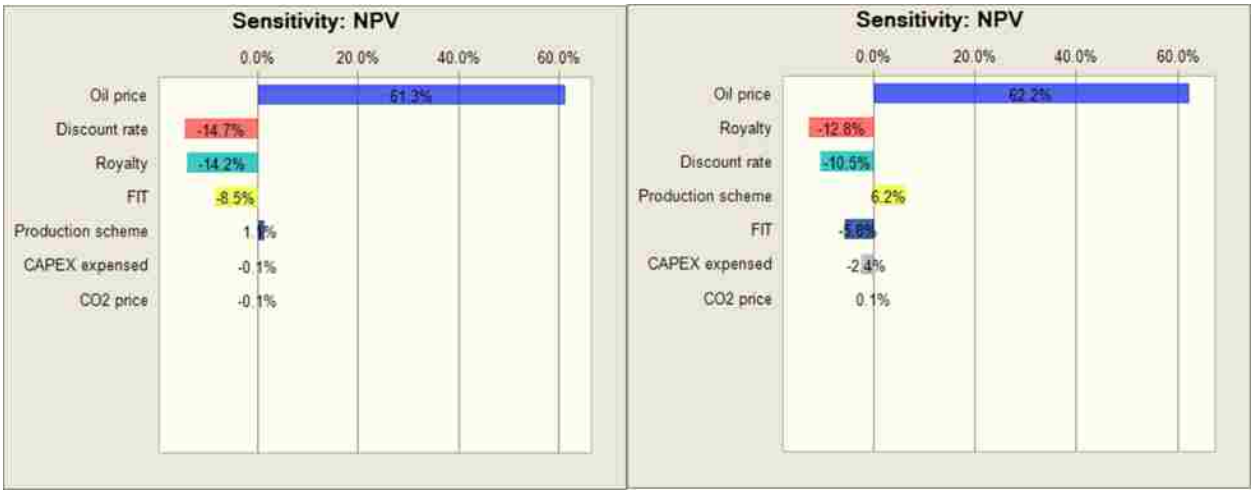

Figure 4.60: Sensitivity Charts of the NPV – Vertical (Left) and Horizontal GAGD (Right)

A comparative economic assessment of various project options is always based on certain economic performance indicators, including the ones selected in this study. These are then used to not only determine whether a particular project will be deemed profitable, but can also be used as a way of ranking the candidate projects if there are capital investment constraints in place. Some of the more commonly used project screening criteria are summarized in Table 4.18 (after Mian, 2002). In this table the i_d-variable is a pre-determined, internally acceptable corporate discount rate, usually taken as 10 percent.

Table 4.18: Economic Project Screening Criteria (Mian, 2002)

Profitability Measure	Accept If:	Reject If:
Payback Period @ i_d	≤ Desired	≥ Desired
Net Present Value (NPV) @ i_d	> 0	< 0
Internal Rate of Return (IRR)	> i_d	< i_d
Profitability Index (PI) @ i_d	> 1	< 1
Present Value Ratio (PVR) @ i_d	> 0	< 0
Technical Cost @ i_d	< Average Product	> Average Product Price
Growth Rate of Return (GRR) @ i_d	> i_d	< i_d

Based on these economic screening criteria and the previously summarized results, it is clear that all of the investigated EOR development plans for the Buckhorn Field would be profitable under the current assumptions. Since all of the EOR projects would result in positive NPVs, any ranking of the various EOR-options would be usually based on PI or IRR. The IRR is often utilized when there are no restrictions on the venture capital amount that can be invested. However, when there are limitations in effect, the PI is often regarded as the proper way of ranking competing projects as it indicates what the return on the invested capital would be. This provides alternative ways of viewing the profitability of the various EOR processes. The possible EOR candidate processes for application in the Buckhorn Field have thusly been ranked based on these aforementioned economic performance indicators. The ranking is depicted in Figures 4.61 and 4.62. Even though the ranking of the various EOR processes is different from one selected economic performance indicator to another, it is still evident that in either case all versions of the GAGD process ranked better than the alternative EOR processes. The latter is also true if the ranking would have been performed based on the NPV, however, the vertical SWGAGD process comes out on top in both ranking systems.

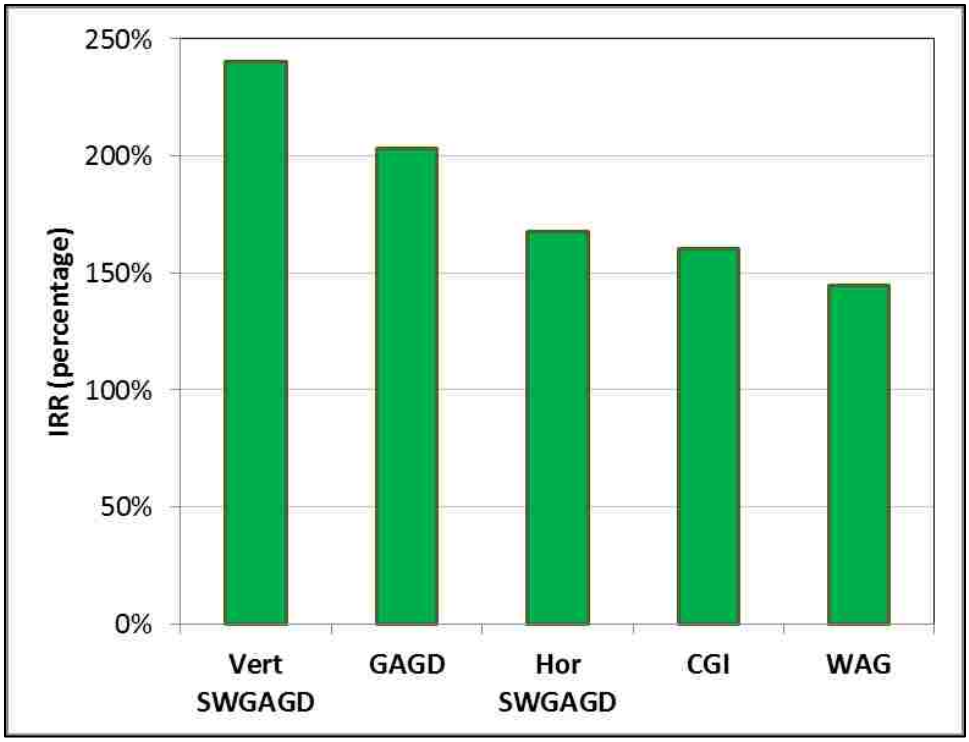

Figure 4.61: Ranking of EOR Processes Based on IRR

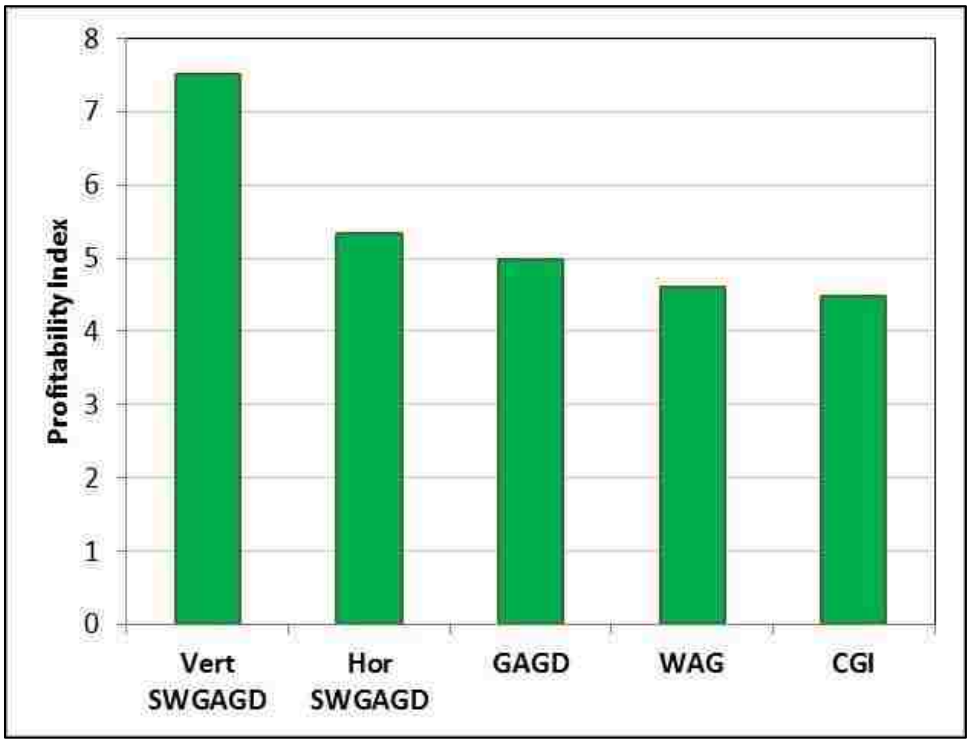

Figure 4.62: Ranking of EOR Processes Based on PI

The preceding economic assessment was based on the simulated oil production profiles resulting from the application of the various gas injection EOR processes in the Buckhorn Field. The following section discusses how the economic assessment changes when the reported field recovery factors for the CGI and WAG process are taken into account.

4.6.1 Economic Assessment of Alternative Gas Injection EOR Processes Reflecting Reported Field Experience

The aforementioned discussion of the results was based solely on the cashflow analysis performed with the simulated production profiles of the various EOR processes as the basis. The simulation study revealed that, on average, the application of the CGI and the WAG process in the Buckhorn Field would potentially result in an ultimate recovery of 61.2 and 59.4%OOIP, respectively. However, the recovery factors for either of these EOR processes have been reported to be quite lower in the literature: the CGI recovery factor was reported as 17%OOIP in Denbury's 2011 Annual Report (Denbury Resources Inc., 2011); Christensen *et al.* (2001) noted a WAG recovery factor of up to 20%OOIP based on 59 reviewed field cases, while the range of the incremental recovery was "generally about 5 to 10%". In order to reflect these reported recovery factors from the reported field cases, the simulated oil production profiles were appropriately scaled down. An example of this is depicted in Figure 4.63 showing both the original as well as the scaled down CGI oil production profiles (in this example: maximum CO_2 injection rate: 1 MMscf/day; maximum oil production rate: 500 STB/day). This scaling down procedure was applied to all of the simulated oil production profiles of the CGI and WAG process to reflect the reported ultimate recovery numbers from the field projects mentioned previously. These scaled down oil production profiles were then used as input for an updated cashflow analysis the results of which are tabulated in Tables 4.19 and 4.20.

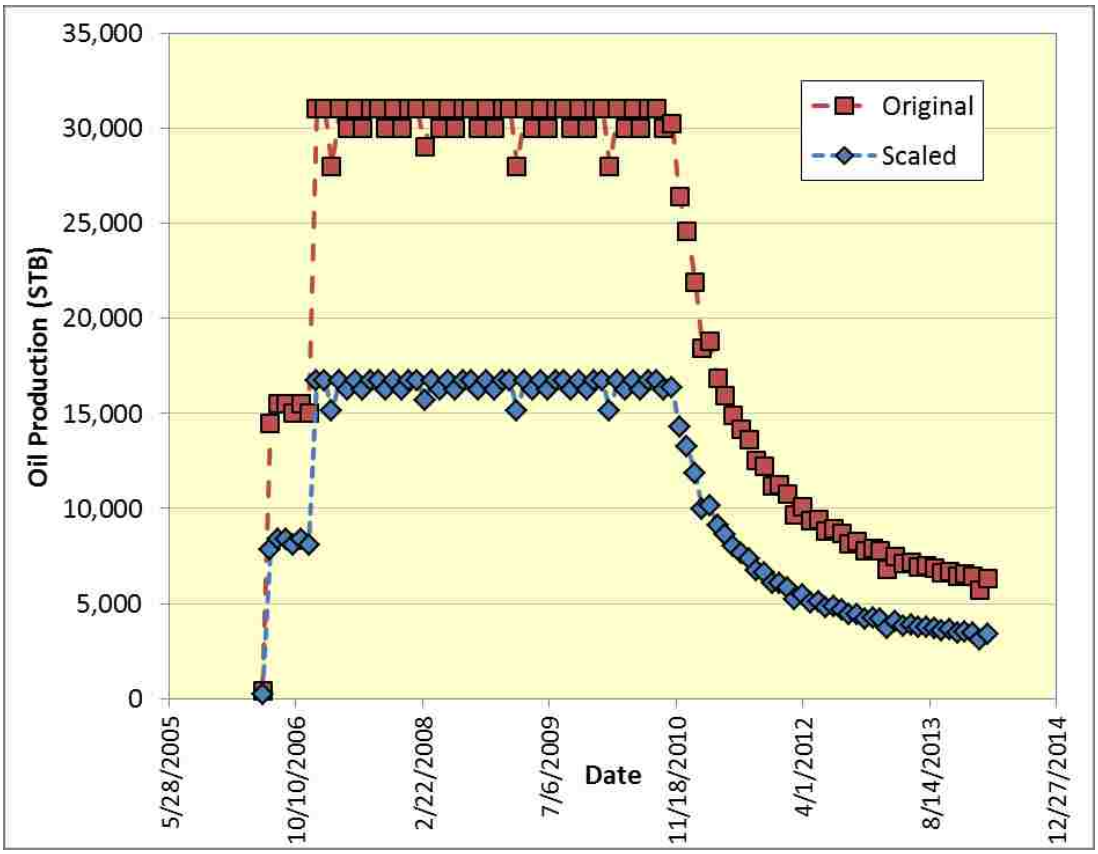

Figure 4.63: CGI Production Profile Scaling – 1 MMSCF/D & 500 STB/D

Table 4.19: Probability Distribution Description of Economic Performance Indicators – Scaled CGI Based on Literature

Statistics	NPV ($)	PI	GRR	IRR
Mean	3,249,449	1.4	12.8%	45%
Median	3,990,481	1.5	15.9%	44%
Standard Deviation	6,302,376	0.8	11.8%	37%
Variance	3.97E+13	0.6	0.01	0.14
Skewness	-0.1330	0.0229	-1.56	0.30
Kurtosis	2.41	2.61	5.2373	2.67
Coeff. of Variability	1.94	0.5469	0.92	0.8182
Minimum	-10,122,199	0.0	-38.2%	-28%
Maximum	20,734,391	3.8	31.8%	159%
Range Width	30,856,590	3.8	70.0%	187%
Mean Std. Error	199,299	0.0	0.37%	1.23%

Table 4.20: Probability Distribution Description of Economic Performance Indicators – Scaled WAG Based on Literature

Statistics	NPV ($)	PI	GRR	IRR
Mean	6,848,715	1.8	18.9%	49%
Median	6,461,420	1.8	18.9%	49%
Standard Deviation	4,744,757	0.6	4.9%	24%
Variance	2.25E+13	0.4	0.2%	6%
Skewness	0.4897	0.6960	-0.08	0.17
Kurtosis	3.19	3.63	2.93	2.91
Coeff. of Variability	0.69	0.3300	0.2585	0.49
Minimum	-3,961,180	0.6	2.7%	-14%
Maximum	24,239,161	4.3	33.1%	125%
Range Width	28,200,341	3.7	30.4%	139%
Mean Std. Error	150,042	0.0	0.2%	1%

The tabulated results above indicate that should the CGI application perform in the Buckhorn Field in a similar manner as to what was reported in the literature, it would result in substantially lower mean NPV than was the case beforehand. This is highlighted in Figure 4.64, showing a comparison of the scaled EOR processes' performance to the original results. If the economic project screening criteria (Mian, 2002) are applied on the mean CGI economic performance indicators reflecting field experience, the field-scaled CGI application would still remain profitable: mean NPV ($3,249,449) is greater than zero, mean IRR (45%) is greater than 10% while the mean PI (1.4) is greater than one. These numbers are reflected in Figures 4.65 and 4.66. Even though two of the considered economic performance indicators meet the minimum profitability screening standards, the PI is only marginally larger than 1.0. As such, scaling down the CGI process to reflect the reported field experience reveals a much more cautious economic profitability picture than before.

The updated results also revealed that the scaled WAG process could be considered profitable if the economic project screening criteria as tabulated in Table 4.18 are applied: the

mean NPV is positive ($6,848,715), the mean PI (1.8) is larger than 1.0 while the mean IRR (49%) is larger than the usually employed benchmark discount factor of 10%. But as was the case with the CGI application that was more reflective of the reported field recoveries, scaling down the WAG application in the Buckhorn Field again results in a more cautious economic assessment than was the case before.

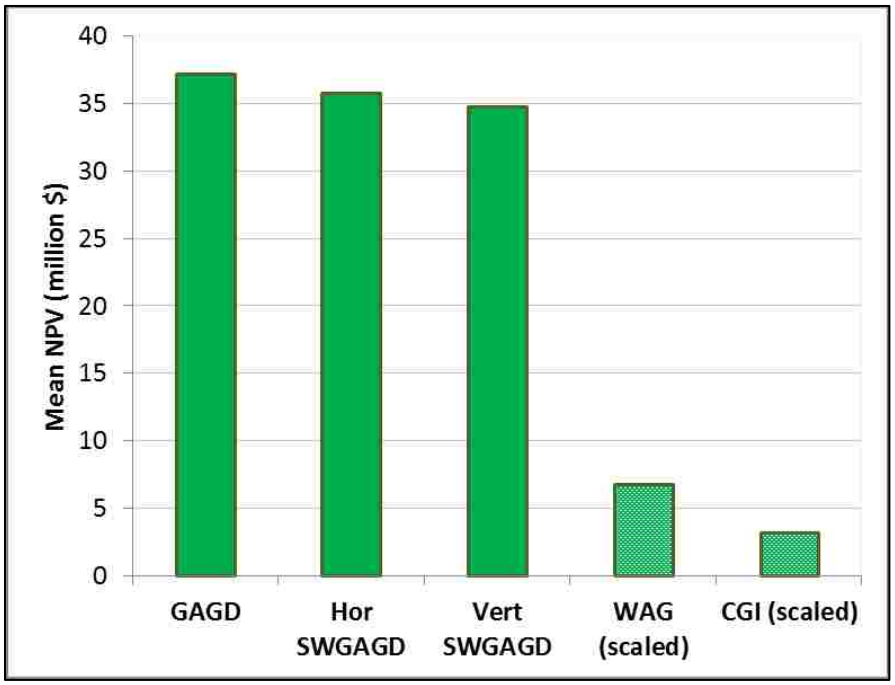

Figure 4.64: Comparison of Mean NPV Performance of the Field-Scaled EOR Processes to the Original Analysis Results

It must be mentioned that the original simulated oil recovery results for all variations of the GAGD process would also need to be re-assessed in a similar manner as described above, however, due to the fact that there are no reported field GAGD recovery factors in the literature this will have to be relegated to the future as more operators start to implement this novel EOR process in their fields. However, it should also be noted here that the GAGD process could be expected to still do well in the field (better than either the CGI or the WAG process) as it does

not fight against nature when trying to recover more oil, but rather uses the naturally occurring gravity segregation to its advantage.

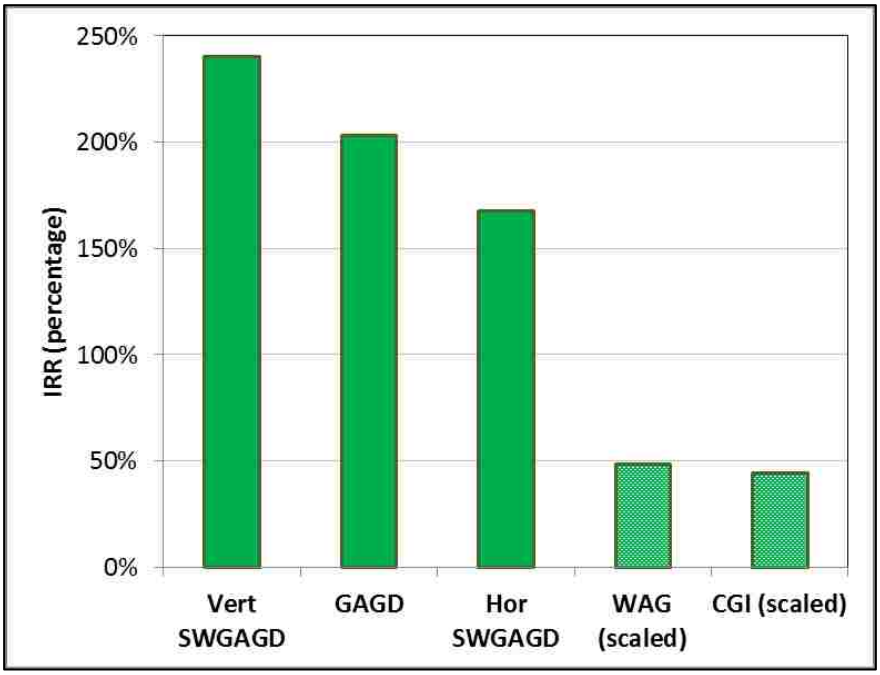

Figure 4.65: Updated Ranking of EOR Processes Based on IRR

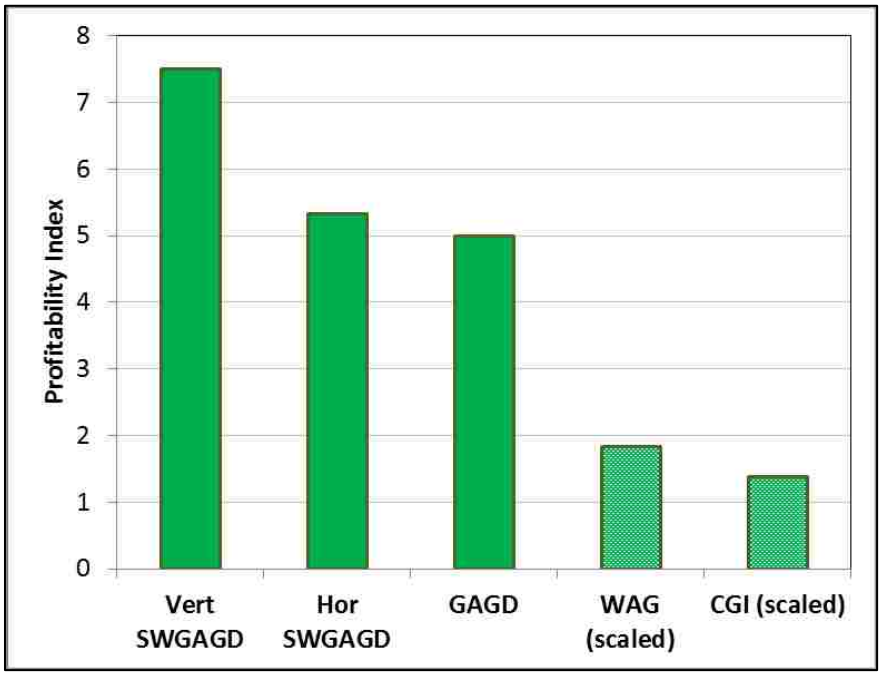

Figure 4.66: Updated Ranking of EOR Processes Based on PI

5. CONCLUSIONS AND RECOMMENDATIONS

5.1 Summary of Findings and Conclusions

1. Two sequences of experiments using reservoir cores from the Buckhorn Field were conducted with the aim of assessing the GAGD recovery in the field and to calculate the relative permeability curves needed for a field-scale numerical simulation study. These experiments were performed in addition to the earlier ones in which Berea sandstone cores were used. In the reservoir core experiments, the tertiary mode CO_2 GAGD flood in the first sequence was not successful due to possible plugging of the core, however, a secondary mode CO_2 GAGD flood during the subsequent experimental round was able to recover 80.7 percent of the original oil in place.
2. Use of reservoir cores in GAGD coreflooding experiments resulted in different relative permeability curves compared to those obtained with the Berea core indicating a possibly different (less water-wet) reservoir wettability for the Buckhorn reservoir rock-fluid system. This was also supported by the generated fractional flow curves.
3. When reservoir core experimental data were used in simulations, the results were slightly different from the results when the Berea relative permeability curves were used. However, the conclusion remained the same: GAGD application in the candidate field could potentially result in significant additional recovery. Both the coreflooding results as well as the results from the simulation study indicated that the GAGD process could possibly lead to a very favorable recovery factor when applied in the Buckhorn Field.
4. Two single-well variations of the conventional GAGD process were proposed and their process performance or technical feasibility in the Buckhorn Field was simulated using two SWGAGD wells, i.e. wells that contained separate injection and production completions

along the same wellbore. The vertical SWGAGD process used vertical wellbores for both the injection as well as the production completions, while the horizontal SWGAGD process housed the production completions in the horizontal leg of its single wellbore. The horizontal SWGAGD performed better than the vertical SWGAGD recovery, although both variations of the SWGAGD process recovered seemingly less oil than the multi-well GAGD process. Due to the fact that the operational parameters were not identical between the three aforementioned development plans, a one-to-one comparison based solely on recovery was not straight-forward.

5. The technical feasibility of two alternative EOR processes, continuous gas injection and Water-Alternating-Gas, were also investigated in the numerical simulation study, and although in terms of oil recovery factor they did not perform as well as the conventional GAGD process a direct comparison was again difficult due to the differences in the operational parameters.
6. A cashflow analysis was conducted for all of the mentioned potential EOR development plans focusing primarily on the economic performance indicators NPV, PI, GRR and IRR. Louisiana's petroleum fiscal system, a concessionary system also known as a royalty/tax system, formed the basis for this cashflow analysis. Based on the selected economic performance indicators, it was concluded that all of the envisioned development plans would be profitable under the stated economic parameter assumptions with both varieties of the SWGAGD process performing just as well (or better) than the multi-well GAGD process.
7. The CGI and WAG process were both outperformed by all variations of the GAGD process, especially if the oil production profiles were to be scaled down to reflect the much lower field-reported recovery results for either EOR process.

8. The multi-well GAGD process came out on top if the various EOR processes were to be ranked based solely on NPV, while the vertical single-well GAGD process ranked the highest when the IRR or the PI were used as the ranking criterion. In the offshore environment where each well costs in excess of $200 Million, these results could possibly provide the impetus for the consideration of this single-well GAGD process in offshore reservoirs as a viable EOR option.

5.2 Recommendations

1. Additional reservoir coreflooding experiments using longer reservoir cores (exceeding the recommended length-to-diameter ratio of about eight (Chugh & Fatt, 1970) should be conducted covering all consecutive stages of the GAGD application in the Buckhorn Field to further confirm the validity of the relative permeability curves used in this study and to emphasize the importance of these two-phase flow relationships in a simulation study.
2. In order to simplify the economic comparison of the various EOR processes the well count in the simulation study was restricted to two "characteristic well units", e.g. in the multi-well GAGD process two well pairs, consisting of one vertical injection well and one horizontal production well, were used compared to the horizontal SWGAGD process where two multi-use wells were used with the production occurring along the horizontal section of the wells, etc. To expand on the economic analysis, the well count itself needs to be optimized by maximizing the oil recovery through smart placement in the field of additional characteristic well units.
3. In the economic evaluation of the WAG process no specific consideration was given to the water disposal costs, but for a true analysis of the process' profitability these (sometimes

substantial) costs need to be included in the cashflow analysis as well. The same holds true for the gas disposal/re-injection cost considerations for all of the studied EOR options.

4. Apart from the already considered CGI and WAG process, other viable EOR processes need to be considered for application in the Buckhorn Field and their technical and economic performance need to be compared to the various configurations of the GAGD process. One of these other alternative EOR options could be the huff 'n' puff process. In this process the gas would initially be injected at very high rates until gas breakthrough occurred in the production wells after which all of the wells would be shut in. This shut-in period would allow for the injected gas slug to segregate from the reservoir oil/brine thereby displacing them nearer the production wells. Once the production wells were once again opened, there would be an instant peak in the oil production as a result of allowing the reservoir fluid distribution to reach equilibrium during shut-in. The effectiveness of these options should be first examined through laboratory experimentation and reservoir simulations prior to implementing a pilot study in the field(s).
5. Another way of optimizing the GAGD processes would be to improve the gas utilization factor, GUF, by incorporating a "blow down" period towards the end of the project during which the gas injection is ceased and any additional oil recovery would be the result of the depletion of the reservoir pressure. The added energy of the previously injected gas volume is utilized to recover additional oil thereby possibly improving the gas utilization factor.

REFERENCES

1. Adamache, I., Kantzas, A., McIntyre, F., and Sigmund, P.M., "Effect of Cyclic Flow Interruptions on Performance of Vertically Directed Miscible Floods," SPE Reservoir Engineering, February 1994.

2. Al-Kaabi, A.O., Al-Afaleg, N.I., Pham, T., Al-Muallem, A.S., Al-Bani, F.A., Hart, R.G., and Hembling, D.E., "Haradh-III: Industry's Largest Field Development With Maximum-Reservoir-Contact-Wells, Smart-Well Completions, and the iField Concept," SPE Production & Operations, Volume 23, Number 4, November 2008, pp. 444-447.

3. Arps, J.J., "Estimation of Primary Oil Reserves," Trans., AIME, 1956, 207, pp. 183-186.

4. Brock, W.R., & Bryan, L.A., "Summary Results of CO_2 EOR Field Tests, 1972-1987," SPE 18977 presented at the Low Permeability Reservoirs Symposium, 6-8 March 1989, Denver, Colorado.

5. Christensen, J.R., Stenby, E.H., and Skauge, A., "Review of WAG Field Experience," SPEREE, vol. 4, no. 2, pp. 97-106, 2001.

6. Chugh, S.C., and Fatt, I., "Influence of Core Plug Dimensions on Frontal Advance," unsolicited SPE paper 2894, 1970.

7. Compressor Systems Inc., Dan Nelson 432-563-1170.

8. Craig, F.J. (1993). SPE Monograph – The Reservoir Engineering Aspects of Water Flooding (Vol. 3). Richardson, TX.

9. Craze, R.C., and Buckley, S.E., "A Factual Analysis of the Effect of Well Spacing on Oil Recovery," Drill. & Prod. Prac., API, 1945, pp. 144-155.

10. Denbury Resources Inc., "2011 Annual Report," downloaded on April 8, 2013 from: http://www.denbury.com/files/doc_downloads/2011%20Annual%20Report.pdf.

11. Denbury Resources Inc., "May 7th 2009 Corporate Investor's Presentation," downloaded on May 9, 2009 from: http://phx.corporate-ir.net/phoenix.zhtml?c=72374&p=irol-presentations.

12. Denoyelle, L.C., and Lemonnier, P., "Simulation of CO_2 Huff 'n' Puff using Relative Permeability Hysteresis," SPE 16710 presented at the 62nd ATCE in Dallas, TX, September 27-30, 1987.

13. Dresser-Rand Company, Baton Rouge Sales Representative Mr. Fisher, 225-273-7313.

14. Gao, Ch., & Rajeswaran, T., "A Literature Review on Smart Well Technology," SPE 10611 presented at the 2007 SPE Drilling and Operations Symposium in Oklahoma City, 31 March-3 April 2007.

15. Glandt, C.A., "Reservoir Management Employing Smart Wells: A Review," SPE Drilling & Completion, Volume 20, Number 4, December 2005, pp. 281-288.

16. Goddard, D.A., "Louisiana Wellbore Schematics and Formation Tops," Center for Energy Studies, Louisiana State University, Baton Rouge, LA, 2006.

17. Gondiken, S., "Camurlu Field Immiscible CO_2 Huff and Puff Pilot project," SPE 15749 presented at the 5th SPE Middle East Oil Show in Manama, Bahrain, March 7-10, 1987.

18. Haines, H.K., and Monger, T.G., "A Laboratory Study of Natural Gas Huff 'n' Puff," CIM/SPE 90-78 or SPE 21576 presented at the CIM/SPE International Technical Meeting, Calgary, Canada, 10-13 June 1990.

19. Haskin, H.K., and Alston, R.B., "An Evaluation of CO_2 Huff 'n' Puff Tests in Texas," Journal of Petroleum Technology, February 1989.

20. Hinkley, R.E., and Davis, L.A., "Capillary Discontinuities and End Effects in Homogeneous Composite Cores: Effect of Flow Rate and Wettability," SPE paper 15596 presented at the 61st Annual Technical Conference and Exhibition of the Society of Petroleum Engineers held in New Orleans, LA October 5-8, 1986.

21. Holtz, M.H., "Summary of Gulf Coast Sandstone CO_2 EOR Flooding application and Response," SPE 113368 presented at the 2008 SPE 89356 presented at the 2004 SPE/DOE Symposium on Improved Oil Recovery, Tulsa, OK, 19-23 April 2008.

22. Iledare, O.O., "Analyzing the Impact of Petroleum Fiscal Arrangements and Contract Terms on Petroleum E&P Economics," SPE 88969, presented at Nigeria Annual International Conference and Exhibition, 2-4 August 2004, Abuja, Nigeria.

23. Kinder Morgan Inc., CO_2 marketing manager Doug McMurrey, 713-369-9159.

24. Kulkarni, M.M., and Rao, D.N., "Is Gravity Drainage an Effective Alternative to WAG?" presented at the AIChE Annual Meeting, Austin, TX, November 7-12, 2004.

25. Lau, H.C., Deutman, R., Al-Sikaiti, S., and Adimora, V., "Intelligent Internal Gas Injection Wells Revitalise Mature S.W. Ampa Field," SPE 72108 presented at the SPE Asia Pacific Improved Oil Recovery Conference, 6-9 October 2001, Kuala Lumpur, Malaysia.

26. Lino, U. de R.A., " An Evaluation of Natural Gas Huff 'n' Puff Field Tests in Brazil," SPE 26974 presented at the IIIrd Latin American/Caribbean Petroleum Engineering Conference in Buenos Aires, Argentina, 27-29 April 1994.

27. MacPhail, W.F., & Konopczynzki, M., "From Intelligent Injectors to Smart Flood Management: Realizing the Value of Intelligent Completion Technology in the Moderate Rate Industry Segment," SPE 112240 presented at the 2008 SPE Intelligent Energy Conference and Exhibition in Amsterdam, 25-27 February 2008.

28. Mahmoud, T., & Rao, D.N., "Mechanisms and Performance Demonstration of the Gas-Assisted Gravity-Drainage Process Using Visual Models," SPE conference paper 110132-MS, 2007.

29. Mahmoud, T.N., and Rao, D.N. "Range of Operability of Gas-Assisted Gravity Drainage Process." SPE/DOE IOR Symposium. Tulsa, OK: Society of Petroleum Engineers, 2008.

30. Mian, M.A., Project Economics and Decision Analysis, Volume 1 - Deterministic Models, PennWell, 2002.

31. Miller, B.J., and Bardon, C.P., "CO_2 Huff 'n' Puff Field Case: Five-Year Program Update," SPE 27677 presented at the SPE Permian Basin Oil and Gas Recovery Conference held in Midland, TX, 16-18 March, 1994.

32. Miller, B.J., and Hamilton-Smith, T., "Field Case: Cyclic Gas Recovery for Light Oil-Using Carbon Dioxide/Nitrogen/Natural Gas," SPE 49169 presented at the 1998 SPE ATCE in New Orleans, LA, 27-30 September, 1998.

33. Mohammed-Singh, L., Singhal, A.K., and Sim, S., "Screening Criteria for carbon Dioxide Huff 'n' Puff Operations," SPE 100044 presented at the 2006 SPE/DOE Symposium on Improved Oil Recovery, Tulsa, OK, 22-26 April, 2006.

34. Monger, T.G., and Coma, J.M., "A Laboratory and Field Evaluation of the CO_2 Huff 'n' Puff Process for Light-Oil Recovery," SPE Reservoir Engineering, November 1988.

35. Monger, T.G., and Trujillo, D.E., "Organic Deposition during CO_2 and Rich Gas Flooding," SPE Reservoir Engineering, February, 1991.

36. Monger, T.G., Ramos, J.C., and Thomas, J., "Light Oil Recovery from Cyclic CO_2 Injection: Influence of Low Pressures, Impure CO_2, and Reservoir Gas," SPE Reservoir Engineering, February, 1991.

37. Murray, M.D., Frailey, S.M., and Lawal, A.S., "New Approach to CO_2 Flood: Soak Alternating Gas," SPE 70023 presented at the SPE Permian Basin Oil and Gas Recovery Conference held in Midland, TX, 15-16 May, 2001.

38. Nadeson, G., Sayegh, S.G., and Girard, M., "Assessment of Dulang Field Immiscible Water-Alternating-Gas (WAG) Injection through Composite Core Displacement Studies," SPE paper 72140 presented at the SPE Asia Pacific IOR Conference in Kuala Lumpur, Malaysia, 8-9 October, 2001.

39. Oudomugsorn, P, “Geology of the Buckhorn Field, Tensas Parish, Louisiana,” M.S. Thesis, Louisiana Tech University, 1971.

40. Paidin, W.R., and Rao, D.N. "Physical Model Experiments to Evaluate the Effect of Wettability and Fractures on the Performance of the Gas Assisted Gravity Drainage (GAGD) Process," prepared for poster presentation at the International Symposium of the Society of Core Analysts, Calgary, 2007.

41. Palmer, F.S., Landry, R.W., and Bou-Mikael, S., “Design and Implementation of Immiscible Carbon Dioxide Displacement Projects (CO_2 Huff-Puff) in South Louisiana,” SPE 15497 presented at the 61st ATCE in New Orleans, LA, September 5-8, 1986.

42. Parker, N.C., “Using Natural Gas Transmission Pipeline Costs to Estimate Hydrogen Pipeline Costs,” Institute of Transportation Studies, University of California, Davis, CA, 2004.

43. Potsch, K., Ramberger, R., Glantschnig, J., Baumgarthuber, S., and Gößnitzer, F., “Gas Injection Pilot in the Hochleiten Field,” SPE 89356 presented at the 2004 SPE/DOE 14th Symposium on Improved Oil Recovery, Tulsa, OK, 17-21 April 2004.

44. Rao, D.N. (2006). Summary Simulation Report – Northern Dense Pod Buckhorn Field.

45. Rao, D.N., Ayirala, S.C., Kulkarni, M.M., and Sharma, A.P., “Development of the Gas Assisted Gravity Drainage (GAGD) Process for Improved Light Oil Recovery”, SPE 89357, Presented at the 2004 SPE/DOE Fourteenth Symposium on Improved Oil Recovery, Tulsa, OK, April 17 – 21, 2004.

46. Rao, D.N., Ayirala, S.C., Kulkarni, M.M., Mahmoud, T.N., & Paidin, W.R., “Development of Gas Assisted Gravity Drainage (GAGD) Process for Improved Light Oil Recovery,” 4095-NETL, 2011.

47. Rao, D.N., Ayirala, S.C., Kulkarni, M.M., and Sharma, A.P., “Development of the Gas Assisted Gravity Drainage (GAGD) Process for Improved Light Oil Recovery”, SPE 89357, Presented at the 2004 SPE/DOE Fourteenth Symposium on Improved Oil Recovery, Tulsa, OK, April 17 – 21, 2004.

48. Rapoport, L.A., & Leas, W.J., “Properties of Linear Waterfloods,” Petroleum Transactions, AIME, vol. 198, pp. 139-148, 1953.

49. Saikia, B.S., “SW-GAGD Schematic,” private e-mail correspondence.

50. Schenewerk, P.A., Thomas, J., Bassiouni, Z., and Wolcott, J., “Evaluation of a South Louisiana CO2 Huff ‘n’ Puff Field Test,” SPE/DOE 24143 presented at the SPE/DOE 8th Symposium on Improved Oil Recovery, Tulsa, OK, April 22-24, 1992.

51. Schiozer, D.J., and. Da Silva, J.-P.Q.G., "Methodology to Compare Smart and Conventional Wells," SPE 124949 presented at the SPE Annual Technical Conference and Exhibition, 4-7 October 2009, New Orleans, Louisiana.

52. Sharma, A.P., and Rao, D.N., "Scaled Physical Model Experiments to Characterize the Gas-Assisted Gravity Drainage EOR Process." SPE/DOE IOR Symposium. Tulsa, OK, 2008.

53. Shayegi, S., Jin, Z., Schenewerk, P., and Wolcott, J., "Improved Cyclic Stimulation using Gas Mixtures," SPE 36687 presented at the 1996 ATCE in Denver, CO, 6-9 October, 1996.

54. Shelton, J.L., and Morris, E.E., "Cyclic Injection of Rich Gas into Producing Wells to Increase Rates from Viscous-Oil Reservoirs," Journal of Petroleum Technology, August 1973.

55. Simpson, M.R., "The CO_2 Huff 'n' Puff Process in a Bottomwater-Drive Reservoir," JPT, Volume 40, Number 7, pp. 887-893, July 1988.

56. Spooner, H.V., "Basal Tuscaloosa Sediments, East-Central Louisiana," Bulletin of the American Association of Petroleum Geologists, vol. 48, no. 1, pp. 1-21, 1964.

57. Thomas, G.A., and Monger-McClure, T.G., "Feasibility of Cyclic CO_2 Injection for Light-Oil Recovery," SPE Reservoir Engineering, May 1991.

58. Thomas, J., Berzins, T.V., Monger, T.G., and Bassiouni, Z., "Light Oil Recovery from Cyclic CO_2 Injection: Influence of Gravity Segregation and Remaining Oil," SPE 20531 presented at the 65th ATCE in New Orleans, LA, September 23-26, 1990.

59. United States Energy Administration, "Oil and Gas Lease Equipment and Operating Costs 1994 Through 2009," retrieved from: http://www.eia.gov/pub/oil_gas/natural_gas/data_publications/cost_indices_equipment_production/current/coststudy.xls

60. Veazey and Associates, Louisiana Oil and Gas consultants Mike Veazey & Jim Veazey, 225-765-1914.

61. Zekri, A.Y., and Almehaideb, R.A., "Relative Permeability Measurements of Composite Cores, and Experimental Approach," SPE paper 77939 presented at the SPE Asia Pacific IOR Conference in Kuala Lumpur, Malaysia, 8-10 October, 2002.

VITA

Wagirin Ruiz Paidin was born in Paramaribo, Suriname, in 1977, the son of Wagimin Samben Paidin and Toegijem Trirarbijah Paidin-Resowidjojo. After completing his high school studies at the Algemene Middelbare School, Paramaribo, Suriname, he joined the Department of Mining and Geology of the School of Natural Sciences at the Anton De Kom University of Suriname, and obtained the degree Bachelor of Science in Mining in 2001. He worked as a junior geologist in charge of sampling and borehole logging for the Gold Division of the ALCOA, L.L.C. in Merian Creek, Suriname, from 2001 to 2002. In 2003, he enrolled in the post-graduate diploma course petroleum technology offered through the cooperation of the State Oil Company of Suriname (Staatsolie Maatschappij Suriname N.V.), the University of Suriname and the Technical University at Delft. As a result of completing the course at the top of the class he joined the Graduate School of the Louisiana State University, Baton Rouge, U.S.A. in August 2004. The degree of Master of Science in Petroleum Engineering was conferred in May 2006 for his part in the development of the Gas-Assisted Gravity Drainage (GAGD) process by conducting physical model experiments to assess the effect of wettability and fractures on process performance.

Soon afterwards he joined the Ph.D. program at LSU working on a gas condensate banking remediation project sponsored by ConocoPhillips which included an extended campus work project during the summer of 2007 at their Technology Center in Bartlesville, OK. There he primarily worked on a feasibility study on CO_2 sequestration in a depleted gas reservoir in the North Sea, as well as working with CoP's X-ray equipment that is routinely used for the determination of fluid saturations in cores during/after displacement experiments under extreme

conditions. After unsuccessfully trying to secure a representative gas condensate sample from CoP for coreflooding experiments, the research focus was shifted towards investigating the application of IOR processes in deepwater Gulf of Mexico reservoirs which is (in)directly related to his current dissertation research, the development and optimization of a single-well adaptation of the GAGD process for application in an onshore Louisiana reservoir.